ANNALS OF THE NEW YORK ACADEMY OF SCIENCES

Volume 72, Art. 13 Pages 559–785

*Editor in Chief*

Otto v. St. Whitelock

*Managing Editor*
Franklin N. Furness

*Associate Editor*
Marguerite Selzer

# THE ANALYSIS OF MIXTURES OF VOLATILE SUBSTANCES

BY

Emil F. Williams (*Conference Chairman*), W. J. Baker, R. K. Beerthuis, M. Bier, R. L. Bowman, N. Brenner, D. R. Bresky, J. E. Callen, J. O. Chase, E. Cieplinski, H. N. Claudy, J. F. Combs, G. Dijkstra, E. E. Dubský, R. D. Eanes, G. Fukayama, J. Greenspan, E. Glueckauf, L. F. Hatch, C. C. Helms, K. J. Hughes, R. W. Hurn, A. T. James, J. Janák, A. Karmen, J. G. Keppler, L. W. Kinsell, M. Krejčí, R. A. Landowne, S. R. Lipsky, J. E. Lovelock, G. D. Michaels, C. H. Orr, J. S. Payne, Jr., E. A. Piper, J. H. Purnell, J. H. Recourt, P. R. Scholly, C. W. Skarstrom, F. C. Snowden, P. Teitelbaum, R. F. Wall, P. Wheeler, W. A. Wiseman, T. L. Zinn

*Consulting Editor*

Emil F. Williams

NEW YORK

*PUBLISHED BY THE ACADEMY*

March 20, 1959

THE NEW YORK ACADEMY OF SCIENCES

(Founded in 1817)

COUNCIL, 1959

*President*

HILARY KOPROWSKI

*President-Elect*

M. J. KOPAC

*Vice-Presidents*

LYLE BORST
C. P. RHOADS

*Recording Secretary*

EMERSON DAY

*Corresponding Secretary*

FREDERICK Y. WISELOGLE

*Treasurer*

GUSTAV J. MARTIN

*Elected Councilors*

1957–1959

GEORGE H. MANGUN
MINA REES
HAYDEN C. NICHOLSON
WILLIAM W. WALCOTT

1958–1960

DAVID A. KARNOFSKY
WAYNE W. UMBREIT
GUSTAV J. MARTIN
JOHN E. VANCE

1959–1961

JOHN E. DEITRICK
ROBERT S. MORISON
CHARLES W. MUSHETT
E. L. TATUM

*Finance Committee*

HARDEN F. TAYLOR, *Chairman*
GORDON Y. BILLARD
ROBERT F. LIGHT

*Executive Director*

EUNICE THOMAS MINER

*SECTION OF BIOLOGICAL AND MEDICAL SCIENCES*

ROBERT L. KROC, *Chairman*
CHARLES NOBACK, *Secretary*

*DIVISION OF ANTHROPOLOGY*

DOROTHY L. KEUR, *Chairman*
DOROTHY CROSS JENSEN, *Secretary*

*DIVISION OF INSTRUMENTATION*

DUNCAN A. HOLADAY, *Chairman*
ANDRES FERRARI, *Secretary*

*DIVISION OF MYCOLOGY*

KARL MARAMOROSCH, *Chairman*
EMANUEL GRUNBERG, *Secretary*

*DIVISION OF PSYCHOLOGY*

GREGORY RAZRAN, *Chairman*

*SECTION OF CHEMICAL SCIENCES*

KARL FOLKERS, *Chairman*
FREDERICK R. EIRICH, *Secretary*

*SECTION OF GEOLOGICAL SCIENCES*

KURT LOWE, *Chairman*
FREDERICK P. YOUNG, Jr., *Secretary*

*DIVISION OF OCEANOGRAPHY AND METEOROLOGY*

ABRAHAM S. KUSSMAN, *Chairman*
CHARLES KNUDSEN, *Secretary*

*SECTION OF PHYSICAL SCIENCES*

EMANUEL R. PIORE, *Chairman*
E. BROMBERG, *Secretary*

*DIVISION OF ENGINEERING*

THOMAS B. DREW, *Chairman*

*Past Presidents*

WILLIAM K. GREGORY
VICTOR K. LAMER
HORACE W. STUNKARD
M. L. CROSSLEY
ROSS F. NIGRELLI
HARDEN F. TAYLOR
BORIS PREGEL

The Sections and the Divisions hold meetings regularly, one evening each month, during the academic year, October to May, inclusive. All meetings are held at the building of The New York Academy of Sciences, 2 East Sixty-third Street, New York 21, New York.

Conferences are also held at irregular intervals at times announced by special programs.

ANNALS OF THE NEW YORK ACADEMY OF SCIENCES
Volume 72, Art. 13 Pages 559–785
March 20, 1959

*Editor in Chief*
Otto v. St. Whitelock

*Managing Editor*
Franklin N. Furness

*Associate Editor*
Marguerite Selzer

# THE ANALYSIS OF MIXTURES OF VOLATILE SUBSTANCES*

*Consulting Editor*
Emil F. Williams

CONTENTS

Introduction. *By* Joseph Greenspan ........ 561

**Part I. Theoretical Considerations**

The Movement of Highly Radioactive Gases in Adsorption Tubes. *By* E. Glueckauf .. 562
The Development of Highly Efficient Gas-Liquid Chromatographic Columns. *By* J. H. Purnell ........ 592
Chromatography in the Gas-Solid System. *By* Jaroslav Janák ........ 606
Discussion: Part I ........ 612

**Part II. Medicine, Public Health, and Food Chemistry**

Gas-Liquid Chromatographic Analysis of Higher Fatty Acids and Fatty Acid Methyl Esters. *By* R. K. Beerthuis, G. Dijkstra, J. G. Keppler, and J. H. Recourt .... 616
Plasma Cholesterol Fatty Acids in Human Subjects as Determined by Alkaline Isomerization and by Gas Chromatography. *By* George D. Michaels, Priscilla Wheeler, George Fukayama, and Laurance W. Kinsell ........ 633
Gas Chromatography in Amino Acid Analysis. *By* M. Bier and Priscilla Teitelbaum ........ 641
Recent Advances in the Gas Chromatographic Separation of Methyl Esters of Fatty Acids. *By* C. H. Orr and J. E. Callen ........ 649
Evaluation of a Stationary Phase for Fatty Acid Analysis by Gas-Liquid Chromatography. *By* S. R. Lipsky and R. A. Landowne ........ 666
A Multistage Analyzer for Exhaust Gas Analysis. *By* R. W. Hurn, J. O. Chase, and K. J. Hughes ........ 675

**Part III. General Laboratory**

Katharometer Behavior. *By* W. A. Wiseman ........ 685

---

* This series of papers is the result of a conference on *The Analysis of Mixtures of Volatile Substances* held by The New York Academy of Sciences on April 10 and 11, 1958.

The 1,2-Dibromo-1-Propenes. *By* LEWIS F. HATCH AND JIMMIE S. PAYNE, JR. .......... 698
Gas Chromatographic Analysis of Mixtures Containing Oxygen, Nitrogen, and Carbon Dioxide. *By* NATHANIEL BRENNER AND EDWARD CIEPLINSKI .......... 705
A Radio Frequency Glow Detector for Gas Chromatography. *By* ARTHUR KARMEN AND ROBERT L. BOWMAN .......... 714
A New Type of Ionization Detector for Gas Chromatography. *By* J. E. LOVELOCK, A. T. JAMES, AND E. A. PIPER .......... 720
Properties of the Calcium Zeolite as Adsorbent for Gas Chromatography. *By* J. JANÁK, M. KREJČÍ, AND E. E. DUBSKÝ .......... 731

## Part IV. Process Control and Instrumentation

Process Control by Gas Chromatography in the Chemical Industry. *By* R. F. WALL, W. J. BAKER, T. L. ZINN, AND J. F. COMBS .......... 739
Use of Adsorption Phenomena in Automatic Plant-Type Gas Analyzers. *By* CHARLES W. SKARSTROM .......... 751
Thermal Conductivity Detectors for Process Control. *By* F. C. SNOWDEN AND R. D. EANES .......... 764
Adapting Gas Chromatography to Automatic Process Stream Analysis. *By* H. N. CLAUDY, C. C. HELMS, P. R. SCHOLLY, AND D. R. BRESKY .......... 779

*Copyright, 1959, by The New York Academy of Sciences*

# INTRODUCTION

Joseph Greenspan
*Process & Instruments, Brooklyn, N. Y.*

The entire field of chromatography is a rapidly developing one. It was only a few years ago that sorption effects were just an annoying, and not at all understood, obstacle encountered in attempts to secure high vacuums or to recover small amounts of substances from solution. However, a more careful examination of these phenomena has resulted in the conversion of a misunderstood hindrance into a valuable technique for the chemist. Liquid-solid chromatography, paper chromatography, and paper electrophoresis are now well-established experimental methods for separation, purification, and identification of all types of substances. References to exchange resins, exchange columns, zeolites, and ion exchangers are now commonplace.

The latest and most rapidly developing branch of chromatography is that of separations based on *gas* chromatography. Methods for separation of closely allied chemical compounds on the basis of adsorption and exchange from the gas phase are being developed almost daily. The separations of a number of especially difficult mixtures are discussed in this monograph.

An interesting aspect of gas chromatography is the intensive theoretical study that accompanies its practical laboratory and industrial applications. Such theoretical treatment will lead, not only to a better understanding of the complex mechanisms of differential exchange adsorption, but also to sounder design of equipment and selection of absorbents for specific problems.

The papers in this monograph show that gas chromatography is not confined to laboratory procedure, but is rapidly becoming a part of chemical plant process engineering, both as a basic unit process and as an analytical control.

Paralleling the development of the theory and practice of this form of adsorption is the development of the instrumentation necessary to follow the separations effected by gas chromatography. Thus it is heartening to see the much neglected katharometer or thermal conductivity cell, previously relegated to occasional low-accuracy analyses of special gas mixtures, now performing high-accuracy analyses of a wide variety of gaseous mixtures. Furthermore, several papers in this monograph indicate that novel instrumentation methods, other than thermal conductivity, are in the offing.

# Part I. Theoretical Considerations

## THE MOVEMENT OF HIGHLY RADIOACTIVE GASES IN ADSORPTION TUBES

E. Glueckauf

*Atomic Energy Research Establishment, Harwell, England*

### Introduction

The adsorption of highly radioactive gases can be employed for a variety of purposes. It can be used, as for example the homogeneous aqueous reactor test at Oak Ridge, Tenn., to retain the gases for a time sufficiently long for their radioactivity to decay, or at least, for most of it to decay. It may be used for the separation of radioactive, long-lived krypton-85, an isotope of considerable commercial value, from xenon or other impurities, or it may be used as a convenient method for concentrating radioactive gases into a small volume. Moreover, it may be assumed that freshly generated radioactive gases from certain reactors, during their passage through adsorption tubes, may be used in the future as valuable sources of high-intensity $\gamma$-radiation. Two problems in particular are of practical interest and will be discussed in detail.

In every case, the normal behavior of gases in adsorption tubes is altered and, in some circumstances, fundamentally so by heat generated by the radioactivity, chiefly as the result of the adsorption of $\beta$-rays in the adsorbent.

The effects produced vary according to whether the outside of the adsorption tube is kept at a constant temperature, in which case a radial temperature gradient is set up in the tube, or whether the tube is insulated against heat loss, in which case the passage of a band of active gas produces a temperature wave traveling along the axis.

In either case the adsorption capacity and the adsorption coefficient, which are usually functions of the temperature, are substantially altered and, as the changed adsorption coefficient results in a reduced adsorption and, hence, reduced local heat production, a complex equilibrium arises.

Moreover, radioactive substances decay with time, so that heat production is reduced the farther the distance from the entrance of the adsorption tube, resulting in an axial temperature gradient even under steady-state conditions.

The conventional theory of gas chromatography does not accommodate these complexities, and a new approach is necessary to obtain a clearer picture of the behavior of such gases in adsorption tubes.

### List of Symbols

$A, B$ = constants of the adsorption isochore (see EQUATION 1).
$a, a_0$ = parameter (see EQUATIONS 8$a$ and 22).
$b$ = parameter (see EQUATION 43$a$).
$C$ = specific heat of tube content (watts/cc. absorbent × degrees C.).
$C_p$ = specific heat of carrier gas (watts/cc. of gas × degrees C.).

$c$ = concentration (moles/cc.) of adsorbed gas.
$D$ = diffusion coefficient of adsorbed gas in carrier gas. (sq. cm./sec.)
$E$ = specific radioactivity in a given section of the tube.
$F$ = flow rate of carrier gas (cc./sec.).
$g_{(t)}$ = decay function of the activity.
$h$ = specific activity in watts per cc. of carrier gas at $T$ degrees K.
$H$ = total activity of band (watts).
$K$ = thermal conductivity of tube content (watts/cm. × degrees C.).
$K_1$ = one half theoretical plate height (cc. of adsorbent).
$l$ = length of adsorbent tube.
$m$ = $v_0c_0$ = moles of adsorbate.
$N$ = number of theoretical plates.
$P$ = reactor power in watts.
$R$ = radius of adsorption tube (cm.).
$r$ = distance from center of tube (cm.).
$S$ = specific $\beta$-radio activity of adsorbed gas (watts/mole).
$T$ = temperature (degrees K).
$t$ = time (sec.).
$t_0$ = time of entry into adsorption tube.
$v$ = volume of carrier gas (cc.).
$v_0$ = feed volume of adsorbate (cc.).
$v_\beta$ = mean band width of eluted band (cc.).
$\bar{v}$ = elution volume of peak (cc.).
$X$ = total volume of adsorption tube (cc.).
$x$ = volume of adsorption tube, from entrance to a given length (cc.).
$\lambda$ = decay constant (sec.$^{-1}$).
$\phi$ = effective distribution coefficient

$$= \frac{\text{moles of adsorbed gas/cc. of adsorbent space}}{\text{moles of adsorbed gas per cc. of gas space at } T \text{ degrees K.}}$$

$\tilde{\phi}$ = radial mean of distribution coefficient.
$\bar{\phi}$ = value of $\phi$ at peak maximum.
$\eta$ = parameter (see EQUATION 45$c$).
Subscripts: 0 refers to state before passage of band,
$\infty$ refers to state after passage of band,
ss refers to steady state.

## Distribution of Activity and Delay of Radioactive Gas in an Adsorbent Tube, Cooled at the Outside, Under Constant Feed and Steady-State Conditions

### *Radial Temperature and Concentration Gradient, and Mean Adsorption Coefficient $\tilde{\phi}$*

If a carrier gas that has, outside the column, a temperature $\bar{T}$ and a radioactivity content of $h$ watts/cc. of gas space enters a region of a higher temperature $T$, the gas expands and its radioactivity content becomes $\bar{T}h/T$. The amount adsorbed per cc. of adsorbing space is $\bar{T}\cdot h\cdot f/T$, where $f$ is a true adsorption coefficient of the dimension cc. of gas per cc. of adsorbent space. For the expression $\bar{T}\cdot f/T$ we use the symbol $\phi$, a "modified" adsorption coefficient. Both $f$ and $\phi$, if we have linear adsorption coefficients, are functions of the temperature only and, for convenience, we choose the function

$$\phi = \exp(A - BT) \tag{1}$$

in preference to the usually employed Clausius-Clapeyron equation. EQUATION 1 generally holds true over a limited temperature interval. From 300 to 500° K we have, for adsorption on charcoal (Sutcliffe Speakman 208 C):

for Kr, $A = 7.80$ and $B = 0.0168$

for Xe, $A = 11.74$ and $B = 0.0214$

Visualize an adsorbing tube of 1 cm. length and of radius $R$. Consider the energy $dE$ released in a ring of width $dr$ at a distance $r$ from the center of the tube. This is given by

$$dE = 2\pi r h \phi \, dr$$

and the total heat flux through this ring is

$$E_r = 2\pi h \int_{r=0}^{r} r\phi \, dr \tag{2}$$

According to Fick's law, the heat flux is given also by

$$E_r = -2\pi r K \frac{dT}{dr} \tag{3}$$

and equating (3) and (2) gives

$$\frac{h}{K} \int_0^r \phi r \, dr = -\frac{r \, dT}{dr} \tag{4}$$

so that one obtains the differential equation

$$\frac{h\phi}{K} + \frac{dT}{r \, dr} + \frac{d^2T}{dr^2} = 0 \tag{5}$$

Eliminating $T$ by means of EQUATION 1, EQUATION 5 gives the differential equation

$$\frac{Bh\phi}{K} = \frac{d \ln \phi}{r \, dr} + \frac{d^2 \ln \phi}{dr^2} \tag{6}$$

The boundary conditions are

$$r = R \qquad \phi = \phi_R$$

(defined by the outside temperature $T_R$, see EQUATION 1)

and

$$r = 0 \qquad \frac{d\phi}{dr} = 0 \tag{7}$$

The solution is

$$\frac{\phi_0}{\phi_r} = \left[1 - a\phi_0 \left(\frac{r}{R}\right)^2\right]^2 \tag{8}$$

where the dimensionless parameter is

$$a = \frac{\mathrm{B}}{8} \cdot \frac{\mathrm{h}}{K} \cdot R^2 \tag{8a}$$

and $\phi_0$, the value of $\phi$ at $r = 0$, is defined by the quadratic

$$\frac{\phi_0}{\phi_R} = (1 - a\phi_0)^2 \tag{8b}$$

EQUATION 8 gives us the adsorption coefficient $\phi$ as function of the radius and also, by means of EQUATION 1, the radial temperature distribution.

$$T_r = T_0 + \frac{2}{B} \ln \left[ 1 - a\phi_0 \left( \frac{r}{R} \right)^2 \right] \tag{9}$$

The total heat flux through the outer surface, that is, the heat produced in 1 cm. length of tube, is given by EQUATION 3. Replacing $T$ from EQUATION 9 with $r = R$ we obtain

$$E_R = \frac{\pi R^2 \cdot h\phi_0}{1 - a\phi_0}$$

Eliminating the denominator with EQUATION 8$b$ we obtain

$$E_R = \pi R^2 \cdot h \cdot \sqrt{\phi_0 \phi_R} \tag{10}$$

and the mean adsorption coefficient follows as

$$\tilde{\phi} = \frac{E_R}{h\pi R^2} = \sqrt{\phi_0 \phi_R} \tag{11}$$

It follows from EQUATION 8$b$ and 11 that $\tilde{\phi}$ is defined by the quadratic

$$a\tilde{\phi}^2 + \tilde{\phi} - \phi_R = 0 \tag{12}$$

FIGURE 1 shows the radial variation of the effective adsorption coefficient $\phi_r$ for a number of values of the parameter $a$. The adsorption coefficients are calculated for Xe at an outside-wall temperature of 50° C. It is apparent that for values of $a > 10^{-2}$ most of the adsorption takes place near the circumference of the tube.

*Example: adsorption of radioactive xenon on charcoal.* This can be illustrated by the case of Xe-fission products carried in a helium gas stream with a total $\beta$-heat evolution of 50 watts/liter at 273° K., that is, $h = 0.05$. This is a moderate activity for purge gas from a reactor. The heat conductivity, $K$, in a charcoal tube filled with helium is

$$K = 2.8 \times 10^{-3} \text{ watts/cm./° C.}$$

The parameter $a = (B/8)(h/K) \cdot R^2$ has, for several values of $R$, the values given in colume 2, TABLE 1. Assuming that the tube is cooled at the outside to 50° C. ($\phi_R = 126$), we obtain for the mean adsorption coefficient $\tilde{\phi}$ the data in column 3; for $\phi_0$, those in column 4; and for the heat produced in watts per

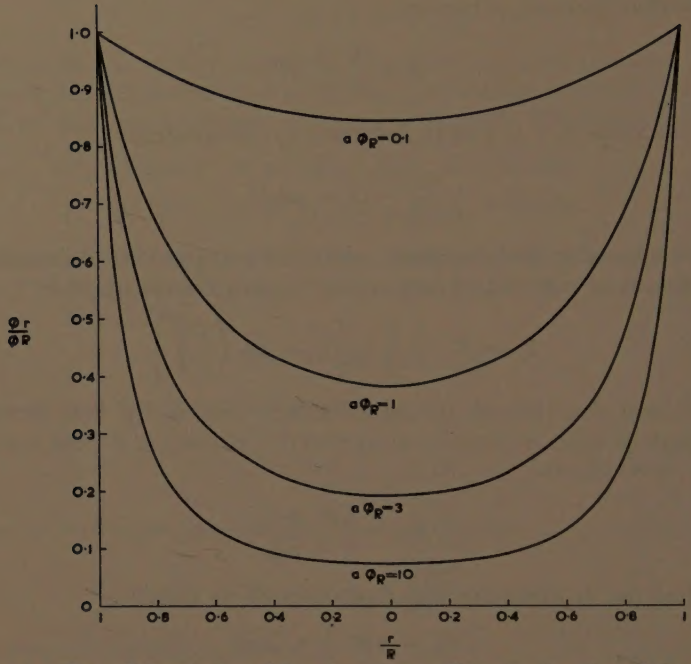

FIGURE 1. The radial variation of the adsorption coefficient as function of the parameter $a\phi_R$ in cooled adsorption tube.

TABLE 1

| $R$ cm. | $a$ $\times 10^3$ | $\phi$ | $\phi_0$ | $E_R$ watts/cm. | $T_0$ (max.) degrees C. |
|---|---|---|---|---|---|
| 0.5 | 12.2 | 68.5 | 37 | 2.7 | 108 |
| 1 | 48.8 | 41.6 | 14 | 6.5 | 152 |
| 1.5 | 110 | 29.5 | 6.9 | 10.4 | 186 |
| 2 | 196 | 23 | 4.2 | 14.3 | 209 |

1 cm. of tube, $E_R$, those in column 5. The temperature $T_0$ at the center of the tube rises rapidly with increasing diameter (see column 6). It is interesting to note that, at these high heat transfers, the heat rating per sq. cm. surface of tube is independent of the tube diameter. It is given by

$$\frac{E_R}{2\pi R} = \sqrt{\frac{2\phi_R K h}{B}}$$

that is, for the given values of $K$ and $h$, it is 1.3 watts/sq. cm. surface.

*Adsorption from a gas mixture* ($Kr + Xe$). If we deal, not with a single gas, but with a mixture of radioactive gases (for example, krypton and xenon), EQUATION 4 changes to

$$\frac{1}{K}(h_1\phi_1 + h_2\phi_2) + \frac{dT}{r\,dr} + \frac{d^2T}{dr^2} = 0 \tag{13}$$

and EQUATION 7 becomes

$$\frac{B_1}{K}(h_1\phi_1 + h_2\phi_2) = \frac{d \ln \phi_1}{r\, dr} + \frac{d^2 \ln \phi_1}{dr^2} \tag{14}$$

where the subscripts 1 and 2 refer to krypton and xenon, respectively.

We can solve this problem of the radial distribution only if the ratio of the adsorption coefficients of the two gases is the same at all temperatures. This leads to the equation for the mean adsorption $\bar{\phi}_1$

$$\frac{1}{\bar{\phi}_1} = \frac{1}{2\phi_{1R}}\left[1 + \sqrt{1 + \frac{BR^2}{2K}(\phi_{1R}h_1 + \phi_{2R}h_2)}\right] \tag{15}$$

If the temperature coefficient ($B$) of $\ln \phi_1$ is not the same as that of $\ln \phi_2$, one would expect that, although the solution of EQUATION 14 no longer leads to an equation of the type of EQUATION 15, a very good approximation would be the symmetrical expression:

$$\frac{\phi_{1R}}{\bar{\phi}_1} \simeq \frac{\phi_{2R}}{\bar{\phi}_2} \simeq \frac{1}{2}\left[1 + \sqrt{1 + \frac{R^2}{2K}(B_1\phi_{1R}h_1 + B_2\phi_{2R}h_2)}\right] \tag{16}$$

### *Continuous Flow of Radioactive Gases Through a Cooled Adsorption Tube*

$\alpha$ (*One chemical species*). Consider a continuous flow into an adsorption tube of an inert gas, for example, helium, that carries radioactive Kr or Xe of constant concentration. At the time ($t_0$) of entry into the adsorption tube, the specific activity may be $h_0$ watts/cc.

In the case of a nonradioactive gas, a breakthrough at the other end would occur, and the gas in the tube would then everywhere have the concentration $c_0$. In the case of a radioactive gas, neither the concentration nor the activity will remain constant, because of the radioactive decay; instead, the local activity will depend on the time it takes for the gas to travel from the point of entry to a given position in the tube. If a point $x$ cc. distant from the point of entry, where $t = t_0$, is reached at the time $t$, its activity $h$ is

$$h = h_0 \cdot g(t)/g(t_0) \tag{17}$$

where $g(t)$ is the decay function of the gas.

The problem of the retention time is complicated by two factors: (1) The retention time per unit length is not constant, because the decaying radioactivity causes a variation of the temperature along the tube and, hence, a variation of the mean adsorptive capacity of the adsorbent. (2) The adsorptive capacity of a unit length depends also on the retention time in the preceding length of tube, as this affects the radioactive heat production.

For a gas with a linear isotherm, such as Kr and Xe at the concentrations with which we are concerned, the average movement of any individual particle of adsorbed gas proceeds according to the equation

$$\frac{dx}{dt} = \frac{F}{\bar{\phi}} \tag{18}$$

where $x$, measured in cc. of adsorption tube, is the distance travelled in the time $t$, and where $F$ is the gas flow rate given in cc. per second. The distance $x$ is therefore obtained at any given time $t$ by

$$x = F \int_{t_0}^{t} \frac{dt}{\bar{\phi}} \tag{19}$$

Eliminating $\bar{\phi}$ with EQUATIONS 12 and 17

$$\frac{1}{\bar{\phi}} = \frac{1}{2\phi_R}\left[1 + \left(1 + 4a_0\phi_R\,\frac{g(t)}{g(t_0)}\right)^{\frac{1}{2}}\right] \tag{20}$$

and

$$x = \frac{F}{2\phi_R}\left[t - t_0 + \int_{t_0}^{t}\left(1 + 4a_0\phi_R\,\frac{g(t)}{g(t_0)}\right)^{\frac{1}{2}} dt\right] \tag{21}$$

where

$$a_0 = \frac{BR^2h_0}{8K} \tag{22}$$

The knowledge of the $t$ to $x$ relation then gives us the specific radioactivity at any given point along the tube, which for a 1-cm. length of adsorption tube has the value

$$E_x = \pi R^2 \bar{\phi}\,\frac{g(t_x)}{g(t_0)} \cdot h_0 \tag{23}$$

If the gas consists of a single radioactive species, the decay follows the well-known function

$$\frac{g(t)}{g(t_0)} = e^{-\lambda(t-t_0)} = e^{-\lambda\tau} \tag{24}$$

where $\lambda$ is the decay constant. The integration of EQUATION 21 gives

$$x = \frac{F\tau}{\phi_R}\left\{\frac{1}{2} + \frac{1}{\lambda\tau}\left[u_0 - u + \frac{1}{2}\ln\frac{(u_0 - 1)(u + 1)}{(u - 1)(u_0 + 1)}\right]\right\} \tag{25}$$

where

$$u_0 = (1 + 4a_0\phi_R)^{\frac{1}{2}} \tag{25a}$$

and

$$u = (1 + 4a_0\phi_R e^{-\lambda\tau})^{\frac{1}{2}} \tag{25b}$$

FIGURE 2 shows the result of these calculations for a case where radioactive $Xe^{137}$ is carried in a continuous stream of a nonadsorbed gas through a charcoal tube. The assumed conditions, in addition to EQUATION 1 for the adsorption isotherm are:

Radius of tube $R = 2.5$ cm.

| | |
|---|---|
| Flow of gas | $F = 167$ cc./sec. |
| Wall temperature | $T_R = 25°$ C. ($\phi_R = 214$) |
| Thermal conductivity | $K = 2.8 \times 10^{-3}$ watts cm.$^{-1}$ (degrees C.)$^{-1}$ |
| Specific radioactivity of gas feed | $h_0 = 0.1$ watts/cc. |
| Decay constant | $\lambda = 0.003$ sec.$^{-1}$ |

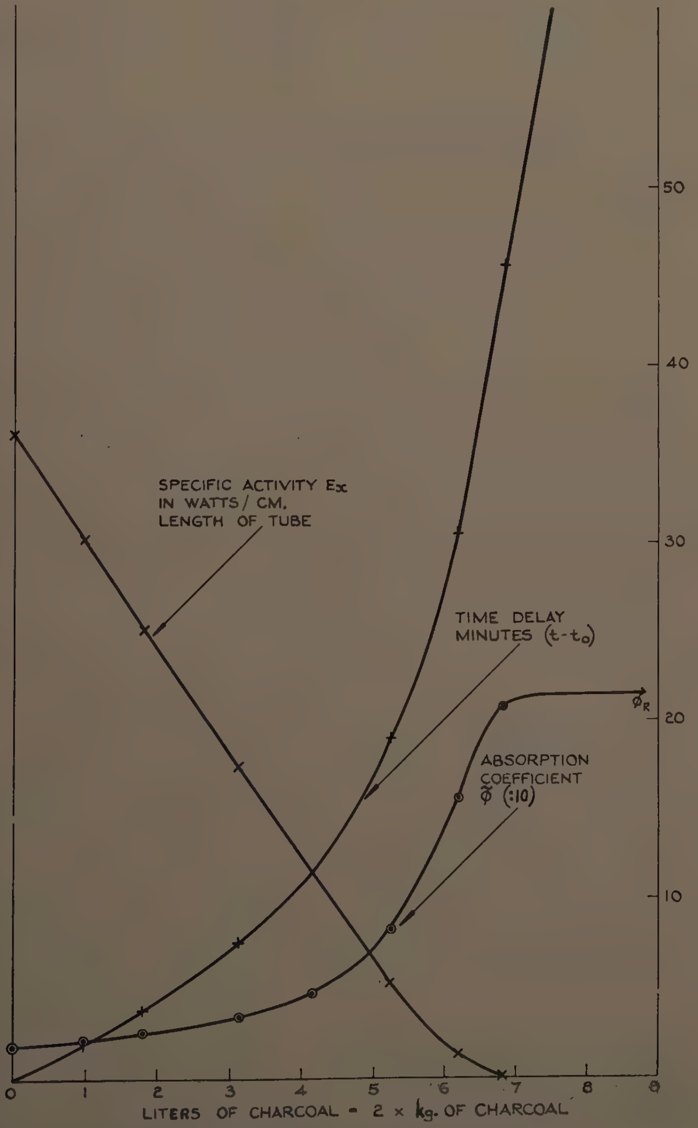

FIGURE 2. Variation of specific activity, adsorption coefficient, and delay time along a charcoal column continuously fed with radioactive $Xe^{137}$.

The curves for the time delay and for the local mean adsorption coefficients show the typical effects of the high temperatures that are generated by the $\beta$-radiation of the adsorbed xenon in the first section of the adsorption tube. Near the entrance ($x = 0$) the temperature is raised by 125°, that is, to 150° C.

A surprising feature is the linear fall of the activity along the tube. This is not a coincidence; it applies to all single-species gases.

One can easily see that when the activity is sufficiently high for

$$4a_0\phi_R \cdot e^{-\lambda\tau} \gg 1$$

and

$$\frac{2(u_0 - u)}{\lambda\tau} \gg 1$$

one obtains

$$x \simeq \frac{2F}{\lambda}\sqrt{\frac{a_0}{\phi_R}}\left[1 - \exp\left(-\frac{\lambda\tau}{2}\right)\right] \qquad \text{(25 approx.)}$$

$$\tilde{\phi} \simeq \sqrt{\frac{\phi_R}{a_0}}\exp\left(\frac{\lambda\tau}{2}\right) \qquad \text{(20 approx.)}$$

and the linear relation (see EQUATION 11):

$$E \simeq \pi R^2 h_0 \sqrt{\frac{\phi_R}{a_0}}\left(1 - \frac{\lambda\sqrt{\phi_R}}{2F\sqrt{a_0}} \cdot x\right) \qquad (26)$$

This leads to the simple relation that the amount $x$ of adsorbent that will allow most of the activity of a single species to decay is given by $E \simeq 0$, or

$$x = \frac{FR}{\lambda}\left(\frac{Bh_0}{2\phi_R K}\right)^{\frac{1}{2}} \qquad (27)$$

It is worthwhile to note that the amount of adsorbent required for almost complete decay is proportional to $R$, so that smaller tube diameters lead to a saving in adsorbent.

$\beta$ (*Two chemical species*). If we have a continuous feed of two chemical species, for example, Kr (subscript 1) and Xe (subscript 2) produced in a reactor at the time $t = 0$, under steady-state conditions, every point $x$ in the adsorption column is associated with two times. The krypton isotopes will have taken a time $t_1 - t_0$ to reach the point and the more strongly adsorbed xenon isotopes will have taken the much longer time $t_2 - t_0$.

The movement of krypton along the column is defined by (see EQUATION 19)

$$x = F\int_{t_0}^{t_1}\frac{dt}{\tilde{\phi}_1} \qquad (28a)$$

and movement of xenon is defined by

$$x = F\int_{t_0}^{t_2}\frac{dt}{\tilde{\phi}_2} \qquad (28b)$$

where $t_0$ is the time of entry into the column. It follows from this that $t_1$ and $t_2$ are related by the equation

$$\frac{t_1 - t_0}{t_2 - t_0} = \frac{\tilde{\phi}_1}{\tilde{\phi}_2} = \frac{\phi_{1R}}{\phi_{2R}} = \alpha \tag{29}$$

(see EQUATION 16). This is important for EQUATION 16, where $h_1$ and $h_2$ are the specific activities of the gas at different times: we know that if $h_2$ refers to the activity at the time $\tau_2 = t_2 - t_0$, then $h_1$ at the same point of the column refers to

$$\tau_1 = t_1 - t_0 = \alpha\tau_2$$

The specific activities $h_1$ and $h_2$ (watts/cc.) are functions of the reactor power $P$ (watts) and the flow rate $F$ (cc./sec.) of the sweeping gas that carries away the gaseous fission product activity:

$$h_1 = \frac{P}{F} g_1(t_1) = \frac{P}{F} g_1(t_0 + \alpha\tau_2) \tag{30a}$$

and

$$h_2 = \frac{P}{F} g_2(t_2) = \frac{P}{F} g_2(t_0 + \tau_2) \tag{30b}$$

The functions $g_1(t)$ and $g_2(t)$ can be computed easily from the fission yields and the physical constants of the dozen or more different isotopes of krypton and xenon and their radioactive, solid daughter products that, given sufficient time to reach the steady state are, at every point along the adsorption tube, in equilibrium with the parent gas activity at that point.

$$g_1(t) = \frac{1}{180} \sum_i (\eta_i \lambda_i e^{-\lambda_i t} \cdot \sum E_j\beta) \text{ sec.}^{-1} \tag{31}$$

for krypton, and similarly $g_2(t)$ for xenon. Here

$\eta_i$ = fission yield of the rare gas isotope

$\sum E_j\beta$ = sum of the mean $\beta$-energies in million electron volts (Mev.) of the parent gas isotope and its active daughters,

and the summation is carried out over all isotopes of one rare gas species (Kr or Xe). We now have a single time variable $\tau$ and, combining EQUATIONS 16, 28*b*, and 30*a*, *b*, we obtain the relation between $x$ and $\tau$ (the residence time of xenon in the column when reaching the point $x$).

$$x = \frac{F}{2\phi_{2R}} \left\{ \tau + \int_0^\tau \left( 1 + \frac{R^2P}{2KF} [B_1\phi_{1R}g_1(t_0 + \alpha\tau) + B_2\phi_{2R}g_2(t_0 + \tau)] \right)^{\frac{1}{2}} d\tau \right\} \tag{32}$$

The specific activities $E_x$ of krypton and xenon, at different positions of $x$ along the adsorption column expressed in watts per cc. of tube content are for the krypton contribution

$$E_1(x) = \bar{\phi}_1 \frac{P}{F} g_1(t_0 + \alpha\tau) \tag{33a}$$

and for the xenon contributions

$$E_2(x) = \bar{\phi}_2 \frac{P}{F} g_2(t_0 + \tau) \tag{33b}$$

An example is provided by the calculation of the distribution of activities that arise when the krypton and xenon are carried out from a small homogeneous reactor of $P = 10^7$ watts by a stream of non-adsorbed gas ($F = 2000$ cc./sec.) through a charcoal tube or a parallel series of charcoal tubes of $R = 5$ cm. radius and is cooled to a wall temperature of 25° C. Assume that, before reaching the adsorption tube, the gases suffer a delay of $t_0 = 72$ sec. FIGURE

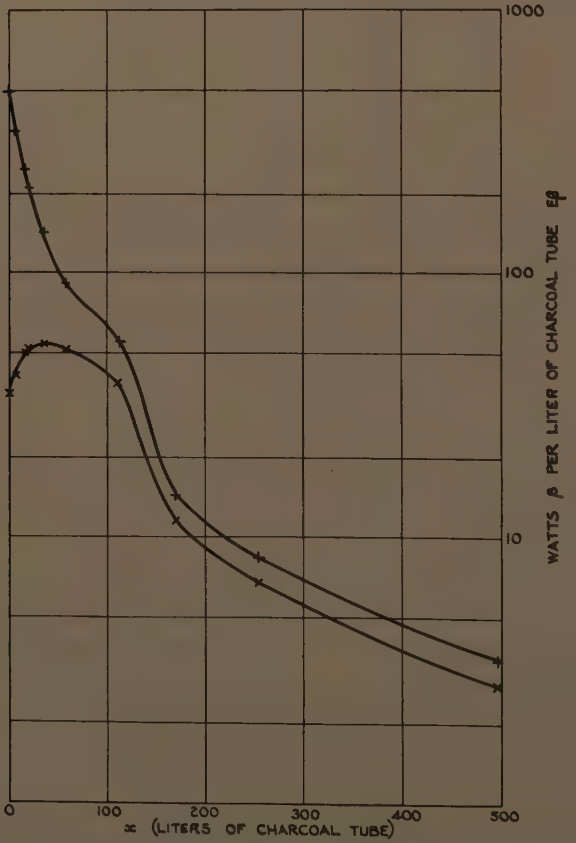

FIGURE 3. Distribution of $\beta$-radiation power along a charcoal column continuously fed with a reactor mixture of radioactive krypton and xenon. Upper curve: Kr + Xe. Lower curve: Kr alone.

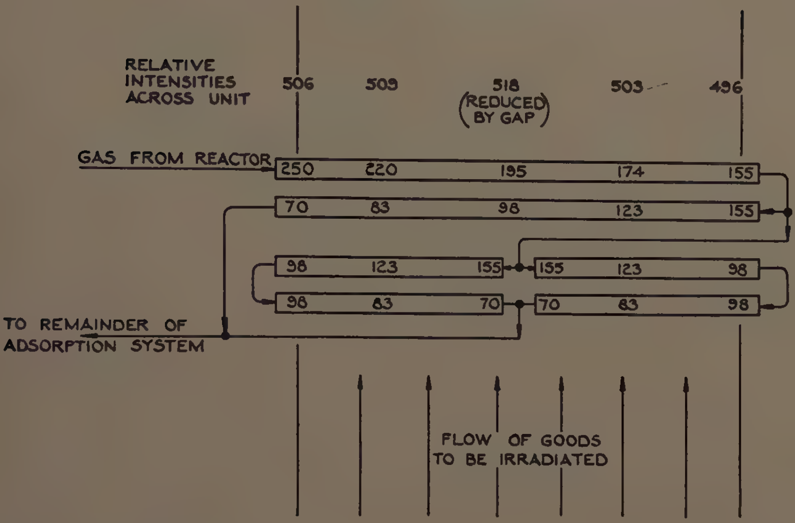

FIGURE 4. Scheme of a 40-liter adsorption system, giving uniform radiation dose (watts $\gamma$ per liter of adsorption system).

3 shows the distribution of radioactivity in the column both for the individual gases and the combined effects. As might be expected, the more strongly adsorbed xenon dominates the part near the entrance to the adsorption tube, whereas krypton, which is much less delayed, falls off less rapidly. The reason for the lower values of the krypton activity near the entrance is that the high temperature generated by the xenon reduces its adsorption. The most important aspect of this exercise is, however, that a knowledge of the age of the individual fission gases in a given section of the adsorption tube also characterizes the $\gamma$-radiation emitted from this section. As a rough approximation, the same kind of curve as in FIGURE 3 with half the watts per liter value as $\gamma$-radiation is obtained.

This permits the designing of $\gamma$-irradiation units of suitable properties. For example, if it is desired to produce a unit that gives a uniform irradiation to goods traveling on a moving band at right angles to the direction of the adsorption tubes, one can, with the help of FIGURE 3, construct a tube system as shown in FIGURE 4, which is so arranged that every article on the moving band receives the same dose.

$\gamma$ (*Channeling effects*). Column 6 in TABLE 2 gives the values of $\phi_0/\tilde{\phi}$ existing at the different positions $x$ of the column. As the rate of movement of any particle of adsorbable gas is inversely proportional to $\phi$, these values indicate that in the first section of the tube the krypton and xenon at the center of the tube move about 5 to 10 times faster than the corresponding radial mean rate. This means that a severe channeling effect is produced as the result of the higher temperatures and lower adsorption coefficients in the center of the tube. The channeling gas in the center will eventually dissipate by radial diffusion, and the result is that gases that had entered the adsorption tube simultaneously

TABLE 2

RESULTS CALCULATED FOR THE GASES FROM A 10 MW. REACTOR EXPERIMENT UNDER STATED CONDITIONS

| Delay times | | Positions $x$ in liters of adsorbent | $\beta$-power watts per liter of adsorbent | $\beta$-power from Kr, watts per liter of adsorbent | $\frac{\tilde{\phi}}{\phi_R} = \frac{\phi_0}{\bar{\phi}}$ | $\Delta x$ liters $= \Delta l \pi R^2 \eta$ |
|---|---|---|---|---|---|---|
| $t_1$ hours | $t_2$ hours | | | | | |
| 0.02 | 0.02 | 0 | 500 | 35 | 0.081 | 100 |
| 0.04 | 0.0215 | 6.8 | 349 | 41 | 0.114 | 97 |
| 0.08 | 0.0246 | 16.9 | 250 | 50 | 0.163 | 92 |
| 0.10 | 0.0261 | 20.9 | 213 | 52 | 0.174 | 91 |
| 0.2 | 0.0337 | 37.2 | 146 | 54 | 0.238 | 84 |
| 0.4 | 0.0489 | 58.7 | 90 | 51 | 0.293 | 78 |
| 1 | 0.096 | 114 | 55 | 38.4 | 0.446 | 61 |
| 2 | 0.170 | 171 | 14.5 | 11.6 | 0.76 | 26 |
| 4 | 0.324 | 255 | 8.5 | 6.8 | 0.91 | 10 |
| 10 | 0.78 | 495 | 3.5 | 2.8 | 0.93 | 8 |
| 20 | 1.54 | 850 | 1.8 | 1.4 | 0.96 | 4 |
| Total power in 850 liters of adsorbent: | | | 20.2 kw. | 8.6 kw. | | |

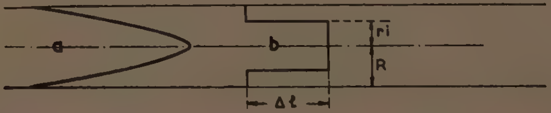

FIGURE 5. Channeling effect in a cooled charcoal tube. (*a*) Paraboloid surface of gas that simultaneously entered the adsorption tube. (*b*) Discontinuous representation of channeling effect for the purpose of approximate calculation.

will be distributed in the tube in a paraboloid shape, as indicated at *a* in FIGURE 5.

In order to estimate roughly the extent of channeling, we replace the curved diffuse boundary representing adsorbed Xe of equal age (see *a* in FIGURE 5) by a discontinuous sharp boundary of the type shown at *b* in FIGURE 5. We can make a rough mass balance that will give us an estimate of the length $\Delta l$ or the volume $\Delta x = n\pi R^2 \Delta l$, where $n$ = number of parallel tubes. In the steady state the amount of adsorbate carried into the "bulge" $(F/n)\cdot c\cdot(r_i/R)^2$ minus the amount lost by the shortening of the bulge through the advancing front $(F/n)\cdot c\cdot(\phi_0/\bar{\phi})(r_i/R)^2$ must be lost by diffusion into the surrounding cylinder $2\pi r_i\cdot\Delta l\cdot D\cdot(dc/dr) \simeq 2\pi r_i\cdot\Delta l\cdot D\cdot c/(R - r_i)$. This leads to a mass balance equation, resulting in

$$\Delta l \simeq \frac{F\cdot r_i(R - r_i)}{2\pi D\cdot nR^2}\left(1 - \frac{\phi_0}{\bar{\phi}}\right) \tag{34}$$

or

$$\Delta x \simeq \frac{F\cdot r_i(R - r_i)}{2D}\left(1 - \frac{\phi_0}{\bar{\phi}}\right) \tag{35}$$

Due to the form of EQUATION 35 the value of $\Delta x$ is not critically dependent on

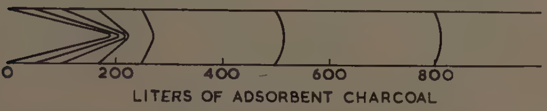

FIGURE 6. Channeling effect of radioactive gases from a 10 Mw. reactor when passing through a cooled charcoal tube system of 4-in. diameter.

the choice of $r_i/R$, and choosing a value of approximately ⅔, which seems a reasonable cut according to FIGURE 1, one obtains

$$\Delta x \simeq \frac{FR^2}{9D}\left(1 - \frac{\tilde{\phi}}{\phi_R}\right) \tag{36}$$

as

$$\frac{\phi_0}{\tilde{\phi}} = \frac{\tilde{\phi}}{\phi_R}$$

In the example of TABLE 2, the equal-age profiles therefore will spread out over volumes of the adsorption tube, as shown in column 7, leading to a distribution of profiles as shown in FIGURE 6. Such a situation, of course, would upset completely the calculated distribution in the first 150 to 200 liters of the adsorption system.

We must come therefore to the conclusion that in this example we have not chosen the correct conditions for the adsorption of the radioactive gases.

As shown in EQUATION 12, $\tilde{\phi}/\phi_R$ is directly dependent on the parameter $a$. Indeed, for large values of parameter $a$

$$\frac{\tilde{\phi}}{\phi_R} \simeq \sqrt{\frac{1}{a\phi_R}} \simeq \frac{1}{R}\sqrt{\frac{8K}{Bh\phi_R}} \tag{37}$$

that is, approximately inverse with the tube radius. In the given example, the channeling effect can be reduced to acceptable dimensions, by reducing the tube diameter from 4 in. to 1 in. for the first 200 liters of the adsorption tube, and simultaneously increasing the number of parallel tubes, so as not to interfere with the pressure drop.

An alternative method would be to reduce the channeling by radial mixing devices, for example, baffles of a suitable shape that need be used in the first sections of the adsorption tube only.

## MOVEMENT OF A BAND OF RADIOACTIVE GAS IN AN ADSORBENT COLUMN, AND THE SEPARATION OF Kr AND Xe

When separating radioactive gases of moderate activity by gas chromatography, the phenomena are in no way different from those of ordinary gas chromatography. However, when we deal with highly active gases emitting $\beta$-rays, the latter are adsorbed in the column material and produce a rise in temperature of the adsorbent during the passage of a band of a radioactive component. This temperature rise affects profoundly not only the separating power of an adsorbent column, but also the time of passage and the shape of the bands. As the adsorption coefficient $\phi$ falls with increasing temperature, the rear of a band will tend to move faster than its front; this has the result of contracting the band. Eventually, a steady state is attained when the contracting tendencies are just compensated by longitudinal diffusion, and the shape of the band no longer alters.

To begin with, we have the usual mass-balance equation derived from the "theoretical plate theory[1]"

$$\left(\frac{\partial c}{\partial x}\right)_v + \left(\frac{\partial(\phi c)}{\partial v}\right)_x - K_1\left(\frac{\partial^2 c}{\partial x^2}\right)_v = 0 \tag{38}$$

where $c$ = concentration in moles per cc. and $v$ = volume of the carrier gas. In addition, a heat balance is established in such a way that the heat carried by a small gas volume $\Delta v$ into any section $\Delta x$ of the column, together with the radioactive heat produced in that section during the time $\Delta t$ of passage of the volume $\Delta v$, ($\Delta t = \Delta v/F$), increases the heat content of this section; longitudinal heat conduction is small and has been neglected.

$$\underset{\substack{\uparrow\\ \text{radio}\\ \text{activity}\\ \text{term}}}{\frac{\phi}{F}s\cdot c} - \underset{\substack{\uparrow\\ \text{heat}\\ \text{convection}\\ \text{term}}}{C_p\left(\frac{\partial T}{\partial x}\right)_v} - \underset{\substack{\uparrow\\ \text{heat}\\ \text{content}\\ \text{term}}}{C\left(\frac{\partial T}{\partial v}\right)_x} = 0 \tag{39}$$

Here $s$ is the specific radioactivity of the adsorbate in watts per mole. The relation between the adsorption coefficient $\phi$ and the local temperature $T$ can be adequately expressed by EQUATION 1.

EQUATION 39 assumes: (1) that there are no radioactive daughters; (2) that the radioactive half life of the species is of sufficient length to give a constant heat release; and (3) that there is no loss of heat from the tube to the surrounding air.

The effect of the first two limitations on any experiments is not severe: (1) The heat effect caused by radioactive daughters during the passage of the narrow band is only small.

(2) If the radioactive species decay somewhat during passage, the final band will have a shape approximating that calculated for the final activity. Its arrival time will approximate that calculated for the mean activity during the passage through the column.

Loss of heat must be prevented under all circumstances and radial uniformity of temperature must be improved by the addition of thermally conducting materials, such as layers of wire netting, to the adsorbent filling; otherwise the inner parts of the tube will get hotter and give a channeling effect that will greatly distort and widen the band.

EQUATIONS 1, 38, and 39, together with the boundary conditions, referring to the feed into the column, describe the system fully. These boundary conditions will usually have the form:

$$v, t = 0 \qquad c = 0 \qquad \text{for all } x \tag{40a}$$

(column empty in the beginning).

$$0 < v, t < v_0, t_0 \qquad x = 0 \qquad c = c^0 \tag{40b}$$

(describing period of feed at $x = 0$).

$$v, t > v_0, t_0 \qquad x = 0 \qquad c = 0 \tag{40c}$$

(describing the subsequent elution of the band with carrier gas).

*Steady-State Conditions (Rate of Movement, Height and Width of the Band)*

When the steady state has been attained, all points of the band move at the same rate ($dx/dv$) down the column. This rate is governed by the adsorption coefficient $\bar{\phi}$ that exists at the peak of the band. At this point diffusion is inoperative, as here the concentration gradient is zero, and all movement of adsorbate is therefore convective. It then follows from EQUATION 1 that

$$\left(\frac{\partial x}{\partial v}\right)_{c,T,\phi} = \frac{1}{\bar{\phi}} \tag{41}$$

From EQUATIONS 38, 39, 40, and 41 one obtains $\bar{\phi}$ and $\bar{c}$ (see APPENDIX, section 1).

The value of $\bar{\phi}$, the adsorption coefficient at the maximum of the band and, hence, the rate of motion of the band are determined by

$$\frac{\bar{\phi}}{\phi_0} = \frac{1}{b} \ln (1 + \mathrm{b}) \simeq \frac{1}{1 + b/2} \qquad \text{for } b < 1 \tag{42}$$

where

$$b = \frac{BH\phi_0}{F(C - C_p\bar{\phi})} \tag{43}$$

that is,

$$b \simeq \frac{BH\phi_0}{F[C - C_p\phi_0/(1 + b/2)]} \tag{43a}$$

This equation enables one to obtain $b$ conveniently from the experimental parameters.

For the concentration at the maximum, $\bar{c}$, under steady-state conditions, one obtains

$$\bar{c} = \frac{BH^2}{8K_1sF(C - C_p\bar{\phi})} = \frac{b \cdot H}{8\phi_0K_1s} \tag{44}$$

The shape of the band can be obtained only with an explicit equation by making the approximation that $b \ll 1$, but it is a very good approximation, even for higher values ($b \simeq 1$).

The relation between the concentration $c$ of the adsorbate and the elution volume $v$ is then obtained (see APPENDIX, section 2) as

$$|v - \bar{v}| = \frac{1}{\eta} \ln \frac{1 + (1 - c/\bar{c})^{\frac{1}{2}}}{1 - (1 - c/\bar{c})^{\frac{1}{2}}} \tag{45a}$$

or

$$\frac{c}{\bar{c}} = \frac{4e^{\eta|v-\bar{v}|}}{(1 + e^{\eta|v-\bar{v}|})^2} \tag{45b}$$

where

$$\eta = \frac{b}{2K_1\phi_0} \tag{45c}$$

with $b$ from EQUATION 43$a$ (see FIGURE 7). From EQUATION 45$a$ it follows that the band width $v_\beta$ at the concentration $c_e$ given by $c_e/\bar{c} = 1/e$ has the value

$$v_\beta = 2(v_e - \bar{v}) = \frac{2}{\eta} \ln \frac{1 + (1 - 1/e)^{\frac{1}{2}}}{1 - (1 - 1/e)^{\frac{1}{2}}} = \frac{4.34}{\eta} = \frac{8.68K_1\phi_0}{b} \tag{46}$$

For inactive gases one would obtain, according to the "theoretical plate" theory, if the feed band was very narrow,

$$v_\beta = \bar{v}\sqrt{\frac{8}{N}} \tag{47}$$

(See Glueckauf,[1] Equation 30.)

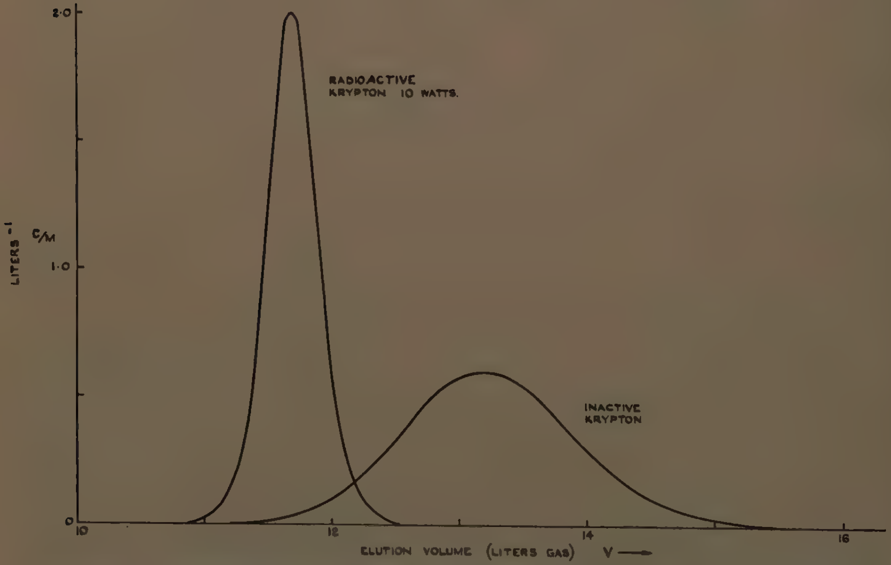

FIGURE 7. Comparison of the elution bands of inactive and radioactive krypton during separate elutions under otherwise identical conditions.

where $N$ is the number of theoretical plates of the chromatographic column. As

$$N = \frac{X}{2K_1} = \frac{\bar{v}}{2\phi_0 K_1} \tag{48}$$

(See Glueckauf,[1] Equation 12a.)

we have

$$v_{\beta(\text{inactive})} = 4\sqrt{\bar{v}K_1\phi_0} \tag{49}$$

or

$$\left(\frac{v_\beta}{v}\right)_{\text{inactive}} = 4\left(\frac{K_1\phi_0}{\bar{v}}\right)^{\frac{1}{2}} = \frac{2.828}{\sqrt{N}} \tag{49a}$$

while

$$\left(\frac{v_\beta}{\bar{v}}\right)_{\text{active}} = \frac{8.68}{b}\left(\frac{K_1\phi_0}{\bar{v}}\right) = \frac{8.68}{bN} \tag{46a}$$

FIGURE 8 gives the values of $v_\beta/\bar{v}$ as function of $N$ for various values of the parameter $b$, which (see EQUATION 43$a$) varies primarily with the ratio $H/F$, that is, with the total radioactive power of the band $H$ and the flow rate $F$. If the column is not long enough for the radioactive band to attain its steady-state width, the actual width will lie below the values given by EQUATIONS 49$a$ and 46$a$.

FIGURE 8 gives a clear indication of the substantial band contraction with increasing value of the parameters $b$ or $H/F$.

FIGURE 7 shows, as an example, the comparison between the elution curves of an inactive band of krypton and that of radioactive krypton with an $H/F$ value of 0.3 joules/cc. of $\beta$-radiation, in a column of 400 theoretical plates, under otherwise identical conditions: $\phi_0 = 16.6$ cc. gas/cc. charcoal, $B = 0.0168$

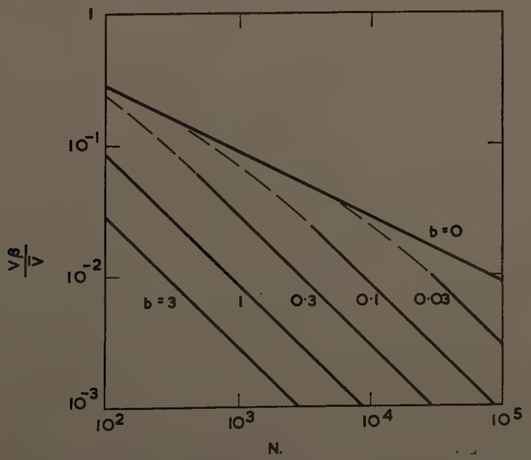

FIGURE 8. Ratio of band width to peak elution volume as function of the parameter $b$.

(degrees C.)$^{-1}$, $C = 0.32$ joules/cc. of column content/° C., $C_p = 0.94 \times 10^{-3}$ joules/cc. of monoatomic carrier gas at $NTP$/° C., $K_1 = 1$ cc. of adsorbent and $X = 800$ cc. of adsorbent. With these data $b = 0.271$.

FIGURE 7 shows clearly the somewhat shorter breakthrough time in the case of radioactive krypton as well as the very considerable band contraction. The general shape of the bands, in spite of the different form of the equations, is not visibly altered.

### *Contraction of an Originally Wide Band*

It is of particular interest to note that the steady-state values of the final band width are independent of the width of original feed band that may have been many times larger. This creates the possibility of concentrating a batch of highly radioactive gas simply by a passage through an adsorbing column. This process of contraction of an originally wide band is therefore treated in some detail. In order to obtain a solution to the general EQUATIONS 1, 38, 39, and 40 for conditions other than the steady state, it is necessary to introduce an approximation.

When we deal with a wide band, diffusion has a much smaller role than convective motion because concentration gradients are much smaller. Therefore, we can omit tentatively the diffusion term in EQUATION 38 that then results in

$$\left(\frac{\partial c}{\partial x}\right)_v + \left(\frac{\partial \phi c}{\partial v}\right)_x = 0 \tag{50}$$

Omission of the "disturbance" term is a useful step that has often been taken in chromatographic theory, when otherwise the solution of the problem would have become impossible.[2, 3] The approximation gives fairly reliable information on the position in the column of the boundaries occurring with substances with nonlinear isotherms. A very similar situation applies here.

As is shown in detail in section 3 of the APPENDIX, one can demonstrate that a band of radioactive gas, which before entering the column was contained in a volume $v_0$, will contract to its steady-state width when the total volume of gas passed through the column is

$$v_{ss} \simeq v_0 \left(\frac{4}{3} + \frac{1}{b}\right) \tag{51}$$

and this takes place at a point in the column defined by

$$x_{ss} \simeq \frac{v_0}{\phi_0}\left(\frac{4}{3} + \frac{1}{b}\right) = \frac{1}{\bar{\phi}}\,(v_{ss} - v_0/2) \tag{52}$$

As after reaching the steady state, the band moves on at the rate given by EQUATION 41, one obtains for the breakthrough volume of such a band through a column of volume $X$ the value

$$v_B \simeq X\bar{\phi} + \frac{v_0}{2} \tag{53}$$

It should be noted that, according to the definitions used in EQUATION 40, $v_B$

includes the feed volume $v_0$. For an inactive wide band of linear isotherm, using the same boundary conditions, the breakthrough volume of the center of the band would be

$$v_{B(\text{inactive})} = X\phi_0 + \frac{v_0}{2} \tag{54}$$

FIGURE 9 shows the band contraction calculated for the same example as in FIGURE 7, the case $H/F = 0.3$ joules/cc. gas, the activity being fed into the column in a volume of 1000 cc. of carrier gas.

The ordinate represents the local concentration ($\phi c$) in the column (moles per cc. of adsorbent) divided by $\phi_0 c_0$ (calculated with EQUATION A39 of the APPENDIX). The full lines show the band shape as calculated when neglecting diffusion phenomena. In practice, diffusion will affect the sharp frontal and rear boundaries to a degree that varies with the height of the theoretical plate; the high peaks, too, will be smoothed out. The dotted lines represent approximately the situation that would arise if the plate height were about 0.25 cc. of adsorbent. For the steady-state shape, the dotted lines represent height and shape as calculated from EQUATIONS 43, 44, and 45.

TABLE 3 gives a summary of the essential equations both for radioactive and nonactive gas chromatography.

It is necessary to draw attention to the fact that a steady state is attained only if $C > C_p\bar{\phi}$. Otherwise, the rear of the band is cooled by the normally

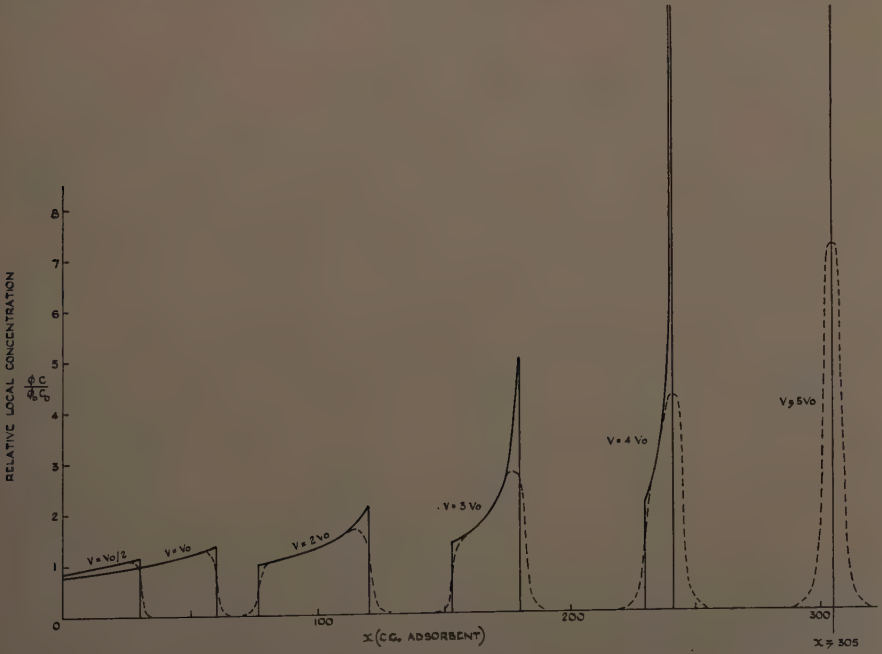

FIGURE 9. Contraction of an originally wide band of radioactive gas during passage along a column.

TABLE 3

SUMMARY OF ESSENTIAL EQUATIONS

| | Radioactive | Nonactive |
|---|---|---|
| Breakthrough volume of peak maximum | $\bar{v} = X\bar{\phi} + \frac{v_0}{2} = \frac{X\phi_0}{b}\ln(1+b) + \frac{v_0}{2}$ | $\bar{v} = X\phi_0 + \frac{v_0}{2}$ |
| Elution curve | $\frac{c}{\bar{c}} = \frac{4e^{\eta\lvert v-\bar{v}\rvert}}{(1+e^{\eta\lvert v-\bar{v}\rvert})^2}$ | $\frac{c}{\bar{c}} = \exp\left(-\frac{N(\bar{v}-v)^2}{2v\bar{v}}\right)$ |
| Concentration at peak maximum | $\bar{c} = \frac{BHm}{8K_1F\left[C - C_p\phi_0\Big/\left(1+\frac{b}{2}\right)\right]}$<br>$\bar{c} = \frac{BH^2}{8K_1Fs\left[C - C_p\phi_0\Big/\left(1+\frac{b}{2}\right)\right]}$ | $\bar{c} = \frac{m}{\bar{v}}\sqrt{\frac{N}{2\pi}} = \frac{m}{2\sqrt{\pi\bar{v}K_1\phi_0}}$ |
| Mean band width of elution band at $c = \bar{c}/e$ | $v_\beta = \frac{4.34}{\eta} = \frac{8.68K_1\phi_0}{b}$ | $v_\beta = \bar{v}\sqrt{\frac{8}{N}} = 4\sqrt{\bar{v}\phi_0K_1}$ |
| Minimum adsorbent to reach steady state | $x_{ss} \simeq \frac{v_0}{\phi_0}\left(\frac{4}{3} + \frac{1}{b}\right)$ | |
| Definition of $b$ | $b = \frac{BH\phi_0}{F\left[C - C_p\phi_0\Big/\left(1+\frac{b}{2}\right)\right]}$ | |

cold carrier gas, which would result in a "tailing" effect. If, however, $C > C_p\bar{\phi}$, the cold front of the carrier gas travels slower than the band and does not interfere.

## SEPARATION OF A MIXTURE OF TWO RADIOACTIVE GASES

While a moderate amount of radioactive heat dissipation will improve the separation of two species with widely different separation factors such as Kr and Xe, due to the sharpening of the bands, a point is reached where increasing the dissipated heat will no longer improve the separation, as the slower species (Xe) is adsorbed at a higher temperature, that is, with a lowered adsorption coefficient and, consequently, is moving at an increased rate as compared with the preceding species (Kr). Indeed, a value of $H/F$ can occur where this effect will result in an equal advance rate for the two peaks. For this and larger values of $H/F$, separation, although very substantial, remains incomplete, the two bands following each other closely and overlapping in the region of contact. The situation that arises then may be compared with that occurring in displacement chromatography, except that the displacing agent here is not the adsorption of the second species but the heat developed by it in the overlap region. This results in a further contraction of the preceding band with more diffusion in the forward direction until both bands move with an equal velocity governed by the following band of adsorbate. As both bands under these conditions are exceedingly narrow (which need not be the case in ordinary displacement chromatography), this case need not be examined in detail, as it is useless from a separation point of view.

It is of interest, however, to find out at which value of $H/F$ separations between krypton and xenon no longer occur.

The two peaks will move at the same rate when

$$\bar{\phi}_1 = \bar{\phi}_2 \tag{55}$$

As the peaks are practically symmetrical we have for krypton (subscript 1)

$$\frac{1}{\bar{\phi}_1} = \frac{1}{\phi_1^0} + \frac{B_1 s_1}{FC_1} \int_{-\infty}^{v=v_1} c_1\, dv \simeq \frac{1}{\phi_1^0} + \frac{B_1 H_1}{2FC_1} \tag{56}$$

where $C_1 = (C - C_p\bar{\phi})_1$. At the rear end of the krypton band, we have the value $\phi_{1z}$ at the temperature $T_z$ giving

$$\frac{1}{\phi_{1z}} = \frac{1}{\phi_1^0} + \frac{B_1 H_1}{FC_1} \tag{57}$$

The more strongly adsorbed xenon band (subscript 2) finds the column already at the temperature $T_z$. For its maximum, we have therefore (see EQUATION 56)

$$\frac{1}{\bar{\phi}_2} = \frac{1}{\phi_{2z}} + \frac{B_2 H_2}{2FC_2} \tag{58}$$

$\phi_{1z}$ and $\phi_{2z}$ are related by the isochores

$$\ln \phi_{1z} = A_1 - B_1 T_z \tag{59a}$$

$$\ln \phi_{2z} = A_2 - B_2 T_z \tag{59b}$$

leading to

$$B_2 \ln \phi_{1z} - B_1 \ln \phi_{2z} = A_1 B_2 - A_2 B_1 \tag{60}$$

The EQUATIONS 55 to 60 permit elimination of all the $\phi$-values except $\phi_1^0$ which is known.

$$\frac{\dfrac{1}{\phi_1^0} + \dfrac{B_1 H_1}{C_1 F}}{\left(\dfrac{1}{\phi_1^0} + \dfrac{B_1 H_1}{2C_1 F} - \dfrac{B_2 H_2}{2C_2 F}\right)^{B_1/B_2}} = \exp\left(\frac{A_2 B_1}{B_2} - A_1\right) \tag{61}$$

With the previously given figures at 25° C. for $A$, $B$, and $C$, EQUATION 61 indicates that a complete separation will no longer occur when $(H_1 + H_2)/F > 8$ joules/cc. of gas. By increasing the gas flow rate through the column in an appropriate manner, it should generally be possible to remain well below this limit. To give an extreme example; if one were to deal with a Kr-Xe mixture of million Mev.-curies of $\beta$-activity ($\simeq$6 kw. of $\beta$-radiation), it would be necessary to operate the column with a gas flow of considerably more than $\frac{3}{4}$ l./sec. With the much smaller activities likely to be involved in practice, the beneficial effect of band sharpening can be made to outweigh considerably the reduction of the separation factor caused by the higher temperature at which the following band must be adsorbed.

## SUMMARY

The behavior of highly radioactive gases in adsorption tubes differs materially from that of other adsorbates. First, heat is generated locally in the adsorption tube by the absorption of radiation (chiefly $\beta$-rays) by the adsorbent. This results in a rise of the temperature of the adsorbent, causing both radial and longitudinal variations of the adsorption coefficients. Second, if the radioactivity is short-lived, the heat development and the temperature effects decrease as the gas travels along the adsorption tube. On first thought, such conditions might appear too complex for a theoretical treatment. In fact, however, comparatively simple, explicit solutions are obtained for gas adsorbed with a linear isotherm.

The following problems, which are of practical interest for a number of reactor types, have been treated.

(1) The breakthrough volumes and times through externally cooled columns of adsorption charcoal under constant feed conditions, the radial temperature distributions, and the heat to be removed at different points along the column have been studied for: (*a*) one radioactive species of one chemical type (Kr or Xe); (*b*) a mixture of radioactive species of one chemical type (Kr or Xe); (*c*) a mixture of radioactive species of two chemical types (Kr and Xe).

An estimate is also made of the channeling effects arising from the higher temperature (and lower adsorbing power) in the central regions of the adsorption tubes, and these factors determine the maximum tube diameters that can be tolerated.

(2) The elution of a finite band of radioactive gas through a thermally insulated chromatographic column is discussed in detail. Here, as a result of the temperature rise occurring in the adsorbent of the column during the passage of a highly radioactive band, the rear end of the band travels in a region of lowered adsorption coefficient and, consequently, tends to move faster than the front. This results in a marked contraction of the bands that finally reach a width independent of the original width of the feed band and of the length of the column. This effect is opposite to the behavior of ordinary (inactive) gases in a column.

One of the most useful aspects of this feature is that it affords a simple means of concentrating dilute radioactive gases into small volumes, without the need for refrigeration, provided that the total radioactive power is in the multiwatt range.

Explicit expressions are derived for the breakthrough volume, the shape of the elution curve, the peak maximum, and the mean band width under steady-

state conditions, as well as for the volume of column required to attain the steady state.

Finally, the effect of radioactive heating on the separation into isolated bands of the fission gases krypton and xenon is discussed. It is shown that as long as the radioactive power of the adsorbed gases is moderate, separation is slightly more efficient, due to band contraction, although the separation of the peak maxima is less. However, for higher radioactive power the latter effect gains in importance and, when the ratio of power to gas flow rate approaches a value of 8 joules/cc. of gas, separation is no longer possible for these gases.

## REFERENCES

1. GLUECKAUF, E. 1955. Theory of chromatography. IX. The "theoretical plate" concept in column separations. Trans. Faraday Soc. **51:** 34–44.
2. DE VAULT, D. 1943. Theory of chromatography. J. Am. Chem. Soc. **65:** 532–540.
3. GLUECKAUF, E. 1946. Contributions to the theory of chromatography. I. Proc. Roy. Soc. London. **A186:** 35–37.

## APPENDIX

### *Section 1 ($\bar{c}$ and $\bar{\phi}$) Steady State*

It is a mathematical axiom that

$$\left(\frac{\partial y}{\partial x}\right)_v = -\left(\frac{\partial y}{\partial v}\right)_x \cdot \left(\frac{\partial v}{\partial x}\right)_y \tag{A0}$$

Thus (from EQUATION 41)

$$\left(\frac{\partial y}{\partial x}\right)_v = -\bar{\phi}\cdot\left(\frac{\partial y}{\partial v}\right)_x \tag{A1}$$

where $y$ may be $c$, $T$ or $\phi$.

Therefore by replacing $\partial x$ in EQUATION 38 by $-\delta v/\bar{\phi}$, we obtain

$$\bar{\phi}\frac{\partial c}{\partial v} - \frac{\partial \phi c}{\partial v} + K_1\bar{\phi}^2\frac{\partial^2 c}{\partial v^2} = 0 \tag{A2}$$

and integrating with respect to $v$:

$$c\bar{\phi} - c\phi + K_1\bar{\phi}^2\cdot\frac{dc}{dv} = 0 \tag{A3}$$

Making the same substitution in EQUATION 39 we obtain

$$\left(\frac{\partial T}{\partial v}\right)_x = \frac{s\phi c}{F(C - C_p\bar{\phi})} \tag{A4}$$

Eliminating $T$ in EQUATION A4 by means of EQUATION 1

$$c = -\frac{F(C - C_p\bar{\phi})}{Bs}\cdot\frac{d\phi}{\phi^2\,dv} = -p\cdot\frac{d\phi}{\phi^2\,dv} \tag{A5}$$

One can now partly eliminate $c$ in EQUATION A3, which becomes

$$\bar{\phi}\frac{d(1/\phi)}{dv} + \frac{d\ln\phi}{dv} + \frac{K_1\bar{\phi}^2}{p}\cdot\frac{dc}{dv} = 0 \tag{A6}$$

Integrating with respect to $v$

$$\frac{\bar{\phi}}{\phi} + \ln\phi + \frac{K_1}{p}\bar{\phi}^2 c - K_2 = 0 \tag{A7}$$

The values of $\bar{\phi}$ and of the integration constant $K_2$ can now be obtained by applying the boundary conditions:

$$\phi = \phi_0 \quad \text{when} \quad c = 0 \qquad (v = -\infty)$$

$$\phi = \phi_\infty \quad \text{when} \quad c = 0 \qquad (v = +\infty)$$

where $\phi_\infty$ follows from EQUATION A5

$$\frac{1}{\phi_\infty} - \frac{1}{\phi_0} = \frac{1}{p}\int_{-\infty}^{+\infty} c\,dv = \frac{c_0 v_0}{p} \quad \text{or} \quad \frac{H}{sp} \quad \text{or} \quad \frac{b}{\phi_0} \tag{A8}$$

where $c_0v_0$ is the total amount of adsorbate in the band. This gives

$$\bar{\phi} = \frac{\ln \phi_0/\phi_\infty}{\dfrac{1}{\phi_\infty} - \dfrac{1}{\phi_0}} = \frac{ps}{H}\ln\left(1 + \frac{H\phi_0}{sp}\right) \tag{A9}$$

Replacing $p$ (see EQUATION A5), we obtain

$$\frac{\bar{\phi}}{\phi_0} = \frac{1}{b}\ln(1+b) \tag{A10 = 42}$$

where $b$ is defined by EQUATION 43, and similarly

$$K_2 = \ln\phi_0 + \frac{1}{b}\ln(1+b) \tag{A11}$$

EQUATION A7 now gives directly the value of $\bar{c}$, that is, the maximum peak height by putting $\phi = \bar{\phi}$. This gives

$$\bar{c} = \frac{p}{K_1\phi_0^2}\cdot\frac{\dfrac{1}{b}\ln(1+b) - \ln\left[\dfrac{1}{b}\ln(1+b)\right] - 1}{\left[\dfrac{1}{b}\ln(1+b)\right]^2} = \frac{p}{K_1\phi_0^2}\cdot Q \tag{A12}$$

This complicated quotient $Q$ can be expanded into a series

$$\frac{b^2}{8}\left(1 - \frac{b^2}{72} - \cdots\right)$$

but in fact, the value $b^2/8$ is not only fully adequate, but covers a wider range of $b$ (see TABLE A1) than the expansion.

TABLE APPENDIX 1

| $b$ | 0.1 | 0.25 | 0.5 | 1 | 3 | 5 | 10 |
|---|---|---|---|---|---|---|---|
| $Q$ | 0.00125 | 0.00780 | 0.0312 | 0.124 | 1.098 | 3.00 | 11.6 |
| $b^2/8$ | 0.00125 | 0.00782 | 0.0313 | 0.125 | 1.125 | 3.12 | 12.5 |

Thus we can write instead of EQUATION A12

$$\bar{c} = \frac{pb^2}{8K_1\phi_0^2} = \frac{BH^2}{8K_1 sF(C - C_p\bar{\phi})} \qquad \text{(A13 = 44)}$$

Although EQUATION A7 defines the relation between $c$ and $\phi$, and together with EQUATION A5 the relation between $\phi$ and $v$, it is not possible to obtain an explicit expression for the elution curve ($c$–$v$ relation). In order to obtain this, an approximation has to be introduced, which limits the solution to small values of $b$.

### *Section 2 (Shape of Band)* *Steady State*

Equation A5 in its integrated form reads

$$\phi = \phi_0\left(1 + \frac{\phi_0}{p}\int_{-\infty}^{v} c\,dv\right)^{-1} \qquad \text{(A14)}$$

The integral term reaches, for $v = \infty$, a maximum value of $b$, when $\phi = \phi_\infty$.

When $b \ll 1$, one can write for EQUATION A14 with good approximation:

$$\phi = \phi_0\left(1 - \frac{\phi_0}{p}\int_{-\infty}^{v} c\,dv\right) \qquad \text{(A15)}$$

which gives

$$c = -\frac{p}{\phi_0^2}\left(\frac{\partial\phi}{\partial v}\right)_x \qquad \text{(A16)}$$

(compare EQUATION A5). Substituting $c$ from A16 into A3 and integrating with respect to $v$ gives

$$\frac{1}{\phi_0^2}\left(\frac{\phi^2}{2} - \phi\bar{\phi}\right) + \frac{K_1}{p}\bar{\phi}^2 c - K_3 = 0 \qquad \text{(A17)}$$

(compare EQUATION A7), and applying the boundary conditions in the same manner as before, gives

$$\bar{\phi} = \frac{\phi_0 + \phi_\infty}{2} \qquad \text{(A18)}$$

(compare EQUATION A9). EQUATION A15, applied to $v = \infty$, gives

$$\frac{\phi_\infty}{\phi_0} = 1 - b \qquad \text{(A19)}$$

(compare EQUATION A8). Whence it follows that

$$\frac{\bar{\phi}}{\phi_0} = 1 - b/2 \qquad \text{(A20)}$$

(compare EQUATION A10). In the same way

$$K_3 = -\tfrac{1}{2}(1 - b) \qquad \text{(A21)}$$

It follows then from EQUATION A17 for $c = \bar{c}$, $\phi = \bar{\phi}$ that

$$\bar{c} = \frac{p}{8K_1\phi_0^2}\,\frac{b^2}{(1 - b/2)^2} \qquad \text{(A22)}$$

(compare EQUATION A13). In order to obtain the desired $c$–$v$ relation, we differentiate EQUATION A3 in the form

$$\bar{\phi} - \phi + K_1\bar{\phi}^2 \frac{d \ln c}{dv} = 0 \tag{A3}$$

with respect to $v$:

$$K_1\bar{\phi}^2 \frac{d^2 \ln c}{dv^2} = \frac{d\phi}{dv} \tag{A23}$$

Replacing $d\phi/dv$ from EQUATION A16 then gives

$$\frac{d^2 \ln c}{dv^2} = -\frac{\phi_0^2}{K_1 p\bar{\phi}^2}\cdot c \tag{A24}$$

Bearing in mind that at the peak $c = \bar{c}$ and $(dc/dv)_{\bar{c}} = 0$, we obtain with the first integration of EQUATION A24

$$\pm\frac{d \ln c}{dv} = \frac{\phi_0}{\bar{\phi}} \sqrt{\frac{2}{K_1 p}}\cdot\sqrt{\bar{c} - c} \tag{A25}$$

and the final integration gives EQUATIONS 45$a$ and $b$ in the text, with

$$\eta = \frac{b}{2K_1\phi_0(1 - b/2)^2}$$

Inspection of A22 and A13 shows that the approximation made in A15 has led to the appearance of the term $(1 - b/2)^2$. Although EQUATION 45 is still an approximation, it is clearly a better approximation if this term is deleted in both $\bar{c}$ and $\eta$ (see EQUATION 45$c$). The two parameters must be changed together as the area under the elution curve, which has the value $H/s = 4\bar{c}/\eta$, must remain unchanged.

### *Section 3 (Contraction of Wide Band)*

The system is described by EQUATIONS 1, 39, 40$a$, $b$, $c$, and 50. These conditions imply that the front of the band where no temperature change has been taking place moves, as in normal chromatography, at the rate

$$\left(\frac{\partial x}{\partial v}\right)_{\phi=\phi_0} = \frac{1}{\phi_0} \tag{A26}$$

which represents the combination of EQUATIONS 39 and 50, and can be considered as a boundary condition.

Eliminating $T$ in EQUATION 39 with EQUATION 1 we have

$$\phi c = -\frac{C_pF}{Bs}\left(\frac{\partial \ln \phi}{\partial x}\right)_v - \frac{CF}{Bs}\left(\frac{\partial \ln \phi}{\partial v}\right)_x \tag{A27}$$

Applying EQUATION A0

$$\phi c = -\frac{F}{Bs}\left[C - C_p\left(\frac{\partial v}{\partial x}\right)_\phi\right]\frac{\partial \ln \phi}{\partial v} = -z\cdot\frac{\partial \ln \phi}{\partial v} \tag{A28}$$

hence

$$c = z \cdot \frac{\partial(1/\phi)}{\partial v} \tag{A29}$$

where $z$ generally $\neq 0$. Eliminating, with EQUATIONS A28 and A29, $c$ and $c\phi$ in EQUATION 50 one obtains

$$-\frac{\partial^2(1/\phi)}{\partial v\,\partial x} + \frac{\partial^2 \ln \phi}{\partial v^2} = 0 \tag{A30}$$

Integrating with respect to $v$ at constant $x$

$$\frac{\partial \phi}{\partial x} + \phi \frac{d\phi}{\partial v} = \phi^2 f(x) \tag{A31}$$

Employing once more EQUATION A0 to eliminate $\partial\phi/\partial v$

$$\frac{\partial \phi}{\partial x}\left[1 - \phi \frac{dx}{dv}\right]_\phi = \phi^2 f(x) \tag{A31}$$

It follows from EQUATION A26 that, for $\phi = \phi_0$, the square bracket has the value zero. As, within the radioactive band,

$$\frac{\partial \phi}{\partial x} \neq \infty$$

it follows that $f(x) = 0$. Hence quite generally

$$\left(\frac{\partial x}{\partial v}\right)_\phi = \frac{1}{\phi} \tag{A32}$$

EQUATION A29 now becomes

$$c = \frac{FC}{Bs}\left(\frac{\partial 1/\phi}{\partial v} + \frac{C_p}{C} \cdot \frac{\partial \ln \phi}{\partial v}\right)_x \tag{A33}$$

We can integrate EQUATION A33 for the point $x = 0$, where $c = c_0$ (see EQUATION 40*b*), and obtain

$$(v)_{x=0} = \frac{FC}{Bsc_0}\left[\frac{1}{\phi} - \frac{1}{\phi_0} + \frac{C_p}{C} \ln \frac{\phi}{\phi_0}\right] \tag{A34}$$

using EQUATION 40*a* as boundary condition for the integration.

We now integrate EQUATION A32, using EQUATION A34 as boundary condition and obtain

$$v = \phi x + \frac{FC}{Bsc_0}\left[\frac{1}{\phi} - \frac{1}{\phi_0} + \frac{C_p}{C} \ln \frac{\phi}{\phi_0}\right] \tag{A35}$$

which is the general equation relating $v$, $x$ and $\phi$ in the column. Knowing the distribution of $\phi$, we can obtain $c$ from A33.

In order to obtain explicit functions for $c$, we introduce the approximation

$$\ln \frac{\phi}{\phi_0} \simeq -\bar{\phi}\left(\frac{1}{\phi} - \frac{1}{\phi_0}\right) \tag{A36}$$

which is valid to the same degree as the approximation made earlier for EQUATION A15.

This gives

$$v = \phi x + \frac{F(C - C_p\bar{\phi})}{Bsc_0}\left(\frac{1}{\phi} - \frac{1}{\phi_0}\right) \tag{A37}$$

As

$$sc_0v_0 = H \quad \text{and} \quad \frac{BH\phi_0}{F(C - C_p\bar{\phi})} = b$$

(see EQUATION 43), EQUATION A37 becomes

$$v = \phi x + \frac{v_0}{b}\left(\frac{\phi_0}{\phi} - 1\right) \tag{A37a}$$

and EQUATION A33 becomes (with the same approximation)

$$\frac{c}{c_0} = \frac{v_0\phi_0}{b}\cdot\left(\frac{\partial^1/\phi}{\partial v}\right)_x \tag{A33a}$$

Solving EQUATION A37*a* for $1/\phi$ and eliminating $\phi$ in EQUATION A33*a* gives

$$\frac{c}{c_0} = \frac{1}{2}\left[1 + \left(1 - \frac{4bxv_0\phi_0}{(bv + v_0)^2}\right)^{-\frac{1}{2}}\right] \tag{A38}$$

and the local concentration in the column is

$$c\phi = c_0\phi_0\left[\left(1 + \frac{bv}{v_0}\right)^2 - \frac{4bx\phi_0}{v_0}\right]^{-\frac{1}{2}}. \tag{A39}$$

The front of the band (see EQUATION A26) is found at

$$x = \frac{v}{\phi_0} \tag{A40}$$

Hence, the concentration at the front,

$$(c)_f = c_0\left(1 - \frac{bv}{v_0}\right)^{-1} \tag{A41}$$

One can see from EQUATION A41 that the concentration becomes infinite when

$$v = v^* = \frac{v_0}{b} \tag{A42}$$

at a point in the column given by

$$x = x^* = \frac{v_0}{b\phi_0} \tag{A43}$$

Beyond this value of $v = v^*$ some discontinuity occurs in the rate of movement of the front.

That this should be so is clear from the fact that up to this value the front has moved at a constant value of $dx_f/dv = 1/\phi_o$, while the band in its final shape moves at the constant rate of $dx/dv = 1/\bar{\phi}$ (see EQUATION 41).

The point where the band has closed up completely ($v_{ss}$, $x_{ss}$) is of some interest because it determines the breakthrough volume of an originally wide band as well as the minimum of column volume required to attain the steady-state conditions.

As a good approximation, we may assume that between the points $x^*$ and $x_{ss}$, the front moves with the mean value of the rate at either end, that is, for $x^* < x < x_{ss}$,

$$\frac{dx_f}{dv} = \frac{1}{2}\left(\frac{1}{\phi_0} + \frac{1}{\bar{\phi}}\right) \tag{A44}$$

This gives

$$x_f = x^* + \frac{(v - v^*)}{2}\left(\frac{1}{\phi_0} + \frac{1}{\bar{\phi}}\right) \tag{A45}$$

If the feed ($c = c_o$ at $x = 0$) is discontinued after $v = v_o$, the rear end of the band will move away from the top of the column at the rate

$$\left(\frac{dx}{dv}\right)_r = \frac{1}{\phi_{x=0,\,v=v_0}} = \frac{1}{\phi_\infty} = \frac{1 + b}{\phi_0} \tag{A46}$$

(see EQUATION A8), and so will proceed along the column according to

$$x_r = (v - v_0)\,\frac{(1 + b)}{\phi_0} \tag{A47}$$

The band reaches infinitely small thickness (corresponding to the steady state when diffusion takes place) when $x_r$ catches up with $x_f$, which occurs at a value $v = v_{ss}$.

Equating A45 and A47 and replacing $\phi_o/\bar{\phi}$ by $b/[\ln(1 + b)] = 1 + b/2 - b^2/12 + b^3/24$ (see EQUATION 42) leads to

$$v_{ss} = v_0\left(\frac{1}{b} + \frac{4}{3} - \frac{2}{27}\,b \cdots\right) \tag{A47a}$$

and

$$x_{ss} = \frac{v_0}{\phi_0}\left(\frac{1}{b} + \frac{4}{3} + \frac{7}{27}\,b \cdots\right) \tag{A48}$$

which can be written also in the form

$$x_{ss} = \frac{1}{\bar{\phi}}\left(v_{ss} - \frac{v_0}{2}\right) \tag{A49}$$

As all further movement, after the steady state has been reached, proceeds according to

$$\frac{dx}{dv} = \frac{1}{\bar{\phi}} \tag{41}$$

It follows that for any column length $X$ and any feed volume $v_o$, we have the breakthrough volume

$$V_B = X\bar{\phi} + v_o/2 \tag{A50}$$

# THE DEVELOPMENT OF HIGHLY EFFICIENT GAS-LIQUID CHROMATOGRAPHIC COLUMNS

J. H. Purnell

*Department of Physical Chemistry, Cambridge University, Cambridge, England*

The separation attainable with a gas-liquid chromatographic (GLC) column depends primarily upon the solvent efficiency, that is, the ratio of the partition coefficients of the substances to be separated. This ratio determines the relative position of the peaks, but clearly, no matter how great the separation of the peaks, it is essential that they should not overlap. The factor that primarily determines whether this occurs is the column efficiency, the magnitude of which is reflected in the sharpness of the eluted bands. Acceptable solvent efficiencies have been obtained so readily in practice that the major effort in GLC has been expended in the study of the characteristics of various involatile solvents; by comparison, relatively little effort has been devoted to the study of the factors contributing to column efficiency. Although column efficiency is dependent to some extent upon the partition coefficients concerned, the solvent and column efficiencies can most profitably be considered separately. The work reported in this paper constitutes a study of some factors, the understanding of which leads to improvement in GLC column performance.

All the processes contributing to band spreading in a column can be regarded as some form of diffusion, but an exact mathematical solution of the diffusion equations concerned is extremely difficult. If certain simplifying assumptions are made, the treatment becomes much easier and, by assuming that only eddy diffusion and molecular diffusion in the gas and liquid phases are of importance, van Deemter *et al.*[1] have obtained an expression for the column efficiency in terms of the theoretical plate height $H$, which can be written

$$H = A + B/u + Cu \tag{1}$$

$A$, $B$, and $C$ are constants relating, respectively, to the characteristics of the column packing, the diffusivity in the gas phase, and the diffusivity in solution; $u$ represents the average carrier-gas velocity. Recently, Bohemen and Purnell[2] have suggested that the eddy diffusion is inversely dependent on the gas velocity and have obtained experimental evidence in support of this view which, in mathematical terms, can be written

$$H = (A + B)/u + Cu \tag{2}$$

In either event, a plot of $H$ against $u$ should be hyperbolic in form with minimum values of $H$ and $u$ given by

$$H_{\text{min.}} = A + 2(BC)^{1/2}, \qquad u_{\text{min.}} = (B/C)^{1/2} \qquad \text{EQUATION 1}$$

or,

$$H_{\text{min.}} = 2[C(A + B)]^{1/2}, \qquad u_{\text{min.}} = [(A + B)/C]^{1/2} \qquad \text{EQUATION 2}$$

There is now no doubt that the general form of the plots of $H$ against $u$ is hyperbolic and this lends weight to the view that the form of the equations is correct. If this is accepted, it immediately follows that there is a particular velocity at which any column, however efficient, should be operated if the maximum efficiency is to be attained, and that any attempt to improve column performance is best carried out after consideration of the equations.

The magnitude of the constants $A$ and $C$ is determined, either wholly or partially, by the characteristics of the column itself; $B$ is determined only by the experimental conditions. It should be borne in mind that in addition to reducing $H$ a desirable end is an increase in $u_{\text{min.}}$ since rapidity of analysis is thereby facilitated. If we consider the ratio $(H/u)_{\text{min.}}$ we see from EQUATION 2 that

$$(H/u)_{\text{min.}} = 2C[(A + B)/(A + B)]^{1/2} = 2C$$

Therefore the most effective way of decreasing the ratio is by reduction of $C$, since this has the effect of increasing $u_{\text{min.}}$. It is important, however, that any steps taken in this direction do not affect adversely the value of $A$.

Consider the means of reducing $A$ and $C$. According to van Deemter *et al.*,[1] $A = 2\lambda d_p$, $\lambda$ being a constant and $d_p$ the support solid particle diameter. In principle, therefore, $A$ and thus $H$ should be reduced by use of particles of very small diameter and, intuitively, one would suppose that the use of very uniform particle size would minimize $\lambda$. Keulemans and Kwantes,[3] however, reported that $A$ passes through a minimum at about $d_p = 0.3$ mm., and they suggested that the most suitable support for GLC was a 50 to 80 mesh range, a suggestion that seems to have been widely accepted. If this is true, it is a finding of great significance since calculation shows that the minimum $A$ is about 1 mm.; this must represent the minimum value of $H$ attainable, even if $B$ and $C$ are zero. A study of the effect of particle size and size distribution on the efficiency is thus an important one.

The constant $C$ is identified by van Deemter *et al.*[1] by the equation

$$C = \frac{8FK}{\pi^2(1 + FK)^2} \cdot \frac{d_f^2}{D_1}$$

$F$ being the ratio of solvent to free gas volume, $K$ the partition coefficient $(c_{\text{liq.}}/c_{\text{gas}})$, $d_f$ the effective film thickness, and $D_1$ the interdiffusion coefficient of the solute in solution. Whether or not this detailed interpretation survives the test of experiment has yet to be established; nevertheless, it is likely to give at least qualitative guidance in our attempts to reduce the value of $C$.

If $K$ is greater than about 20, $C \propto d_f/KD_1$ since both $F$ and $d_f$ are functions of the solvent weight, provided a uniform distribution can be achieved from column to column. Since we can expect $d_f$ to be at least approximately linearly dependent on $d_p$, the value of $C$ should be reduced either by use of fine particles of support or by reducing the amount of solvent used in the column. In the same way, any method of increasing the product $KD$ will lead to higher efficiencies.

A further consideration in this connection that is not implicit in the equations given previously is the question of the effect of solute load. Van Deemter *et al.*[1] have shown that, provided the feed volume in which the solutes enter the column is less than $KV_s/2N^{1/2}$ in which $V_s$ represents the volume of solvent in the column, solute load has no effect on the plate height. On the other hand, the theory assumes a linear partition isotherm; that is, the partition coefficient is independent of concentration, but that this is not necessarily so in the early stages of an elution can be calculated readily. Suppose that 0.1 ml. of a gaseous solute ($4 \times 10^{-6}$ moles) is introduced wholly into the first plate of a 1-m. column of 1000 plates. Such a column, composed of packing containing 20 per cent by weight of solvent, contains about 2 gm. solvent/meter if the tube diameter is about 5 mm. Thus, we have 2 mg. of solvent/plate and, if the molecular weight is 400, this corresponds to $5 \times 10^{-6}$ moles. The solute concentration in the plate is thus about 45 moles per cent. Linearity of the isotherm can be expected only for ideal solutions at this concentration, and it must be expected that mixed solutes will interact also. In consequence of these views it is not surprising that a marked concentration dependence of $H$ has been observed by most workers even though, in practice, injection into a single plate is never achieved. Even so, amounts up to 100 times that used in the calculation are conventionally employed; therefore the concentrations will correspond to those quoted, even if injection corresponds to spreading over 100 plates.

The following experimental results will show to what extent the views outlined are borne out in practice; auxiliary measures necessary to the realization of high efficiencies are considered also.

### *Experimental*

The apparatus and procedures employed differed little from the conventional. Columns were constructed in glass, the support material used throughout being Sil-O-Cel* firebrick. Fractions of this were sieved to size and further graded by sedimentation in water, after which they were dried intensively. The solvent was introduced by deposition from acetone or ether solution, the packing then being heated under vacuum to a temperature higher than any used in the subsequent experiments.

Columns were contained in an efficient air thermostat; the carrier gas flow was controlled by a series of needle valves and measured by use of a soap bubble meter situated at the column outlet. Temperature and flow control were sufficiently good to make possible the use of a single-channel, hot-wire katharometer that proved noiseless and driftless when connected with a 1 mv. recorder. Sample injection was made from a micrometer syringe or high pressure capillary and the column preheater was maintained at 50° C. above the boiling point of the highest boiling liquid eluted. Except when stated to the contrary, the column outlet was maintained at atmospheric pressure.

Four solutes were chosen for study; these were cyclohexane, acetone, benzene and isopropanol, the choice being made on the grounds of the difference in partition coefficients and chemical type. Preliminary experiments showed that as long as the total sample was less than 4 $\mu$l., results obtained with a mixture were the same as with individual solutes. This accelerated the experiments considerably and also facilitated introduction of very small amounts of any solute by dilution in the other.

---

* Product of Johns-Manville Sales Corporation, New York, N. Y.

### *Results*

It is not possible to illustrate all the results obtained, but those presented are representative. FIGURE 1 illustrates plots of $H$ against $u$ for the elution by nitrogen at 47° C. of 0.6 $\mu$l. benzene from 20 per cent by weight polyethylene glycol columns. The values of $H$ were measured with the aid of the equation of Glueckauf[5] and the values of $u$ were averaged by use of the pressure drop correction of James and Martin.[6] The curves are hyperbolic in form, as predicted by theory; the coarser meshed columns yielded pronounced minima. There is an obvious reduction of $H$ with diminishing particle size that continues to the smallest particle size studied. The results illustrate the linear dependence of the constant $C$ on the particle diameter; this is brought out by the data contained in TABLE 1, in particular by the near constancy of the ratio $C$/mean $d_p$. An interesting feature is that, as the particle size is reduced, the high velocity end of the hyperbolas becomes more nearly horizontal. In such circumstances high velocities can be used without loss of efficiency and the duration of analysis proportionately reduced.

The importance of maintaining a close size distribution is well illustrated by the data presented in FIGURE 2. These relate to the elution of 0.5 $\mu$l. acetone by nitrogen at 47° C. from columns containing 20 per cent by weight polyethylene glycol supported by various mixtures of 30 to 40 and 50 to 60 mesh firebrick. Addition of 25 per cent of the finer mesh to the 30 to 40 mesh leads to a marked loss of efficiency and, even at 50 per cent, the efficiency is still

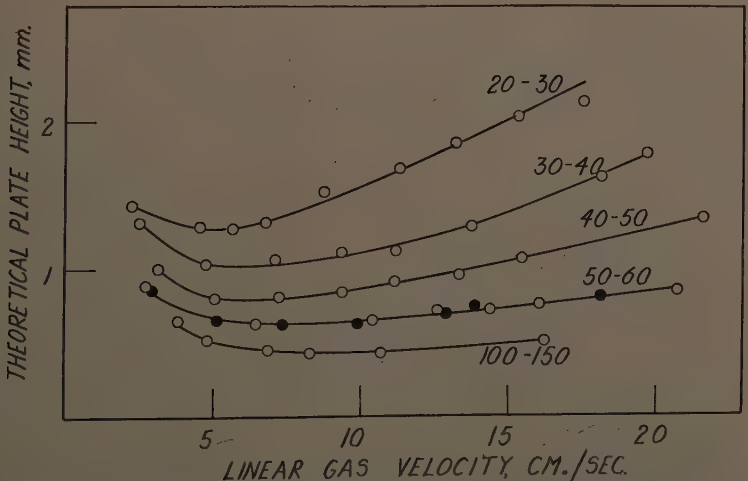

FIGURE 1. Effect of change of particle size on column efficiency. Columns contain 20 per cent polyethylene glycol. Elution data for 0.6 $\mu$l. benzene at 47° C. Carrier gas, nitrogen.

TABLE 1

VALUES OF $B' = A + B$ AND $C$, CALCULATED ACCORDING TO EQUATION 2

Elution of 0.5 μl. Acetone by Nitrogen at 47° C. from Columns Containing 20 per cent by Weight Polyethylene Glycol (M.W. 400) and with Atmospheric Column Outlet Pressure

| Particle size range | $B'$ | $C$ | $10^2\ C/\text{mean}\ d_p$ |
|---|---|---|---|
| 20–30 | 0.360 | 0.0100 | 16.7 |
| 30–40 | 0.304 | 0.0073 | 17.4 |
| 40–50 | 0.290 | 0.0053 | 15.9 |
| 50–60 | 0.278 | 0.0037 | 13.0 |
| 100–150 | 0.220 | 0.0021 | 16.8 |

The constant λ, calculated from particle size dependence of $B'$, is 1.5.

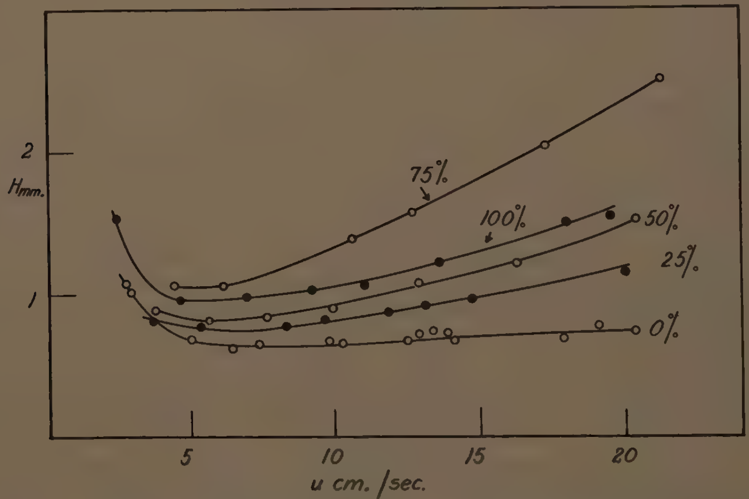

FIGURE 2. Effect of broad size distribution of support material. Elution of 0.5 μl. acetone by nitrogen at 47° C. Columns, 20 per cent polyethylene glycol. Percentage of 30 to 40 mesh in mixture with 50 to 60 mesh is stated on diagram.

less than that of the 30 to 40 column. It is only when the proportion of 50 to 60 mesh rises above about 60 per cent that any improvement is observed. Identical results have been obtained on mixing other sized particles and for ternary mixtures. They show conclusively that the high efficiencies corresponding to small-particle diameters can be achieved only if the spread of sizes is kept small. At this time it appears that the ratio of the largest to the smallest particle diameter within a fraction should not exceed 1.5. It is probable that the anomalous results of Keulemans and Kwantes[3] stemmed from the use of supports of wide size distribution.

The values of the constants $A$, $B$, and $C$, calculated from data similar to those in FIGURES 1 and 2, are more consistent and reasonable in magnitude if they are derived from EQUATION 2, rather than from EQUATION 1. Thus, if calculated from EQUATION 1, $A$ is frequently negative, which is entirely inadmissible, and the corresponding values of $B$ are both too great and vary in

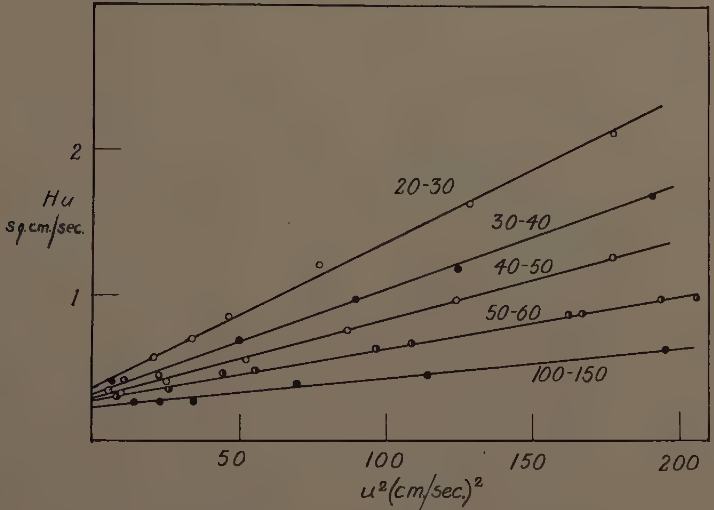

FIGURE 3. Plots of $Hu$ against $u^2$ for elution of 0.5 $\mu$l. acetone. Conditions are as in FIGURE 1.

an erratic manner. According to EQUATION 2, a plot of $Hu$ against $u^2$ should be linear, of slope $C$, and intercept $(A + B)$. FIGURE 3 shows such plots and there is obviously agreement over the whole range of velocities, which both supports EQUATION 2 and makes for convenience in interpolation, accuracy, and ease in calculation of the constants from the experimental data. Evidently, a plot of $H/u$ against $1/u^2$ will be linear also, of slope $(A + B)$, and intercept $C$. This form of plot has also been discussed by Brennan and Kemball.[7] The constants calculated from EQUATION 2 for the experiments with the mixed-mesh size supports are listed in TABLE 2. It is of interest that the consequence of wide size distribution appears to be not only an increase in $A$ but, initially, also in $C$. This somewhat unexpected result may be due to a preferential uptake of solvent by the coarser particles of the mixture that would yield an effectively thicker film. This, however, may not be the whole explanation; the phenomenon merits more detailed study.

TABLE 2

VALUES OF $B' = A + B$ AND $C$, CALCULATED FROM EQUATION 2 FOR THE ELUTION OF 0.5 $\mu$l. ACETONE FROM 20 PER CENT BY WEIGHT POLYETHYLENE GLYCOL COLUMNS

Solid Support, Mixed 30 to 40 and 50 to 60 Mesh Firebrick. Column Outlet Pressure is Atmospheric

| Percentage 30 to 40 mesh in mixture | $B'$ | $C$ |
|---|---|---|
| 100 | 0.304 | 0.0073 |
| 75 | 0.270 | 0.0107 |
| 50 | 0.255 | 0.0066 |
| 25 | 0.250 | 0.0054 |
| 0 | 0.265 | 0.0037 |

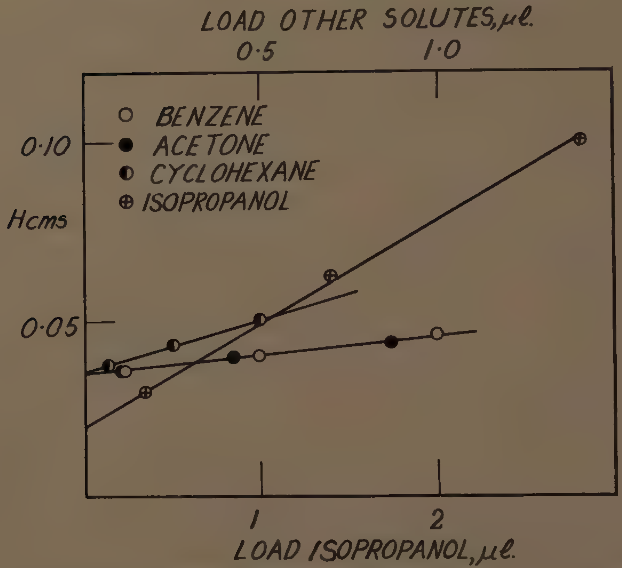

FIGURE 4. Dependence of column efficiency on sample size. Columns contain 20 per cent polyethylene glycol on 100 to 150 mesh Sil-O-Cel.

The variation of $H$ with sample size is depicted in FIGURE 4 and is seen to be reasonably linear over the range studied. The data were obtained during elution from a 20 per cent polyethylene glycol-100 to 150 mesh firebrick column at the optimum velocity. With loads of about 0.5 μl., efficiencies between 800 to 1000 theoretical plates per foot of column ($H \simeq 0.4$ mm.) are obtained. The values extrapolated to zero load ($H_0$) are over 1000 plates per foot for all the solutes, whereas for isopropanol it is about 1500. Due to the insensitivity of the detector the maximum efficiency realized in these experiments was only 1320 plates per foot, and it would require a detector such as the discharge tube to achieve the maximum.

The improvement resulting from a reduction of the weight of solvent contained in the column is illustrated in FIGURE 5, which pertains to the elution of 2 μl. samples of isopropanol. Again, the results suggest a linear relation between $C$ and $d_f$, but they are not particularly reproducible, probably in consequence of the occurrence of adsorption at low coverage and the difficulty of obtaining a uniform distribution of solvent. However, even though no great quantitative value can be placed on the results, it seems safe to say that there is at least no loss of efficiency on reducing the proportion of solvent employed in the column. As little as 1 per cent by weight can be very profitably used, as evidenced by the work of Scott and Cheshire.[4] This, as will be seen later, is a finding of considerable importance.

Changing the product $KD_1$ is illustrated in FIGURE 6, which shows $H$ versus $u$ plots for benzene and cyclohexane eluted from columns of 16 per cent dinonyl phthalate, squalene and polyethylene glycol. The curves for benzene for all three solvents are superimposed, as are those for cyclohexane, for the phthalate

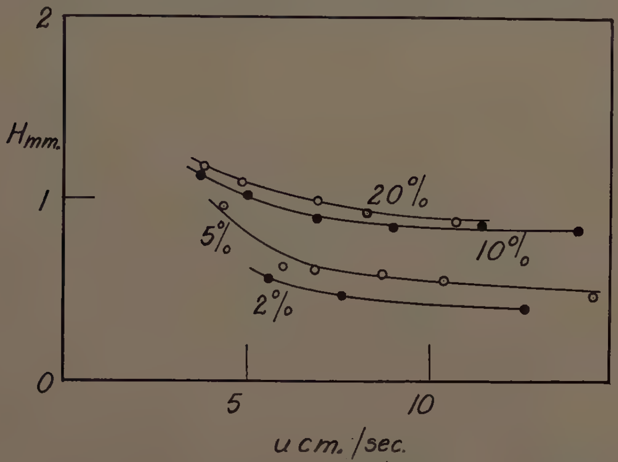

FIGURE 5. Illustration of improvement in column efficiency with reduction of proportion of solvent in column. Conditions are as in FIGURE 1; 2 μl. samples of isopropanol eluted.

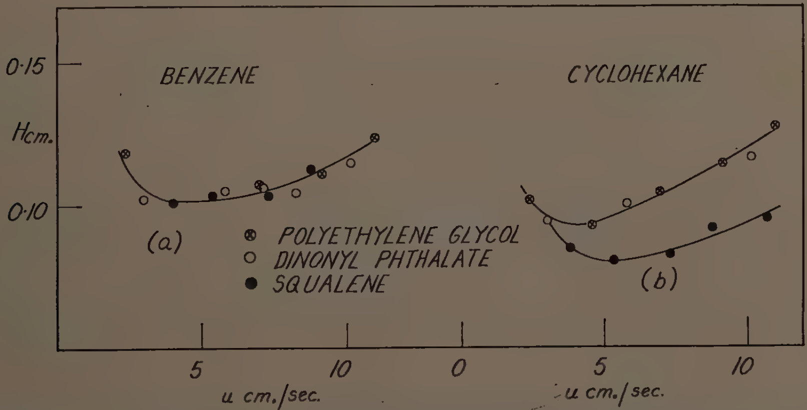

FIGURE 6. Comparison of efficiencies attained for benzene and cyclohexane with various solvents.

and for the glycol. Elution of cyclohexane from squalene yields smaller values of $H$ than when the other two solvents are used. The results obtained with acetone are not presented because, with the glycol, the curve is identical to that for benzene; with the other two solvents the values of $H$ obtained are so large (0.15–0.4 cm.) that they cannot be plotted on the same scale. The peaks are so broad and distorted that these solvents are clearly of little use for analyses involving acetone. These results illustrate the general finding that the product $KD_1$ very frequently is approximately constant for a solute from solvent to solvent or, alternatively, for a series of solutes in a given solvent. This is not unexpected, perhaps, since $K$ in ideal or regular solution may be expected to increase with molecular diameter of the solute, while $D_1$ should decrease at about the same rate.

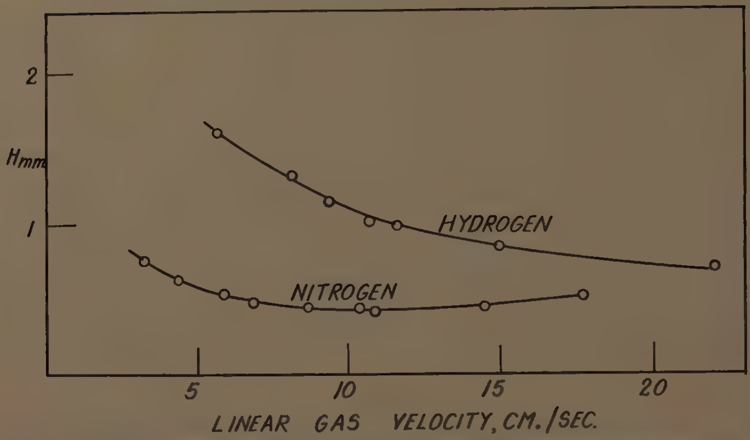

FIGURE 7. Elution curves for 0.15 μl. benzene from 5 per cent polyethylene glycol in 100 to 150 mesh Sil-O-Cel columns. Carrier gases, hydrogen and nitrogen.

There seems to be no doubt that the rate theory has proved very successful in predicting the means of reducing the values of the constants $A$ and $C$. We may now consider how experimental conditions may be adapted to reduce the value of $B$. It can be deduced readily that $B \propto D_g$, $D_g$ being the coefficient of interdiffusion of the solute in the carrier gas. It follows, therefore, that $B$ should be reducible either by use of a carrier gas of large collision cross section or by operation of the column at elevated pressures. A comparison of the relative merits of hydrogen and nitrogen as carrier gases is shown in FIGURE 7. The column containing 5 per cent polyethylene glycol was supported by 100 to 150 mesh firebrick and the elution of 0.15 μl. benzene was carried out, in each case, with a column outlet pressure of 1 atm. The difference between the curves is striking; it is clear that at these pressures the use of hydrogen or helium is justified only if detector sensitivity is thereby improved and the solvent efficiency is considerable.

The remarkable improvement resulting from high pressure operation is shown in FIGURE 8, which compares the elution of 0.5 μl. acetone from a 20 per cent polyethylene glycol-100 to 150 mesh support column with the outlet at 1 and 3 atm. pressure, respectively. The carrier gas is hydrogen and the efficiency corresponding to the higher pressure is comparable to that obtained when nitrogen is used at 1 atm. At both pressures the theoretical plate height continues to decrease up to the maximum velocity employed; therefore it seems that, in general, the faster the elutions in hydrogen are carried out, the better they will be. The effect of increased pressure on nitrogen elution is illustrated in FIGURE 9, which compares the concentration dependence of $H$ for isopropanol at the two pressures. $H_0$ at 1 atm. was found earlier to correspond to about 1500 theoretical plates per foot; at 3 atm. it is about 2000. However, it has not proved possible to realize more than about 1400 plates per foot since, at the higher pressure, the deficiencies of the katharometer are even more marked in consequence of the greater dilution of the sample and the effect

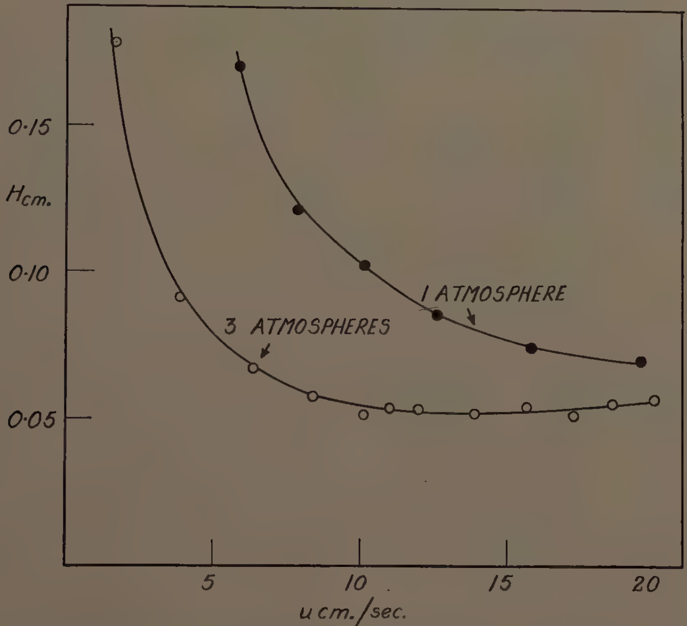

FIGURE 8. Effect of change of column pressure on efficiency. Elution of 0.5 $\mu$l. acetone by hydrogen from 20 per cent polyethylene glycol column at 47° C.

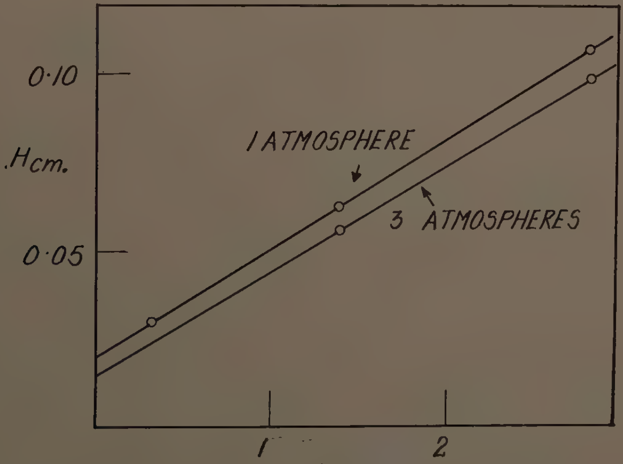

FIGURE 9. Concentration dependence of column efficiency at two pressures. Elution of isopropanol by nitrogen.

of the greater mass flow.[8, 9] The development of such detectors as the discharge tube and flame-ionization gauge are undoubtedly timely, and experiments in progress should help considerably in evaluating their possibilities in connection with the problem of achieving $H_0$ in practice.

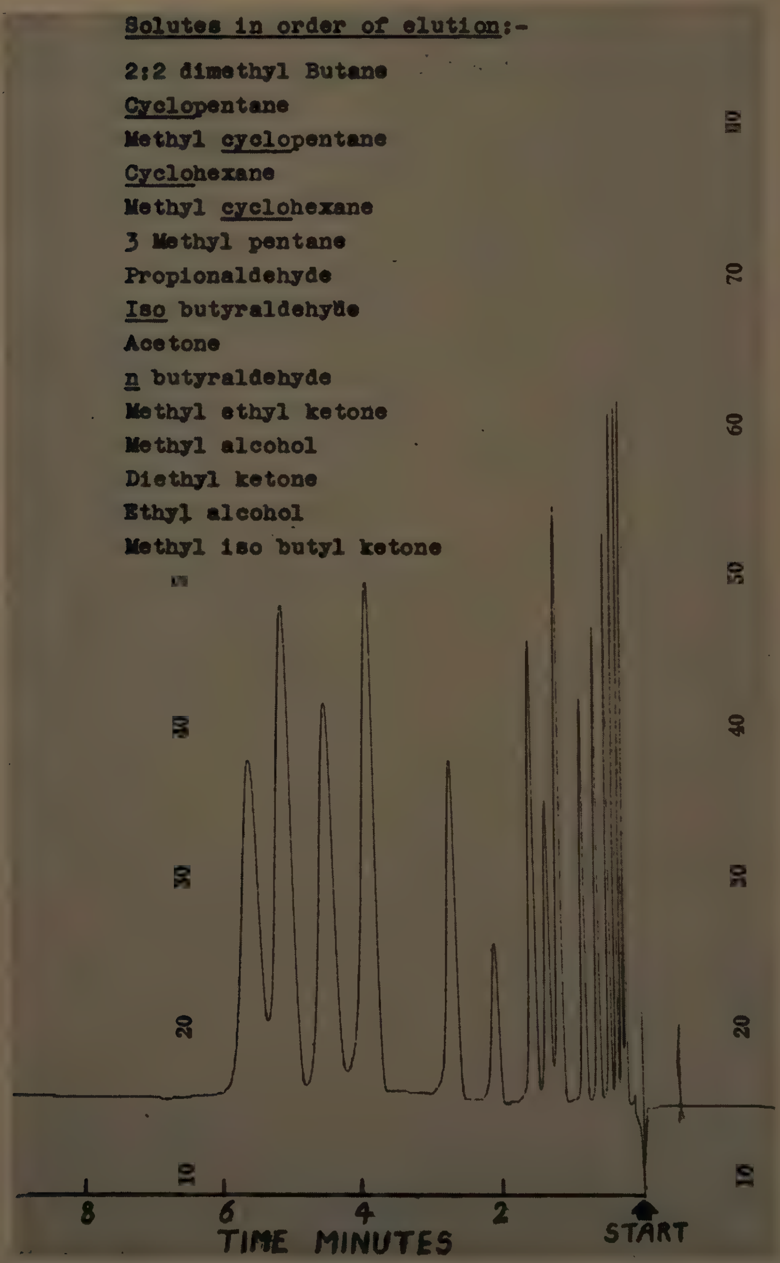

FIGURE 10. Chromatogram of synthetic mixture. Column, 104 cm. by 0.4 cm.; 20 per cent polyethylene glycol on 100 to 150 mesh Sil-O-Cel. Carrier gas, hydrogen; column outlet pressure, 3 atm.

As an illustration of what can easily be attained experimentally, FIGURE 10 reproduces a chromatogram of a synthetic mixture of hydrocarbons, ketones, and alcohols such as might be used in combustion studies. The analysis was carried out at 47° C. with a column 3 ft. long containing 20 per cent of polyethylene glycol supported by 100 to 150 mesh brick, the carrier gas being hydrogen and the column outlet pressure 3 atm. The total time required is only 6 min., but this could have been reduced proportionately by use of leaner columns. The efficiencies for the various solutes vary between about 2200 and 3000 plates.

## *Discussion*

All the experiments described were carried out at a single temperature and it is probable that at some other temperature quite different results would have been obtained. However, it would be coincidental if this work was conducted at the most favorable value; therefore, even higher values of the column efficiency might be possible. It would be anticipated that a lower temperature would lead to improvement, since gaseous diffusion decreases approximately as the square of the reduction of temperature. Although diffusivity in the liquid would be reduced, the increased partition coefficient would probably more than offset this, since its temperature dependence is generally greater than that of diffusion.

The high efficiencies quoted for the columns described here can be considered in another way: namely, in the light of the performance index $P$ proposed by Golay.[10] The index is defined by the equation

$$P = \frac{\Delta t^4 \cdot t_a \cdot \Delta p}{t^3(t - t_a)}$$

$\Delta t$ being the peak half width, $t_a$ the retention time for air, $t$ the retention time for the solute, and $\Delta p$ the pressure drop across the column. According to Golay, the ideal column has $P = 0.8$.

The values of $P$ obtained are typified by those in TABLE 3, which pertains to elution of a standard load from 20 per cent columns, nitrogen being the carrier. Even though these values do not represent, by any means, the lowest attainable values, they are considerably smaller than those calculable from

TABLE 3

PERFORMANCE INDEXES FOR ELUTION BY NITROGEN AT 47° C. OF 0.5 μl. ACETONE FROM COLUMNS LISTED IN TABLE 1

Column Outlet Pressure is Atmospheric

| Particle size range | $P$ |
|---|---|
| 20–30 | 40 |
| 30–40 | 67 |
| 40–50 | 80 |
| 50–60 | 82 |
| 90–100 | 110 |
| 100–150 | 118 |

TABLE 4

CONCENTRATION DEPENDENCE OF PERFORMANCE INDEX

Data for Isopropanol Eluted at 47° C. by Nitrogen from Polyethylene Glycol Supported by 100 to 150 Mesh Brick

| Sample volume μl. liquid | Column outlet, one atmosphere $P$ | Column outlet, three atmospheres $P$ |
|---|---|---|
| 5.6 | 2175 | 1690 |
| 2.8 | 750 | 480 |
| 1.4 | 285 | 157 |
| 0.4 | 60 | 36 |
| $H_0$ | 30 | 15 |

the literature and quoted by Golay. The variation of $P$ with load is shown in TABLE 4, which lists data for elution of isopropanol by nitrogen at 1- and 3-atm. outlet pressure. At the lower pressure, the value of $P$ corresponding to $H_0$ is 30; at the higher pressure it is 15. With further increase in pressure, or any other expedient available for improving the column efficiency, values of $P$ below 10 should not be too difficult to achieve.

The most significant improvement in column efficiency results undoubtedly from the use of very uniform samples of the finest possible size. Next in order of importance are the use of the smallest possible samples for analysis and the use of high column pressures. A necessary consequence of these is the need for detectors that will work satisfactorily with quantities very much less than a microgram; a further experimental point is the question of the means of introduction of such small amounts. Since the operation of columns at high pressures results in a reduced linear velocity for a given volume flow rate, the time of analysis is proportionately lengthened. In addition, the value of $u_{\text{min.}}$ is reduced under these conditions. It is, therefore, a fortunate finding that the use of lean columns is advantageous, since this nullifies the above drawback. Many reasons can be advanced in support of more rapid analyses; among these there are the applications of GLC to plant-process control and the fact that high boiling materials can be eluted at relatively low temperatures. Work in this direction suggests the possibility of the use of solvents in which partition coefficients are very low, separation being chiefly a consequence of the high column efficiency rather than the solvent efficiency. That this is possible is shown in FIGURE 10, in which the five hydrocarbons are separated within 1 min., although their partition coefficients in polyethylene glycol at the column temperature are only of the order of 20. The importance of this for the analysis of high boiling liquids is evident.

The results obtained in this investigation lend considerable support to the general assumptions of the rate theory and leave little doubt that, provided all the necessary requirements are observed, packed columns can be made and operated in such a way as to realize an efficiency close to ideal. At present, conventional columns have efficiencies of 100 to 500 plates/ft., but in the near future we may look forward to very considerable improvements of such magnitude that columns of 20,000 theoretical plates may become commonplace.

### *Acknowledgment*

I am indebted to J. Bohemen for his assistance in these investigations and to Imperial Chemical Industries Ltd., London, England, for the loan of a recorder.

### *References*

1. van Deemter, J. J., F. J. Zuiderweg & A. Klinkenberg. 1956. Chem. Eng. Sci. **5:** 271.
2. Bohemen, J. & J. H. Purnell. 1958. Second Gas Chromatography Symposium Inst. Petroleum. In press.
3. Keulemans, A. I. M. & A. Kwantes. 1956. Vapour Phase Chromatography. : 15. Butterworths. London, England.
4. Scott, R. P. W. & J. D. Cheshire. 1957. Second Informal Symposium of the Gas Chromatography Discussion Group, Cambridge, England.
5. Glueckauf, E. 1955. Trans. Faraday Soc. **51:** 34.
6. James, A. T. & A. J. P. Martin. 1952. Biochem. J. **50:** 679.
7. Brennan, D. & C. Kemball. 1958. J. Inst. Petroleum, **44:** 14.
8. Bohemen, J. & J. H. Purnell. 1957. Chem. Ind. : 815.
9. Bohemen, J. & J. H. Purnell. 1958. J. Appl. Chem. **8:** 433.
10. Golay, M. J. E. 1957. Nature. **180:** 435.

### *Discussion of the Paper*

C. W. Skarstrom (*Esso Research and Engineering Company, Linden, N. J.*): How can the loss of efficiency on going to wide columns be explained?

Purnell: There seems to be no obvious reason why wide columns should lose efficiency other than that they may require more careful packing and load scaling. In fact, I understand that certain workers in the United States have succeeded in scaling up to several inches diameter. I think the main problem is in the injection; it must be remembered that rapid vaporization of, for example, 0.5 gm. of liquid will require considerable heat, and will require it very suddenly. I doubt that conventional column preheaters are capable of this. Vaporization of 1 gm. of water, for example, requires 500 calories, a very large amount for a small electric heater to provide in a few seconds.

# CHROMATOGRAPHY IN THE GAS-SOLID SYSTEM

Jaroslav Janák

*Laboratory for Gas Analysis, Czechoslovak Academy of Sciences, Brno, Czechoslovakia*

The development of gas chromatography is largely the result of efforts made during the last six years. It began with simple experiments with carbon and other materials that showed remarkable sorption capacities for gases.

The first work that led to the development of this method was done in the period 1920 to 1930; it began with the experiments of Berl (1921, 1923, 1924) on the separation of gases by sorption and desorption at low temperatures. These experiments had little in common with today's conception of gas chromatography, but they led to the systematic studies of Peters (1930, 1937), whose work shows a thorough knowledge of the effect of pressure variation on the sorption processes. These studies were the predecessors of displacement chromatography.

The first developments in displacement chromatography utilized increased temperature to effect separation. It was initiated by Eucken and Knick (1936) who treated both the empirical and theoretical aspects of the problem. Contributions were made by Henjes (1938) and by Ferber and Luther (1940). Further progress was realized when Tiselius (1943) introduced a highly adsorbed substance as a displacing agent. These early studies culminated in the mastering of displacement chromatography from both the theoretical (Claeson, 1946, 1949) and methodological points of view (Turner, 1943; Phillips, 1949, 1952; Clough, 1955). In the period 1950 to 1952 this type of gas chromatography was superseded by the more advantageous elution method.

The frontal type of chromatographic analysis (Roth *et al.*, 1942; Claeson, 1946, 1949) was an outgrowth of the earlier work, but it achieved only limited importance.

Schuftan (1930, 1931) introduced the use of a gas as a desorption agent. His work is outstanding in that it shows a close relation to the modern concept of elution gas chromatography. The general theoretical concept of elution chromatography was formulated later in the important work of Martin and Synge (1941).

Until 1940 the experiments in gas chromatography were concerned only with the separation of gases. The papers of Martin and Synge (1941), Hesse (1941), and Damkoehler and Teile (1943) consider the separation of liquids showing sufficient volatility to permit their handling in the vapor phase. Although interrputed by World War II, gas chromatography is rapidly coming of age, as evidenced by the large amount of work being reported. Among the papers relating to gas-solid systems, some outstanding ones are those of Phillips (1949), Turkeltaub (1950), Cremer (1951), Zhukhovitskii and his co-workers (1951), Janák (1953), N. H. Ray (1954), and Patton *et al.* (1955). The reviews by C. G. B. Hammar (1951), Janák (1956), Zhukhovitskii and Turkeltaub (1957), and Cremer and Roselius (1958) list other important papers relating to gas-solid chromatography.

It is generally accepted that gas-solid chromatography is limited in its application to the analysis of gases or easily volatilized compounds. However, it does have considerable technological promise.

Among the more common surface-active substances used in gas-solid chromatography are active charcoal, silica gel, alumina, and various aluminum silicates. The properties of these adsorbents depend upon the size of the sorption-active surface and on its physical and chemical characteristics. The surface area determines the sorption capacity expressed in terms of grams or milliliters of the sorbent. Irregularities in the surface and the internal (crystalline) structure determine the number of sorption centers and their distribution. The chemical makeup of the adsorbent is a major factor in determining its selectivity.

If $K_1$ is Henry's coefficient relating the distribution of the compound in question to the carrier gas and adsorbent, its relation to the adsorption energy (expressed as adsorption heat) will be

$$K_1 = A \cdot e^{(Q_1/R)T} \tag{1}$$

Neglecting the process of inner diffusion, the spread of compound 1 at any point in the column is expressed by the equation:

$$C = C_{\text{max.}} \cdot e^{X^2 K_1/4Dt} \tag{2}$$

in which $X$ is the distance of the point from the peak, $t$ is the time, and $D$ the coefficient of longitudinal diffusion.

The value $K_1$ depends upon the properties of the sorbing agent and the sorbed substance. In a gas-liquid system $K_1$ has a constant value over a wide concentration range. The structure of the conventional adsorbents is such that centers of different adsorption energy exist and the adsorption is not uniform throughout. Therefore $K_1$ is not constant, but varies with the concentration of the adsorbed substance.

### *Shape of the Elution Curve*

When the sample is introduced into the adsorption column and the required active centers are occupied, that section of the column is eliminated from sorption. This is not true only when a minimum volume of sample is introduced; when a larger volume of sample is introduced the elution peak does not start at the inlet, but at a certain distance from it (FIGURE 1). Measurements of the $U_g{}^0$ value (corresponding to the $V_g{}^0$ of gas-liquid chromatography, Janák, 1953*a*, *b*) may be greatly influenced by the sample size, especially in the case of low surface adsorbents. In the calculations the correction for zero volume is even more important than in gas-liquid chromatography.

If one type of adsorption center is involved, Henry's coefficient should not depend upon the molar concentration of the chromatographed substance. When the centers are of different types and of different adsorption energies, Henry's coefficient calculated for the total number of centers should depend upon the molar concentration of the chromatographed substance. A series of equilibrium curves, corresponding to the sorption of individual centers of the

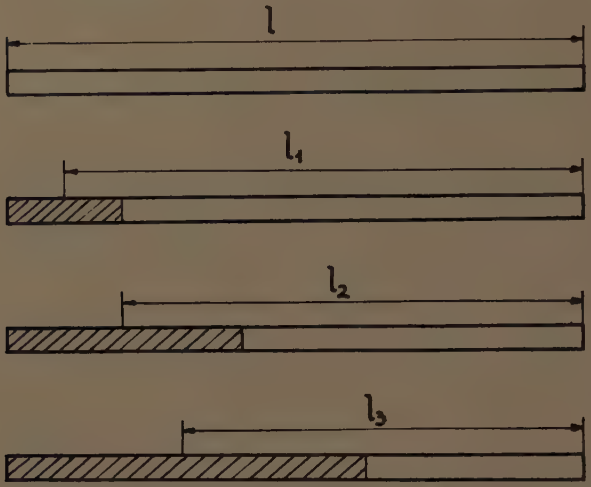

FIGURE 1. Dependence of the elution curve shape and the $U_g^0$ values on the sample size.

same type, can be derived from EQUATION 2. Separation requires that

$$Q' < Q'' < Q'''$$

The resulting elution curve represents the sum of the partial elution curves and shows characteristic tailing (FIGURE 2).

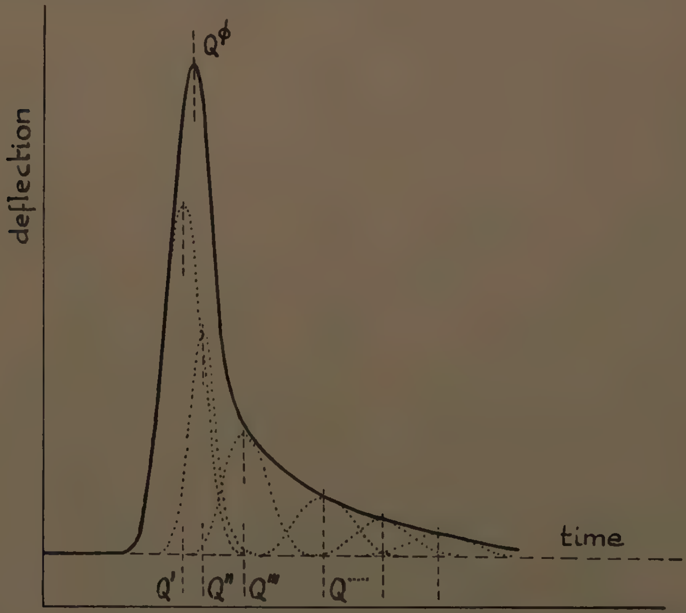

FIGURE 2. Development of the tailing effect in the course of gas-solid chromatography.

TABLE 1

| Carrier gas | $U_g{}^0$ for krypton |
|---|---|
| Hydrogen | 21.2 |
| Helium | 20.8 |
| Argon | 19.2 |
| Nitrogen | 19.0 |
| Methane | 11.4 |
| Carbon dioxide | 7.7 |
| Ammonia | 5.8 |

### *Influence of the Carrier Gas on Elution Curve Shape*

Thus far in this paper it has been assumed that the carrier gas is not adsorbed. If the carrier gas is sorbed and

$$Q_{\text{carrier gas}} > Q_{\text{substance}}$$

the adsorption centers remain blocked for that sorbate. This results in a decrease in the effective surface and in the number and strength of effective centers and, consequently, in a decrease in the $U_g{}^0$ values (TABLE 1) for weakly adsorbed compounds. For those components in which

$$Q_{\text{carrier gas}} < Q_{\text{substance}}$$

all sites will be available and the elution curves of these materials will tail. Those compounds having

$$Q_{\text{carrier gas}} = Q_{\text{substance}}$$

will show a symmetrical elution curve as given by EQUATION 2. A reverse asymmetry of the elution curve is characteristic for those components in which

$$Q_{\text{carrier gas}} > Q_{\text{substance}}$$

These conditions are illustrated in FIGURE 3, which shows the elution curves of He and Ne from active charcoal with hydrogen at −180° C. and the elution curves for $H_2$ and $N_2$ from the same adsorbent using $CO_2$ as the carrier gas.

### *Modification of the Surface and Homogeneous Sorption*

To be suitable for gas-solid chromatography an adsorbent should have only one type of adsorption center. This can be achieved by: (1) preparing solids with the proper lattice (Barrer, 1949; Janák, 1957); (2) blocking the centers that cause the variation in adsorptive forces with a proper liquid (Eggertsen *et al*, 1956; Janák, 1957); (3) blocking the centers with a highly adsorbed carrier gas (Janák, 1953*a*, *b*), for example, gases such as $CO_2$ and $NH_3$ ; and (4) preparing "homogeneous" sorption-active centers on suitable carriers.

The first three methods have been described already. I shall discuss the fourth method by citing some of its practical possibilities. Glueckauf and his co-workers (1949, 1956) reported on the separation of the isotopes of hydrogen by displacement development on palladium black. Glueckauf had chosen

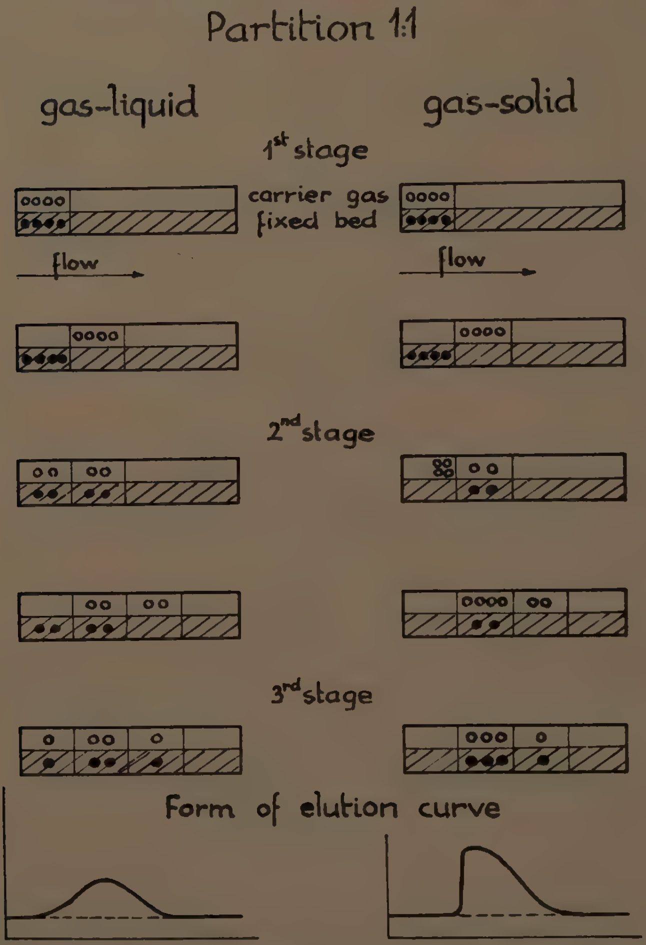

FIGURE 3. Shape of the elution curve in the gas-liquid and gas-solid chromatography systems using a highly sorbed carrier gas.

this procedure since separation by elution was incomplete, probably due to tailing. As a consequence of previously cited considerations, such tailing is the result of a variation in the magnitude of the forces surrounding the hydrogen molecules, brought about by nonuniform distribution of the Pd atoms. If a uniform distribution of palladium atoms is attained, elution development will give symmetrical peaks. This is illustrated in FIGURE 4, which shows a series of curves obtained by chromatographing hydrogen on such a column. The adsorbent was palladium, 0.3 gm. on 20 gm. of Celite. The palladium was added to the Celite as an undissociated organic complex and reduced to metallic palladium at 400° C. The operation was carried out in such a way as to isolate the individual palladium atoms. It should be noted that the elution curves are reasonably symmetrical. If the volume of the hydrogen sample is

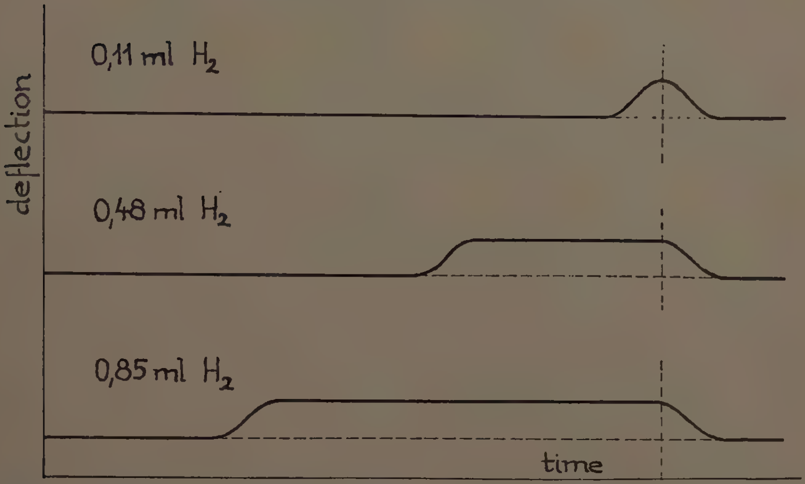

FIGURE 4. Elution curve shape for hydrogen on a carrier containing a low ratio of palladium. Carrier gas, argon. Temperature is 20° C.

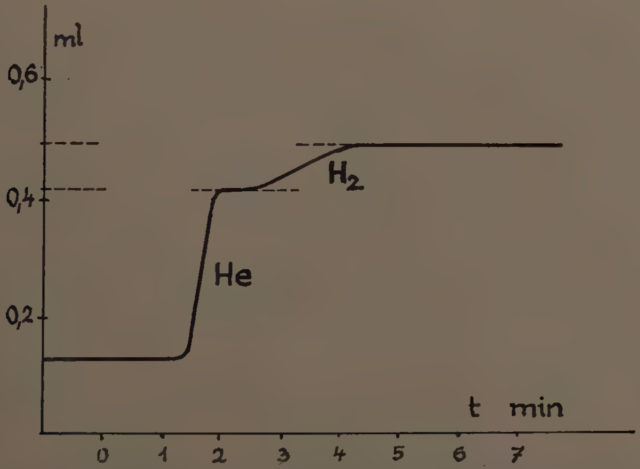

FIGURE 5. Separation of helium and hydrogen on a palladium carrier by elution chromatography. Carrier gas is carbon dioxide; temperature 20° C.; and $U_g^0$ for hydrogen, 380.

increased the column becomes saturated, but there is no asymmetry of the elution curve.

This method has been used (FIGURE 5) for the volume determination of hydrogen and helium in various mixtures. Its potential is such that this approach to the preparation of solid adsorbents warrants further investigation.

## *References*

BARRER, R. M. 1949. Discussions Faraday Soc. **7:** 135.
BERL, E., K. ANDRESS & W. MÜLLER. 1921. Z. angew. Chem. **34:** 125–127; 278–279.

Berl, E. & W. Schwebel. 1923. Z. angew. Chem. **36:** 541–545; 552–554.
Berl, E. & E. Wachendorff. 1924. Z. angew. Chem. **37:** 205–206.
Claeson, S. 1946. Arkiv Kemi Mineral. Geol. **A23:** 1.
Claeson, S. 1949. Discussions Faraday Soc. **7:** 34.
Clough, K. H. 1955. Petrol. Engr. **27:** 686.
Cremer, E. & R. Mueller. 1951. Z. Elektrochem. **55:** 217.
Cremer, E. & F. Prior. 1951. Z. Elektrochem. **55:** 66.
Cremer, E. & L. Roselius. 1958. Angew. Chem. **70:** 42.
Damkoehler, G. & H. Teile. 1943. Die Chemie. **56:** 353.
Eggertsen, F. T., H. S. Knight & S. Groennings. 1956. Anal. Chem. **28:** 303.
Eucken, A. & H. Knick. 1936. Brennstoff-Chem. **17:** 241.
Ferber, E. & H. Luther. 1940. Angew. Chem. **53:** 31.
Glueckauf, E., K. H. Barker & G. P. Kitt. 1949. Discussions Faraday Soc. **7:** 199.
Glueckauf, E. & G. P. Kitt. 1956. *In* Vapour Phase Chromatography. : 422–427. D. H. Desty, Ed. Butterworths. London, England.
Griffiths, J. H., D. H. James & C. S. G. Phillips. 1952. Analyst. **77:** 897.
Hammar, C. G. B. 1951. Svensk Kem. Tidskr. **63:** 125.
Henjes, R. 1938. Oel u. Kohle ver. Erdoel u. Teer. **14:** 1075–1085.
Hesse, G. & H. Eilbrecht. 1941. Liebigs Ann. Chem. **546:** 405.
Hesse, G., H. Werther & W. Schnorrenberg. 1951. Z. Elektrochem. **55:** 60.
Janák, J. 1953a. Chem. listy. **47:** 464; 817; 1184.
Janák, J. 1953b. Collection Czechoslov. Chem. Commun. **18:** 798. **19:** 684; 917.
Janák, J. 1956. Mikrochim. Acta. : 1038.
Janák, J. 1957. Erdoel u. Kohle. **10:** 442.
Martin, A. J. P. & R. L. M. Synge. 1941. Biochem. J. **35:** 1958.
Patton, H. W., J. S. Lewis & W. I. Kaye. 1955. Anal. Chem. **27:** 170–174.
Peters, K. 1937. Z. physik. Chem. Leipzig. **A180:** 44.
Peters, K. & W. Lohmar. 1937. Angew. Chem. **50:** 40.
Peters, K. & K. Weil. 1930. Z. physik. Chem. Leipzig. **A148:** 1.
Phillips, C. S. G. 1949. Discussions Faraday Soc. **7:** 241.
Ray, N. H. 1954. J. Appl. Chem. London. **4:** 21–25; 82–85.
Roth, F., W. Ohme & A. Nikish. 1942. Oel u. Kohle. **37:** 1133.
Schuftan, P. 1930. *In* Das Erdoel. **4:** 448. Engler & Hofer, Eds. 2nd. ed. Hirzel. Leipzig, Germany.
Schuftan, P. 1931. Gasanalyse in der Technik. Hirzel. Leipzig, Germany.
Tiselius, A. 1943. Arkiv Kemi Mineral. Geol. **A16:** 5.
Turner, W. C. 1943. Natl. Petrol. News. **35:** 234. Oil Gas J. **41:** 48. Petrol. Refiner. **22:** 140.
Turkeltaub, N. M. 1950. Zhur. Anal. Khim. **5:** 200.
Zhukhovitskii, A. A. & N. M. Turkeltaub. 1957. Uspekhi Khim. **26:** 992.
Zhukhovitskii, A. A., O. V. Zolotareva, V. A. Sokolov & N. M. Turkeltaub. 1951. Doklady Akad. Nauk S. S. S. R. **77:** 435.

## DISCUSSION: PART I

Marcel J. E. Golay, *Discussion Leader*
*The Perkin-Elmer Corporation, Norwalk, Conn.*

M. J. E. Golay: A brief look into the theory of gas-liquid partition chromatography for open and coated capillaries can serve two purposes. First, it leads to a rigorous expression for the HETP that may serve as a basis for the unrigorous expression for the HETP of packed columns. Second, with some slight compromise, these rigorous equations can be transformed into a convenient and nearly rigorous expression for the performance index (P.I.)[1] of any column.

When we compare the van Deemter expression for

$$HETP = (A + (B/u) + Cu)$$

with the rigorous expression reached for open and coated capillaries, we note two things. First, the $A$ term disappears completely. This is easily understood: the $A$ term, misleadingly called the eddy diffusion term (there are no eddies in the essentially streamlined flow of gas in any chromatographic column) is due to the anastomosis of a packed column, and there is no anastomosis in an open capillary. Second, the $C$ term splits into two terms, a new term containing $1/D_g$ and the regular van Deemter term containing $1/D_1$, where $D_g$ and $D_1$ are the diffusion constants of the sample molecules in the carrier gas and in the partition liquid, respectively.

With respect to the disappearance of the $A$ term, it can be speculated that very uniformly packed columns, such as the ones realized in the course of the work of J. H. Purnell reported elsewhere in this monograph, have a lower $A$ term than irregularly packed columns, and that the explanation for slightly positive or slightly negative $A$ terms should be looked for elsewhere. In addition, lumping the $A$ term with $B$ to obtain an $(A + B)/u$ term, as Purnell has done, constitutes a nomographic device, but a physical explanation of his results is needed.

The $B$ term is easily understood. It corresponds simply to the static diffusion in the gas phase that would take place whether or not there is flow and, of course, the slower the flow, the more time there is for diffusion in the gas phase, hence the velocity is in the denominator.

The $C$ term, or its two counterparts in $1/D_g$ and $1/D_1$ for the capillaries, arose because there are statistical fluctuations in the fractional occupancy of the several phases of a column, some molecules remaining longer in the fast-moving gas phase, others remaining longer in the slow-moving gas phase, and still others remaining longer in the liquid phase.

In capillaries, the largest of the two terms is the one in $1/D_1$; fortunately, it is one about which something can be done by increasing the surface area and decreasing the thickness of the liquid phase. On the other hand, nothing can be done about the $1/D_g$ term, since any increase in the horizontal diffusion, which is desirable, is accompanied by an increase in the longitudinal diffusion, which is undesirable.

The relative importance of the terms in $1/D_g$ and $1/D_1$ in packed columns is a matter of speculation. Of course, in the case of air peaks the $1/D_g$ term alone operates. Since the relative band width $\Delta t/t$ of air peaks in packed columns is closer to the value of the relative band width of components than is the case for capillaries, I have surmised that the $1/D_g$ term is relatively more important than the $1/D_1$ term in packed columns when the latter are compared to open capillary columns. Therefore, I have been led to form the physical picture that in packed columns the sample molecules spend considerable time diffusing into the gas phase to reach very thin oil patches into which they diffuse rather quickly, whereas the opposite is true in coated capillary columns. Hence the problem of fabricating capillary columns consists in constructing an oil-supporting structure of large area at the capillary walls.

J. H. Purnell: I agree that at least one further term is necessary in the van Deemter equation. We have considered the problem of the parabolic velocity gradient, resulting fom laminar flow of the carrier gas, and find that it can be regarded as another diffusion term. Since the solute molecules close to the particles have little or no longitudinal velocity, they can enter the fast moving stream only by diffusion; if they do not, band-broadening becomes infinite. In consequence, this factor is reduced by increasing the diffusivity, that is, by reducing the pressure and using a carrier gas such as hydrogen. Clearly, this is in contrast to reduction of longitudinal diffusion.

To illustrate this experimentally, we can write the van Deemter equation for elution of a solute by both nitrogen and hydrogen

$$H_{H_2} = A + B_{H_2}/u + Cu$$

$$H_{N_2} = A + B_{N_2}/u + Cu$$

Hence

$$H_{H_2} - H_{N_2} = \Delta H = 1/u \cdot B$$

and a plot of $\Delta H$ against $1/u$ should be linear, of slope $\Delta B$ and zero intercept. In fact, the plots are curved, concave to the $1/u$ axis and cutting it at some finite value.

Also, we see that plots of $H$ against $u$ for the two gases should never intersect, since their limiting slope at high velocities is $C$, which in principle is independent of carrier gas. In fact, they do intersect, particularly if the overall pressure is higher in the hydrogen elutions.

The results are in accord with the idea expressed elsewhere in this monograph, since the nonuniform velocity profile contributes to $C$, that is,

$$H = A + \mathrm{B}/u + (C_e + C_g)u$$

$C_e$ being the usual mass transfer constant and $C_g$ the effective diffusion coefficient corresponding to the process described.

While our calculations yield a simpler relation than do those of Golay, it may be that when his are considered further, both calculations may prove identical. From our equation and the experimental values for the $\Delta H$ versus $1/u$ plots and from the intersections referred to, we can calculate the ratio of the diffusivities of solutes in nitrogen and hydrogen with reasonable accurary.

E. GLUECKAUF: Any nonuniformity of sample introduction will markedly affect column efficiency.

J. H. PURNELL: I think that Glueckauf's statement is correct. For example, assume a solute of diffusion coefficient $5 \times 10^{-2}$. From the Einstein equation

$$x^2 = t/10$$

If $t = 20$ sec., a reasonable value for time spent in the gas phase, and *cf* represents the air peak times, $x^2 = 2$ or $x = 1.4$ cm. Therefore, in a 5-mm. tube molecules can make only three lateral traverses during the elution. Therefore, if the sample introduction is nonuniform, it is likely to remain that way and, in effect, the column is grossly overloaded. It may well be that a multichannel injector or an atomizer would solve the problem.

E. GLUECKAUF: It has been suggested by Purnell that the $A$ term of the van Deemter equation

$$HTP = A + B/u + Cu$$

can be neglected. This requires some comment.

A term of this kind must exist in any discontinuously packed column and its value is of the order of the particle diameter; the second term is independent of particle size. This means that $A$ can be neglected only as long as the particle size is small enough. However, one can easily see that if the $B/u$ term is reduced more and more as the result of improved operating conditions, $A$ can not be neglected any more. For example, for a 150 to 200mesh column material $A$ would be approximately 0.01 cm. When $B/u + Cu$ is a minimum, the sum has the value 2 $B/u$, so that the value of $A$ must be compared with 2 $B/u$. The latter usually has values of approximately 0.1 cm. (for example, for $N_2$ at 1 atm. and for $H_2$ at 5 atm.). Under these conditions the $A$ term is clearly negligible, and then Purnell's equation is justified. However, for example, when we consider the use of $N_2$ at 10 atm., the value of 2 $B/u$ becomes comparable in size to that of $A$, and with further improvements the latter tends to become the limiting factor in the height of the theoretical plate. It would appear from this that Golay's suggestion to use fine capillary tubes, thus removing the discontinuity convection term $A$, may have valuable application.

### *Reference*

1. Golay, M. J. E. 1957. Nature. **180:** 435.

## Part II. Medicine, Public Health, and Food Chemistry

# GAS-LIQUID CHROMATOGRAPHIC ANALYSIS OF HIGHER FATTY ACIDS AND FATTY ACID METHYL ESTERS

R. K. Beerthuis, G. Dijkstra, J. G. Keppler, and J. H. Recourt
*Unilever Research Laboratory, Vlaardingen, The Netherlands*

### INTRODUCTION

The analysis of free fatty acids is interfered with by the association phenomenon of the carboxylic groups. It now appears that this disturbing factor can be eliminated. By their investigations, Szabo and Dijkstra[1, 2] have indicated that, above a given temperature, association decreases greatly. This is independent of the chain length of the fatty acids. It is now possible to analyze in a simple way the even-numbered free fatty acids $C_{12}$ to $C_{22}$ by carrying out gas-chromatographic analyses at high temperatures.

The detection is accomplished by combustion of the escaping acids over copper oxide at 1000° C.; the carbon dioxide thus obtained is measured in a katharometer at room temperature.

The separation of saturated and unsaturated fatty acid methyl esters in the range from dodecanoic acid ($C_{12}$) up to and including triacontanoic acid ($C_{30}$) will be discussed in the light of the results obtained from the analysis of the component fatty acids of menhaden oil, *Ximenia caffra* oil, and various model substances. The gas-density balance has been used as detector and has proved to be extremely suitable; it was also found suitable when used in combination with the combustion method.

The reaction products obtained by alkali isomerization of naturally occurring linoleic acid have been analyzed by means of gas chromatography. It appeared that *trans-trans* conjugation of the double bonds also occurs during the isomerization reaction.

### GAS-LIQUID CHROMATOGRAPHIC SEPARATION OF HIGHER MONOCARBOXYLIC ACIDS

The gas-liquid chromatographic separation of higher monocarboxylic acids is made difficult by the fact that the acids tend to associate.

In their earliest attempts to separate the lower fatty acids, James and Martin[3] obtained asymmetric zones resulting from dimerization of the acids in the liquid phase. The monomeric content is dependent upon the fatty acid concentration, as a result of which the regions of low acid concentration move more rapidly down the column than do regions of high acid concentration.

These investigators solved the problem by adding a long-chain fatty acid (stearic acid) of low vapor pressure to the liquid phase. In consequence, the concentration of the monomer and the self-dimerization by association were reduced to such an extent that almost symmetrical zones were obtained.

In this way it was possible to separate the fatty acids up to and including lauric acid.

The same principle would be applicable also to the separation of higher fatty acids were it not for the fact that no long-chain fatty acid that is only slightly volatile and adequately stable at high temperature is available. It is possible that favorable results might be obtained by the addition of, for example, polyacrylic acid to the liquid phase.

We have carried out experiments using silicone oil to which $\beta$-anthroquinone carboxylic acid had been added. At higher column temperatures, however, this acid eluted.

Another possibility was opened up by the investigation of Szabo and Dijkstra[1, 2] in which the association of fatty acids was studied with the aid of infrared absorption measurements.

The infrared absorption of the C═O stretching frequency displayed, for the fatty acids, a double bond; for the C═O dimer, an absorption at 1717 cm.$^{-1}$ (5.832 $\mu$); for the C═O monomer, an absorption at 1767 cm.$^{-1}$ (5.66 $\mu$). These absorption maxima are eminently suitable for quantitative determinations (FIGURE 1).

The degree of association from 25° C. to 220° C. was determined in an inert solvent, that is, paraffin wax or oil (FIGURE 2).

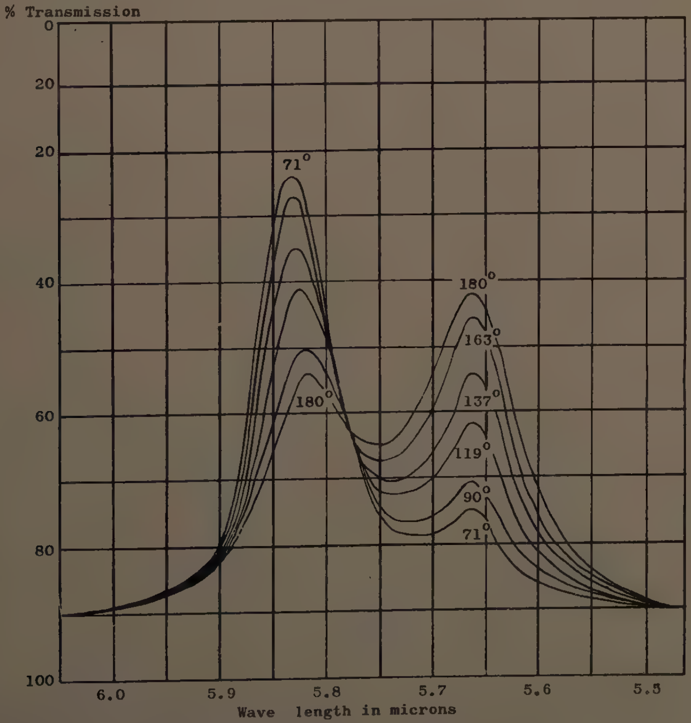

FIGURE 1. Carbonyl group absorptions of 0.05 M/l. stearic acid in paraffin wax.

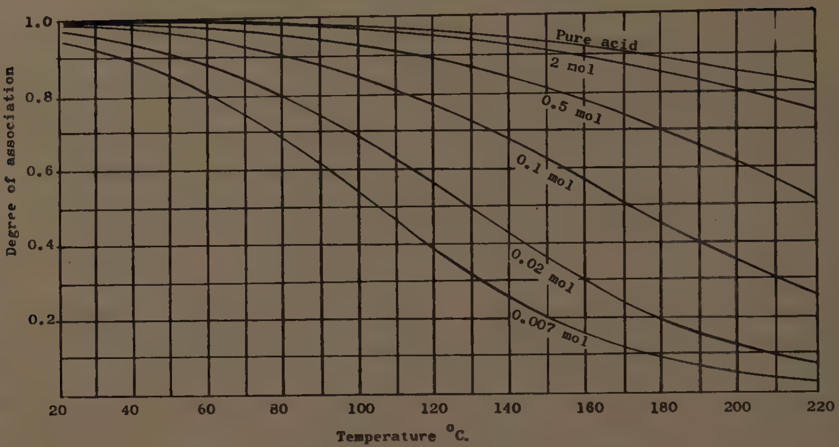

FIGURE 2. Association of stearic acid in paraffin.

From this investigation it was established that:

(1) Even in diluted solution, complete association is asymptotically approached; at room temperature, for example, 90 per cent of the molecules of a 0.007 M stearic acid solution are associated.

(2) Only very slight dissociation occurs in the undiluted acid; at 220° C., at least 80 per cent is still associated.

(3) However, in dilute solution, stronger dissociation occurs and approaches complete dissociation asymptotically. At 200° C. only 0.5 per cent of the stearic acid in a 0.007 M solution is associated.

(4) The association is constant for all chain lengths and the degree of unsaturation of the chain in no way influences the degree of association.

On the basis of these data, it may be concluded that separation by means of gas chromatography is possible, provided: (1) a sufficiently high temperature is applied; and (2) low concentration in the liquid phase is maintained.

## *Experimental Results*

*Apparatus.* A katharometer is used as detector, in which, after combustion, the fatty acids are detected as $CO_2$.

For the detection of fatty acids as such, the katharometer is unsuitable, as the acids around the hot platinum wire would display decomposition phenomena.

Moreover, the combustion method has the following advantages.

(1) The carbon present in a compound is oxidized to carbon dioxide and this gives a greater change in the composition of the eluted gas mixture than occurs when only the organic vapor is measured.

(2) The carbon dioxide can be detected at room temperature in the katharometer, in contrast to the detection of organic vapors; for this purpose the detector must be heated to a temperature sufficiently high to prevent condensation. The sensitivity of the katharometer is favorably influenced by as low

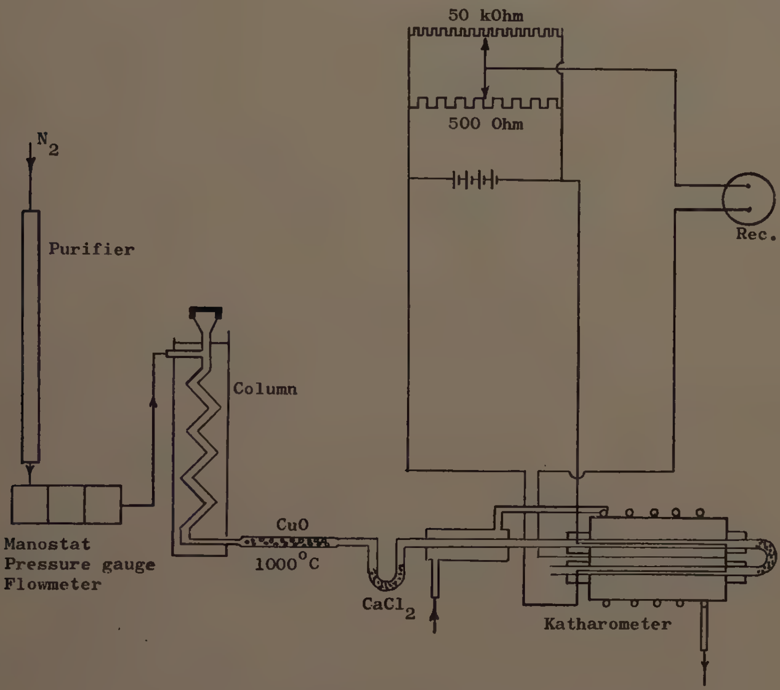

FIGURE 3. Flow sheet of the combustion method with a katharometer.

an operational temperature as possible, for the temperature gradient between the platinum wire and the wall of the detector is dependent, at a certain voltage, upon the temperature of the environment in such a way that this gradient becomes smaller as the temperature of the environment increases.

(3) Because only one substance, $CO_2$, is invariably detected, the difficulty involved in calibrating for the heat conductivity of many substances is eliminated.

The apparatus is depicted diagrammatically in FIGURE 3. The columns are arranged spirally or are folded in an aluminum tube that is electrically heated with resistance wire and well insulated with asbestos cloth.

Combustion of the components takes place in a quartz tube with an internal diameter of 6 mm. and an effective length of 8 cm.; the tube is filled with pieces of copper oxide. The quartz tube is held at 1000° C. by means of an electric oven. The water is removed with $CaCl_2$, and the gas stream is then cooled to room temperature in a copper tube (internal diameter, 4 mm.; length, 10 cm.) filled with copper turnings. This copper tube is fitted with a cooling jacket through which thermostat water flows, and is connected with the katharometer.

The katharometer consists of a cylindrical copper block 5 cm. in diameter, through which two channels 2 mm. in diameter and 10 cm. in length are bored. Threaded tautly and centrally through each channel is a 20 $\mu$ platinum wire 10 cm. in length and having a resistance of 40 $\Omega$.

The platinum wires are each connected by a resistance of approximately 250 Ω (500 Ω potentiometer) in a Wheatstone bridge; accurate adjustment of the bridge balance is achieved with a variable resistance of 50 kΩ.

Using a current of 85 mAmp. through the platinum wires, a static base line is obtained on a recorder with 1 mv. full-scale deflection and a chart width of 10 in.

The katharometer is kept at constant temperature by means of a cooling spiral through which flows thermostat water from the previously described cooling jacket of the cooling tube.

The cooling tube and katharometer are assembled in a sealed Dewar vessel.

*Separation of fatty acids.* The first attempts to separate fatty acids were made over a Celite-silicone oil filling. For this purpose, a slightly volatile fraction obtained from silicone oil (D.C. M.S. 550) by molecular distillation at 250° C. and 7 μ was used.

For the separation of the higher fatty acids ($C_{12}$ and higher), however, silicone oil was found to be unsuitable. The chromatograms invariably displayed a disjointed base line; moreover, even at high temperatures, acid in low concentration can be detected for a considerable time in the gas emerging from the column.

Despite high column temperatures, considerable association occurs, probably promoted by the silicone oil. In later experiments, Apiezon L grease was used as liquid phase. When Apiezon L grease is used in combination with high column temperatures, small amounts of volatile products elute above

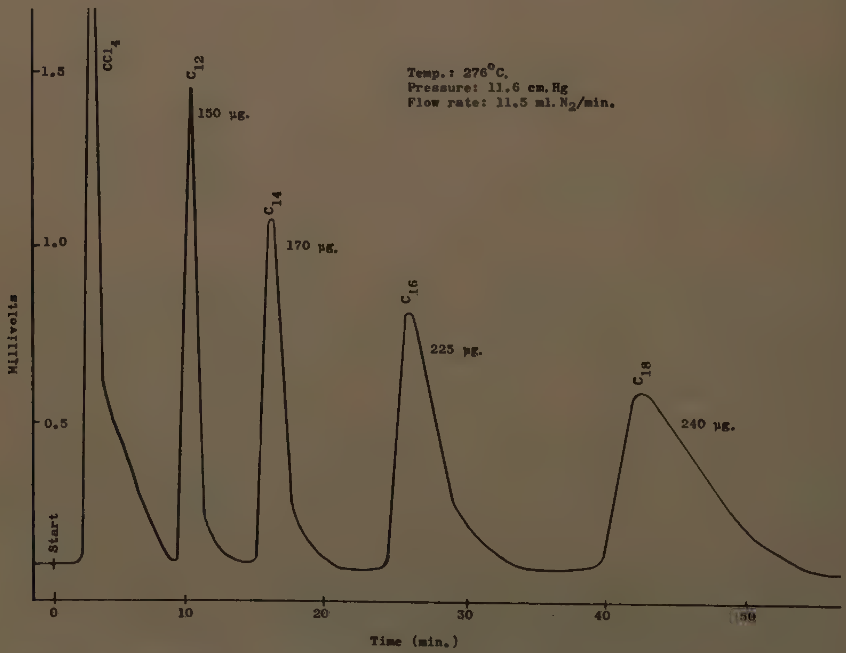

FIGURE 4. Separation of normal fatty acids dissolved in carbon tetrachloride ($CCl_4$).

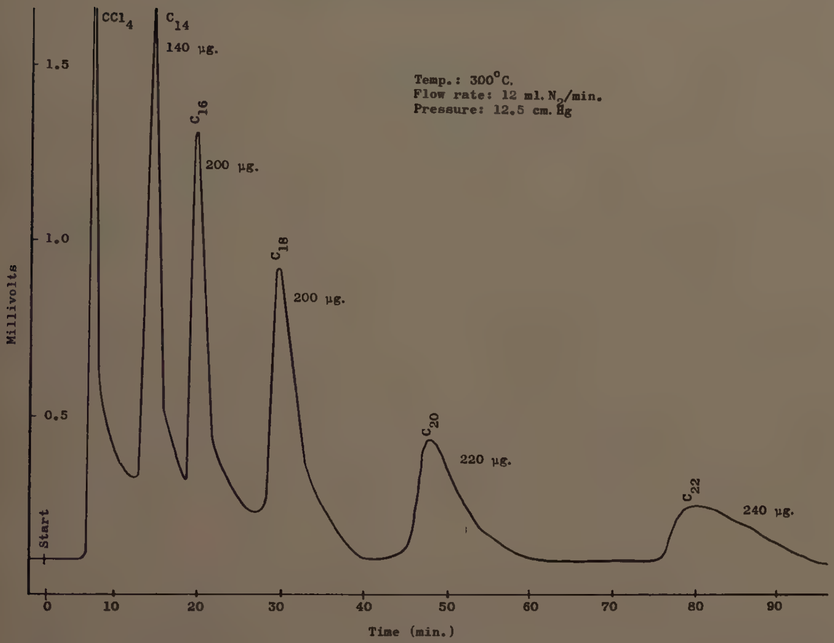

FIGURE 5. Separation of normal fatty acids $C_{14}$ to $C_{22}$ dissolved in carbon tetrachloride ($CCl_4$).

240° C. If, however, Apiezon-impregnated Celite is held at 300° C. and 10 mm. Hg in a nitrogen atmosphere for 5 hours, the filling thus prepared was found to be stable.

The separation of the monocarboxylic acids was finally investigated using a column having a length of 150 cm.; an internal diameter of 0.4 cm.; and a filling of 9 gm. Apiezon L/Celite (50 to 100 $\mu$) in 1:4 ratio.

The results obtained are represented in FIGURES 4 and 5.

All curves display a certain amount of tailing; this is reduced but not completely eliminated by increase in temperature.

The interference caused by silicone oil can be seen in FIGURE 6.

On comparing FIGURES 4 and 6, it is again apparent that the tailing effect is more pronounced at low than at high temperatures; this accords with the fact that association decreases with increase in temperature.

From TABLE 1 it will be seen that the quantitative determination of the fatty acids from these curves gives very good results. The areas were compared mutually by copying and cutting out the curves and weighing them.

From the provisional results it appears that the association of the free fatty acids at high temperature can be suppressed sufficiently to enable gas-chromatographic separation to be carried out. If, however, a greater differentiation and a more accurate analysis of the higher fatty acids is desired (for example, the separation of uneven from even numbered fatty acids or the separation of unsaturated from saturated fatty acids of equal chain length), analysis with the aid of the methyl esters is still the recommended method.

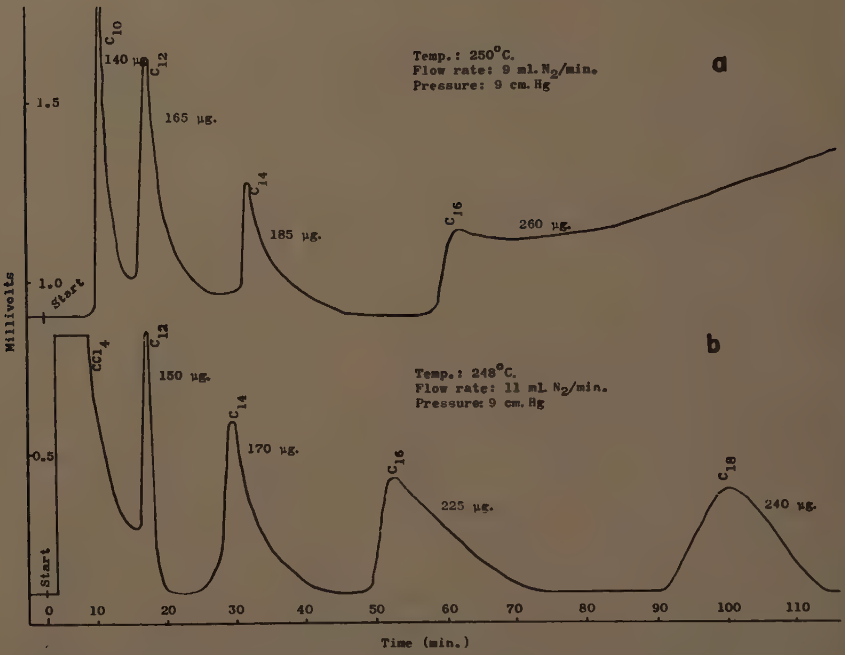

FIGURE 6. (a) Fatty acids $C_{10}$ to $C_{18}$ dissolved in silicone oil. (b) Fatty acids $C_{12}$ to $C_1$ dissolved in $CCl_4$.

TABLE 1

MIXTURE OF FATTY ACIDS FROM $C_{12}$ UP TO AND INCLUDING $C_{18}$

| Component | Composition (percentages) | Calculated from area of the curves (percentages) |
|---|---|---|
| Lauric acid | 17.2 | 17.5 |
| Myristic acid | 19.3 | 18.8 |
| Palmitic acid | 30.0 | 29.0 |
| Stearic acid | 33.5 | 34.7 |

Analysis of the fatty acids may be especially suitable for the monitoring of factory distillations.

## GAS-LIQUID CHROMATOGRAPHY OF HIGHER FATTY ACID METHYL ESTERS

The gas-liquid chromatography of fatty acid methyl esters to behenic acid at temperatures exceeding 200° C. is described by Cropper and Heywood,[4] and by Keppler *et al.*[5]

James and Martin[6] achieved excellent separations of unsaturated and saturated methyl esters at temperatures up to 204° C. In 1957 the analysis of methyl esters up to and including cerotic acid at 256° C. was described by Beerthuis and Keppler.[7]

It was found that the analysis of fatty acid methyl esters having chain lengths up to and including 30 carbon atoms is possible with column temperatures up to 286° C.

*Apparatus.* As detector, the gas-density balance developed by Martin and James[8] was used. The columns and detector were heated by means of a vapor bath that enabled analysis at 256° C. to be carried out with ease.

However, the application of the vapor bath to achieve high temperatures has the disadvantage that few liquids remain stable during prolonged boiling. Moreover, few liquids suitable for boiling at these high temperatures are to be found.

For these reasons, electric heating is always preferable, especially as any desired temperature can be obtained without the time-consuming replacement of one liquid by another.

In addition to the original apparatus with vapor jacket, we constructed a simple device in which the column is electrically warmed while the gas-density balance remains at room temperature. After separation, the substances are converted through combustion to carbon dioxide and water and the $CO_2$ is detected (FIGURE 7).

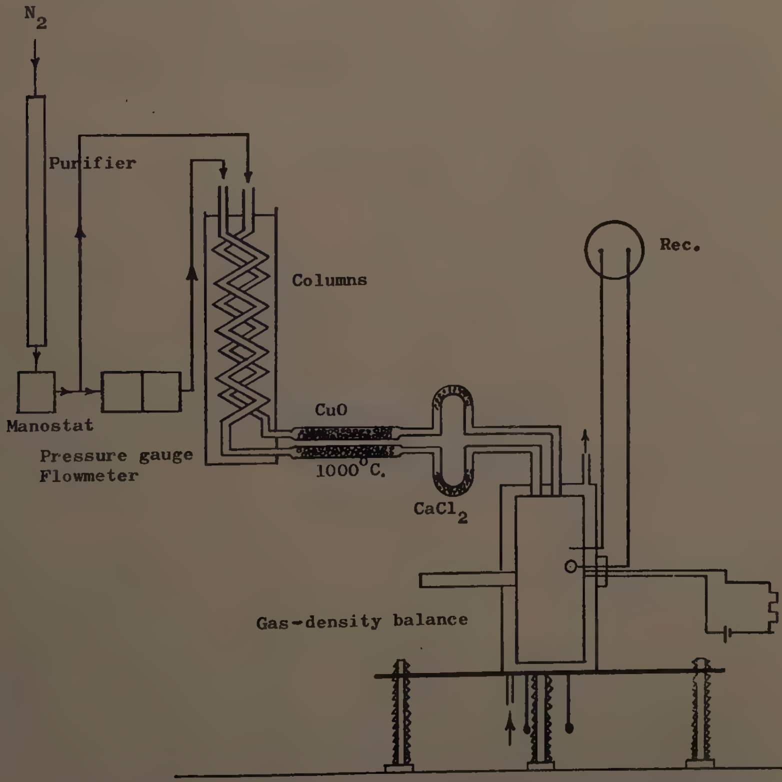

FIGURE 7. Flow sheet of the combustion method with a gas-density balance.

TABLE 2

RETENTION VOLUME RELATIVE TO METHYL LAURATE

| Methyl ester | Apiezon L | Silicone grease | Silicone oil |
|---|---|---|---|
| Laurate | 2.52 | 2 | 2 |
| Palmitate | 6.19 | 4.35 | 4.36 |
| Oleate | 12.9 | 8.23 | 10 |
| Stearate | 15.47 | 9.17 | 11 |

The gas-density balance is built into a copper housing through which water from a thermostat is pumped to ensure constant temperature. In opposition to the disadvantage that substances are lost by combustion is the advantage that the detection sensitivity is enhanced. The difference in gas density between carrier gas and carrier gas plus component is larger after combustion to $CO_2$ than prior to combustion.

An additional advantage is that with this apparatus it is possible continually to raise the temperature during the analysis. The construction and heating of the columns are identical with those described in FIGURE 3.

### *Support Material and Phases*

Celite 545 from which the finest particles had been removed by sedimentation was used invariably as carrier. In this high-temperature range the choice of liquid phase is rather limited.

From tests made with various phases, the best separation was found to be obtained with Apiezon L grease. This can be seen from TABLE 2, which shows the results obtained with equal amounts of filling, namely, 4 gm. Celite 545 treated with 1 gm. liquid phase, at 197° C.

The Celite-Apiezon fillings were treated as described previously. Oxygen-free nitrogen was used as carrier gas. The columns were filled by repeatedly sucking small amounts of the filling into the column, maintaining a vacuum of approximately 15 cm. Hg for several minutes and then suddenly breaking the vacuum. In this way, both spiral-shaped and straight columns could be filled.

Recently Orr and Callen[9] introduced a new polar liquid phase "Reoplex 400 plasticizer" that is more suitable for the separation of saturated and unsaturated fatty acid methyl esters than Apiezon L grease.

### *Applications*

*Separation of menhaden oil fatty acids.* No description of a gas-chromatographic analysis of the fatty acids from menhaden oil is given in the literature, and the data available from this source are not always in agreement.

In order to obtain a broad impression of the composition, in particular of the higher fatty acids, a qualitative analysis was carried out over a column of low separating power at 231° C. (vapor bath: decanol).

It was found that fatty acids higher than lignoceric acid ($C_{24}$) were not present in this sample (FIGURE 8).

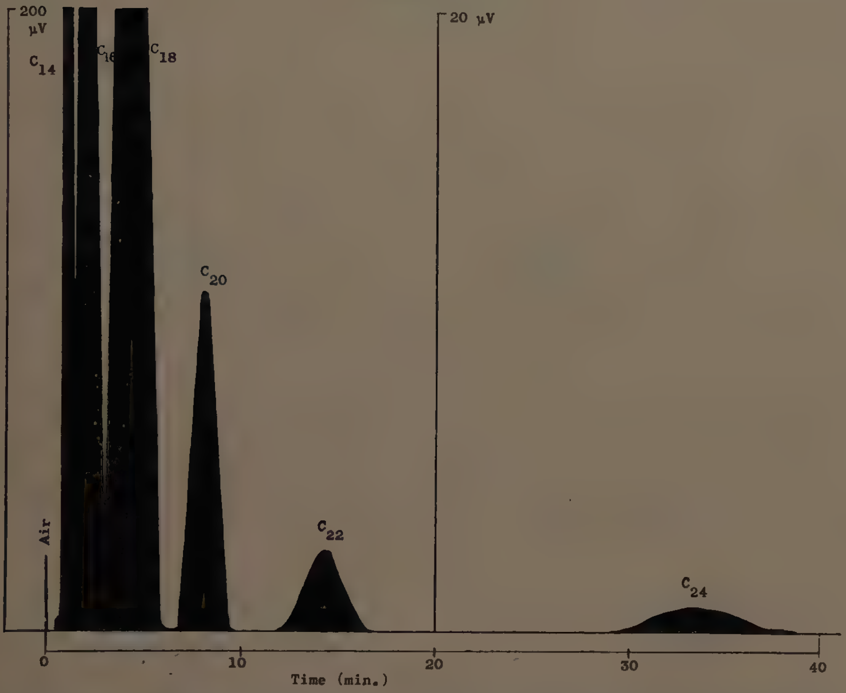

FIGURE 8. Menhaden oil methyl esters. Conditions: temperature, 231° C. (vapor bath); overpressure, 38.5 cm. Hg; gas flow, 29 ml. $N_2$/min.; filling, 3 gm. Celite 545/Apiezon L, 10:1 ratio; column, 110 cm., 0.4 cm.

The complete analysis could be carried out in two stages: (1) at 197° C., for the $C_{12}$ to $C_{18}$ range; and (2) at 231° C., for the $C_{18}$ to $C_{22}$ range.

The results of the separation of the fatty acid methyl esters from $C_{12}$ up to and including $C_{18}$ are represented in FIGURE 9.

The separation factor (the time of emergence of a substance relative to its next lowest homologue) was found to be 1.56 for one $CH_2$ group. The unsaturated fatty acids were detected by hydrogenating and again chromatographing the sample.

In another run the $C_{16}$ unsaturated methyl esters were condensed; after rechromatographing on a column with Reoplex 400 as stationary phase, four different unsaturated acids could be detected. In this way overlapping of the branched and normal heptadecanoate by the unsaturated $C_{16}$ acids was avoided.

The same procedure was applied to the unsaturated $C_{18}$ group and, in this case, four different acids were detected.

The retention volumes of oleate, linoleate, and linolenate were the same as those of the respective eluted unsaturated $C_{18}$ acids and, in addition to these three acids, a higher unsaturated acid, probably one with four double bonds, was present. The acids are not yet completely identified. However, the provisional results are in agreement with those reported by Schlenk *et al.*[10] who,

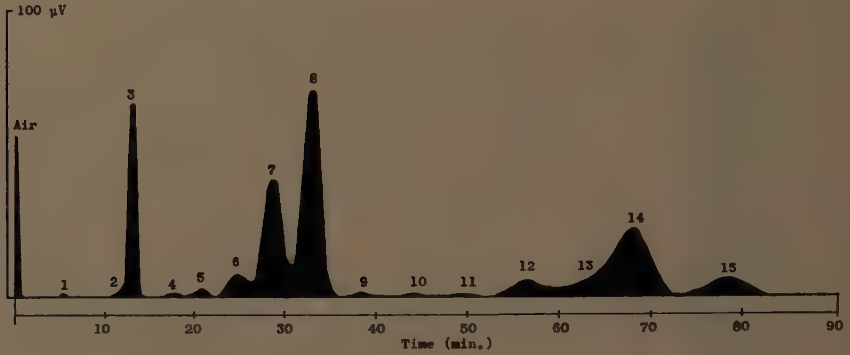

FIGURE 9. Menhaden oil methyl esters. Conditions: temperature, 197° C. (vapor bath); overpressure, 49.3 cm. Hg; gas flow, 24 ml. $N_2$/min.; filling, 4.7 gm. Celite 545/Apiezon L, 9:1 ratio; column, 104 cm., 0.4 cm.; amount introduced, 2 mg. (of which 1.4 mg. was detected). The peaks (the fatty acids are indicated by their chain lengths) were obtained in the following order: (1) $C_{12}$; (2) unsaturated $C_{14}$; (3) $C_{14}$; (4) branched $C_{15}$; (5) $C_{15}$; (6) polyunsaturated $C_{16}$; (7) unsaturated $C_{16}$; (8) $C_{16}$; (9) highly branched (?) $C_{17}$; (10) branched $C_{17}$; (11) $C_{17}$; (12) polyunsaturated $C_{18}$; (13) di- and triunsaturated $C_{18}$; (14) monounsaturated $C_{18}$; (15) $C_{18}$.

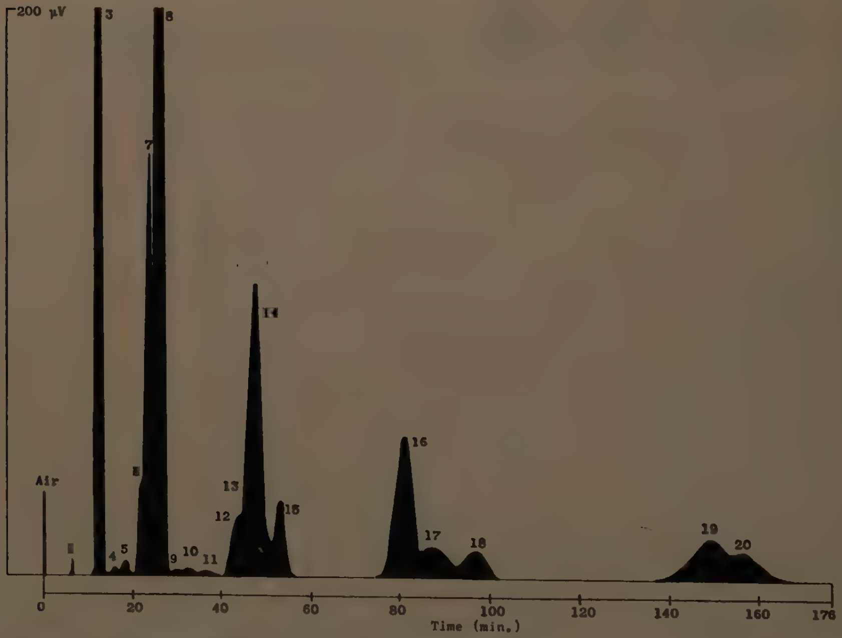

FIGURE 10. Menhaden oil methyl esters. Conditions: temperature, 231° C. (vapor bath); overpressure, 50.7 cm. Hg; gas flow, 20 ml. $N_2$/min.; filling, 7.7 gm. Celite/Apiezon L, 4:1 ratio; column, 116 cm., 0.4 cm.; amount introduced, 6 mg. The numbers of the peaks correspond with those given in FIGURE 9. From peak 16, onward: (16 and 17) polyunsaturated $C_{20}$; (18) unsaturated $C_{20}$; (19 and 20) polyunsaturated $C_{22}$.

TABLE 3

| Peak | | Weight percentages of methyl esters |
|---|---|---|
| 1 | Dodecanoate | 0.1 |
| 2 | Tetradecenoate | 0.1 |
| 3 | Tetradecanoate | 8.4 |
| 4 | Branched pentadecanoate | 0.3 |
| 5 | Pentadecanoate | 0.7 |
| 6 | Hexadecatetraenoate | 0.3 |
| | Hexadecatrienoate | 1.3 |
| 7 | Hexadecadienoate | 1.8 |
| | Hexadecenoate | 11.9 |
| 8 | Hexadecanoate | 20.7 |
| 9 | Highly branched heptadecanoate | 0.3 |
| 10 | Branched heptadecanoate | 0.5 |
| 11 | Heptadecanoate | 0.5 |
| 12 | Octadecatetraenoate | 2.5 |
| 13 | Octadecatrienoate | 0.9 |
| 14 | Octadecadienoate | 2.0 |
| | Octadecenoate | 15.6 |
| 15 | Octadecanoate | 3.8 |
| 16/17 | Polyunsaturated eicosanoate | 12.5 resp. 2.9 |
| 18 | Unsaturated eicosanoate | 2.8 |
| 19/20 | Polyunsaturated docosanoate | 6.4 resp. 3.3 |
| 21 | Saturated or unsaturated tetracosanoate | 0.4 |

by means of paper chromatography, found mono-, di-, tri-, and tetra-unsaturated $C_{16}$ and $C_{18}$ acids in the component fatty acids of menhaden oil.

The separation in the range $C_{18}$ up to and including $C_{22}$ is represented in FIGURE 10. In this case, the separation factor for one $CH_2$ group was 1.46. Peak 19 was found to coincide with the model substance docosahexaenoic acid.*

A mono- and a penta-unsaturated $C_{20}$ acid were detected in menhaden oil by Baldwin and Parks;[11] the presence of docosapentaenoic acid was detected by Armstrong and Allan.[12] Presumably, the latter is the acid represented by peak 20.

The percentage composition can be calculated from the curves obtained; correction for the expected and known molecular weights of the substances, according to James and Wheatley,[13] is made as follows:

Corrected surface area =

$$\frac{M_1 - 28}{M_2 - 28} \times \frac{M_2}{M_1} \times \text{surface area found}$$

In this equation, $M_1$ is the molecular weight of reference substance and $M_2$ is the molecular weight of the substance to be identified. The composition is given in TABLE 3.

*Separation of the fatty acids of Ximenia caffra oil.* It has long been known that *Ximenia* oils contain very high-component fatty acids.[14] Ligthelm *et al.*[15]

---

* Isolated from cod-liver oil by O. Notevarp (Norway).

demonstrated the presence of fatty acids up to and including a chain length of 30 carbon atoms. They proved the presence of a series of oleic acid homologous to triacontenoic acid in addition to the saturated series. The separation of the higher fatty acids from behenic acid has been investigated by us.

With a column temperature of 274° C. the range up to and including $C_{32}$ can be covered easily. From an analysis carried out at this temperature it appeared that fatty acids up to and including $C_{28}$ were present in the sample (FIGURE 11). On overdosing, $C_{30}$ and higher acids could not be detected.

From the retentions it appeared that the peaks for the saturated acids $C_{22}$, $C_{24}$, $C_{26}$, and $C_{28}$ form a homologue series. After hydrogenation, this series of prepeaks shifted to the saturated series, thus proving that they originate from unsaturated acids.

The results of experiments carried out to permit further identification are represented in FIGURE 12. The positions of the saturated and unsaturated fatty acids appear from the curves. The results of Ligthelm *et al.*,[15] who found only monounsaturated fatty acids of the homologue series of oleic acid, almost certainly exclude the possibility of the presence of higher unsaturated acids.

It was found that the analysis of fatty acids up to and including $C_{28}$ was also possible at lower column temperatures; namely, at 231° C., as shown in FIGURE 13.

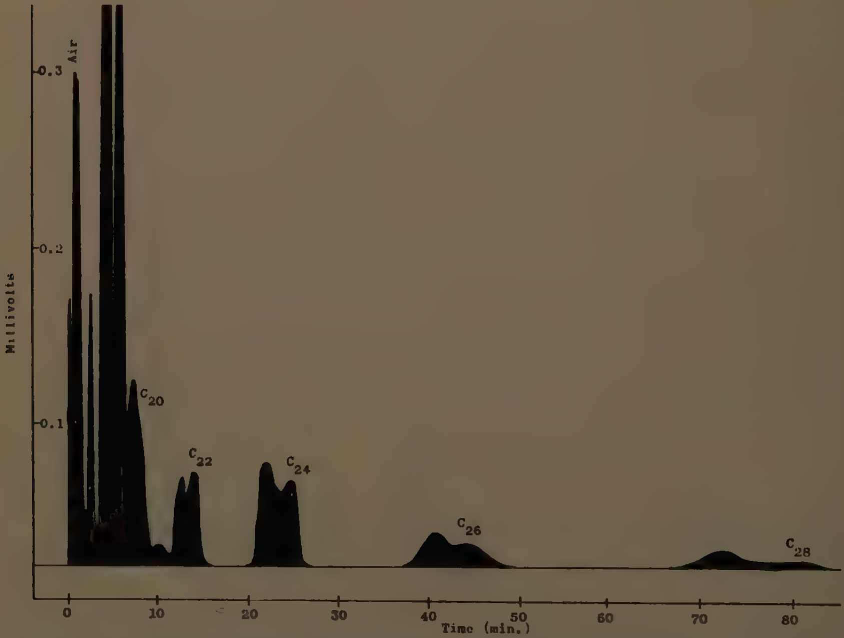

FIGURE 11. *Ximenia caffra* oil methyl esters. Conditions: temperature, 274° C.; overpressure, 29 cm. Hg; gas flow, 25 ml. $N_2$/min.; filling, 4 gm. Celite 545/Apiezon L, 9.9:1 ratio; column, 115 cm., 0.4 cm.; amount introduced, approximately 4 mg.; detection, $CO_2$, after combustion.

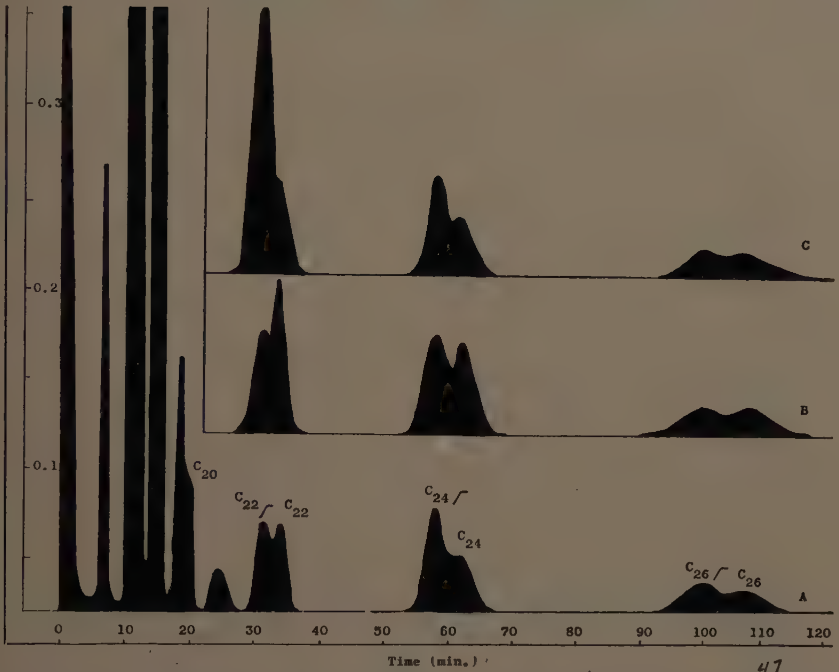

47

FIGURE 12. Conditions: temperature, 286° C.; overpressure, 49 cm. Hg; gas flow, 20 ml $N_2$/min.; filling, 5 gm. Celite 545/Apiezon L, 4:1 ratio; column, 114 cm., 0.4 cm.; amount introduced, invariably approximately 6 mg.; detection, $CO_2$, after combustion. Curve *A*: methylesters of *Ximenia caffra* oil. Curve *B*: Methylesters of *Ximenia caffra* oil + $C_{22}$, $C_{24}$, $C_{26}$. Curve *C*: methylesters of *Ximenia caffra* oil + erucic acid.

*Separation of model substances up to and including triacontanoic acid* ($C_{30}$). The separation of the saturated, even fatty acid methyl esters of $C_{24}$ up to and including $C_{30}$ is shown in FIGURE 14.

### *Isomerization Reactions*

Rearrangements of 1,4-double bonds of di- and polyolefinic compounds to the conjugated position have been shown to occur during treatment with catalysts such as nickel or alkali at high temperatures.

Various geometrical isomers are produced during these reactions. Nichols *et al.*[16] demonstrated that on alkali isomerization of 9-*cis*, 12-*cis*-linoleic acid, 90 to 95 per cent conjugated dienoic acid is formed, the 9-*cis*, 11-*trans*, and the 10-*trans*, 12-*cis* isomers predominating.

The yield from this reaction and the reaction products thus obtained can be studied with the aid of gas-chromatography since the conjugation of the double bonds appears to exercise great influence upon the retention time. Under standard conditions[17] 9-*cis*, 12-*cis*-linoleic acid (isolated by urea-adduct formation from safflower oil, and 99 per cent pure) was isomerized with alkali, after which the acid was esterified with diazomethane and the methyl ester analyzed gas-chromatographically. The result of one of the experiments is given in FIGURE 15*A*.

Apart from unconverted linoleate (peak *a*), two other peaks were obtained that were identified by means of infrared spectroscopy as conjugated *cis*-

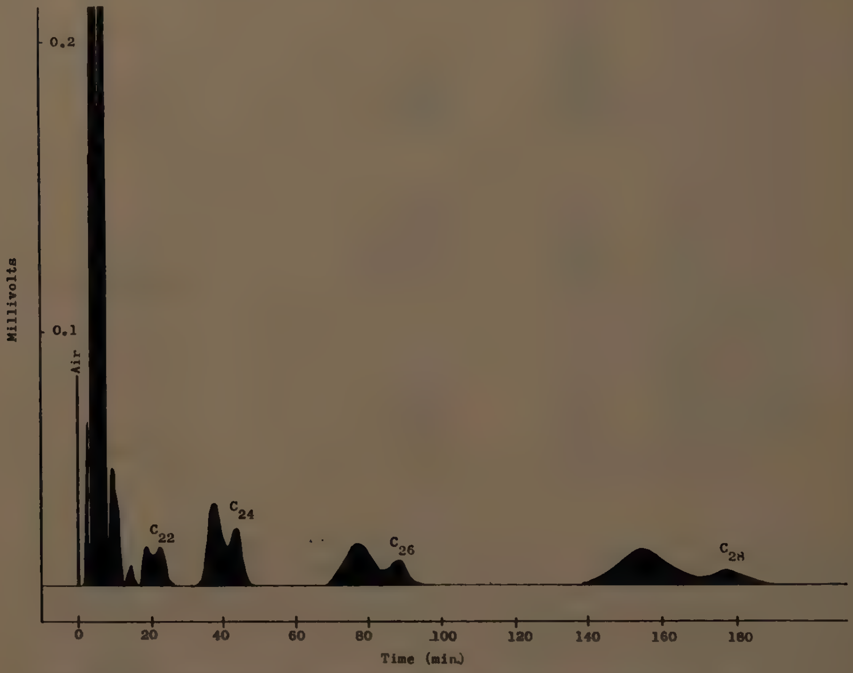

FIGURE 13. *Ximenia caffra* oil methyl esters. Conditions: temperature, 231° C. (vapor bath); overpressure, 45.5 cm. Hg; gas flow, 50 ml. $N_2$/min.; filling, 3 gm. Celite/Apiezon L, 9:1 ratio; column, 110 cm, 0.4 cm.; amount introduced, approximately 14 mg.

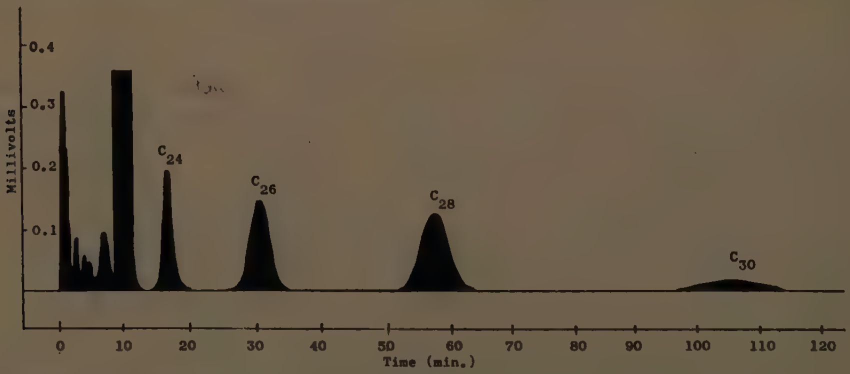

FIGURE 14. Conditions: temperature, 270° C.; overpressure, 42 cm. Hg; gas flow, 29 ml. $N_2$/min.; filling, 4 gm. Celite 545/Apiezon L, 9:1 ratio; column, 115 cm., 0.4 cm.; amount introduced, approximately 2 mg.; detection, $CO_2$, after combustion. The lower components, which eluted before $C_{24}$ methyl ester, originate from the impure triacontanoic acid.

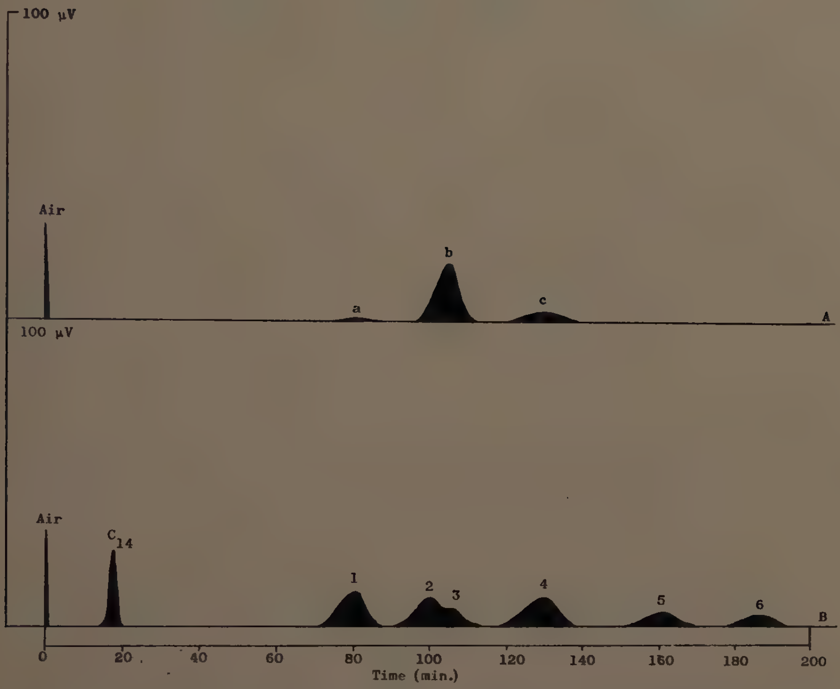

FIGURE 15. Conditions: temperature, 197° C. (vapor bath); overpressure, 59.5 cm. Hg; gas flow, 10 ml. $N_2$/min.; filling, 6 gm. Celite 545/Apiezon L, 9:1 ratio; column, 116 cm., 0.4 cm. Curve *A*: alkali isomerized 9-*cis*, 12-*cis*-linoleic acid. Curve *B*, mixture of the methyl esters: ($C_{14}$) tetradecanoate; (1) octadeca-9-*cis*, 12-*cis*-dienoate; (2) octadecanoate; (3) octadeca-9-*cis*, 11-*trans* + 10-*trans*, 12-*cis*-dienoate; (4) octadeca-9-*trans*, 11-*trans* + 10-*trans*, 12-*trans*-dienoate; (5) octadeca-9-*cis*, 11-*trans*, 13-*trans*-trienoate; (6) octadeca-9-*trans*, 11-*trans*, 13-*trans*-trienoate.

*trans* (peak *b*) and conjugated *trans-trans* (peak *c*). In the second peak the isomers 9-*cis*, 11-*trans* and 10-*trans*, 11-*cis* apparently coincide. The third peak was further identified as follows:

(1) The retention volume appeared to be the same as that of the model substance 10-*trans*, 12-*trans* linoleate (von Mikusch's acid).

(2) The substance was obtained in pure state after separation by condensation from the gas current. The condensate was then ozonized, and the aldehydes and aldehyde esters so formed were then identified as 2,4-dinitrophenylhydrazones by means of paper chromatography.[18] Hexanal, heptanal, and

TABLE 4
RETENTION VOLUMES RELATIVE TO METHYL MYRISTATE

| | |
|---|---|
| Octadeca-9-*cis*, 12-*cis*-dienoate | 4.45 |
| Octadecanoate | 5.52 |
| Octadeca-9-*cis*, 11-*trans* + 10-*trans*, 12-*cis*-dienoate | 6.00 |
| Octadeca-9-*trans*, 11-*trans* + 10-*trans*, 12-*trans*-dienoate | 7.23 |
| Octadeca-9-*cis*, 11-*trans*, 13-*trans*-trienoate | 8.94 |
| Octadeca-9-*trans*, 11-*trans*, 13-*trans*-trienoate | 10.39 |

the methyl esters of 9-aldononanoic acid and 10-aldodecanoic acid were present in equal molecular amounts.

In the third peak, therefore, 10-*trans*, 12-*trans* and 9-*trans*, 11-*trans*-linoleate (Mangold's acid) coincide.

The occurrence of *trans-trans* conjugation during the standardized alkali isomerization was hitherto unknown.

The difference in retention time between *trans*, *trans* and *cis*, *trans* conjugated double bonds in isomers appears to be great (these are evidently caused by the stretching of the molecular configuration by the *trans* double bond and the accompanying decrease in volatility). This can be seen from FIGURE 15*B*.

The relative retention volumes of the separated components are given in TABLE 4.

From the examples given it follows that: (1) during standardized alkali isomerization of linoleic acid, various isomers may form, including *trans-trans* conjugated linoleic acid; and (2) isomerization reactions can be studied with the aid of gas-liquid chromatography.

## ACKNOWLEDGMENTS

We thank C. J. Duyverman for his assistance in separating the free fatty acids, J. C. M. Schogt and J. de Bruyn for the syntheses of the $C_{26}$, $C_{28}$ and $C_{30}$ acids, S. Sparreboom for the pure linoleic acid and its isomerization, and K. de Jong for the paper-chromatographic identifications.

We also thank the management of Unilever N. V., Rotterdam, The Netherlands, for permission to publish this paper.

## REFERENCES

1. SZABO SARKADI, D. 1956. Thesis. Delft, Netherlands.
2. DIJKSTRA, G Chem. Weekblad. To be published.
3. JAMES, A. T. & A. J. P. MARTIN. 1952. Biochem. J. **50:** 679.
4. CROPPER, F. R. & A. HEYWOOD. 1953. Nature. **172:** 1101. Ibid., 1954. **174:** 1063.
5. KEPPLER, J. G., G. DIJKSTRA & J. A. SCHOLS. 1957. *In* Vapour-Phase Chromatography. : 222. D. H. Desty & C. L. A. Harbourn, Eds. Butterworths. London, England.
6. JAMES, A. T. & A. J. P. MARTIN. 1956. Biochem. J. **63:** 144.
7. BEERTHUIS, R. K. & J. G. KEPPLER. 1957. Nature **179:** 731.
8. MARTIN, A. J. P. & A. T. JAMES. 1956. Biochem. J. **63:** 138.
9. ORR, C. H. & J. E. CALLEN. 1958. J. Am. Chem. Soc. **80:** 249.
10. SCHLENK, H., J. L. GELLERMAN, J. A. TILLOTSON & H. K. MANGOLD. 1957. J. Am. Oil Chem. Soc. **34:** 384.
11. BALDWIN, W. H. & L. E. PARKS. 1943. Oil & Soap **20:** 101.
12. ARMSTRONG, E. F. & J. ALLAN. 1924. J. Soc. Chem. Ind. **43:** 216T.
13. JAMES, A. T. & V. R. WHEATLEY. 1956. Biochem. J. **63:** 269.
14. BOEKENOOGEN, H. A. 1939. Fette u. Seifen. **46:** 717.
15. LIGTHELM, S. P., D. H. S. HORN, N. M. SCHWARTZ & M. M. VON HOLDT. 1954. J. Sci. Food Agr. **5:** 281.
16. NICHOLS, P. L. JR., S. F. HERB & R. W. RIEMENSCHNEIDER. 1951. J. Am. Chem. Soc. **73:** 247.
17. AMERICAN OIL CHEMISTS' SOCIETY. 1946. Official and tentative methods. 2nd ed. V. C. Mehlenbacher, Ed. Rev. to April 1956. Chicago, Ill.
18. KLEIN, F. & K. DE JONG. 1956. Rec. trav. chim. **75:** 1285.

# PLASMA CHOLESTEROL FATTY ACIDS IN HUMAN SUBJECTS AS DETERMINED BY ALKALINE ISOMERIZATION AND BY GAS CHROMATOGRAPHY*

George D. Michaels, Priscilla Wheeler, George Fukayama,
and Laurance W. Kinsell
*Institute for Metabolic Research, Highland-Alameda County Hospital, Oakland, Calif.*

This paper presents data on the plasma cholesterol ester fatty acid composition (1) in patients studied in the metabolic ward during quantitatively constant intakes of either purified ethyl oleate or linoleate, and (2) in 35 normal males and 6 normal females whose diets were "general" at the time blood was obtained for analysis.

## *Methods*

*Extraction procedure.* Fasting plasma lipids are extracted with 25 volumes of solution containing equal parts of ethanol and acetone. The plasma is added slowly to the solvent with shaking; this is brought to a boil and filtered rapidly, using fat-free filter paper. Aliquots of this extract are used for the column separation of the cholesterol esters.

*Preparation of solution in petroleum ether.* Two 50-ml. aliquots of the plasma filtrate, each representing 2 ml. of plasma, are evaporated to dryness under partial vacuum at approximately 50° C. Five ml. of petroleum ether is added to the residue to dissolve the fat. This is added to the column. The tube is washed 3 times with 2-ml. portions of petroleum ether and these portions are added to the column. After the absorption of the petroleum ether by the Celite-silicic acid, 100 ml. of petroleum ether is added for complete elution of the cholesterol esters. The rate is adjusted by application of slight positive pressure to attain a flow rate of approximately 1 ml./min.

*Preparation of the column.* The column consists of a 25-ml. burette with a self-lubricating Teflon plug assembly† and a 125-ml. flask fused to the top of the burette as a reservoir. A glass wool plug is introduced and a mixture of equal parts by weight of Celite and silicic acid is added with tamping to a height of 10 cm.

Many investigators who use silicic acid for the separation of the various fat components advise the use of certain mesh sizes and activation by heat[1] or by dehydrating solvents.[2] Such activation will increase the efficiency considerably if one is interested in obtaining the maximum amount of lipid adsorption per gram of silicic acid. However, dehydration of silicic acid below a certain point will eliminate its adsorptive power almost completely. The degree of activation affects not only the amount of fat adsorbed per gram, but also the elution of certain fats. When 100 ml. of petroleum ether is added to the col-

---

* The work reported in this paper was supported in part by grants from The Armour Laboratories, Paterson, N. J.; Carnation Company, Los Angeles, Calif.; Schering Corporation, Bloomfield, N. J.; Alameda County Heart Association, Oakland, Calif.; and the National Institutes of Health, Public Health Service, Bethesda, Md.

† "Ultramax," Fischer and Porter Company, Hatboro, Pa.

umn containing nonactivated silicic acid (22 per cent water, as received from the manufacturer), it will quantitatively elute all cholesterol esters. If activated silicic acid is used, the cholesterol esters will be eluted quantitatively only when diethyl ether is added to the petroleum ether. For the investigation described in this paper, nonactivated silicic acid was used.

*Alkaline isomerization technique.* A solution of 21 per cent KOH ethylene glycol is used for the alkaline isomerization.[3] One ml. of this material is used as described for microisomerization by Holman.[4] We did not find the results of this procedure for the analysis of small amounts of fats to be satisfactory, especially for dienoic acids, with which the error was as high as 50 per cent of the theoretical value in some cases. We believe that this resulted from the high absorption by the blank, especially in the range of 233 m$\mu$, with a resultant wide slit width in the Beckman DU spectrophotometer. This high blank can be lowered considerably by acidifying the alkaline ethylene glycol after isomerization, re-extracting the fatty acids with petroleum ether, evaporating the petroleum ether fractions, and dissolving the fatty acids in sufficient methanol to obtain the proper dilution for spectrophotometric reading. This additional step leaves as residue the bulk of the nonfat material responsible for the high blank.

*Gas phase chromatography.* The cholesterol ester collected by the evaporation of the petroleum ether eluate from the column is hydrolyzed and the resultant fatty acids are converted to their methyl esters. This product is diluted with petroleum ether to a satisfactory volume with a minimum amount of solvent and an appropriate amount is injected into the gas chromatograph.* The column employed in this study consists a 5-foot coiled stainless steel tubing of 4 mm. bore, which is packed with a polymer of adipic acid and ethylene glycol; Celite is used as the supporting material. A temperature of 200° C. and a helium gas flow of 150 ml. are maintained. A katharometer-type detector is used.

*Total cholesterol method.* Cholesterol was determined by a modification of the Schoenheimer-Sperry procedure.[5] In this modification, the initial extraction of the plasma lipids, the hydrolysis, and the precipitation of the cholesterol with digitonin are identical with the Schoenheimer-Sperry method, but the following changes are made. The excesss digitonin is removed by washing with isopropyl alcohol. The isopropyl alcohol is prepared by the addition of sufficient water to bring the concentration to 95 per cent, and sufficient cholesterol digitonide is added with shaking to obtain a saturated solution (the solubility of cholesterol digitonide in 95 per cent isopropyl alcohol is very slight). The amount used each day should be filtered.

Two blanks are prepared, one containing the orcinol and ferric chloride and the other 1 cc. of the 1 per cent digitonin solution in the acetone alcohol; both are carried through the entire procedure. The latter blank is included to check completeness of removal of excess digitonin by the isopropyl wash. The two blanks should yield identical readings.

Orcinol reagent is used for the final colorimetric analysis in place of the standard Lieberman-Burchard reaction. The primary reason for the use of this color reaction is that no demonstrable change in color occurs within two hours if the tubes are kept out of the direct sunlight. The reagent used is easily prepared and remains good for several months.

---

* The Aerograph, manufactured by Wilkens Instrument and Research, Berkeley, Calif., is used for this procedure.

*Total lipids and iodine value method.* The total lipids were determined by Bragdon's method.[6] Iodine values were determined by a colorimetric adaptation of the pyridine dibromide method.[7] The test consists of preparation of a series of standards (oleic acid, 1 to 6 mg.), and the addition of a known quantity of the dibromide solution to each. The color extinction is plotted. The unknown is prepared in the same manner and compared with the standard. Colorimetric analysis by this procedure is faster and more reproducible than by the usual titration methods.

## *Experimental Observations*

Fasting plasma cholesterol fatty acid values in a group of 35 normal adult males and 6 normal females, all under the age of 40, are shown in TABLES 1 and 2. The most impressive finding is the uniformly high content of dienoic acids (50 per cent in the females and 44 per cent in the males). All of these values were determined by alkaline isomerization.

FIGURE 1 shows the patterns obtained by gas chromatography of cholesterol fatty acid samples from one male and one female control, respectively; TABLE 3 shows the comparison of the percentage composition of samples which were

TABLE 1

NORMAL FEMALES (6)

| | Range | Mean | Standard error of the mean ± |
|---|---|---|---|
| Total lipids | 566–719 | 663 | 24.6 |
| Total cholesterol | 168–228 | 201 | 10.5 |
| Cholesterol ester fatty acid iodine values | 124–146 | 140 | 3.4 |
| Cholesterol ester fatty acids saturated | 15–27 | 19 | 1.8 |
| Monoenoic | 14–26 | 20 | 1.7 |
| Dienoic | 43–54 | 50 | 1.5 |
| Trienoic | 2.2–4.8 | 4.2 | 0.41 |
| Tetraenoic | 3.4–6.5 | 5.1 | 0.52 |

TABLE 2

NORMAL MALES (35)

| | Range | Mean | Standard error of the mean ± |
|---|---|---|---|
| Total lipids | 484–984 | 697 | 20.2 |
| Total cholesterol | 148–285 | 202 | 5.1 |
| Cholesterol ester fatty acid iodine values | 117–150 | 133 | 1.6 |
| Cholesterol ester fatty acids saturated | 0–36 | 18 | 1.6 |
| Monoenoic | 9–65 | 30 | 2.2 |
| Dienoic | 33–58 | 44 | 0.92 |
| Trienoic | 0.2–8.1 | 5.4 | 0.23 |
| Tetraenoic | 2.3–8.1 | 5.4 | 0.23 |

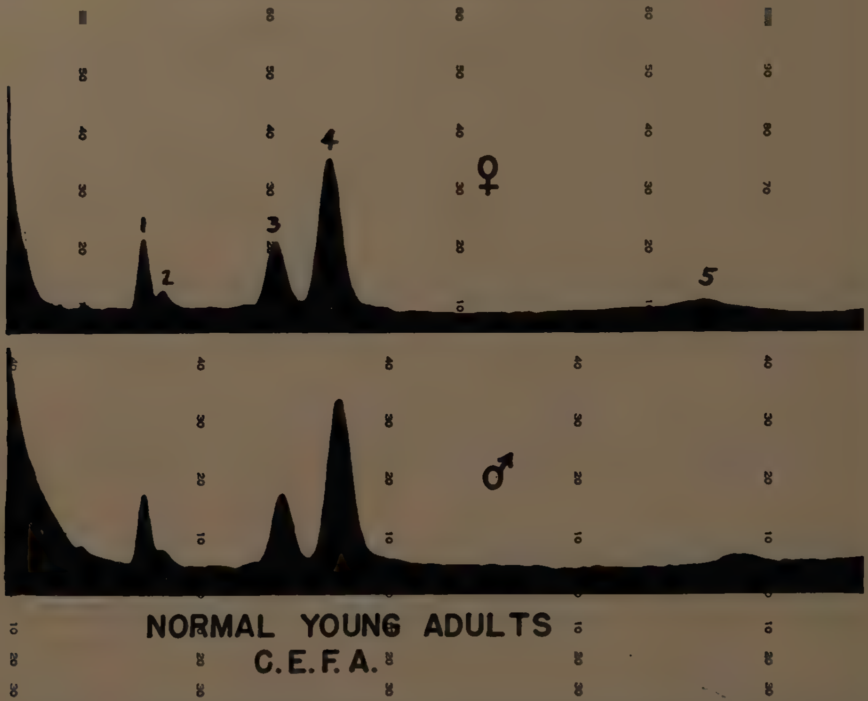

Figure 1. Plasma cholesterol fatty acids in normal males and females: (1) palmitic acid; (2) palmitoleic acid (?); (3) oleic acid; (4) linoleic acid; and (5) arachidonic acid.

Table 3

Cholesterol Ester Fatty Acid Composition

| | Normal male | | Normal female | |
|---|---|---|---|---|
| | Gas chromatography | Alkaline isomerization | Gas chromatography | Alkaline isomerization |
| Saturated | 14.1 | 16.3 | 16.0 | 15.9 |
| Monoenoic | 31.1 | 26.2 | 27.6 | 27.9 |
| Dienoic | 46.7 | 51.1 | 51.7 | 52.2 |
| Tetraenoic | 8.1 | 6.4 | 3.7 | 4.0 |

taken from two patients and were analyzed by both methods. Good agreement is observed in the dienoic acid component and somewhat variable agreement in the other components.

In one study[8] it was found that the administration of ethyl linoleate to a young normal male resulted in striking elevation of the cholesterol ester fatty acid iodine values to levels in excess of 250. Unfortunately, at that time it was impossible to measure the individual fatty acids. In some of the studies that follow, equal or greater amounts of linoleate have been administered to

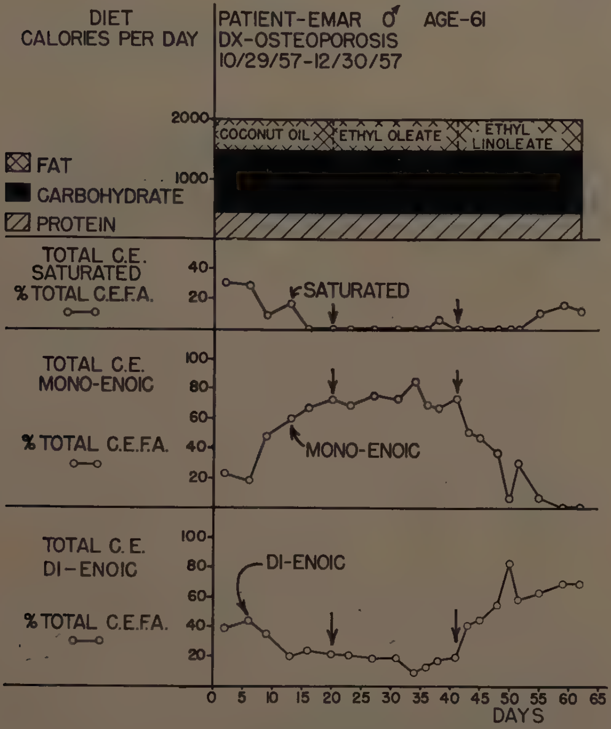

FIGURE 2. Plasma cholesterol fatty acids in relation to food intake in patient EMAR.

patients with a variety of abnormalities. In none of these patients were iodine values in excess of 170 obtained.

Patient EMAR, aged 61, a male patient with marked osteoporosis, during the course of metabolic study received formula diets that were constant except for the type of fat. The fats used were coconut oil, ethyl oleate (99.8 per cent pure), and ethyl linoleate (95 per cent pure). The findings are shown in FIGURE 2. In the case of oleate and linoleate the cholesterol esters essentially mirror the fats that were fed. The monoenoic acid content also increased during coconut oil ingestion.

Patient HMEN, a male, aged 55, with mild diabetes and advanced arteriosclerosis, fed ethyl oleate (85 per cent pure) followed by ethyl linoleate, showed much the same cholesterol ester fatty acid patterns as the previous patient. These findings are shown in FIGURE 3.

A male patient, AING, aged 34, with diabetes of moderate severity, received oleate followed by linoleate in the amounts shown in FIGURE 4. As in the previous patients, the cholesterol esters reflect the composition of the administered fat. On admission to the hospital, this patient was in poor diabetic control. The tetraenoic acid content of his cholesterol esters was about twice the level observed in normal and in most other patients so far studied (FIGURE

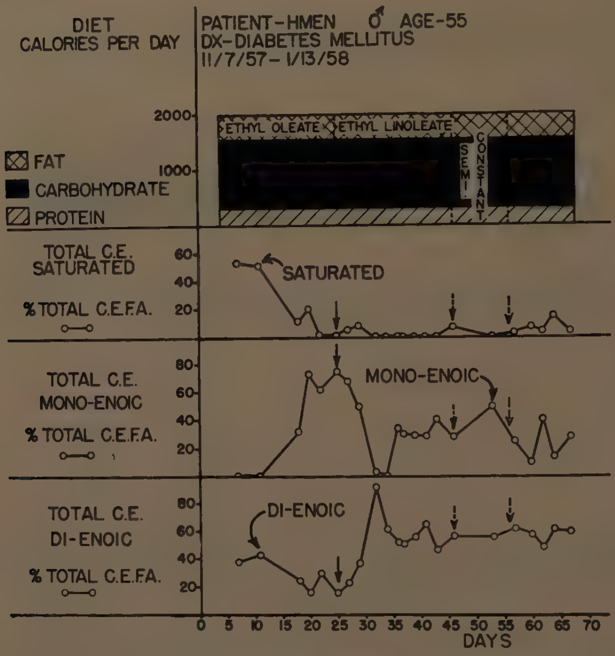

FIGURE 3. Plasma cholesterol fatty acids in relation to food intake in patient HMEN.

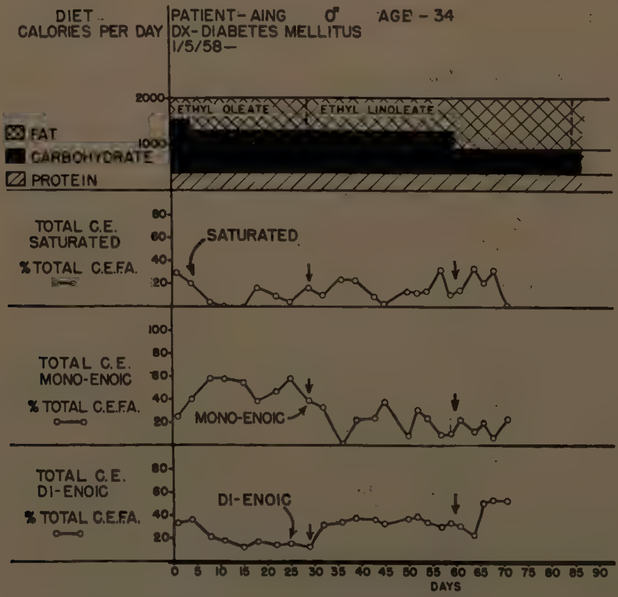

FIGURE 4. Plasma cholesterol fatty acids in patient AING in relation to food intake.

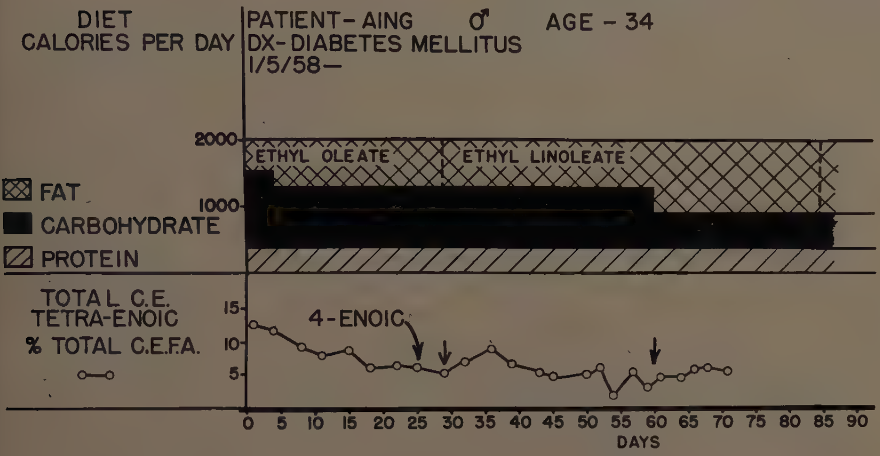

FIGURE 5. Elevated plasma cholesterol tetraenoic acid in patient AING during period of poor diabetic control. As diabetes came under full control, tetraenoic acid reached "normal" levels.

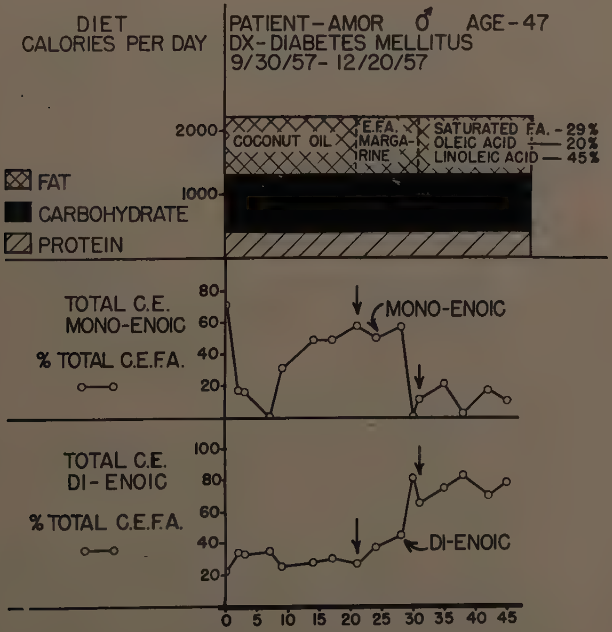

FIGURE 6. Plasma cholesterol mono- and dienoic acids in relation to dietary fat intake.

5). The level of the tetraenoic acid fell to "normal" as diabetic control improved. The significance of this observation is under investigation.

FIGURE 6 shows the findings in a male patient, AMOR, aged 47, with severe, completely insulin-dependent diabetes. Substitution of fats containing relatively large amounts of linoleic acid for coconut oil produced the expected fall in cholesterol and total lipid, and a marked increase in the dienoic acid content of the cholesterol esters at the expense of monoenoic acid.*

## *Summary*

A modification of the Riemenschneider technique for determination of unsaturated fatty acids by alkaline isomerization is presented. Application of this modification permits accurate determination of amounts of material of the magnitude of 0.3 mg.

On the basis of data so far available, reasonably good agreement is obtained between plasma cholesterol ester fatty acid values obtained by alkaline isomerization and by gas phase chromatography.

Normal young males and females on a general diet have a predictable level of dienoic acid in the cholesterol esters. This approaches 50 per cent. The other fatty-acid components of the cholesterol esters are considerably more variable.

The fatty acid composition of the diet modifies to a marked and relatively predictable degree the qualitative and quantitative composition of the cholesterol esters. This statement applies particularly to studies with purified ethyl oleate and ethyl linoleate.

## *Acknowledgments*

We thank H. P. Chin, Yvonne Fisher, Florence Olson, and Sadie Smyrl for their technical assistance.

## *References*

1. TRUEBLOOD, K. N. & E. W. MALMBERG. 1950. J. Am. Chem. Soc. **72:** 4112.
2. HIRSCH, J. 1958. Rept. Committee on Problems of Lipid Analysis. Rockefeller Inst. New York, N. Y.
3. HERB, S. F. & R. W. RIEMENSCHNEIDER. 1953. Anal. Chem. **25:** 953.
4. HOLMAN, R. T. 1957. Measurement of polyunsaturated fatty acids. *In* Methods of Biochemical Analysis. **4:** 99. Interscience. New York, N. Y.
5. MICHAELS, G. D., G. FUKAYAMA, H. P. CHIN & P. WHEELER. 1958. Proc. Soc. Exptl. Biol. Med. **98:** 826.
6. BRAGDON, J. H. 1951. J. Biol. Chem. **190:** 513.
7. YASUDA, M. 1931. J. Biol. Chem. **94:** 401.
8. KINSELL, L. W., R. FRISKEY, S. SPLITTER & G. D. MICHAELS. 1958. Lancet. **1:** 334.

---

* The preparation containing 45 per cent linoleic acid was Whirl, produced by The Procter & Gamble Company, Cincinnati, Ohio.

# GAS CHROMATOGRAPHY IN AMINO ACID ANALYSIS

M. Bier

*Department of Organic Chemistry and Enzymology, Fordham University, New York, N. Y.; Department of Protein and Enzyme Chemistry, Institute of Applied Biology, New York, N. Y.*

Priscilla Teitelbaum

*Institute of Applied Biology, New York, N. Y.*

## *Introduction*

The analysis of amino acids is an essential part of peptide and protein studies. Not only is it of importance for the determination of the over-all composition of these biological materials, but it has acquired added importance in studies of amino acid sequence in peptide chains. The special problems encountered in sequence studies are the limitation of available material and the large number of analyses required. Present available methods fulfilling these requirements are paper chromatography and paper electrophoresis,[1] particularly high-voltage electrophoresis.[2]

Briefly, the advantages of gas chromatography over either of the above two methods are speed, sensitivity, and the automation of the method. Unfortunately, amino acids are nonvolatile and therefore cannot be determined by gas chromatography. However, there are several chemical reactions whereby the amino acids can be converted into volatile derivatives suitable for gas chromatographic analysis. Primarily, this paper will be a survey of available reactions, with suggestions for possible methods of utilizing them.[3] The development of specific procedures will require considerably more time and the cooperative efforts of a number of laboratories.

As an example of possible volatile derivatives, we shall consider various derivatives of alanine (TABLE 1), one of the simplest amino acids. Alanine itself is nonvolatile because of its zwitterion structure. In general, the presence of two functional groups in a molecule, as in glycols or in aminoalcohols, results in relatively elevated boiling points, due to hydrogen bonding. Therefore there is a distinct advantage in using the degradation products obtained by decarboxylation; these products not only have one less carbon, but also have lost one functional group. Most volatile are the aldehydes and the amines, there being a definite advantage in favor of the latter.

## *Ninhydrin Oxidation*

The oxidation with ninhydrin of amino acids to corresponding aldehydes containing one less carbon is one of the most extensively studied chemical reactions of amino acids. It is frequently employed for the quantitative estimation of total amino nitrogen in hydrolyzates, either colorimetrically or by measurement of the $CO_2$ liberated. Virtanen and Rautanen[4] have shown that the formation of aldehydes is quantitative by determining titrimetrically the aldehydes obtained by distillation of volatile reaction products. This result

Table 1

Melting or Boiling Points of Alanine and its Derivatives

| Compound | M.P. (°C.) | B.P. (°C.) |
|---|---|---|
| Alanine | 297 | |
| Methyl alanine | | 38 at 15 mm. |
| Acetyl alanine | 137 | |
| 2-Aminopropanol | | 176 |
| Propylene glycol | | 188 |
| Acetic acid | | 118 |
| Ethanol | | 78 |
| Acetaldehyde | | 21 |
| Ethylamine | | 17 |

was confirmed recently by Hunter and Potter,[5] who also employed a distillation procedure. Hunter *et al.*[6] have also shown that the aldehydes in the distillate can be separated by gas chromatography.

By dispensing with the distillation, we were able to develop a microrpocedure for determining the volatile aldehydes gas chromatographically. The procedure is based upon the extraction of the aldehydes from the reaction mixture with organic solvents, water being undesirable as a carrier in gas chromatography. The amino acid and ninhydrin solutions and the appropriate organic solvent are introduced into a 1-ml. medical glass ampule. Chlorinated hydrocarbons, such as carbon tetrachloride and tetrachloroethane, available in spectral grades, are best for this purpose because their specific density is greater than that of water. The ampule is sealed and shaken constantly for 20 to 30 min. in boiling water. It is then cooled in an ice bath and centrifuged in an upside-down position in order to force all the liquid into the small conical top portion of the ampule, the heavy hydrocarbon settling at the bottom. When the ampule is opened, the bottom hydrocarbon layer can be withdrawn conveniently with the syringe used for the injection of the sample into the gas chromatography apparatus, the sample size being between 20 and 40 $\mu$l. In this way, a minimum of 0.1 ml. of an amino acid solution of a concentration yielding about 25 $\mu$g. of aldehyde and containing about 2 to 10 $\mu$g. of amino nitrogen can be treated with 0.1 ml. of ninhydrin and extracted with 0.1 ml. of the organic solvent. This procedure requires far less material than distillation (10 ml. of an amino acid solution containing about 3 mg. of amino acid[6]) and the necessary amount of material is of the order of magnitude easily obtainable from paper chromatographic separation of peptides or amino acids. No loss of aldehydes due to evaporation or transfer can occur, and the whole procedure, including oxidation, extraction, and analysis, requires about 40 min. If a number of samples are run simultaneously, this time is further reduced to the actual time of gas-chromatographic separation which, at 80° C. and with carbon tetrachloride, is about 10 min. for the more volatile aldehydes.

The aqueous solvent for the amino acid–ninhydrin mixture can be that recommended for the quantitative color development of the ninhydrin reaction.[7] To facilitate the extraction step, an almost saturated salt solution is preferable; a 10 per cent $KH_2PO_4$–21 per cent NaCl solution was also employed, as utilized by Virtanen and Rautanen[4] in the distillation of the aldehydes. The salts are added to the ampule in dry form. Nevertheless, the partition quotient of acetaldehyde is not very favorable, and either repeated extraction or a correction factor is necessary. The ninhydrin employed is in 50 per cent excess over that stoichiometrically required, that is, approximately 1.5 × 25.4 mg. ninhydrin/mg. amino nitrogen. If larger amounts of material are available, the reaction can be carried out in screw-topped conical centrifuge tubes with 1 ml. of the amino acid and ninhydrin solution and 1 ml. of the organic solvent. No substantial difference was observed if the organic solvent was present during the reaction or if it was added after cooling. Upon centrifugation, a substantial volume of solvent can be transferred to another tube and there dried with a desiccant, so that repeated analyses are possible.

For quantitative estimation of amino acids, standard curves were prepared by analyzing the corresponding aldehydes in solutions of known concentrations. FIGURE 1 shows the standard curve for isobutyraldehyde; the indicated points correspond to the values obtained on the analysis of valine solutions of various concentrations. A good quantitative agreement is observed.

FIGURE 2 represents the diagram resulting from the analysis of a mixture of

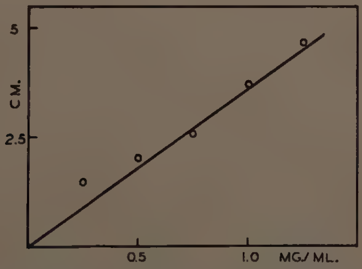

FIGURE 1. Solid line: standard curve for isobutyraldehyde in $CCl_4$. Circles: ninhydrin oxidation products of valine. Silicone Dow-Corning 200 column, 78° C., 20 psi, sample size 20 μl. Vapor fractometer at highest sensitivity.

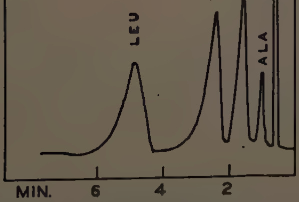

FIGURE 2. Chromatogram of the oxidation products of a mixture of alanine, 2-aminobutyric acid, valine, and leucine in ethane tetrachloride. Silicone Dow-Corning 200 column, 78° C., 20 psi, sample size 20 μl.

TABLE 2

VOLATILE NINHYDRIN OXIDATION PRODUCTS

| Amino acid | Aldehyde | B.P. (°C.) |
|---|---|---|
| Glycine | Formaldehyde | −21 |
| Alanine | Acetaldehyde | 21 |
| 2-Aminobutyric acid | Propionaldehyde | 48 |
| Valine | Isobutyraldehyde | 63 |
| Leucine | Isovaleraldehyde | 92.5 |
| Isoleucine | Methylethylacetaldehyde | 93 |
| Norleucine | Valeraldehyde | 103 |
| Methionine | Methylmercaptopropionaldehyde | 60 at 12 mm. |
| Phenylalanine | Phenylacetaldehyde | 194 |

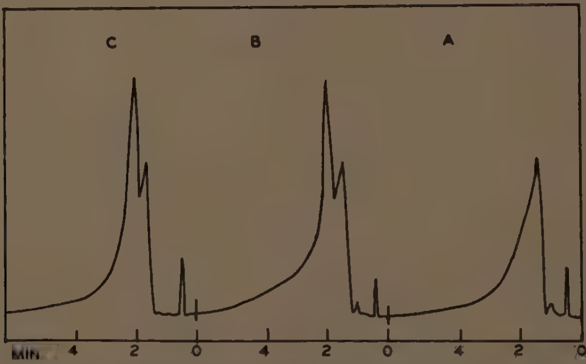

FIGURE 3. (A) volatile impurity present in dimethylsulfoxide; (B) 0.25 per cent isovaleraldehyde in dimethylsulfoxide; and (C) Oxidation product of equimolecular leucine in dimethylsulfoxide. Dodecylphthalate column, 150° C., 25 psi.

four amino acids—alanine, α-aminobutyric acid, valine, and leucine—in proportions giving equal amounts of aldehyde. The reduced size of the acetaldehyde peak in the amino acid extract will be noted; this is due to the unfavorable partition coefficient.

A list of naturally occurring amino acids giving volatile aldehydes is given in TABLE 2. Although it was not assayed, glycine is included in the list.

The possibility of carrying out the ninhydrin oxidation in organic solvents was also explored. Strongly polar solvents in which the amino acids are readily soluble would be particularly useful; such a solvent is dimethylsulfoxide. FIGURE 3 presents the diagrams obtained on analysis of the oxidation product of leucine, of pure dimethylsulfoxide, and of a control solution of isovaleraldehyde in dimethylsulfoxide. While this reaction medium does not require extraction, its usefulness is limited by the strong absorption of the solvent on the column.

### *Decarboxylation*

Only about eight amino acids are accessible to analysis by the above method. Fortunately, the list can be extended by decarboxylation. TABLE 3 lists the

TABLE 3

ENZYMATIC DECARBOXYLATION PRODUCTS

| Amino acid | Amine | B.P. (°C.) |
|---|---|---|
| Lysine | Cadaverine | 180 |
| Ornithine | Putrescine | 158 |
| Tyrosine | Tyramine | 220 |
| Histidine | Histamine | 210 at 18 mm. |
| Arginine | Agmatine | — |
| Glutamic acid | 4-Aminobutyric acid | — |

amino acids for which specific bacterial decarboxylating enzymes are available. These enzymes can be used for the quantiative determination of the individual amino acids by determining the amount of $CO_2$ liberated in a Warburg apparatus.[8] This requires the use of enzymes specific for the individual amino acids. At least two of the amines, cadaverine and putrescine, and possibly a third one, tyramine, could be determined by gas chromatography simultaneously.

It is well known that all the decarboxylating enzymes have pyridoxal phosphate as their coenzyme. The mechanism of their catalytic action was postulated as follows:

$$\mathrm{XCHO} + \mathrm{H_2NCHRCO_2H} \xrightarrow[-\mathrm{H_2O}]{} \mathrm{XCH{=}NCHRCO_2H} \xrightarrow[-\mathrm{CO_2}]{}$$

$$\mathrm{XCH{=}NCH_2R} \xrightarrow[\mathrm{H_2O}]{} \mathrm{XCHO} + \mathrm{H_2NCH_2R}$$

where $X$ stands for the ring system of pyridoxine attached to the apoenzyme· An active carbonyl group is thus involved in the reaction. The catalytic action of three aromatic aldehydes on amino acid decarboxylation was recently studied by Dose.[9] Benzaldehyde was shown to be the least suitable catalyst, the cleavage of the intermediate product formed with valine giving a mixture of both benzylamine and isobutylamine in proportions of 2:1. *p*-Anisaldehyde was more satisfactory, yielding the corresponding derivatives in proportions of 1:1. The reaction of valine with *p*-dimethylaminobenzaldehyde was most satisfactory, giving only the desired isobutylamine. The same catalyst was employed also on other amino acids at temperatures ranging from 150 to 200° C.; the yields of the corresponding amines were only 25 to 75 per cent, but all amino acids reacted except cysteine, cystine, and tryptophan. More important is the fact that the results with the three aldehydes fitted the theoretical views of the mechanism of the reaction and open a definite approach toward finding more efficient catalysts.

A more empirical decarboxylation procedure was employed by Abderhalden and Gebelein,[10] who reported that, by heating tyrosine in diphenylmethane at 240° C., a 95 per cent yield of tyramine was obtained. The reaction was found to proceed also for glycine and alanine, but no yields were reported. Other catalysts, suggested at various times, were barite in glycol or glycerol solutions[11] for the decarboxylation of methylated amino acids, and various metal salts, notably cupric chloride,[12] for pyrolytic decarboxylation.

TABLE 4

YIELD OF AMINES OBTAINABLE BY DECARBOXYLATION OF AMINO ACIDS

| Amino acid | Decarboxylation with | | | |
|---|---|---|---|---|
| | Diphenylmethane | | *p*-Dimethylaminobenzaldehyde | |
| | Percentage yield | Temperature (°C.) | Percentage yield | Temperature (°C.) |
| Alanine | 78 | 240 | 48 | 180 |
| Glycine | 29 | 235 | 71 | 180 |
| Leucine | 84 | 235 | 78 | 190 |
| Lysine | 10 | 260 | 80 | 210 |
| Methionine | 77 | 240 | 48 | 190 |
| Phenylalanine | 88 | 225 | 36 | 175 |
| Proline | 70 | 235 | 40 | 180 |
| Serine | 32 | 245 | 66 | 195 |
| Threonine | 44 | 250 | 78 | 180 |
| Valine | 83 | 240 | 80 | 190 |
| 2-Aminovaleric acid | 85 | 235 | 72 | 180 |

We have studied two of the above reactions: decarboxylation with *p*-dimethylaminobenzaldehyde and decarboxylation in diphenylmethane. The procedure employed was as follows. The amino acid (0.1 mM) was weighed directly into an ampule, and either 50 mg. of the aldehyde or 1 ml. of the hydrocarbon was added. The ampule was sealed and heated in an oil bath until the reaction was terminated, as judged by evolvement of $CO_2$. In general, the reaction with the aldehyde was faster and proceeded at a lower temperature than in the hydrocarbon. With the aldehyde, a homogeneous melt was obtained; in the hydrocarbon the amino acid dissolved only upon decarboxylation. The contents of the ampule were transferred to a distillation apparatus and the amine formed was steam-distilled into 0.01 N HCl. The extent of the reaction was determined by back-titrating the excess acid with 0.01 N NaOH. The data obtained are summarized in TABLE 4.

In no case was a quantitative decarboxylation obtained. The diphenylmethane procedure gave higher yields in all cases, except with glycine, lysine, serine, and threonine. With these amino acids, charring occurred during the heating process, which probably accounts for the lower yields.

Gas chromatographic analysis of the reaction products of the decarboxylation was also attempted. James and Martin[13] reported the separation of amines on a liquid paraffin column. Using a hexadecane column, we obtained chromatographs only at relatively high concentrations of amines (above 1 to 2 per cent), considerable tailing always being present. At lower concentrations, no satisfactory diagrams could be obtained, and the results were not better with other columns tried, namely dodecylphthalate, silicone oil Dow-Corning 200, and polyethyleneglycol. The difficulty may be either in the column or in the injection system, and it is believed that a vapor injection of amines may give better results.

For reference, a list of amino acids giving volatile amine derivatives is presented in TABLE 5; it includes 16 amino acids. Some of the most important

TABLE 5
VOLATILE DECARBOXYLATION PRODUCTS OF AMINO ACIDS

| Amino acid | Amine | B.P. (°C.) |
|---|---|---|
| Alanine | Ethylamine | 17 |
| Glycine | Methylamine | −7 |
| Histidine | Histamine | 210 at 18 mm. |
| Isoleucine | 2-Methylbutylamine | 92 |
| Leucine | Isoamylamine | 95 |
| Lysine | Cadaverine | 180 |
| Methionine | Methylmercaptopropylamine | 170 |
| Norleucine | Amylamine | 104 |
| Phenylalanine | Phenethylamine | 195 |
| Proline | Pyrrolidine | 89 |
| Serine | Ethanolamine | 172 |
| Threonine | 1-Amino-2-propanol | 160 |
| Tyrosine | Tyramine | 220 |
| Valine | Isobutylamine | 68 |
| 2-Aminobutyric acid | Propylamine | 49 |
| Ornithine | Putrescine | 158 |

amino acids, however, including cysteine, arginine, histidine, tryptophan, and the dicarboxylic acids, aspartic and glutamic, are not accessible to gas chromatographic analysis by any of the methods discussed.

## *Conclusion*

The possible application of gas chromatography to the analysis of a number of amino acids was demonstrated by employing two reactions: ninhydrin oxidation and decarboxylation. Only the ninhydrin oxidation gives quantitative results, but it is applicable to fewer amino acids. A study of better catalysts for decarboxylation and the finding of appropriate conditions giving quantitative yields of amines would extend considerably the usefulness of the method. The principal advantage of the method, in its present stage, is its rapidity. Another advantage, at least of the ninhydrin method, is that no desalting of the hydrolyzates prior to analysis appears to be necessary. In addition, gas chromatography may prove to be a valuable tool in the study of reactions of amino acids.

## *Acknowledgment*

We thank E. Cieplinski of the Perkin-Elmer Corp., Norwalk, Conn., for his help in carrying out some of the initial gas chromatographic analyses. We also thank N. Brenner of the same company for the loan of a vapor fractometer.

## *References*

1. BLOCK, R. J., E. DURRUM & G. ZWEIG. 1958. Paper Chromatography and Paper Electrophoresis. 2nd ed. Academic Press. New York, N. Y.
2. WIELAND, T. *In* Electrophoresis, Theory and Applications. M. Bier, Ed. Academic Press. New York, N. Y. In press.
3. BIER, M. & P. TEITELBAUM. 1958. (Abstr.) Federation Proc. **17**(1) : 191.
4. VIRTANEN, A. I. & N. RAUTANEN. 1947. Biochem. J. **41:** 101.
5. HUNTER, I. R. & E. F. POTTER. 1958. Anal. Chem. **30:** 293.

6. HUNTER, I. R., K. P. DIMICK & J. W. CORSE. 1956. Chem. & Ind. London. **16:** 294.
7. HARDING, V. J. & R. M. MACLEAN. 1916. J. Biol. Chem. **24:** 503.
8. NAJJAR, V. A. 1955. *In* Methods in Enzymology. **2:** 185. Colowick & Kaplan, Eds. Academic Press. New York, N. Y.
9. DOSE, K. 1957. Nature. **179:** 734.
10. ABDERHALDEN, E. & F. GEBELEIN. 1926. Z. Physiol. Chem. **152:** 125.
11. WAELE, H. 1931. Ann. physiol. physicochim. biol. **7:** 293.
12. YANAGISAWA, H., Z. HORII & T. NISHIURA. 1933. J. Pharmacol. Soc. Japan. **53:** 1221.
13. JAMES, A. T. & A. J. P. MARTIN. 1952. Analyst. **77:** 915.

# RECENT ADVANCES IN THE GAS CHROMATOGRAPHIC SEPARATION OF METHYL ESTERS OF FATTY ACIDS

C. H. Orr and J. E. Callen
*Miami Valley Laboratories, The Procter & Gamble Company, Cincinnati, Ohio*

The first reported use of gas chromatography in the separation of fatty acids was by James and Martin[1] at the Oxford Congress of Analytical Chemistry in 1952. They described the separation of acids from formic through dodecanoic on silicone–stearic acid columns, and detected the eluted acids by titration.

In 1953, Cropper and Heywood[2] extended the gas chromatographic separation to the methyl esters of the even-numbered fatty acids from $C_{12}$ to $C_{22}$. They used Dow Corning high vacuum silicone grease on Celite columns and employed a platinum-wire thermal conductivity cell as the detector. The efficiency of their columns allowed only a separation based on differences in chain length, and methyl oleate and methyl stearate were not separated.

A major contribution to the field of fatty ester separation and to gas chromatography in general was made with the invention of the gas density balance detector by Martin and James[3] in 1953. The high sensitivity of this ingenious device was largely responsible for improvements in the separation of the methyl esters of the fatty acids containing from 8 to 26 carbon atoms by James and Martin,[4, 5] James and Wheatley,[6] and Beerthuis and Keppler.[7] The high sensitivity allowed the use of extremely small samples that, in turn, reduced the band spreading that results from overloaded columns. These workers found Apiezon M or Apiezon L vacuum greases on Celite to be the preferred partition medium and reported the successful separation of saturated and monounsaturated methyl esters of the same carbon chain length, as well as some branched chain fatty esters prepared from natural lipid sources. However, methyl linoleate and methyl linolenate were not separated.

More recently Insull and James[8, 9] and Lipsky[10] have reported further refinements in the separation of high molecular weight fatty esters using Apiezon greases. These refinements resulted from improved technique in the preparation of the coated Celite and in the packing of columns. Lipsky[10] found that improvements could be made in the separation by precise control of the temperature of the detector, in this case a high-sensitivity thermal conductivity cell, through use of proportional controllers. Using Apiezon L and temperatures in the range of 200 to 250° C., Lipsky and Insull and James obtained excellent separations of methyl stearate, methyl oleate, and methyl linoleate. In no case, however, was it possible to resolve methyl linoleate and methyl linolenate on Apiezon L.

Table 1 summarizes data taken from the best curves published by the above authors and gives the efficiencies of the separations obtained. Theoretical plate calculations are based on the methyl stearate peak and the percentage impurities were calculated using the method of Glueckauf,[11] with a separation factor of 1.15 for methyl stearate relative to methyl oleate. The factor $R$ is

TABLE 1

SEPARATION OF FATTY METHYL ESTERS ON APIEZON GREASES

| $t_R$ (min.) (methyl stearate) | Theoretical plates (methyl stearate) | Resolution[12] $R$ | Percentage methyl oleate in methyl stearate | References |
|---|---|---|---|---|
| 93 | 800 | 1.70 | 3 | James & Martin[4] |
| 127 | 1000 | 1.73 | 1 | James & Wheatley[6] |
| 164 | 1500 | 3.60 | 0.4 | James[5] |
| 180 | 3000 | — | 0.01 | Insull & James[8] |
| 185 | 3500 | 4.57 | 0.001 | Insull[9] |
| 137 | 3700 | 4.15 | 0.001 | Lipsky[10] |

the resolution calculated according to the method of Jones.[12] The measurements made on the curves reproduced in the papers indicated necessarily are not as accurate as if they were made on the original recorder charts, but they are probably accurate to within 10 per cent. This summary shows the marked improvement that has been made during the past two years in the separation of fatty esters, using such nonpolar partition media as Apiezon M and Apiezon L.

FIGURE 1 was prepared from a gas chromatographic curve supplied by S. R. Lipsky of the Yale University Medical School, New Haven, Conn. It is typical of the best separations that have been obtained on methyl stearate, methyl oleate, and methyl linoleate, using Apiezon L as the partition liquid. To obtain such a curve requires optimization of almost every variable and, in addition, excellent instrumentation and technique. However, on a nonpolar partition medium such as Apiezon L, the separations obtained are mainly the result of small volatility differences in the components separated. It is doubtful that the efficiency of separation of these methyl esters on Apiezon L

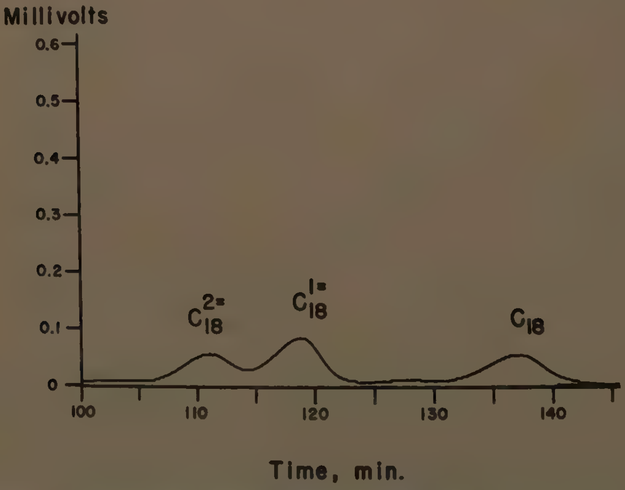

FIGURE 1. Separation of methyl esters of linoleic, oleic, and stearic acids.

can be pushed much beyond 5000 theoretical plates, and a considerably greater increase in number of theoretical plates would be required to separate methyl linoleate and methyl linolenate on this partition medium. Estimating from Glueckauf's relationships[11] and using a separation factor of 1.04 calculated from James and Martin's work,[4] it can be shown that a separation of equal quantities of methyl oleate and methyl linoleate with only 1 per cent impurity in each would require approximately 14,000 theoretical plates.

### *Discussion of Experimental Results*

The data of Insull and James,[8] indicated that nonpolar partition media were to be preferred for the separation of fatty methyl esters. It was our belief, however, that highly polar partition media might yield increased separation of saturated and unsaturated fatty esters. This was based on the fact that silver nitrate in ethylene glycol had been used for the separation of low molecular weight olefins[13] and on the reported work of Phillips[14] describing the use of metal salts of fatty acids as partition agents in the separation of olefins. In each case the materials containing double bonds exhibited longer retention times than did their corresponding saturated derivatives.

A number of materials were tried as partition liquids that on the basis of chemical structure or metal ion content would be expected to exhibit varying degrees of polarity.* These included asphaltenes, didodecylbiphenyl, tetraoctylpyromellitate, polyethylene glycol saturated with silver nitrate, powdered silver nitrate as the supporting solid for Apiezon L grease, and a number of polyether lubricating oils. None was effective in separating high molecular weight saturated and unsaturated methyl esters under the conditions tried.

Our attention was drawn to the polyester materials that are used commercially as plasticizers for vinyl chloride polymers. A large number of different types of these materials is available. Most are copolymers of dibasic acids with di- or polyglycols and have molecular weights in the three- to six-thousand range. Using one of these polyesters, Geigy's Reoplex 400, we were able to demonstrate the expected increased relative retention times of the unsaturated fatty esters on polar partition liquids.† Our preliminary findings have been published.[16]

FIGURE 2 shows two gas chromatographic separations of a mixture of methyl esters of fatty acids. The upper curve *A* was obtained on Reoplex 400 polyester plasticizer under conditions selected to give retention times of the same order of magnitude as that obtained on the same sample using Apiezon L vacuum grease (curve *B*) as the partition liquid. The retention times for the esters in the lower curve *B* are in the order:

$$C_{16}^{1=} < C_{16} < C_{18}^{1=} < C_{18}$$

---

* The term polarity is used here in a general sense to describe all the various types of cohesive forces between solute and solvent that affect retention time. An excellent discussion of these forces has been written by Keulemans.[15]

† Reoplex 400 is manufactured by The Geigy Company, Ltd., Manchester, England. Samples may be obtained through Geigy Chemical Corp., Pharmaceutical Division, Yonkers, N. Y.

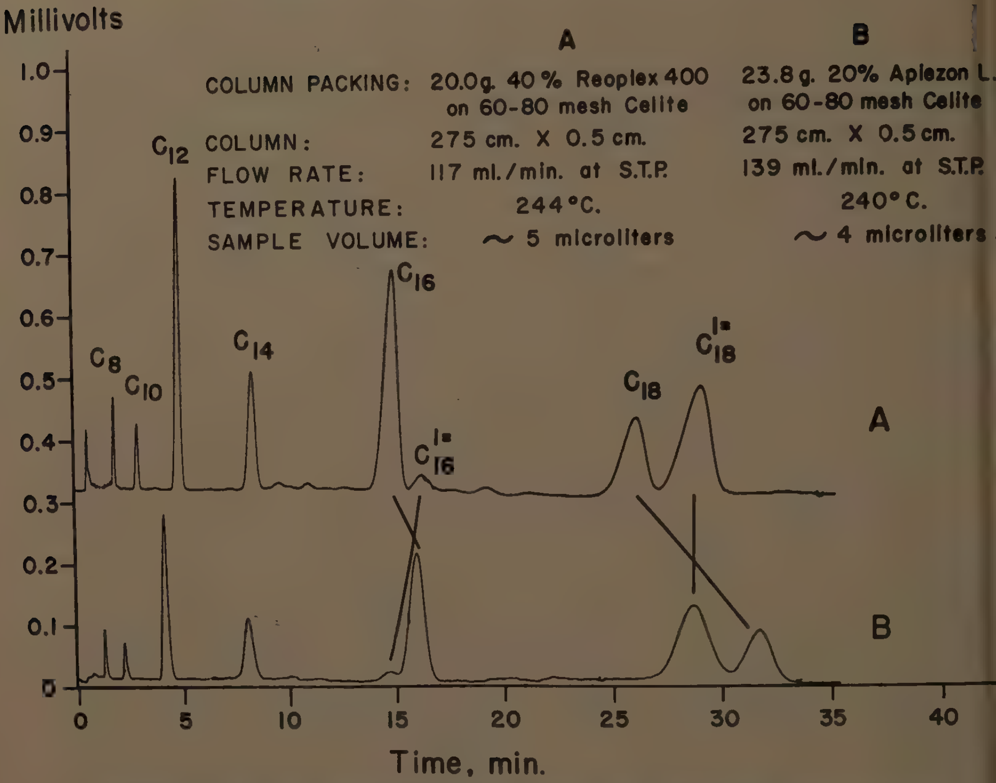

FIGURE 2. Comparison of Reoplex 400 and Apiezon L in the separation of methyl esters of fatty acids from 80 per cent hydrogenated tallow–20 per cent coconut oil.

In the upper curve *A*, a reversal of order of emergence of saturated and unsaturated fatty esters of the same chain length has occurred and it can be seen that the order is:

$$C_{16} < C_{16}^{1-} < C_{18} < C_{18}^{1-}$$

It should be pointed out that the previous workers had tried weakly polar materials such as silicone oils and aromatic compounds as partition liquids. It is reasonable to assume that these materials also have a slight tendency to retard the double bond-containing esters. It is also suggested that the tendency of these slightly polar materials to retard the unsaturated fatty esters was just sufficient to counteract the decrease in retention time that results from the slightly higher volatility of methyl oleate over that of methyl stearate. This would explain the failure of silicones and asphaltenes to effect the separation.

The only explanation that can be offered at this time for the reversal of retention times on polyesters is the simple one that the solubility of unsaturated esters in the polyester partition liquid is greater than that of saturated esters, and that the unsaturated esters show an appreciable negative deviation from Raoult's law. We have no evidence to support the formation of a weak complex such as occurs with olefins on silver ion-containing partition liquids.

A study was made of the effect on the ultraviolet spectra of adding small quantities of Reoplex 400 to solutions of methyl linoleate in carbon tetrachloride. No shifts in wave length in the ultraviolet spectra of these solutions could be detected and no change in the absorptivity of the methyl linoleate was observed. If loose chemical complexes were involved between the polyesters and the double-bond system of the methyl linoleate, changes in the ultraviolet spectrum would be expected. However, in these experiments it was impossible to maintain the same stoichiometric relationships that occur in the gas chromatography column.

FIGURE 3 shows the separation of a mixture of methyl esters of fatty acids under conditions that allow the emergence of methyl arachidonate in a reasonable time. The arachidonate was added as an enriched fraction from hog ovary fatty methyl esters. Under these conditions the methyl oleate and methyl stearate are not completely separated. Two thousand theoretical plates at methyl oleate are calculated from these data and the methyl stearate and methyl oleate are mutually contaminated to the extent of approximately 3 per cent. Methyl linolenate is separated cleanly from methyl arachidate. The peak at 49 min. is believed to be methyl arachidonate, although this retention time is lower than predicted by an extrapolation based on the multiple double-bond $C_{18}$ methyl esters. A peak of this same retention time has been obtained for samples from two different sources that were shown by ultraviolet analysis to contain methyl arachidonate. It is interesting that the peak occurs where a $C_{20}$ methyl ester with three double bonds would be expected.

Several different polyesters have been evaluated. Some have almost equaled Reoplex 400 in efficiency of separation of unsaturated fatty methyl esters, but as yet none has been found that surpasses it. In TABLE 2 there is listed a cross section of the various kinds of polyesters tested. These partition media were compared, using the separation of methyl stearate and methyl linoleate as the criterion. This was necessary because the less efficient polyesters were incapable of separating methyl stearate from methyl oleate. The data listed in TABLE 3 were obtained at 200° C. with a flow rate of 74 ml./min. of helium, using 12 ft. × ¼ in. columns packed with 60 to 80 mesh Celite 545 containing 15 per cent by weight of polyester.

Wide variations in retention times, theoretical plates, and separation factors for methyl stearate and methyl linoleate are evident from these data. They point up particularly the fact that a consideration of numbers of theoretical plates alone is insufficient to describe separation efficiency. For example, Reoplex 110 gives a column of 5100 theoretical plates at linoleate, but with a separation factor of only 1.06; the methyl linoleate peak overlaps the methyl stearate to the extent of 2 per cent, and methyl oleate and methyl stearate are not separated. On the other hand, Polyester 210-A with only 1500 theoretical plates separates methyl stearate and methyl linoleate very effectively because of the relatively high separation factor of 1.28.

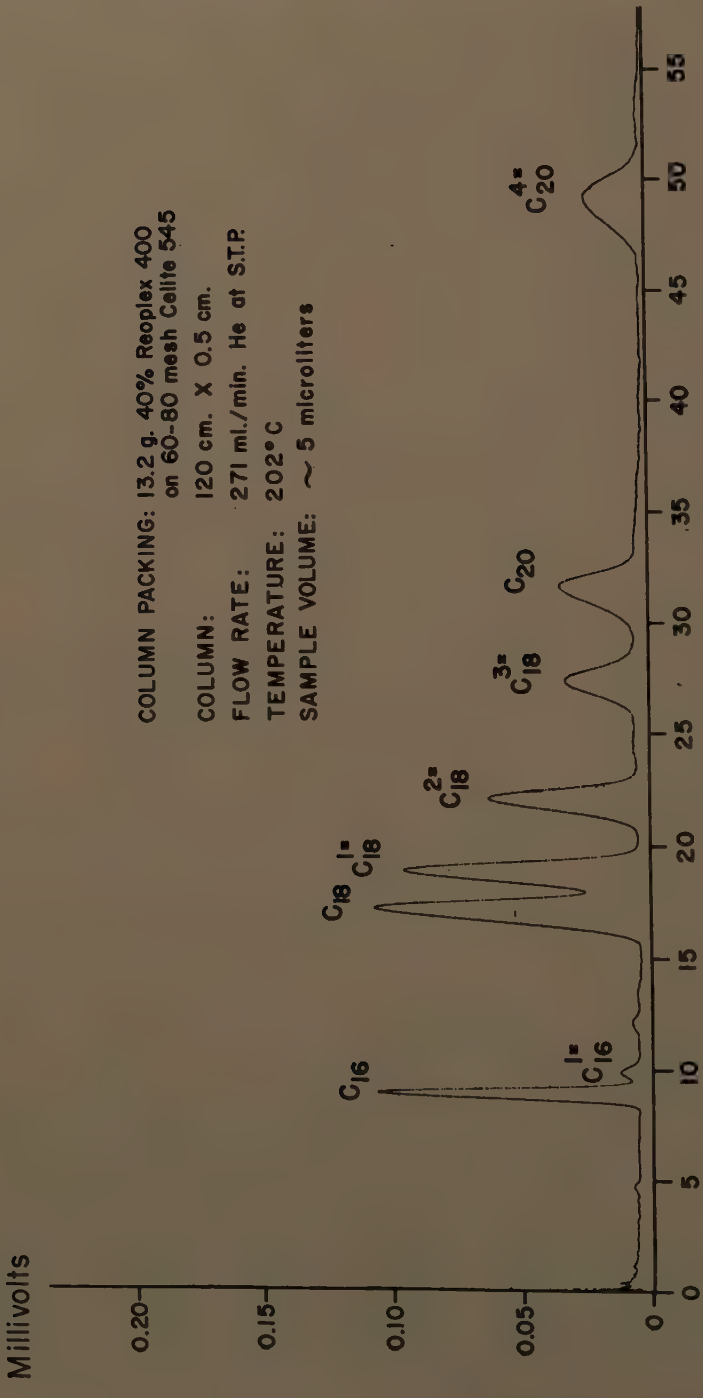

COLUMN PACKING: 13.2 g. 40% Reoplex 400 on 60-80 mesh Celite 545
COLUMN: 120 cm. X 0.5 cm.
FLOW RATE: 271 ml./min. He at S.T.P.
TEMPERATURE: 202° C
SAMPLE VOLUME: ~ 5 microliters

FIGURE 3. Separation of mixture of fatty methyl esters containing methyl arachidonate.

TABLE 2
POLYESTERS

| Trade name | Structural type |
|---|---|
| Reoplex 100* | Polypropylene sebacate |
| Reoplex 110* | Polypropylene sebacate/phthalate |
| Reoplex 220* | Polypropylene sebacate/laurate |
| Reoplex 300* | Butyl glyceryl sebacate |
| Reoplex 400* | Polyoxyalkalene adipate |
| Paraplex G-40† | Polyester |
| Paraplex G-25† | Polyester |
| Polyester 210-A‡ | Polyethylene sebacate |
| LAC-R-296§ | Polydiethyleneglycol adipate |
| LAC-2-R446§ | Polydiethyleneglycol/pentaerythritol adipate |

* The Geigy Company, Ltd., Manchester, England.
† Rohm & Haas Company, Philadelphia, Pa.
‡ Wallace & Tiernan Inc., Belleville, N. J.
§ Cambridge Industries Co., Inc., Cambridge, Mass.

TABLE 3
COMPARISON OF POLYESTER PARTITION MEDIA: SEPARATION OF METHYL STEARATE AND METHYL LINOLEATE

| Trade name | $t_R$ (min.) methyl stearate | Theoretical plates at methyl linoleate | Separation factor $\alpha$ | Weight fraction methyl stearate in methyl linoleate |
|---|---|---|---|---|
| Reoplex 100 | 145 | 7300 | 1.06 | $6 \times 10^{-3}$ |
| Reoplex 110 | 131 | 5100 | 1.06 | $2 \times 10^{-2}$ |
| Reoplex 220 | no separation | | | |
| Reoplex 300 | 94 | 4900 | 1.05 | $4.5 \times 10^{-2}$ |
| Reoplex 400 | 30 | 4700 | 1.29 | $1 \times 10^{-16}$ |
| Paraplex G-40 | 25 | 2850 | 1.21 | $1 \times 10^{-6}$ |
| Paraplex G-25 | 70 | 3200 | 1.08 | $1.5 \times 10^{-2}$ |
| Polyester 210-A | 95 | 1500 | 1.28 | $1 \times 10^{-6}$ |
| LAC-R-296 | 23 | 2600 | 1.10 | $1 \times 10^{-2}$ |
| LAC-2-R446 | 23 | 2560 | 1.32 | $5 \times 10^{-12}$ |

Conditions: 12 ft. × ¼ in. column with 15 per cent polyester on 60 to 80 mesh Celite 545 at 200° C. and 74 ml. helium/min. at S.T.P.
Sample: 5 λ containing 7 per cent $C_{18}$, 7 per cent $C_{18}^{1=}$, 11 per cent $C_{18}^{2=}$.

The four best polyester partition liquids are compared in TABLE 4, using a more stringent criterion, the separation of methyl oleate and methyl stearate. These data show that Reoplex 400 and LAC-2-R446 polyesters are the most efficient of all the materials tried. Each has its advantages. The Reoplex 400 is slightly more effective in the separation of methyl oleate and methyl stearate under the specific conditions used. The LAC-2-R446 polyester gives approximately 25 per cent shorter retention times for methyl esters under the conditions used and thus may be slightly preferred for the longer chain fatty esters. However, because of the greater polarity of the LAC-2-R446, as evidenced by the lower retention times for the saturated methyl esters, and its somewhat larger separation factor for methyl oleate and methyl stearate, the $C_{18}$ unsaturated materials are sufficiently spread to cause the peaks for methyl

TABLE 4

COMPARISON OF POLYESTER PARTITION MEDIA: SEPARATION OF METHYL STEARATE AND METHYL OLEATE

| Trade name | $t_R$ (min.) methyl stearate | Theoretical plates at methyl oleate | Separation factor $\alpha$ | Percentage methyl stearate in methyl oleate |
|---|---|---|---|---|
| Reoplex 400 | 30 | 3260 | 1.09 | 0.6 |
| Paraplex G-40 | 25 | 1890 | 1.09 | 3.0 |
| LAC-R-296 | 23 | 1100 | 1.09 | 7.0 |
| LAC-2-R446 | 23 | 1825 | 1.11 | 1.5 |

Conditions: 12 ft. × ¼ in. column with 15 per cent polyester on 60 to 80 mesh Celite 545 at 200° C. and 74 ml. helium/min. at S.T.P.

Sample: 5 λ containing 7 per cent $C_{18}$, 7 per cent $C_{18}^{1=}$, 11 per cent $C_{18}^{2=}$.

linolenate to overlap those of methyl arachidate, the first member of the $C_{20}$ fatty esters. In this respect Reoplex 400 appears to effect the optimum separation within the $C_{18}$ series without overlapping the first member of the $C_{20}$ series. Methyl esters from odd-numbered chain lengths would interfere, of course, when using either polyester. In these cases, it would be preferable to make a chain-length separation using Apiezon L or silicone grease and then separate each chain-length fraction into its various components on a polyester column.

FIGURE 4 is a plot of the logarithm of the corrected retention volumes of the saturated fatty methyl esters relative to the number of carbon atoms in the fatty chain. The relationship is linear over the range 8 to 22 carbons. A similar plot (FIGURE 5) can be made for the monoethenoid fatty esters series, three members of which were available. The slope of this plot is the same as that for the saturated esters and results in a separation factor in terms of retention volumes for both series of 1.38 per —$CH_2$— group.

A plot of the logarithms of the retention volumes of the unsaturated $C_{18}$ fatty

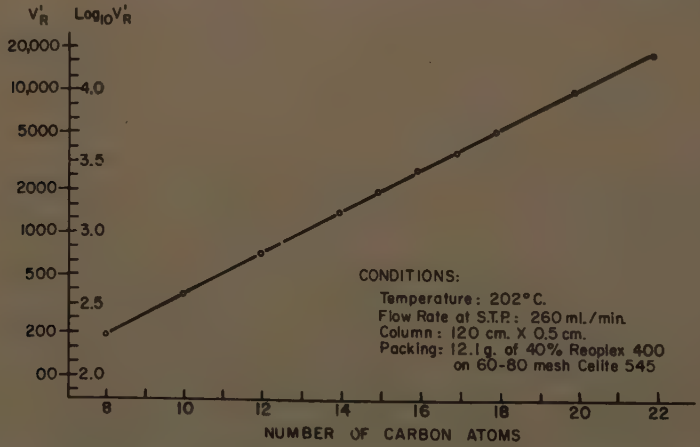

FIGURE 4. Methyl esters of saturated fatty acids. $\log_{10} V'_R$ vs. number of carbon atoms in fatty acid.

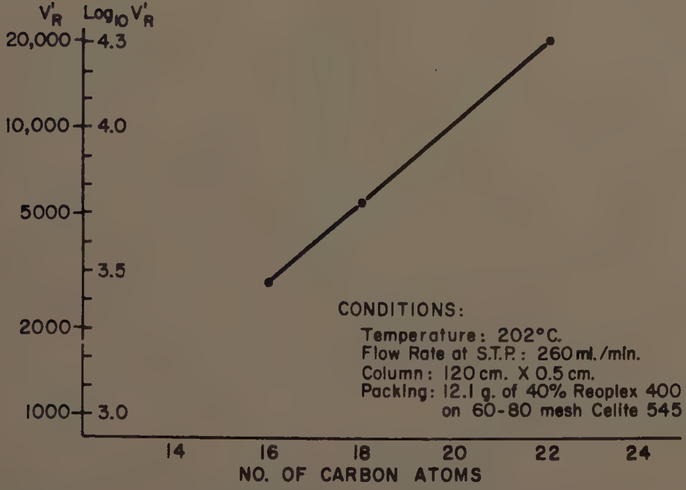

FIGURE 5. Methyl esters of monoethenoid fatty acids. $\log_{10} V'_R$ vs. number of carbon atoms in fatty acid.

methyl esters relative to the number of double bonds in the fatty ester (FIGURE 6) is also linear. The separation factor in this case is 1.21 per double bond.

The most satisfactory method of reporting retention volume data is on a relative basis with reference to an internal standard. In practice, small differences (2 or 3 per cent) in flow rate and column temperature that may be encountered from day to day on the same column cause marked differences in retention volume, but do not appreciably affect the relative retention volumes. It is also difficult to prepare two identical columns that will give exactly the same retention volumes under the same conditions. By use of relative retention volumes, however, the data from similar columns are found to agree,

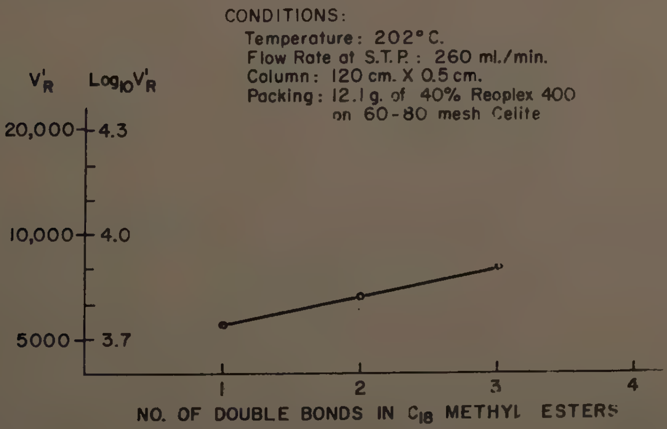

FIGURE 6. Methyl esters of $C_{18}$ fatty acids. $\log_{10} V'_R$ vs. number of double bonds.

TABLE 5

RETENTION VOLUMES ON REOPLEX 400 COLUMNS AT 200° C. RELATIVE TO METHYL PALMITATE

| | | | |
|---|---|---|---|
| Methyl caprylate | 0.073 | Methyl oleate | 2.10 |
| Methyl caprate | 0.138 | Methyl linoleate | 2.50 |
| Methyl laurate | 0.268 | Methyl linolenate | 3.11 |
| Methyl myristate | 0.511 | Methyl arachidate | 3.53 |
| Methyl palmitate | 1.00 | Methyl arachidonate | 5.52 |
| Methyl palmitoleate | 1.10 | Methyl behenate | 6.62 |
| Methyl stearate | 1.90 | Methyl erucate | 7.24 |

and qualitative identifications are simplified. TABLE 5 lists the retention volumes relative to methyl palmitate for all the methyl esters for which data are available.

### *Quantitative Use of Polyester Partition Liquids*

There are some important problems involving the use of polyester partition media for quantitative analysis that for the moment remain unsolved. These arise from the volatility and thermal instability of the currently available polyesters.

In the polymerization of a dibasic acid and a diol the resultant product usually consists of polymers having a broad molecular weight range. It is often difficult to drive the polymerization reactions to completion. Consequently, all the commercial polyesters contain small amounts of monomer substances and varying amounts of low molecular weight polymers having sufficient volatility to bleed slowly out of the column. Therefore, it is necessary to pretreat columns prepared from these polyesters for several hours at use temperature with nitrogen or helium flowing through them before they will give a steady baseline on the recorder.

An additional source of difficulty encountered with the polyesters derives from their chemical structure. Being esters, they will slowly undergo transesterification reactions with the sample esters at elevated temperatures. This effect is demonstrated in TABLE 6, which gives the quantitative results on a synthetic mixture separated on a Reoplex 400 column at 240° C. All of the component esters undoubtedly reacted to some extent with the column polyesters. However, because the residence time in the column was different for

TABLE 6

QUANTITATIVE ANALYSIS OF SYNTHETIC MIXTURES OF FATTY METHYL ESTERS ON REOPLEX 400 AT 240° C.

| | Percentage weighed | Percentage found (percentage peak area) | Difference |
|---|---|---|---|
| Methyl palmitate | 24.9 | 35.7 | +10.8 |
| Methyl stearate | 25.0 | 26.1 | +1.1 |
| Methyl oleate | 25.0 | 22.5 | −2.5 |
| Methyl linoleate | 25.1 | 15.7 | −9.4 |

TABLE 7

QUANTITATIVE ANALYSIS OF SYNTHETIC MIXTURES OF FATTY METHYL ESTERS ON REOPLEX 400 AT 200° C.

| | Synthetic Mixture 1 | | | Synthetic Mixture 2 | | |
|---|---|---|---|---|---|---|
| | Percentage weighed | Percentage found | Difference | Percentage weighed | Percentage found | Difference |
| Methyl palmitate | 10.8 | 13.2 | +2.4 | 24.9 | 26.7 | +1.8 |
| Methyl stearate | 18.8 | 19.2 | +0.4 | 25.0 | 25.8 | +0.8 |
| Methyl oleate | 23.8 | 24.8 | +1.0 | 25.0 | 25.6 | +0.6 |
| Methyl linoleate | 32.1 | 29.3 | −2.8 | 25.1 | 21.8 | −3.3 |
| Methyl linolenate | 14.5 | 13.5 | −1.0 | | | |

each component, more reaction would be expected to have occurred for the peaks emerging last. When calulated on a per cent-peak-area basis, this effect should result in high values for the fast components and low values for the slow components. The data bear this out and make quantitative use of the polyester partition media unattractive at 240° C.

Lowering the temperature to 200° C. results in considerable improvement over the results obtained at 240° C. The quantitative analysis of the above mixture at 200° C. is tabulated as Synthetic Mixture 2 in TABLE 7; also tabulated is a five-component mixture containing methyl linolenate. Although further reductions in the transesterification reaction certainly can be made by using even lower temperatures, it is expected that the low volatility of the sample fatty esters will make 185° C. the approximate lower limit. Even at this temperature, the retention times of esters such as methyl arachidonate and methyl erucate will be quite high. It is important for biological studies to be able to analyze these esters rapidly and accurately. A possible solution to the problem would be the use of a combination of two internal standards, one a high molecular weight hydrocarbon of suitable retention time that would not react with the polyester and the other a methyl ester of an odd-numbered fatty acid such as methyl *n*-heptadecanoate that would not overlap the fatty esters normally encountered. Calibration of the internal standard mixture on a nonreactive column would be required to establish the relative response of the detector for the two components. Addition of the internal standard to ester mixtures to be analyzed would then allow calculation of peak areas in absolute terms, and the decrease in peak area for the ester internal standard relative to the hydrocarbon internal standard would serve as the basis for a correction factor to apply to the sample esters. Of course, a better solution is the development of a partition liquid having the stability of Apiezon L and the polarity of Reoplex 400. Materials that might be expected to exhibit such properties are certain polyethers and polyamides, as well as sterically hindered polyesters.

### *Experimental Procedure*

Since the complete separation of the methyl esters of high molecular weight fatty acids that occur in natural products is such a difficult one to accomplish, it is necessary to take special measures in the packing of columns and in the design and operation of the apparatus. Factors considered to be of importance are as follows.

*Preparation of column packing materials.* The Celite 545 used in this work was first screened to narrow mesh ranges. Mesh sizes 60 to 80, 80 to 100, and 100 to 120 may be used. In the present work, 60 to 80 mesh was preferred because of the lower pressure drop across the columns that it permits. The screened Celite was washed with concentrated hydrochloric acid to remove soluble metal impurities. It was then washed with distilled water, with 10 per cent methanolic sodium hydroxide, and then with water until neutral. A final wash with methanol aided the air drying, which was carried out in a hood. Final drying was carried out in an oven at 200° C.

The polyester partition liquids were dissolved in just sufficient acetone to cover the Celite. The solution was added to the Celite with stirring, and the slurry was spread out in trays or on a large sheet of aluminum foil to dry under an air stream in a hood. The coated Celite was rescreened prior to the packing of columns.

*Packing of the columns.* Columns were first packed completely with vibration, using a small vibrator marking tool with a short length of quarter-inch steel rod in the chuck. The column was then fitted with gas supply at a pressure at least equal to that to be used in making the chromatograms, and again vibrated thoroughly. The gas pressure was shut off and the pressure was allowed to bleed down through the column. Additional packing material was then added to fill the column, and the gas pressure was reapplied. This cycle of operation was repeated until the column was completely filled. It is very important during the operation and during the following use of the column that, once gas pressure is applied at the head of the column, it should not be released from this end, but always should be allowed to bleed out at the detector end of the column. This practice avoids the blowing back of column packing material and prevents the occurrence of voids in the column that allow diffusion and peak broadening.

*Introduction of samples.* It is important in the gas chromatography of all substances that the sample be introduced as a vapor as nearly instantaneously as possible and thus at as high a concentration in the gas phase as possible. In order to accomplish this with high molecular weight fatty esters, it has been found that the temperature of the sample flashing portion of the column should

TABLE 8
EFFECT OF FLASH CHAMBER TEMPERATURE
(COLUMN TEMPERATURE 200° C.)

| Flash chamber temperature, °C. | Theoretical plates at methyl stearate | Percentage methyl oleate in methyl stearate |
|---|---|---|
| 350 | 1460 | 3.5 |
| 300 | 1380 | 3.8 |
| 250 | 1230 | 4.6 |
| 200 | 920 | 7.0 |

be in the neighborhood of 350° C. TABLE 8 gives the number of theoretical plates obtained on a Reoplex 400 column at 200° C. and a helium flow rate of 266 ml./min. at 4 different flashing chamber temperatures. A 60 per cent increase in number of theoretical plates was obtained by raising the flash chamber temperature from column temperature to 350° C. Under the conditions employed, this was equivalent to a 50 per cent reduction in the overlap of the methyl stearate and methyl oleate peaks. Many commercial instruments employ a flash temperature only 50° C. above that of the column. A gain of 20 per cent in theoretical plates is indicated for an additional increase of 100° C. in the flash chamber temperature.

*Instrumentation.* The gas chromatographic equipment employed in this work was a Burrell Kromotog K-5. The prototype of this instrument was designed by S. R. Lipsky of Yale University Medical School, New Haven, Conn. The thermal conductivity cells and associated circuitry were designed by Lloyd Guild of the Burrell Corporation, Pittsburgh, Pa. We contributed some minor design changes and additions. The instrument is a dual-column unit with columns and detectors separately heated by conduction within large aluminum masses and separately controlled, each with its own saturable core reactor-type proportional controller. It utilizes a split-flow helium system with both reference and sample sides of the high-sensitivity thermal conductivity cells separately supplied with helium at atmospheric pressure. No exact sensitivity figures are available at this time, but the detectors are approximately three times as sensitive as other conventional filament-type thermal conductivity cells that have been used previously in this work.

*Preferred operating conditions.* Although the present work has not covered the entire range of operating variables, the following conditions are thought to be near optimum for the use of Reoplex 400 polyester: packing material, 20 to 40 per cent Reoplex 400 on 60 to 80 or 80 to 100 mesh Celite 545; column dimensions, 0.5 cm. × 120 to 275 cm.; flow rate, 100 to 300 ml./min. helium at S.T.P.; temperature, 200° C.; and flash chamber temperature, 350° C.

FIGURE 7 is a gas chromatographic curve that represents one of the best separations of methyl esters obtained to date. The number of theoretical plates at methyl oleate is 3200 and the methyl oleate and methyl stearate peaks overlap by approximately 0.6 per cent. The sample contains, in addition to the $C_{18}$ series of fatty methyl esters, methyl arachidate, methyl behenate, and methyl erucate. These particular conditions therefore represent a good compromise between efficiency of separation and retention time for the $C_{22}$ fractions.

### *Application of Method to Animal Lipids*

Although the development of the gas chromatographic method described above is not yet complete, it has been applied to a limited number of samples of fatty acids of animal origin. FIGURE 8 is the gas chromatographic curve obtained on a sample of methyl esters of the cholesterol ester fatty acids isolated from the lymph from the thoracic duct of a rat fed a diet containing cholesterol and cottonseed oil as a fat source. FIGURE 9 is a similar curve in

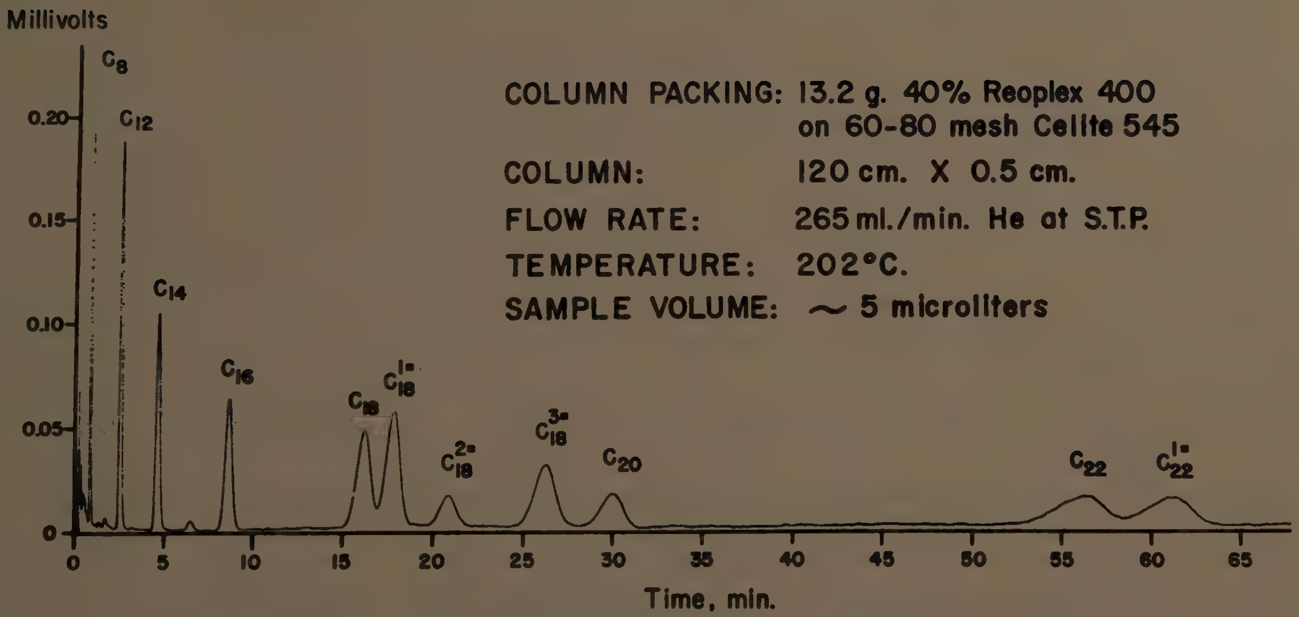

FIGURE 7. Separation of mixture of fatty acid methyl esters under recommended conditions.

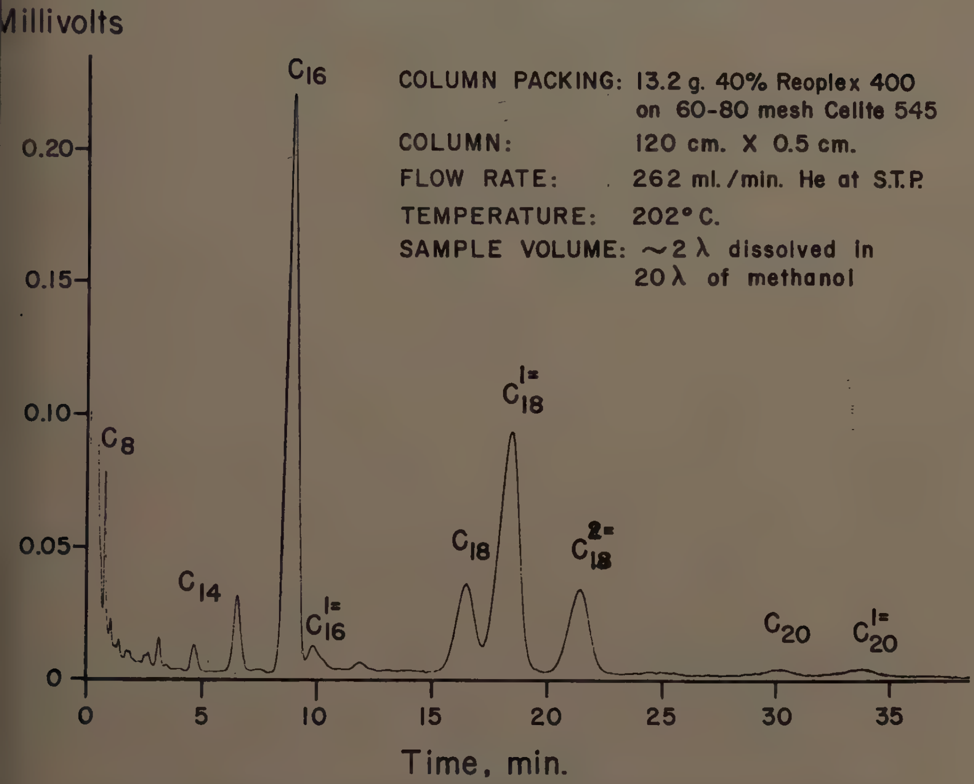

FIGURE 8. Separation of methyl esters prepared from rat thoracic lymph cholesterol esters. Fat in diet was cottonseed oil.

which the only difference was the fat source, in this case, a hydrogenated cottonseed oil shortening. It is too soon to draw conclusions from any compositional differences indicated by these data. It is interesting, however, that the samples show great similarity.

## *Summary*

A new type of partition medium has been discovered for the separation of high molecular weight saturated and unsaturated fatty methyl esters. This material, a polyester plasticizer, Reoplex 400, has been found to give excellent separation of the methyl esters of fatty acids normally encountered in natural fats, including the polyunsaturated esters. The experimental conditions recommended for best separations have been outlined. It also has been pointed out that quantitative results based on samples of known composition are in error in such a way that there is an indication of decomposition of the sample esters, probably by a transesterification reaction between them and the partition liquid. A procedure to compensate for this has been proposed.

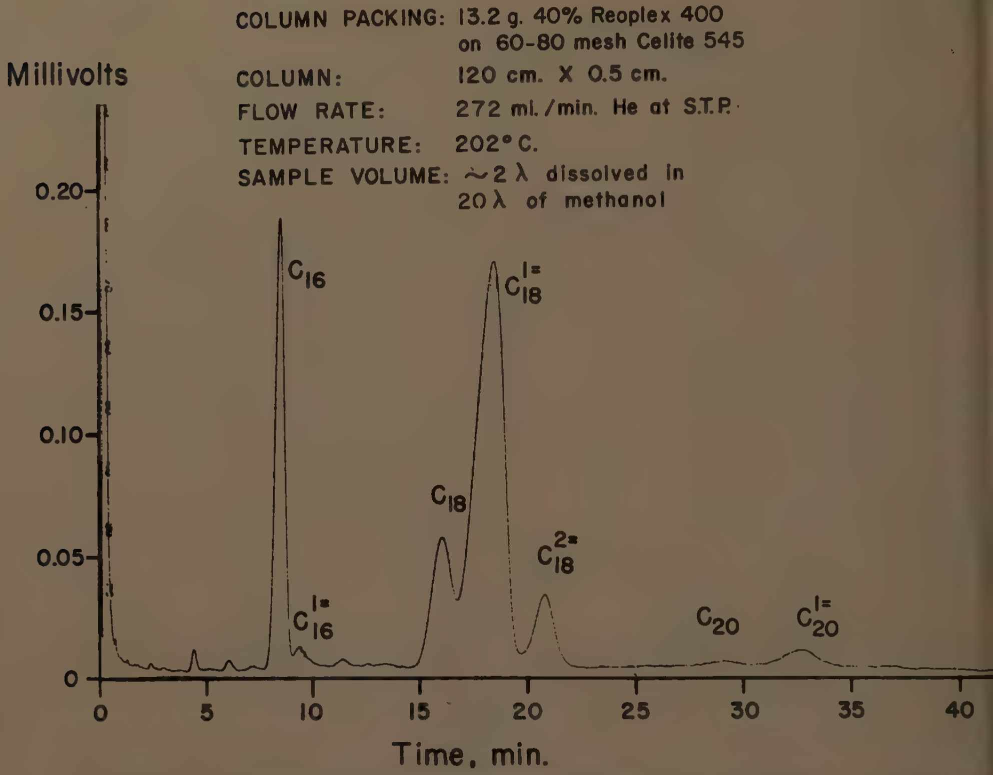

FIGURE 9. Separation of methyl esters prepared from rat thoracic lymph cholesterol esters. Fat in diet was hydrogenated cottonseed oil shortening.

## *Acknowledgments*

We thank S. R. Lipsky for supplying us with samples of Polyester 210-A, LAC-R-296, and LAC-2-R446 for comparison with Reoplex 400. Acknowledgment is made to H. C. Spatz and H. R. Zussman of Geigy Chemical Corp., Ardsley, N. Y., and to Allan Hill of The Geigy Company, Ltd., Manchester, England, for several samples of Reoplex 400, which made it possible to confirm batch-to-batch uniformity. We also express our appreciation to S. T. Preston, through whom we obtained the first sample of Reoplex 400.

## *References*

1. JAMES, A. T. & A. J. P. MARTIN. 1952. Biochem. J. **50:** 679.
2. CROPPER, F. R. & A. HEYWOOD. 1953–1954. Nature. **172:** 1101; **174:** 1063.
3. MARTIN, A. J. P. & A. T. JAMES. 1956. Biochem. J. **63:** 138; U. S. Pat. 2,728,219, December 27, 1955.
4. JAMES, A. T. & A. J. P. MARTIN. 1956. Biochem. J. **63:** 144.
5. JAMES, A. T. 1957. Fette Seifen Anstrichmittel. **59:** 73.
6. JAMES, A. T. & V. R. WHEATLEY. 1956. Biochem. J. **63:** 269.
7. BEERTHUIS, R. K. & J. G. KEPPLER. 1957. Nature. **179:** 731.
8. INSULL, W., JR. & A. T. JAMES. 1957. Am. Chem. Soc. Meeting, New York, N. Y.

9. Insull, W., Jr. Private communication.
10. Lipsky, S. R. Private communication.
11. Glueckauf, E. 1955. Trans. Faraday Soc. **51:** 34.
12. Jones, W. L. 1956. Physical parameters in gas chromatography. Southwide Chem. Conf., Memphis, Tenn.
13. Bradford, B. W., D. Harvey & D. E. Chalkley. 1955. J. Inst. Petroleum. **41:** 80.
14. Phillips, C. 1957. Symposium on Gas Chromatography, Michigan State University, East Lansing, Mich. To be published.
15. Keulemans, A. I. M. 1957. Gas Chromatography. Reinhold. New York, N. Y.
16. Orr, C. H. & J. E. Callen. 1958. J. Am Chem. Soc. **80:** 249.

# EVALUATION OF A STATIONARY PHASE FOR FATTY ACID ANALYSIS BY GAS-LIQUID CHROMATOGRAPHY*

S. R. Lipsky and R. A. Landowne

*Department of Internal Medicine, Yale University School of Medicine, New Haven, Conn.*

Recent developments in the field of gas-liquid chromatography have led to significant improvements in the separation of the individual components of mixtures containing long chain saturated and unsaturated fatty acids. The outstanding accomplishments of James and Martin[1] in this field have now been extended by the use of various types of stationary liquids. In recent studies,[2-4] the resolution of saturated and polyunsaturated acid esters, particularly of the biochemically important $C_{18}$ series of compounds, was readily accomplished by altering the chemical nature of the liquid phase. Under these conditions, the time required for the elution of compounds with chain lengths up to $C_{22}$ was considerably shortened, and the analyses were performed at the usual column temperatures of approximately 200° C. In these instances, certain alkyd resins were used as liquid phases for the first time. The material employed by Orr and Callen[2] was the plasticizer Reoplex 400. Two high molecular weight polymers, LAC-1-R296,† an adipate polyester of diethylene glycol, and LAC-2-R446,† an adipate polyester of diethylene glycol made more polar by partial cross linking with pentaerythritol, were described by Lipsky and Landowne.[3, 4] Since these compounds possessed a high degree of polarity in comparison to the previously employed Apiezon greases,[1] a notable change in the order of emergence of the unsaturated acid esters from the column occurred. The more polar esters, those containing the greater number of double bonds, were retained to a greater extent by the polar stationary liquid and therefore were eluted from the column at a rate slower than their preceding *less* unsaturated acid ester. Therefore, in a typical chromatographic analysis of the $C_{18}$ series of compounds the order of elution became methyl stearate, followed successively by methyl oleate, methyl linoleate, and methyl linolenate. Since the extent of time that a component remains on the column is determined in part by its relative volatility and solubility in the liquid phase, it was apparent that the affinity of these polymers for the long chain fatty acid esters was *comparatively* low. Therefore, the bands that represented esters of chain lengths up to $C_{20}$ were sharp and distinct because they emerged rapidly from the column; furthermore, it appeared possible to elute the saturated $C_{22}$ ester before any appreciable broadening effect was noted.

Another significant and interesting feature of certain polyesters as stationary liquids was their ability to provide excellent resolution of the individual components of mixtures of fatty acid esters with columns yielding as few as 1150 theoretical plates, as calculated for methyl stearate. This was in significant

---

* The work reported in this paper was supported by grants from the National Heart Institute, Public Health Service, Bethesda, Md.; the National Dairy Council, Chicago, Ill.; and the Atomic Energy Commission, Washington, D. C.

† These materials may be obtained from Cambridge Industries Company, Cambridge, Mass.

TABLE 1

COMPOSITION OF A STANDARD MIXTURE OF METHYL ESTERS OF LONG CHAIN FATTY ACIDS

| Compound | Percentages by weight |
|---|---|
| Methyl laurate | 10.1 |
| Methyl myristate | 12.4 |
| Methyl palmitate | 11.7 |
| Methyl palmitoleate | 2.6 |
| Methyl stearate | 11.0 |
| Methyl oleate | 14.3 |
| Methyl linoleate | 10.4 |
| Methyl linolenate | 7.7 |
| Methyl arachidate | 7.5 |
| Methyl behenate | 8.7 |
| Methyl hexacosanoate | 3.6 |

contrast to the calculated efficiencies of columns containing the Apiezon greases. With the latter, the best columns that gave efficiencies of 3000 to 4000 theoretical plates (for methyl stearate) effected only the partial resolution of the linoleate and oleate bands. In addition, it did not appear possible to achieve any degree of separation between the $C_{18}$ diene and the $C_{18}$ triene when the paraffinic vacuum grease was used as a liquid phase.

A wide variety of polyesters of varying chemical composition and molecular weights was studied in an attempt to obtain a series of compounds, that, as liquid phases, could produce the rapid and complete resolution of a wide range of saturated and unsaturated fatty acid esters. This goal was readily attained by increasing the number of polar sites present in the stationary liquid. Dicarboxylic acids of varying chain lengths were reacted with diethylene glycol to produce polymers of molecular weights ranging from 3000 to 30,000. In certain instances additional polarity was obtained by introducing pentaerythritol (about 4 per cent) to the reaction mixture to form a partially cross-linked two-dimensional polymer. From the results of these studies* a distinct relationship was observed to exist between the relative volatility or solubility of the individual saturated and unsaturated acid esters in a particular stationary liquid and the chemical composition of the liquid phase. When the sebacate and azelate polyesters were employed as liquid phases, the separation of linoleate from linolenate was easily accomplished; however, the stearate and oleate bands were frequently indistinguishable. Since these particular polymers had a moderate affinity for fatty acid esters, the elution of components with chain lengths up to $C_{22}$ from the column usually required 1 to 2 hours. High molecular weight, more polar alkyd resins made from smaller chain dibasic acids were then used as stationary liquids. Columns containing the adipate and glutarate polyesters of diethylene glycol[4] provided excellent resolution of the individual components of a mixture similar to that noted in TABLE 1. The elution of the saturated and unsaturated acid esters ranging from $C_{12}$ to $C_{22}$ was accomplished in 30 to 45 min. at column temperatures of approximately 200° C.

* A comprehensive description of this work will be presented elsewhere.

The use of certain polymers as stationary liquids for the gas-liquid chromatographic technique presented some inherent difficulties due to the nature of their physical and chemical properties. Since the analysis of long chain fatty acid esters under present experimental conditions usually requires operating column temperatures above 190° C., a high degree of thermal stability is one of the requirements for an alkyd resin to function satisfactorily as a liquid phase. It is also desirable that these polymers possess vapor pressures of less than 0.5 mm. Hg in this temperature range. A majority of the preparations was found to contain some volatile materials that usually could be removed by allowing a stream of inert gas under pressure to pass through a column maintained at 5 to 10° C. above the usual operating temperatures for 12 to 24 hours prior to use. In a number of instances slow "bleeding" of the phase from the column occurred continuously throughout its use. This probably signified a persistent breakdown of the stationary phase. In many cases, however, it was possible to use a column for one hundred or more analyses before appreciable loss in resolving power was noted. Under these circumstances, a standard sample was frequently analyzed in order to obtain a basis for comparison of the relative retention volumes of various individual fatty acid esters. When preconditioning of the column did not remove the impurities, contamination of the sensing element became a problem. With thermal conductivity cells, the stripping of relatively large quantities of the more volatile liquid phases from the column frequently resulted in the deposition of breakdown products on the hot wire. Baseline instability became prevalent and additional difficulties were encountered in the recovery of sample components. Since ionization chambers containing beta emitters are becoming increasingly popular as detection units because of their increased sensitivity, these devices also have been found to be somewhat susceptible to impurities under certain operating conditions, particularly when argon is used as a carrier gas.[5] At certain applied voltages[6] metastable argon atoms are produced that can collide with the contaminants bleeding from the column and can cause fluctuating increases in the ionization current. This could act as an additional source of background noise and lead to a lower and less desirable signal-to-noise ratio.

One of the more formidable problems that may be encountered in the use of these materials is related directly to their particular chemical structure. Since these compounds are polyesters, it seems possible that at elevated temperatures some transesterification would occur when the fatty acid esters to be analyzed remain in contact with the stationary phase for any appreciable length of time. Indeed, Orr and Callen,[7] employing Reoplex 400 as a liquid phase at 240° C., obtained quantitative evidence that demonstrated the existence of considerable interaction between the volatilized long chain fatty acid esters and the stationary liquid. The substances affected to the greatest degree were those with comparatively long retention times. When the operating temperature of the column was decreased to 200° C., transesterification, although still present, was considerably diminished. Thus, if polyesters are to be feasibly employed as liquid phases for use in the *quantitative* separation of long chain fatty acid esters by gas-liquid chromatography at 200° C., it would be highly desirable to obtain one that would provide excellent resolution and comparatively short retention times for components with chain lengths up to at least 22 carbon atoms. Under these circumstances, interaction should be minimal. A versatile alkyd resin that at this time seems most likely to fulfill these criteria best is described below.

### *Experimental*

The gas-liquid chromatographic equipment used during the course of this investigation was designed in this laboratory in collaboration with Maurice Godet and Harold Henry. A commercially available thermal conductivity cell employing split flow reference and detection paths vented to the atmosphere was originally used as a detection device. Since these elements lacked superior sensitivity and the hot filaments proved to be highly susceptible to oxidation and deposition of carbonaceous material during routine operation at 200° C., they have now been replaced by much more sensitive and stable ionization chambers containing either alpha or beta emitters as radiation sources. The compartments containing the cell and the column were individualized, since it seemed desirable to operate the sensing elements at 25° to 75° C. above the column temperature in order to prevent condensation of high boiling materials in the detector. Each compartment consisted of a large mass of aluminum that served as a heat sink and insured good thermal stability. Each sink was covered by a heating mantle whose voltage was governed by an electronic proportional controller. An error signal was fed from a bridge to an amplifier and two sets of saturable core reactors. The sensing element of this controller consisted of a resistance probe mounted in the bridge. This system provided regulation of the column and cell temperatures to better than 0.01° C. Any temperature in the range of 50 to 300° C. could be attained precisely by "dialing" a given resistance. A small independently controlled "flash" heater operating at a temperature 100° C. higher than that of the column was installed around the injection point of the apparatus in order to ensure complete volatilization of the injected sample.

Accurate control of the carrier gas (helium) was achieved through two sets of pressure regulators mounted in series. It did not appear necessary to preheat the gas prior to its passage onto the column. On the downstream side of the cell, stainless steel packless valves and glass collection tubes allowed for recovery of samples. The gas flow, corrected for temperature and pressure, was measured at the outlet with a standard soap bubble apparatus.

The columns, made of double-thickness Pyrex glass, were U-shaped, 4 to 9 feet in over-all length, and had an internal diameter of 4 to 5 mm. This type of column was preferred to the coiled metal column for ease and uniformity of packing. Acid-washed Celite 545 was used as an inert support. Great care was taken in sieving this material in an effort to obtain almost exclusively 60 to 80 mesh particles. This narrow distribution of particle size usually provided minimal pressure drops across the column. Under these circumstances, high flow rates and optimal resolution were easily attained. In order to minimize variations in the coating of the inert support, 250 to 500 gm. batches were made up at one time and stored in tight, dry containers. One part of the liquid phase was dissolved in acetone in a large beaker on a hot plate. Four parts of the inert support were added to the solution and the slurry was stirred until the last traces of the solvent were removed. When this technique was employed, it did not appear necessary to resieve the coated particles prior to use. Loading was accomplished by adding this material slowly to one leg of the column by means of a small funnel. During the course of this procedure, the column was continuously vibrated. After both legs of the column appeared uniformly packed, an inert gas at 15 psi was allowed to flow through the inlet side and the column was again vibrated for 3 to 4 minutes. The column was then vented and additional coated material was added to within 2 inches of the top. This void in the column that was in close proximity to the "flash" heater was filled with uncoated Celite. A known sample of fatty acid esters contained in a micrometer syringe was placed on the column by piercing a silicone seal.

A succinate polyester of diethylene glycol proved to be the best liquid phase tested thus far in this laboratory. This polymer had a molecular weight of 4450, an acid number of 0.21, and viscosities of 1292 and 61,500 centistokes at 100° C. and 38° C., respectively. FIGURE 1 shows the chromatogram of a standard mixture of methyl esters of saturated and unsaturated fatty acids extending from $C_{12}$ to $C_{26}$. All bands are easily distinguishable, and elution of the saturated $C_{26}$ ester from the column was complete in 38 min. The commonly occurring components up to $C_{22}$ emerged from the column in less

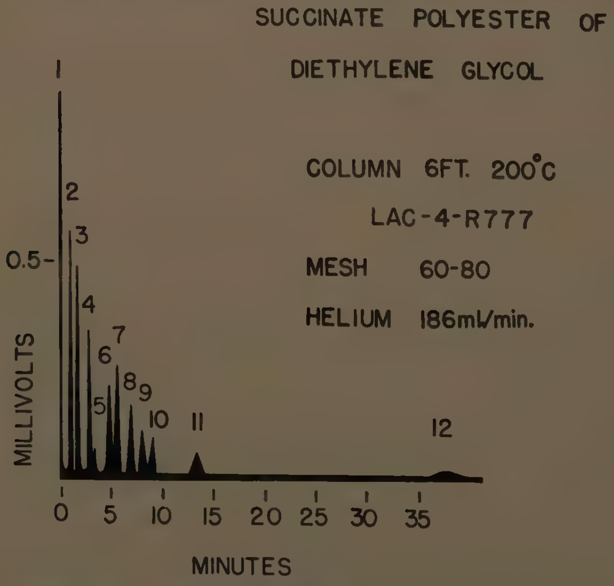

FIGURE 1. Separation of a standard mixture of long chain fatty acid esters: (1) air, (2) methyl laurate, (3) methyl myristate, (4) methyl palmitate, (5) methyl palmitoleate, (6) methyl stearate, (7) methyl oleate, (8) methyl linoleate, (9) methyl linolenate, (10) methyl arachidate, (11) methyl behenate, and (12) methyl hexacosanoate.

TABLE 2
ANALYSIS OF A STANDARD MIXTURE OF METHYL ESTERS OF LONG CHAIN FATTY ACIDS ON A SUCCINATE POLYESTER OF DIETHYLENE GLYCOL AT 203° C.

| | Percentages | | |
|---|---|---|---|
| | Weighed | Found | Difference |
| Methyl palmitate | 13.9 | 15.1 | +1.2 |
| Methyl palmitoleate | 3.0 | 3.3 | +0.3 |
| Methyl stearate | 15.6 | 16.5 | +0.9 |
| Methyl oleate | 20.6 | 21.0 | +0.4 |
| Methyl linoleate | 15.9 | 16.4 | +0.5 |
| Methyl linolenate | 11.3 | 9.6 | −1.7 |
| Methyl arachidate | 10.6 | 9.6 | −1.0 |
| Methyl behenate | 9.1 | 8.5 | −0.6 |
| | 100.0 | | |

than 15 min. Because of the extremely polar nature of this stationary liquid, it was possible for the first time to achieve very rapid elution of the individual components of a wide range of fatty acid esters without sacrificing resolution at the comparatively low operating column temperatures of approximately 200° C. A quantitative analysis of a known mixture of fatty acid esters extending to $C_{22}$ obtained at 203° C. is presented in TABLE 2. Undoubtedly, because of the extremely short retention times, little or no interaction between the component esters and the liquid phase occurred in this preliminary study. The small differences noted conceivably could be attributed to minor errors associated with the technique of calculating areas under the curve. Since many of the $C_{12}$ to $C_{20}$ components emerge from the column in rapid sequence, it may be necessary to collect specific fractions for further identification if branched chain or more highly unsaturated acid esters are thought to exist in an unknown sample. These fractions may then be rechromatographed on a column containing a stationary liquid that affords separation of these different types of compounds. Additional modification of the unsaturated components by bromination, hydrogenation, or oxidation to the corresponding mono- and dicarboxylic acids may also be required for further characterization of the chemical structure of these materials.

A semilogarithmic plot of retention time against the number of carbon atoms is given in FIGURE 2*a*. By extrapolation of this straight line, it is apparent that elution of a saturated fatty acid ester containing 32 carbon atoms would occur within 3 hours. From previous experience, it can be assumed that the $C_{32}$ band would be detectable, although considerably broadened. However, by increasing the temperature of the column by 10° to 20° C. and/or shortening the length of the column, thereby causing a more rapid elution of these bands representing the higher molecular weight components from the column, the broadening effect would be considerably lessened. In FIGURE 2*b* it can be noted that, from an analysis of a series of $C_{18}$ unsaturated compounds, the logarithm of retention times is also linear with respect to the number of

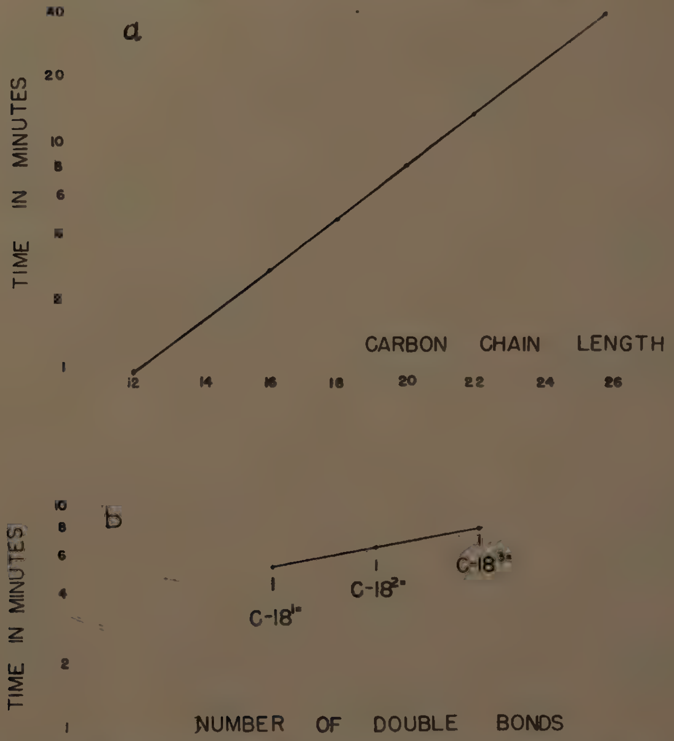

FIGURE 2. Semilogarithmic plot of retention time versus carbon chain length for a standard mixture of long chain fatty acid esters.

double bonds present in the molecule. The retention volumes of some methyl esters of the long chain fatty acid esters relative to methyl myristate are listed in TABLE 3.

Under the conditions of the experiment, the separation factor $\alpha$ for methyl stearate and methyl oleate was 1.16. This is exceptional in view of the very rapid elution of the acid esters from the column. It should be noted (TABLE 1) that, despite the fact that the concentrations of the closely related stearate (11.0 per cent) and oleate (14.3 per cent) and the linoleate (10.4 per cent) and linolenate (7.7 per cent) bands was relatively high and together comprised approximately 43 per cent of the total mixture, the separation of each from the other was practically complete. Since the relative proportions of these commonly encountered $C_{18}$ acid esters may vary considerably in biological preparations, it is encouraging to observe that this particular stationary liquid affords good resolution of these components over a moderate range of concentrations. The cross contamination between the stearate and oleate and the linolenate and arachidate bands amounted to less than 1.0 per cent. This calculation was based on the formula derived by Glueckauf[8] that expresses the relationship of the number of theoretical plates, separation factor, and the fractional band impurity.

TABLE 3

RETENTION VOLUMES OF THE METHYL ESTERS OF THE LONG CHAIN FATTY ACID ESTERS RELATIVE TO METHYL MYRISTATE AT 203° C. STATIONARY PHASE: SUCCINATE POLYESTER OF DIETHYLENE GLYCOL

| Methyl ester | |
|---|---|
| Methyl laurate | 0.60 |
| Methyl myristate | 1.00 |
| Methyl palmitate | 1.67 |
| Methyl palmitoleate | 1.95 |
| Methyl stearate | 2.78 |
| Methyl oleate | 3.22 |
| Methyl linoleate | 4.00 |
| Methyl linolenate | 4.67 |
| Methyl arachidate | 5.12 |
| Methyl behenate | 7.80 |
| Methyl hexacosanoate | 23.00 |

From the experience derived from the analysis of a large number of mixtures of long chain fatty acid esters containing concentrations of linoleate as high as 30 per cent, it was noted further that little or no difficulty was encountered in separating this acid ester from other closely related members of the $C_{18}$ series. These results were obtained by using one part of the liquid phase to 4 parts of the inert support. In instances where the molar ratio of 2 closely related compounds was high, the quantity of stationary phase used was increased to 30 per cent. With the availability of highly sensitive sensing elements in the form of radio frequency glow detectors[9] or chambers in which ionization is effected by means of beta rays from a radioactive source, it should be possible to use much smaller sample loads on columns containing 5 to 10 per cent by weight of liquid phase, thus further improving the resolution. While a wide variation of viscosities was encountered with the various polyesters tested, there seemed to be no correlation between this property and column efficiency. Although columns containing smaller particle diameters of inert support are known to be more efficient, their use is not always practicable with certain of the polyesters since very low flow rates were obtained under these circumstances. Fortunately, these materials in themselves are so efficient that they can be employed readily with larger particle sizes, such as 60 to 80 or 80 to 100 mesh. It is still of great importance that a narrow range of particle size be utilized in order to insure uniform packing within the column. This is necessary in order to avoid channeling and to permit an even distribution of liquid phase throughout the column.

## *Summary*

An extremely efficient stationary liquid for use in the separation of fatty acids by gas liquid chromatography is described. By employing columns containing Celite 545 coated with a high molecular weight succinate polyester of diethylene glycol at 203° C., it was possible to resolve the individual components of saturated and unsaturated acid esters extending from $C_{12}$ to $C_{26}$ in approximately 38 min. Since the retention times were extraordinarily short

even for the higher molecular weight substances, preliminary data indicated that there was little or no loss of the sample on the column by transesterification or degradation.

### *References*

1. James, A. T. & A. J. P. Martin. 1956. Gas-liquid chromatography: the separation and identification of the methyl esters of saturated and unsaturated acids from formic acid to *n*-octadecanoic acid. Biochem. J. **63:** 144.
2. Orr, C. & J. Callen. 1958. Separation of polyunsaturated fatty acid methyl esters by gas chromatography. J. Am. Chem. Soc. **80:** 249.
3. Lipsky, S. R. & R. A. Landowne. 1958. A new partition agent for use in the rapid separation of fatty acid esters by gas-liquid chromatography. Biochem. Biophys. Acta. **27:** 666.
4. Lipsky, S. R. & R. A. Landowne. 1958. Use of different partition agents for separating saturated and unsaturated fatty acids by gas-liquid chromatography. Federation Proc. **17:** 265.
5. Jesse, W. P. & J. Sadauskis. 1955. Ionization by alpha particles in mixtures of gases. Phys. Rev. **100:** 1755.
6. Lovelock, J. E. 1958. A sensitive detector for gas chromatography. J. Chromatography. **1:** 35.
7. Orr, C. H. & J. E. Callen. 1959. Recent advances in the gas-chromatographic separation of methyl esters of fatty acids. Ann. N. Y. Acad. Sci. **72** (13): 649.
8. Glueckauf, E. *Cited by* A. I. M. Keulemans. 1957. *In* Gas Chromatography. Reinhold. New York, N. Y.
9. Karmen, A. & R. L. Bowman. 1959. A radio frequency glow detector for gas chromatography. Ann. N. Y. Acad. Sci. **72** (13): 714.

# A MULTISTAGE ANALYZER FOR EXHAUST GAS ANALYSIS

R. W. Hurn, J. O. Chase, and K. J. Hughes
*Petroleum Experiment Station, Bureau of Mines, United States Department of the Interior, Bartlesville, Okla.*

## *Introduction*

The organic matter in automotive exhaust gas is an extremely complex mixture of hydrocarbons, partially oxidized hydrocarbons, and other products of combustion. As classes, some of these materials are known to be significant precursors of chemical reactions in photochemical processes that form objectionable air pollutants in some metropolitan areas. However, there is little detailed information about the specific reactants to be found in exhaust gas. This information is requisite to a systematic scientific study of the contribution of exhaust gas to the air pollution problem; therefore industry and government have begun work to provide this necessary information. As a contribution to the effort, the Bureau of Mines, Bartlesville, Okla., has conducted research on the composition of the hydrocarbon component of exhaust gas.

During the past decade technical interest in the study of automotive exhaust gases was intensified when some of its components became suspect in air pollution problems in metropolitan areas. Many investigators have reported information implicating the hydrocarbons in exhaust gas as reactants in atmospheric photochemical processes that result in what is commonly termed smog. The current technical status of this problem is well summarized in a report by the Air Pollution Foundation of Los Angeles, Calif.[1] Although air pollution researches are currently the dominant influence in scientific study of automotive exhaust gases, the information obtained is also important in fundamental research on the combustion processes and combustion behavior of fuels.

Primarily because of its activity in the latter field, the Bureau of Mines was prepared to undertake research on the composition of exhaust gases and its Bartlesville Station early became active in the work. During 1956 and the first half of 1957, the automotive and petroleum industries provided funds for the development of an analytical technique using gas chromatography, and the work was continued after June 1957 with support by the Public Health Service under its community air pollution program.* Progress in the application of gas chromatography was rapid, and much experimentally derived information was obtained. The results defined the analytical problems and indicated the capabilities and limitations of the analytical methods.

In this work the objective has been to obtain information about specific components of exhaust gas rather than classes of compounds in it. This approach has been encouraged by those interested in the air pollution problem because there is evidence that hydrocarbons differ significantly in their reactivities in the smog-forming processes.[2, 3]

The exhaust products from a spark-ignition, automotive-type engine form a complex mixture of nitrogen and oxides of nitrogen, oxygen, water, carbon monoxide, carbon dioxide, and other products of fuel decomposition. These decomposition products include hydrogen, oxygenated compounds (principally aldehydes), and hydrocarbons in varied stages of reaction and thermal decomposition. Analysis is difficult because the mixture is complex and the materials to be determined are present only in dilute concentrations; before the advent of gas chromatography there was no satisfactory analytical method for the specific hydrocarbons other than the very light ones. Gas chromatographic techniques offered a method for meeting analytical requirements; this report discusses how gas chromatography has been applied to exhaust gas analysis, the problems encountered, and the limitations and capabilities of the technique developed.

---

* During 1958 the additional development of exhaust gas analytical techniques will be supported at the Bartlesville Station by the automotive and petroleum industries.

### *The Analytical Problem*

The analyses discussed in this report were concerned only with the hydrocarbon component of exhaust gases: other classes of compounds were removed from the sample before it was introduced into the chromatographic analyzer. Methane is not recovered by the exhaust gas concentration techniques used to collect the samples that were analyzed. Therefore, except where specifically mentioned, analysis for methane is not considered.

The hydrocarbon component of exhaust gas varies in concentrations from 200 to several thousand ppm by volume, and specific compounds for which analyses are desired may be present in concentrations of only a few ppm. As an arbitrary choice, it appears reasonable at this time to specify the desired detectability level at about 3 to 5 ppm for hydrocarbons having 1 to 6 carbon atoms per molecule.

The compounds to be identified and quantitatively determined include materials as light as methane and as heavy as decane, and they include all hydrocarbon types. Because of the experimental factors involved in engine test work, it is highly desirable that complete analytical results be available from single samples.

Because the hydrocarbons are dispersed in such a relatively large volume of material extraneous to the analysis, some concentration is necessary if the whole exhaust gas is considered as the sample. This concentration can be accomplished within, or external to, the chromatographic columns but, in the sense of ordinary gas chromatographic techniques, some concentration is necessary. The analytical technique discussed in this report does not provide for the necessary concentration; the discussion assumes the exhaust gas sample to be free of water, carbon dioxide, oxides of nitrogen, and the fixed gases. Methods for sample preparation have been described in a previous paper.[4]

The applicability of gas chromatography to this analytical problem was indicated by the demonstrated capabilities of simple, single-column systems. However, it became evident that no single chromatographic column could effect the desired separation of materials covering the wide molecular weight range of hydrocarbons in the exhaust gas mixture. Detector sensitivity posed another important problem in this research. Because analyses were required on minute quantities of sample, high sensitivity of the detector was a design requisite. However, this latter factor no longer is unique to exhaust gas chromatography, and detector sensitivity in conventional equipment has been increased steadily over the past two years.

Results of experimental laboratory work begun in 1956 showed that the $C_2$ to $C_5$ hydrocarbon constituents of exhaust gas could be separated satisfactorily by a semipolar liquid phase in a relatively long chromatographic column operated at or near room temperature. Furthermore, some useful separation of the $C_6$ to $C_8$ paraffin and naphthenes, $C_5$ to $C_7$ olefins, and $C_6$ and $C_7$ aromatics could be made in a relatively short, nonpolar column operated at room temperature. However, these separations, requiring two different partition columns, could not be made in independent analyses because it was necessary that all data be obtained from a single sample. This necessitated the use of a staged, or series, arrangement of the columns, and an analyzer incorporating this system was evolved. The use of the two-stage analyzer has been reported.[4]

### *Equipment*

Calibration data from a two-stage analyzer are given in TABLES 1 and 2. These show good resolution of the $C_2$ through $C_6$ hydrocarbons. They also show that the analyzer can be used to detect the presence of materials normally considered relatively high in molecular weight for the gasoline boiling range. However, these capabilities do not meet the requirements of all applications of an exhaust gas analyzer in current research; the principal deficiency is lack of sufficient resolution for separating compounds in the $C_6$ through $C_8$ molecular weight range. Exhaust gases contain quantitatively significant amounts of hydrocarbon in this range, and some analyzer capability to resolve them is necessary.

Much improved resolution of the $C_6$ to $C_8$ molecular weight range materials could be had in a 20- to 30-foot length of a slightly polar column operated just above room temperature. A section of this type was a part of the two-stage analyzer mentioned earlier; to obtain resolution of the $C_6$, $C_7$, and some $C_8$ hydrocarbons it was necessary only to utilize its separation potentialities more fully. This intermediate 20-foot column could, in effect, handle and satisfactorily resolve compounds too heavy for the entire 50-foot second stage of the two-stage analyzer and too light for the first stage. A detector unit was provided to monitor the effluent from the intermediate stage; with appropriate flow-control modifications, the changes that resulted in the three-stage unit are shown diagrammatically in FIGURE 1. Calibration data for this unit are included in TABLE 1 for convenient comparison with data from the two-stage unit. Calibration chromatograms are shown in FIGURE 2.

Experimental work with exhaust gases has shown that, to allow minor constituents to produce readable elution peaks, elution times from the respective columns should be held below two hours and preferably below one. These choices of elution time are arbitrary and have no absolute significance; however, they can be used for guidance. After these retention times are exceeded in analyses with the equipment described, the elution peaks must become so wide that the thermal conductivity response to the eluted hydrocarbon quantita-

## TABLE 1
### CALIBRATION DATA FOR MULTISTAGE CHROMATOGRAPHS*

| Compound | Boiling point °C. | Emergence time, min. | | | | |
|---|---|---|---|---|---|---|
| | | 3-Stage unit | | | 2-Stage unit | |
| | | 1st Stage | 2nd Stage | 3rd Stage | 1st Stage | 2nd Stage |
| Air | | | | 6.0 | 1.5 | 5.6 |
| Ethane | −88.7 | | 3.7 | 7.1 | | 7.0 |
| Propane | −42.2 | | 4.8 | 9.4 | | 9.2 |
| Propene | −47.6 | | 5.2 | 10.2 | | 9.7 |
| Isobutane | −10.2 | | 6.0 | 13.0 | | 12.2 |
| *n*-Butane | −.5 | | 7.5 | 16.1 | 3.7 | 15.3 |
| Iso- and butene-1 | −6.1 | | 8.3 | 17.7 | | 16.9 |
| *trans*-Butene-2 | .8 | | 9.1 | 20.6 | | 19.5 |
| *cis*-Butene-2 | 3.7 | | 10.1 | 23.1 | | 21.7 |
| Butadiene-1,3 | −4.7 | | 10.1 | 23.1 | — | — |
| Isopentane | 28.0 | | 11.9 | 27.0 | | 25.8 |
| *n*-Pentane | 36.0 | | 14.4 | 33.6 | 6.6 | 31.8 |
| Pentene-1 | 30.2 | | 16.3 | 37.5 | | 35.6 |
| 2-Methylbutene-1 | 31.2 | | | | | 37.7 |
| *trans*-Pentene-2 | 36.0 | | 18.3 | 43.8 | | 41.4 |
| *cis*-Pentene-2 | 36.9 | 5.4 | 18.3 | 46.5 | | 43.9 |
| 2,2-Dimethylbutane | 49.7 | 5.4 | 18.3 | 43.8 | | |
| 2-Methylbutadiene-1,3 | 34.1 | 5.4 | 23.0 | 55.3 | | 53.6 |
| 2,3-Dimethylbutane | 58.1 | 6.9 | 24.4 | 59.2 | | |
| 2-Methylpentane | 60.2 | 6.9 | 24.4 | 59.2 | | 56.9 |
| 3-Methylpentane | 63.2 | 8.0 | 28.1 | 67.9 | | 65.7 |
| Cyclopentane | 49.3 | 8.0 | 31.1 | 67.9 | | 65.7 |
| *n*-Hexane | 68.7 | 9.2 | 32.8 | 73.3 | 10.6 | 76.3 |
| Hexene-1 | 63.5 | 9.2 | 37.6 | 89.7 | | 87.8 |
| *trans*-Hexene-2 | 67.9 | 11.0 | 45.3 | 108.0 | | 107.5 |
| *cis*-Hexene-2 | 68.8 | 11.2 | 45.3 | 108.0 | | 107.5 |
| 2,4-Dimethylpentane | 80.5 | 11.2 | 40.2 | 99.6 | | 98.0 |
| Methylcyclopentane | 71.8 | 13.1 | 50.6 | 112.8 | | 112.1 |
| 3,3-Dimethylpentene-1 | 77.5 | 12.5 | 49.1 | 122.3 | | |
| 2,2,3-Trimethylbutane | 80.9 | 11.7 | 43.4 | 109.9 | | |
| *trans*-4,4-Dimethylpentene-2 | 76.8 | 11.7 | 46.0 | 112.8 | | |
| 3,3-Dimethylpentane | 86.1 | 14.9 | 51.8 | 130.5 | | |
| 2,4-Dimethylpentene-1 | 81.6 | 14.4 | 57.3 | 142.5 | | |
| 2-Methylhexane | 90.1 | 15.9 | 57.3 | 142.0 | | 142.0 |
| 2,3-Dimethylpentane | 89.8 | 16.1 | 60.6 | 142.0 | | 149.3 |
| 3-Methylhexane | 91.9 | 17.3 | 64.6 | 148.5 | | 149.3 |
| 2,3-Dimethylpentene-1 | 84.3 | 17.3 | 66.2 | 160.0 | | |
| Isooctane | 116.0 | 19.0 | 65.6 | 169.0 | | 171.7 |
| Cyclohexane | 80.7 | 19.0 | 70.8 | 157.0 | | 157.6 |
| 3-Ethylpentane | 93.5 | 19.0 | 70.2 | 170.3 | | |
| 4-Methylhexene-1 | 86.7 | 17.3 | 70.2 | 177.0 | | |
| *trans*-1,2-Dimethylcyclopentane | 91.9 | 25.2 | 75.5 | 180.0 | | |
| *n*-Heptane | 98.4 | 21.4 | 80.7 | 171.3 | 26.3 | 198.3 |
| 2-Methylhexene-1 | 92.0 | 20.6 | 88.0 | | | |
| *cis*-1,2-Dimethylcyclopentane | 99.5 | 55.2 | 80.7 | | | |
| Heptene-1 | 94.9 | 21.7 | 93.2 | | | |
| *trans*-Heptene-3 | 95.7 | 23.6 | 93.2 | | | |
| *trans*-Heptene-2 | 98.0 | 25.2 | 105.6 | | 28.4 | |
| Ethylcyclopentane | 103.5 | 30.0 | 117.2 | | | |
| Methylcyclohexane | 101.2 | 32.8 | 132.0 | | | |
| Benzene | 80.1 | 23.6 | 146.0 | | 33.7 | |
| *n*-Octane | 125.7 | 52.6 | | | 49.0 | |
| Octene-2 | 125.3 | | | | 54.9 | |
| Toluene | 110.6 | 60.6 | | | 58.5 | |
| Ethylcyclohexane | 131.8 | | | | 64.1 | |
| *n*-Nonane | 150.8 | 131.0 | | | 93.3 | |
| Ethylbenzene | 136.2 | | | | 112.2 | |
| *m*-Xylene | 139.2 | 151.0 | | | 124.0 | |
| *p*-Xylene | 138.4 | 151.0 | | | 124.0 | |
| *o*-Xylene | 144.4 | 191.0 | | | 152.2 | |
| *n*-Decane | 174.0 | | | | 204.6 | |

* For description of columns see TABLE 2.

TABLE 2
DESCRIPTION OF COLUMNS
(All columns 0.250 × 0.032-in. wall, copper tubing)

| Stationary phase | Support | | Liquid/solid ratio by weight | Packing wt., gm. | Column length, ft. | Pressures, psig | | Temp., °C. | Flow rate |
|---|---|---|---|---|---|---|---|---|---|
| | Material | Mesh | | | | Inlet | Outlet | | |
| Two-stage analyzer | | | | | | | | | |
| First stage Dibutylphthalate | $C_{22}$ | 28–35 | 25:100 | 6 | 2 | 30 | 25* | 37.8 | 100† |
| Squalene | $C_{22}$ | 28–65 | 20:100 | 30 | 10 | | | 93.3 | 100 |
| Second stage Benzyl ether | $C_{22}$ | 30–40 | 20:100 | 67 | 20 | 25 | 0 | 37.8 | 100 |
| Dibutyl-*n*-maleate | $C_{22}$ | 30–40 | 20:100 | 85 | 30 | | | 37.8 | 100 |
| Three-stage analyzer | | | | | | | | | |
| First Silicone (DC-550) | $C_{22}$ | 40–50 | 20:100 | 18 | 6 | 25 | 22 | 46 | 80 |
| Second Benzyl ether | $C_{22}$ | 30–40 | 20:100 | 56 | 20 | 22 | 16 | 46 | 80 |
| Third Dibutyl-*n*-maleate | $C_{22}$ | 30–40 | 30:100 | 92 | 32 | 16 | 0 | 46 | 80 |

* For accelerated elution during independent, or parallel, operation, outlet is dropped to atmospheric pressure, inlet to approximately 7.5 psig.

† Helium carrier gas; flow rate measured at atmospheric pressure and room temperature with soap-bubble rate meter.

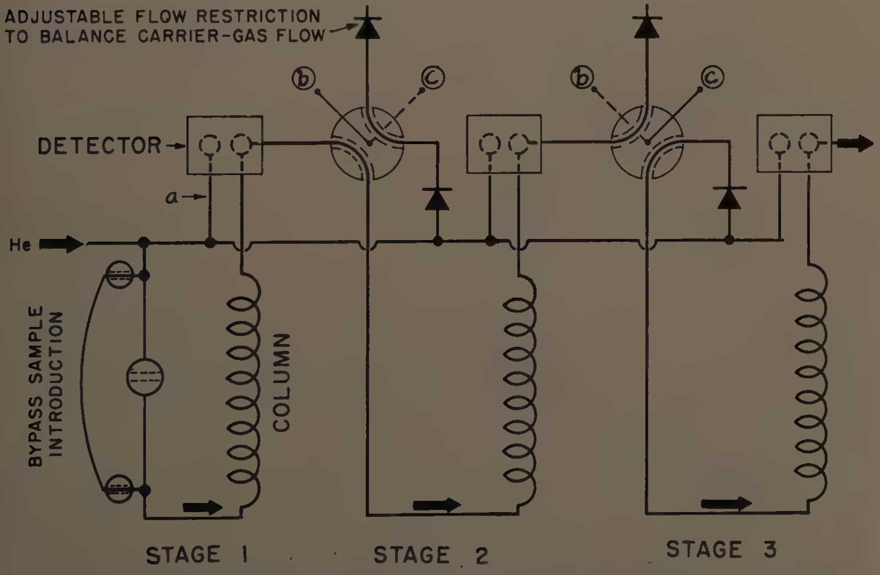
ADJUSTABLE FLOW RESTRICTION TO BALANCE CARRIER-GAS FLOW
ⓑ
ⓒ
ⓑ
ⓒ
DETECTOR
a
He
BYPASS SAMPLE INTRODUCTION
COLUMN
STAGE 1
STAGE 2
STAGE 3

FIGURE 1. Flow schematic of three-stage analyzer. (a) Outlet side of reference cell is closed after purging; (b) following stage is in series with preceding stage; (c) following stage is independent of preceding stage.

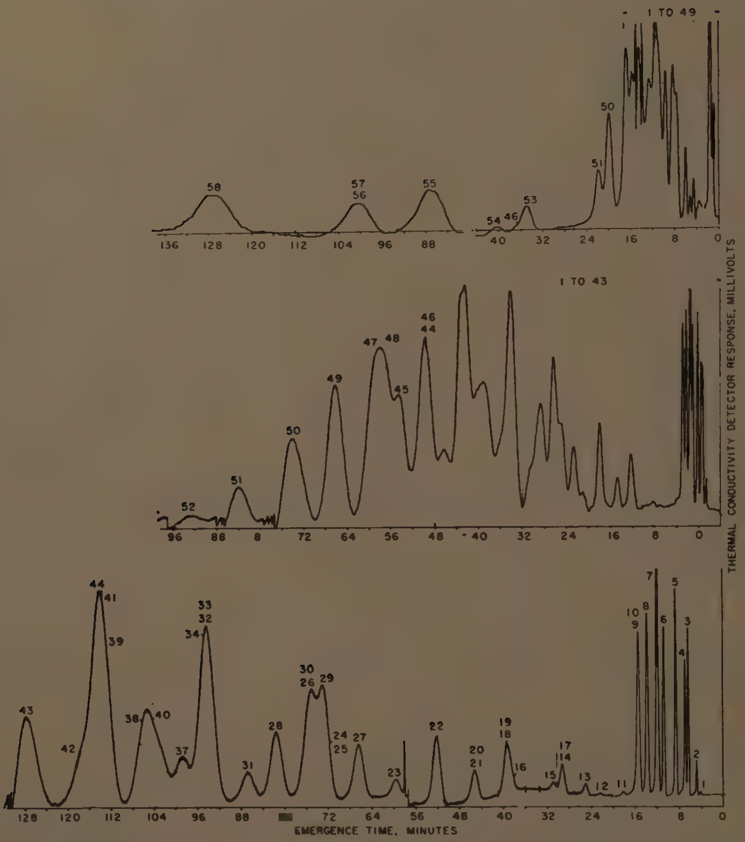

| No. | Compound | No. | Compound | No. | Compound |
|---|---|---|---|---|---|
| 1 | Air | 23 | Hexene-1 | 41 | 3-Ethylpentane |
| 2 | Ethane | 24 | *trans*-Hexene-2 | 42 | 4-Methylhexene-1 |
| 3 | Propane | 25 | *cis*-Hexene-2 | 43 | *trans*-1,2-Dimethylcyclopentane |
| 4 | Propene | 26 | Methylcyclopentane | 44 | *n*-Heptane |
| 5 | Isobutane | 27 | 2,4-Dimethylpentane | 45 | 2-Methylhexene-1 |
| 6 | *n*-Butane | 28 | 3,3-Dimethylpentene-1 | 46 | *cis*-1,2-Dimethylcyclopentane |
| 7 | Isobutene, butene-1 | 29 | 2,2,3-Trimethylbutane | 47 | Heptene-1 |
| 8 | *trans*-Butene-2 | 30 | *trans*-4,4-Dimethylpentene-2 | 48 | *trans*-Heptene-3 |
| 9 | *cis*-Butene-2 | 31 | 3,3-Dimethylpentane | 49 | *trans*-Heptene-2 |
| 10 | Butadiene-1,3 | 32 | 2,3-Dimethylpentane | 50 | Ethylcyclopentane |
| 11 | Isopentane | 33 | 2-Methylhexane | 51 | Methylcyclohexane |
| 12 | *n*-Pentane | 34 | 2,4-Dimethylpentene-1 | 52 | Benzene |
| 13 | Pentene-1 | 35 | *cis*-1,3-Dimethylcyclopentane | 53 | *n*-Octane |
| 14 | *trans*-Pentene-2 | 36 | *trans*-1,3-Dimethylcyclopentane | 54 | Toluene |
| 15 | *cis*-Pentene-2 | 37 | 3-Methylhexane | 55 | *n*-Nonane |
| 16 | 2-Methylbutadiene-1,3 | 38 | 2,3-Dimethylpentene-1 | 56 | *m*-Xylene |
| 17 | 2,2-Dimethylbutane | 39 | Isooctane | 57 | *p*-Xylene |
| 18 | 2,3-Dimethylbutane | 40 | Cyclohexane | 58 | *o*-Xylene |
| 19 | 2-Methylpentane | | | | |
| 20 | 3-Methylpentane | | | | |
| 21 | Cylcopentane | | | | |
| 22 | *n*-Hexane | | | | |

FIGURE 2. Representative separations in three-stage analyzer: actual chromatogram reproductions.

tively approaches the instrumental noise and drift. Accordingly, in the following discussions it will be assumed that the analyzer has limited capabilities for any compounds not eluted within about two hours.

The multistage analyzers are operated to exclude from the successive columns materials heavier than a column is designed to pass with acceptable retention. This is accomplished by diverting the sample stream from a column after the appropriate portion of the total sample has passed into it. After the sample stream has been diverted from a stage, an auxiliary carrier gas source is connected and the stage continues to function independently. By arbitrary choice the three-stage analyzer is operated as follows:

(1) The total sample is taken into and passed through the first stage.

(2) Fractionation in the first stage permits selection of material input to the second. All materials in the first stage with retention times equal to or less than that of methylcyclohexane are passed into the second stage.

(3) All materials in the second stage with retention times equal to or less than that of *n*-hexane are taken into the third stage. Therefore, data from the third stage are used as a basis of analysis for the $C_2$ to $C_6$ paraffins and isoparaffins and the $C_2$ to $C_5$ olefins and cycloparaffins.

The first stage provides analytical data essentially for the $C_8$ and heavier paraffins and isoparaffins, for some of the $C_7$ and heavier olefins, and for all aromatics except benzene. Analyses for the remaining materials, principally $C_6$ and $C_7$ hydrocarbons, are made from data from the second stage.

The improved resolution of the three-stage compared with the two-stage analyzer can be measured by comparing the respective spreads in elution times between *n*-hexane and *n*-heptane. In the two-stage analyzer these elutions from the first stage are separated by about 15 min.; in the intermediate stage of the three-stage analyzer they are separated by more than 45 min. The two-stage unit gives very little separation of the $C_7$ straight chain saturates and $C_7$ isomers, whereas there is a progressive change of approximately 30 min. in elution times for these materials in the intermediate section of the three-stage analyzer. This is the general area in which improved resolution is sometimes needed for exhaust gas analyses.

The restricted analytical range is the principal limitation of the three-stage analyzer when it is operated under the condition for which data are given. The analyzer as described is not suitable to analyze for materials heavier than the $C_9$ straight chain paraffins and $C_7$ olefins and aromatics. For some applications this limitation is acceptable. Where it is not, the operating temperature of the first stage could be increased, thus extending the analytical range well into the $C_{10}$ molecular weight hydrocarbons. (As previously stated, methane is not considered in these analyses, but it may be pointed out that methane is quantitatively an important constituent of exhaust gas. It may be determined in a solid adsorbent column or in a low-temperature system using a gas-liquid partition technique.)

When the increased resolution of the three-stage analyzer is not required and its greater complexity is not justified, the two-stage analyzer already cited may be useful. In the work at the Petroleum Experiment Station the two-stage unit has been used as a good analytical instrument for the $C_2$ through $C_6$ hydrocarbons and as a monitoring instrument for the $C_6$ through $C_{10}$ constituents of exhaust gas. The data in TABLE 1 may be cited as a measure of its capabilities in this application.

In the operation of the two-stage analyzer all materials with retention times in the first stage equal to or less than heptene-1 are taken into the second stage; the rest of the sample is excluded from it. The arbitrary decision to take heptene-1 into the second stage of the analyzer made it necessary to incorporate into the first stage a section that would retain benzene until the heptene had been eluted, because benzene is retained in the second stage about six hours and its presence would obstruct and incapacitate the analyzer for that period. Benzene was retarded in the first stage by adding a two-foot section of dibutylphthalate column operated at 37.8° C. This short section of polar material has no appreciable adverse effect on elution of anything other than the aromatic, but it is a very effective discriminator for that class of compound.

Other modifications of the two- and three-stage arrangements could be made to extend the analytical range of the instrument further or to give better resolution of any one restricted group of hydrocarbons. Possible arrangements are innumerable, and this report can only suggest the available potentialities for fractionation. For example, the technique of changing flow rate during the analysis could be applied to the three-stage analyzer to extend the analytical range of any or all sections. Virtually any change that extends the analytical range will entail some sacrifice of resolution capabilities. Sacrifices can be tolerated in some instances, but not in others. The option selected depends upon the analytical requirement.

### *Thermal Conductivity Detection*

When this laboratory first used gas chromatography in exhaust gas analysis it became evident that detector sensitivity must be improved over that readily available in commercial-type equipment. The analytical requirement was the detection and measurement of hydrocarbons present in concentrations of 3 to 5 parts* of hydrocarbon per million parts of exhaust gas. Quantitatively, this required a detector that would produce a readable response to a hydrocarbon component weighing only 1 to 5 $\mu$g., the quantity depending upon molecular weight.

Experimental data obtained on thermal conductivity equipment indicated that thermistor detectors were sufficiently sensitive. Unfortunately, they were equally responsive to environmental variations. Nevertheless, combined noise and 5-min. drift were reduced below 3 $\mu$v. by careful design of the electric elements, carrier gas flow control, and cell geometry, all in conjunction with the following design and maintenance features.

(1) Thermal conductivity cell block temperature controlled within ±0.002° C. and the external surfaces of the cell body insulated against minute temperature irregularities in its surrounding environment.

(2) Column temperatures controlled within ±0.5° C.

---

* Most frequently expressed in air pollution researches as parts per volume. The term "exhaust gas" is assumed to include all material in the exhaust stream.

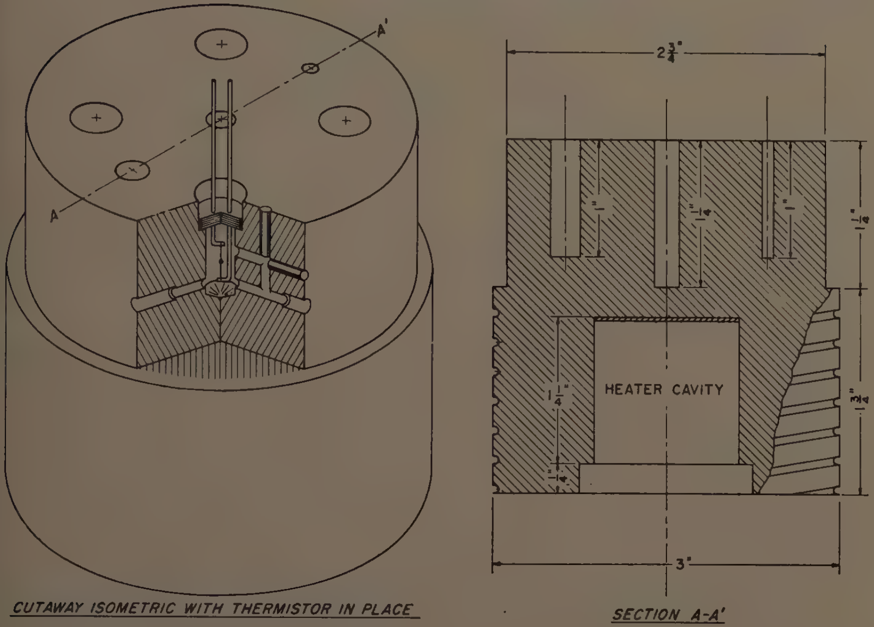

CUTAWAY ISOMETRIC WITH THERMISTOR IN PLACE

SECTION A-A'

FIGURE 3. Thermal conductivity cell with multiple thermistor detectors.

(3) Elimination of minute gas leaks. This precaution may appear obvious, but its neglect is a frequently unsuspected source of system noise and instability.

(4) Adherence to good practice in transfer and measurement of microvolt-level potentials.

One type of cell that was developed for a multistage analyzer has been described.[4] Its essential features are reproduced in FIGURE 3. An internal heater (not shown) in the central cell cavity is used to maintain cell temperature at 37.8° C.; power input to the heater is controlled by a potentiometric-type relay that responds to a thermistor-type temperature control bridge.

A cell of this design was fitted with 8000 Ω (nominal resistance at 25° C.) thermistors and operated in a bridge using 10 mAmp. in each leg through 1200 Ω bridging resistors. Its sensitivity to *n*-butane eluted in a helium carrier* was calculated from experimental data to exceed 5000 mv. ml./mg.

## *Summary*

Gas chromatography was found to be an effective analytical tool in analysis of the composition of the hydrocarbon component of exhaust gas but, in this application, the simple, single-column analyzers were too restricted in the types and boiling range of material they could handle and separate. It was found necessary to analyze for all types of hydrocarbons throughout the molecular weight range $C_2$ to $C_{10}$ hydrocarbons; moreover, the analysis was required from a single sample. To answer these needs, a system of staged columns was so designed that every portion of the sample could be taken through one or more columns suited to the separation of components in that portion. Special attention was given to provisions for effecting type separations in the first stage or stages, so that the aromatic materials were excluded from long columns packed with polar material in which the retention time of the aromatics would be excessive.

---

* Elution time, 15 min.; carrier flow rate, 100 ml./min.

Thermal conductivity detectors in nested arrangement were designed specifically for the multistage analyzer. These were chosen for high sensitivity characteristics so that trace hydrocarbons could be detected in small samples. The entire technique of analysis was developed around the use of small samples to enhance efficiency of separation.

The partition columns, thermal conductivity detectors, and analytical technique as specifically applied to exhaust gas analysis are described. This paper discusses problems that are unique to, or prominent in, the use of gas chromatography for exhaust gas analysis. Therefore it may be helpful both to those interested in doing exhaust analytical work and to those using or evaluating work in this field.

The separations and detection systems that have been described fulfill a need for an analyzer to identify and measure the principal hydrocarbon components of automotive exhaust gas. However, the determinations exclude methane and some of the heavier materials that may be present. The current trend is toward extending exhaust analyses to include methane at one end of the molecular weight range and $C_9$ to $C_{12}$ hydrocarbons at the other. Therefore, the need for an analyzer able to determine from one sample the hydrocarbons, methane through dodecane, or higher, is evident. Unquestionably, the technique of operating gas-liquid partition columns in series will become more important in meeting these difficult requirements.

## *References*

1. Faith, W. L., N. A. Renzetti & L. H. Rogers. 1957. Rept. No. 21. Air Pollution Foundation. Los Angeles, Calif.
2. Mader, P. P., J. Gliksman, M. Eye & L. A. Chambers. 1957. Effects of different motor fuels on photochemical formation of air contaminants from automobile exhaust vapors. *Paper presented at* Natl. Am. Chem. Soc. Meeting.
3. Haagen-Smit, A. J. & A. M. Fox. 1956. Ozone formation in photochemical oxidation of organic substances. Ind. Eng. Chem. **48:** 1484.
4. Hurn, R. W., K. J. Hughes & J. O. Chase. 1958. Applications of gas chromatography to analysis of exhaust gases. *Paper presented at* Natl. Soc. Automotive Engrs. Meeting.

## *Discussion of the Paper*

E. F. Williams (*American Cyanamid Company, Stamford, Conn.*): It would appear that in dealing with such a wide distribution of material types we are concerned with solvent efficiencies, as well as with column efficiencies. I should like to hear some ideas or suggestions regarding such separations.

J. H. Purnell (*Cambridge University, Cambridge, England*): I agree that solvent efficiencies vary markedly from tubstance to substance. This makes analysis of multitype mixtures very difficult at times and is one of the reasons why we were led to the work on column efficiencies. The best solvent I know of in this respect is polyethylene glycol, which only rarely seems to give gross band spreading.

## Part III. General Laboratory

# KATHAROMETER BEHAVIOR

W. A. Wiseman
*Gas Chromatography Limited, London, England*

## *Introduction*

In a previous work[1] an expression was derived for the response of the katharometer under ideal conditions. In this paper the theory is amplified, its conclusions are tested, and the accompanying experimental work is described. The conclusion is that the theory represents a good guide to katharometer behavior in practice.

## *Filament Constant*

The previously derived expression for the response of the katharometer is

$$(dE)_\theta = J\cdot\alpha\cdot\theta^{3/2}\cdot D^{1/2}R^{1/2}2\pi\beta l_k\cdot dk' \qquad (1)$$

where $(dE)_\theta$ volts is the true response of the katharometer; $\theta$° C. is the temperature difference between the wire and the walls; $R$ in ohms is the filament resistance; $\alpha$ its temperature coefficient of resistivity; $l_k$ cm., the katharometer length; $dk'$, the change in thermal conductivity due to the presence of an impurity in the carrier gas; and $\beta = 1/(\ln r_k/r)$, where $r_k$ cm. is the radius of the katharometer tube and $r$ that of the wire.

$D$ was given by

$$Di^2R = \theta$$

but more exactly by

$$Di^2R = \theta + t \qquad (2)$$

The significance of $t$ is given below.

The heat balance of the katharometer was given by

$$i^2R = Jk\theta(l_1 + l_2) + J\cdot k\theta_k(l_1 + l_2) + J\cdot k'\theta 2\pi\beta l_k \qquad (3)$$

where $k$ cal./sec./°C. cm. is the thermal conductivity of the materials of the filament support; $k'$ that of the gas; $l_1$ and $l_2$, the mean length of the heat paths down the filament leads (the 2 ends may be different owing to the design of the filament); and $\theta_k$° C. is the temperature difference between the walls of the katharometer and ambient.

There is an additional mode of heat loss due to the donation of heat to the moving gas and subsequent removal from the system. This is assumed to be proportional to $\theta$ and the rate of gas flow $m$. Therefore the full heat balance becomes

$$i^2R = Jk''m\theta + Jk\theta(l_1 + l_2) + Jk\theta_k(l_1 + l_2) + Jk'\theta 2\pi\beta l_k \qquad (4)$$

whence

$$1/D = Jk'' + Jk(l_1 + l_2) + Jk'2\pi\beta l_k \tag{5}$$

and

$$t = DJk\theta_k(l_1 + l_2) \tag{6}$$

If $R_0$ ohms is the filament resistance when $\theta = 0$, and as $R = R_0(1 + \alpha\theta)$ from (2) and (6),

$$R = \alpha R_0 Di^2R + R_0 - \alpha R_0 DJk\theta_k(l_1 + l_2) \tag{7}$$

If a plot of $i^2R$ against $R$ is made, it should begin, as $i^2R$ is increased, with an upward curve and gradually become a straight line whose slope is $\alpha R_0 D$. At what value of $i^2R$ this occurs depends on the value of $\alpha R_0 DJk\theta_k(l_1 + l_2)$ which, being constant, becomes less significant as $i^2R$ is increased. If the straight portion is extrapolated backward to cross the $R$ axis, the distance in ohms (for example $\rho$) between that point and $R_0$ equals $\alpha R_0 DJk\theta_k(l_1 + l_2)$. Therefore, both $D$ and $k\theta_k(l_1 + l_2)$ may be found from this plot.

From the plot of curves for two different gases whose relative values of $k'$ are known, the values of $2\pi\beta l_k$ and $k(l_1 + l_2)$ may be found from EQUATION 5, provided the contribution to heat loss by the gas flow is negligible, as was found in this case, or equal for the two gases. This contribution may be determined from the wire temperature at different rates of flow, although this was not done here because of its relative insignificance.

Hence the complete heat flow characteristics of a filament may be determined.

### *Katharometer Response*

The katharometer resopnse $(dE)_\theta$ is assumed to be $idR$ volts, where $i$ is the wire current in amperes. This is not measured directly by the conventional Wheatstone bridge. If the response actually measured is $dE$ volts, it can be shown that, provided there is an infinite resistance (approximately obtained with modern potentiometric recorders) across the bridge,

$$(dE)_\theta = \frac{dE \cdot \sum R}{R_3 + R_4} \tag{8}$$

where $R_3$ and $R_4$ are the resistances on the side of the recorder opposite to the katharometer. This is the Wheatstone bridge correction that has been used with all of these results.

Substituting for $D$ in EQUATION 1

$$(dE)_\theta = \alpha \cdot 2\pi\beta l_k \left\{ \frac{JR\theta^3}{k''m + k(l_1 + l_2) + 2\pi\beta l_k k'} \right\}^{1/2} dk' \tag{9}$$

Obviously, heat going down the leads and being carried away by the gas flow is heat wasted, as far as response is concerned. The maximum response is given when $k''m + k(l_1 + l_2) = 0$. In practice these can be made less than 6 per cent of the total heat flow; for the purposes of deciding which factors are otherwise important they will be ignored. However, conclusions reached will refer to maximum responses. The introduction of a theoretically advantageous feature will produce the desired result only if additional heat loss is prevented.

Comparisons of katharometer responses[2] should be made at equal values of $\theta$ as the noise level appears to be approximately proportional to $\theta$.

If the length of the wire $= nl_k$ cm. and its resistivity $= s$,

$$(dE)_\theta = \frac{\alpha l_k}{r}\left\{\frac{2\beta\cdot n\cdot s\cdot J\theta^3}{k'}\right\}^{1/2}\cdot dk' \tag{10}$$

Hence at constant values of $\theta$ the following relationships exist.

(1) The katharometer response is inversely proportional to the filament radius, giving precise definition to the trend predicted by Keulemans[3] for this factor.

(2) For a given filament radius the responses are proportional to $\alpha\sqrt{s}$.

(3) Response is directly proportional to the katharometer length. These two effects have been discussed by Keulemans.

(4) The response is proportional to $\sqrt{n}$, that is, a given length of wire is most profitably used in a straight line, while a given katharometer space is most profitably filled with a coil.

(5) The response is inversely proportional to $\sqrt{k'}$.

It is worthwhile to consider responses at equal bridge current, as many comparisons have been made under such conditions.

Thus

$$(dE)_\theta = \frac{\alpha i^3 R^2 2\pi\beta l_k\cdot dk'}{J\{k(l_1 + l_2) + k''m + 2\pi\beta l_k k'\}^2} \tag{11}$$

Neglected terms as before and substituting $R$

$$(dE)_\theta = \frac{\alpha i^3 s^2 n^2 l_k dk'}{2\pi^3 J\beta r^4 (k')^2} \tag{12}$$

Hence:

(1) The response is inversely proportional to the fourth power of the radius of the wire, obviously a dominating factor.

(2) The response is inversely proportional to $(k')^2$. This leads to the view that the lower the thermal conductivity, the higher the response. Thus it is found that at low bridge currents nitrogen gives a better response for many compounds than does helium. That it does not do so always is due to a fall off in response at higher currents when using nitrogen.

(3) A coil is favorable, as the response is proportional to $n^2$.

### *Effect of Change of Rate of Flow*

Before proceeding to the result of tests of theory, evidence for the negligible effect of rate of flow changes is given. TABLE 1 shows some typical results.

The method of obtaining these results was to make a change in conditions

TABLE 1

| Flow rate, cc./min. | Flow change cc./min. | Wire resistance ohms | $\Delta R$ ohms | $\Delta\theta$ °C. |
|---|---|---|---|---|
| 17.9 | — | 183.5420 | — | — |
| 38.8 | +20.9 | 183.5223 | −0.0197 | −0.044 |
| 20.9 | −17.9 | 183.5316 | +0.0093 | +0.020 |
| 32.7 | +11.8 | 183.5247 | −0.0070 | −0.015 |
| 8 μg. pinene | — | — | ±0.0047 | ±0.010 |
| 75 μg. pinene | — | — | ±0.0386 | ±0.085 |

Conditions: carrier gas, hydrogen; working substance, pinene; katharometer temperature, 161.5° C; $\theta$ = 28.9° C.

and then readjust the base line to its original position. The amount of adjustment necessary is represented by the figures in TABLE 1.

The changes thus given may be compared with a change in wire resistance of about 0.5 ohms when there is a change of 1 mAmp. in the wire current at the wire current used.

## *Tests of Theory*

*Katharometer response.* A brief test of the theory (EQUATION 1) showed that with hydrogen and helium the response was proportional to $\theta^{3/2}$. This can be only approximately true as $R^{1/2}$ is not quite constant. A precise method can be derived from

$$(dE)_\theta = \frac{J\cdot\alpha\theta^2 2\pi\beta l_k dk'}{i} \tag{13}$$

whence $[(dE)_\theta\cdot i]/J\alpha\theta^2$ should be a constant and equal to $2\pi\beta l_k dk'$. This factor is used rather than $dk'$ because of an uncertainty in the value of $\beta$. TABLE 2 gives some typical results.

These results show that:

(1) There is a large measure of constancy in the value of $2\pi\beta l_k dk'$, particularly for hydrogen and helium. The value appears to remain constant over different katharometer temperatures; $\epsilon$ (where $\epsilon = dk'/k'$) falls with rising temperature.[3] This is to be expected from the temperature coefficients of thermal conductivity of these gases and the usual substances to be detected.[3]

(2) There is a tendency for some of the results to be low at low values of $\theta$ and for all results to be low at high values of $\theta$. The former is due to the fact that most results were obtained with samples of equal size. At low sensitivities the peaks were quite small, leaving a substantial percentage of material undetected and giving low values for the response. When larger samples are used, the material undetected is relatively small and the responses are equal to those expected.

The distinct fall off in the value of $2\pi\beta l_k dk'$ at high values of $\theta$ is least noticeable with hydrogen and most noticeable with nitrogen. Eventually, in the latter case, the peaks diminish in size. The fall off of $2\pi\beta l_k dk'$ begins at roughly 25° C., and the fall in peak size at the highest values of $\theta$ is an uninterrupted

TABLE 2

| Carrier gas katharometer temperature | | Nitrogen 80° C. | | Helium 100° C. | | | |
|---|---|---|---|---|---|---|---|
| Current mAmp. | $\theta$ °C. | $(dE)_\theta$ $\mu$v. | $2\pi\beta l_k dk'$ cal./sec./°C. $\times 10^{-6}$ | Current mAmp. | $\theta$ °C. | $(dE)_\theta$ $\mu$v. | $2\pi\beta l_k dk'$ cal./sec./°C. $\times 10^{-6}$ |
| 18 | 12.9 | 64 | 0.56 | 25 | 5.7 | 230 | 19.2 |
| 23½ | 25.0 | 175 | 0.58 | 32½ | 9.0 | 550 | 19.7 |
| 25½ | 29.6 | 242 | 0.63 | 40 | 14.1 | 1100 | 19.7 |
| 31½ | 50.4 | 376 | 0.40 | 49 | 20.3 | 1780 | 18.9 |
| 38 | 78.7 | 560 | 0.31 | 60 | 31.0 | 3640 | 20.3 |
| 44 | 107.1 | 754 | 0.26 | 66½ | 40.8 | 4860 | 17.5 |
| 52 | 167. | 786 | 0.13 | 78½ | 50.2 | 6170 | 16.0 |
| Carrier gas katharometer temperature | | Helium 131° C. | | Hydrogen 100° C. | | | |
| 39 | 12.8 | 790 | 17.0 | 33 | 8.1 | 310 | 15.6 |
| 45 | 17.0 | 1430 | 20.0 | 40 | 12.4 | 640 | 16.7 |
| 51½ | 22.9 | 1990 | 17.4 | 47 | 16.8 | 1100 | 18.4 |
| 58 | 28.6 | 2850 | 18.1 | 54 | 22.4 | 1620 | 17.5 |
| 65 | 36.2 | 4220 | 18.9 | 61 | 29.7 | 2500 | 17.1 |
| 78 | 51.6 | 7300 | 17.6 | 68½ | 37.0 | 3120 | 15.5 |
| 88½ | 72.6 | 12100 | 18.1 | 87½ | 63.0 | 7260 | 15.9 |
| 99 | 93.6 | 15070 | 15.2 | 118 | 126.9 | 17300 | 12.6 |
| Carrier gas katharometer temperature | | Hydrogen 131° C. | | Hydrogen 161° C. | | | |
| 30½ | 6.9 | 300 | 17.1 | 40 | 10.8 | 510 | 18.9 |
| 39 | 10.6 | 514 | 15.8 | 46½ | 14.5 | 910 | 17.9 |
| 46 | 15.1 | 970 | 17.4 | 53½ | 18.3 | 1350 | 19.4 |
| 54 | 20.3 | 1440 | 16.8 | 63½ | 27.2 | 2320 | 17.9 |
| 60 | 26.0 | 2240 | 17.9 | 66½ | 29.8 | 2720 | 18.0 |
| 74 | 39.7 | 4000 | 16.8 | 89 | 56.0 | 6350 | 16.2 |
| 102 | 81.5 | 10750 | 14.7 | 100 | 72.0 | 9160 | 15.9 |

continuation of this effect. With hydrogen and helium the fall off is much less marked.

(3) Helium gives higher values of $2\pi\beta l_k dk'$ than does hydrogen. As $k'$ is lower, $\epsilon$ must be substantially higher. For this reason, helium is the best gas known for use with katharometers.

Many specific points concerning the effect on response of various features referred to above were not tested. However, the question of wire diameter at constant bridge current was examined. The response of the katharometer supplied with the Griffin & George apparatus* was determined under similar conditions. $l_k$ was the same in both cases, as was the material of the filament. $\beta$ was favorable to the Griffin & George instrument, as the wire diameter was double that of the present instrument. The response of the former at equal wire current should then be about one-sixteenth that of the latter; this was found to be true (TABLE 3).

* Griffin & George Ltd., Wembley, Middlesex, England.

TABLE 3

| | | | | |
|---|---|---|---|---|
| Wire current, mAmp. | 41 | 60 | 75 | 99 |
| Griffin response, µv. | 22 | 74 | 138 | 296 |
| Glass response, µv. | 400 | 650 | 1780 | 4800 |
| Ratio | 18.2 | 19.0 | 18.1 | 16.2 |

TABLE 4

| Gas | Temperature, °C. | $D$ (watts/°C.)$^{-1}$ | $\beta$ |
|---|---|---|---|
| Nitrogen | 80 | 324 | 0.159 |
| Helium | 80 | 66.0 | 0.154 |
| Helium | 100 | 56.6 | 0.178 |
| Helium | 131 | 51.2 | 0.197 |
| Hydrogen | 100 | 47.8 | 0.176 |
| Hydrogen | 131 | 41.6 | 0.203 |
| Hydrogen | 161 | 37.6 | 0.223 |

The effect of katharometer length on response was confirmed also by the use of a shorter filament of the same platinum wire as used for these results.

*Filament constants.* $D$ values of the filament at various temperatures are shown in TABLE 4. The values of $\beta$ are calculated, assuming constant values of $k'$ of $41.3 \times 10^{-5}$, $34.3 \times 10^{-5}$, and $5.8 \times 10^{-5}$ cal./sec./°C. cm. for hydrogen,[4] helium,[4] and nitrogen,[3] respectively, and assuming that 20 per cent of the heat goes down the leads with nitrogen and 10 per cent with the other gases. The values of $D$ decrease with rising temperature; the decrease is attributed to rises in the values of $k'$. $\beta$ should equal approximately 0.16, indicating that its values are higher than expected, probably as they are calculated from thermal conductivities at 0 °C. Nevertheless, they are of the right order. The filament did not in any case lie exactly along the axis of the katharometer tube and was somewhat slack.

FIGURE 1 shows a plot of $i^2R$ against $R$ for the filament using nitrogen at 80°

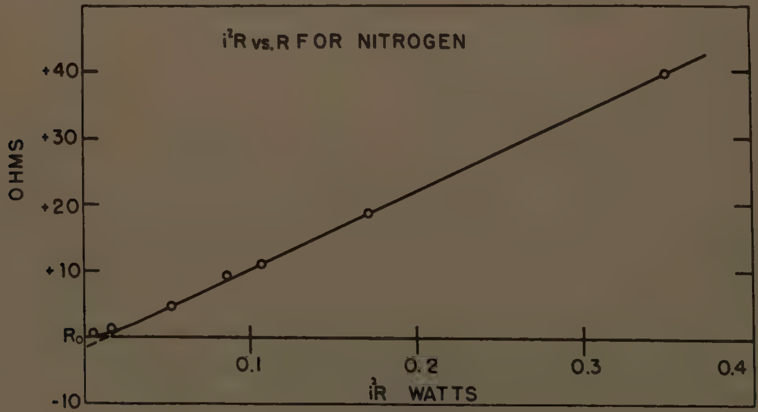

FIGURE 1

C. It shows the curve at low values of $i^2R$, from which $\rho = 1.5$ ohms. Therefore,

$$k \cdot \theta_k(l_1 + l_2) = 3.0 \times 10^{-3} \text{ cal./sec.}$$

As one end of the filament leads touched the katharometer walls, it was assumed that for it $\theta_k = 0$. Furthermore, as for the other end, $\theta_k \approx 60°$ C.,

$$k \cdot l_2 \approx 0.05 \times 10^{-3} \text{ cal./sec./°C.}$$

FIGURE 2 shows a group of plots of $i^2R$ against $R$, particularly the rapid rise in $\theta$ using nitrogen as opposed to that using hydrogen or helium. Where decomposition effects occur the advantages of using these latter gases, in addition to the vastly increased sensitivity obtained, are obvious.

The reciprocal $D$ values for helium and nitrogen at 80° C. are 3.6 and $0.73 \times 10^{-3}$ cal./sec./°C., respectively, and the ratio of their values of $k'$ is 6.0.

Hence:

(1) $k(l_1 + l_2) = 0.16 \times 10^{-3}$ cal./sec./°C.

(2) $kl_1 \approx 0.11 \times 10^{-3}$ cal./sec./°C.

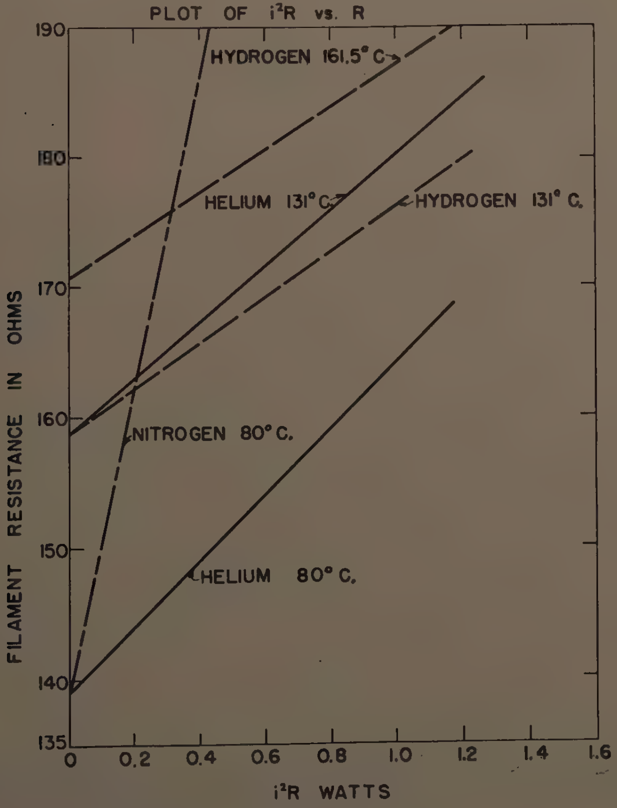

FIGURE 2

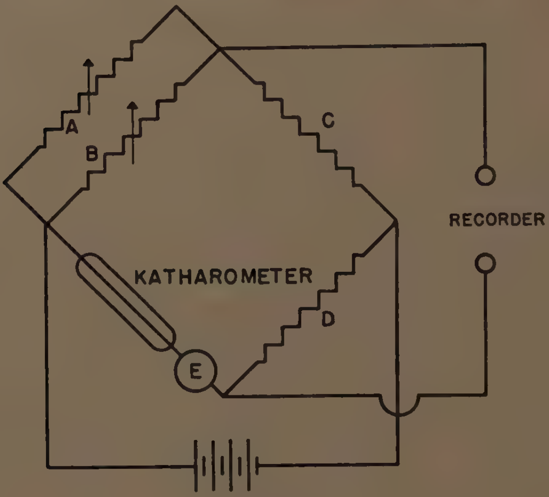

FIGURE 3

(3) 4.5 per cent of the total heat flow goes through the leads using helium, and 22 per cent using nitrogen, permitting the assumptions above to be made when determining $\beta$.

## *Experimental Details*

*Circuit.* FIGURE 3 illustrates the circuit used. *A* and *B* are two 1- to 11,110-ohm resistance boxes in parallel that, while covering a wide range of resistances, enable the wire resistance to be measured to within at least ±0.001 ohms. Such changes were readily detectable on the recording chart in most cases. No amplifier was used to feed the signal into a 2- or 3-mv. Honeywell Brown* recorder.

*C* and *D* are two 100-ohm, standard, manganin-wound resistances.† The ammeter *E* was a milliammeter with a reading of from 0 to 250 mAmp. and of negligible internal resistance.

*Katharometer and other apparatus.* The katharometer used was one with insertable filaments. The filament primarily used for this work had "non-conducting" leads and is illustrated in FIGURE 4. Experimental work shows that the filament was, in fact, virtually thermally nonconducting through the electric leads that were, however, capable of passing all the current necessary for satisfactory filament operation.

The katharometer with column attached fitted into a vapor bath. The katharometer body itself was maintained at a constant temperature by a separate vapor bath and was virtually independent of column conditions. The whole apparatus was constructed of glass.

*Determination of filament resistance.* The resistance of the wire at the tem-

---

* Manufactured by Honeywell Controls Ltd., Motherwell, Lanarkshire, England.
† Manufactured by W. G. Pye Ltd., Cambridge, England.

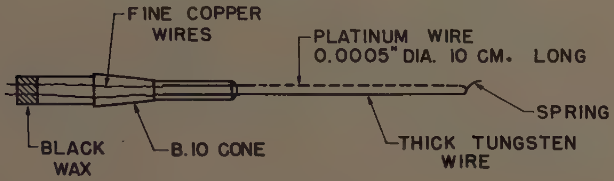

FIGURE 4

perature of the katharometer was determined when only a very small current was passing through it and when hydrogen or helium was used as the mobile phase. No current was passed for a period of time before making this estimation. The value so obtained could be compared with other results at the same temperature from the plot of $i^2R$ againts $R$. It was concluded that the values obtained were in error by no more than 0.1 ohm.

The results, which are linear, are shown in TABLE 5 at different katharometer temperatures and the mean value of $\alpha$ calculated from these is 0.00266. This compares with the published values of approximately 0.004 for platinum. The reason for this discrepancy is not known, but it was probably due to the fact that the wire was not pure platinum.

*Representation of responses.* Responses have been determined as those given in microvolts by a molar dilution in the gas stream of $10^3$ and were found from the peak area $A$ sq. cm. Therefore,

$$dE = 0.0452 \frac{A \cdot C_1 C_2 C_3}{m} \text{ microvolts} \tag{14}$$

using the same symbols, as far as possible, as did Dimbat *et al.*[5] that is, $C_1$ = rate of flow in cc./min. at atmospheric pressure, $C_2$ = chart speed in min./cm., $C_3$ = mv./cm. of scale, and $m$ = moles of substance added.

The response $P$ as determined by Dimbat *et al.* is related directly to the above; therefore

$$dE = 0.0452\, MP \tag{15}$$

where $M$ is the molecular weight of the substance. This method of expression is preferred primarily for two reasons:

(1) The result is given in a simple quantity, that is, microvolts directly relatable to the noise level and the electric properties of any circuit or recording instrument.

(2) It has been found that, with the katharometer at least, most substances when using hydrogen or helium give the same response (within 5 per cent) if calculated in the proposed manner. On the other hand, Dimbat's formula

TABLE 5

| | | | | |
|---|---|---|---|---|
| Temperature of katharometer in °C. | 80 | 100 | 131 | 161.5 |
| Resistance of wire in ohms | 139.2 | 146.4 | 158.9 | 170.4 |

TABLE 6

| | Proposed formula response, $\mu$v. | | | Dimbat & Porter mv. cc./mg. | |
|---|---|---|---|---|---|
| | M.W. | Hydrogen | Helium | Hydrogen | Helium |
| Pinene | 136 | 650 | 1050 | 105 | 170 |
| Ethyl acetate | 88 | 650 | 950 | 160 | 240 |
| *n*-Propyl *n*-butyrate | 130 | 680 | 1000 | 115 | 170 |
| Diethyl ketone | 86 | 540 | 880 | 140 | 225 |
| Ethyl alcohol | 46 | 420 | 620 | 200 | 300 |
| Toluene | 92 | 480 | 640 | 115 | 155 |
| Cineol | 154 | 670 | 970 | 95 | 140 |

gives high values for substances of low molecular weight and low values for substances of high molecular weight (TABLE 6). The figures given are at medium sensitivity.

Ethyl alcohol, which gives the lowest value on the proposed formula, gives the highest on the Dimbat and Porter formula. This serves to emphasize the fact that the latter concerns weight detectable, while the former gives an indication of the instrument's efficiency as a vapor detector in gas streams; obviously, the latter is of more fundamental importance. The weight detectable may always be diminished by various procedures. The dilution detectable in the gas stream remains broadly unaffected by such expedients.

### *Discussion*

*Defects of theory.* The present theory appears to give a good guide to katharometer behavior, but it is not complete. In considering the heat balance, it was assumed that the thermal conductivity of the gas was constant at all values of $\theta$. This is not true, as is shown by the fact that the wire temperature is less than expected at very high values of $i^2R$ (for example, over 1.0 watts). $\epsilon$ decreases with increase of katharometer temperature and it is possible that, by taking into account the variation of $k'$ with $\theta$, the departure from the present theory at high values of $\theta$ may be accounted for. Preliminary examination shows this line of attack to be promising, but it is still not possible to account for $w$ and inverted peaks as reported by many workers.[6, 7] However, these may be due to other causes.[8]

*Rate of flow, pressure, and response.* During the course of this investigation it was shown that the katharometer response for many compounds was independent of the pressure prevailing in the instrument. However, as the thermal conductivity of some vapors is markedly dependent on pressure,[9] this is unlikely to prove an invariable rule.

It was also shown that, except where convection probably was a factor, for example, in vertical katharometers, the response was independent of rate of flow over a very wide range. However, if the contribution by rate of flow to heat loss was made significant, a relationship could be expected, irrespective of changes of $\theta$.

*Good design in katharometers.* The rules drawn up by Keulemans[3] for good design of katharometers may now be amended and expanded.

Two of these rules should be taken in conjunction. Great stress need not be laid on symmetry if temperature control is improved. In this case the wire temperature was constant within ±0.001° C. or ±0.003 per cent at 161.5° C. This was achieved solely by a vapor bath. Evidence for this may be seen in part by examination of TABLE 1. In the conditions under which the figures given were recorded, there was a slight drift of base line that was always present with the apparatus used, due, it is believed, to the polarization of the accumulators. The noise was virtually undetectable; that is, it was less than ±½ mm. This can be compared with the peak given by 8 $\mu$g. of pinene, which was 8 mm. in height, and corresponds to a noise level of not more than 6 $\mu$v. A noise level of this order for katharometers has been quoted by Keulemans.[10] In these cases symmetry is advantageous, but not essential. Flow sensitivity need not be a problem in katharometers.

There seems to be no doubt that these improvements are due to the use of thin wires. Further advantage has been obtained by making the leads thermally as nonconducting as possible. In my opinion, the greatest advantage in symmetry can be obtained by making the filaments of as nearly the same resistance as possible. This is done most readily by using demountable filaments, as a suitable pair can be selected readily.

Undoubtedly convection is a factor in katharometer equilibrium, particularly at low gas flows, but it can be virtually eliminated by the use of a horizontal instrument.

## *Acknowledgment*

I thank the directors of W. & A. Gilbey, Ltd., London, England, for permission to publish this work.

## *References*

1. WISEMAN, W. A. 1957. Chem. & Ind. London. : 1356.
2. WISEMAN, W. A. Unpublished data.
3. KEULEMANS, A. I. M. 1957. Gas Chromatography. : 78–93. Reinhold. New York, N. Y.
4. KANNALUICK, W. G. & L. H. MARTIN. 1934. Proc. Roy. Soc. London. **A144:** 496.
5. DIMBAT, M., P. E. PORTER & F. H. STROSS. 1956. Anal. Chem. **28:** 290.
6. PURNELL, J. H. 1957. Chem. & Ind. London. : 815.
7. HARVEY, D. & C. O. MORGAN. 1956. V. P. C. Symposium, London, England. : 74.
8. KEPPLER, J. G., G. DIJKSTRA & J. A. SCHOLS. 1956. V. P. C. Symposium, London, England. : 222.
9. LAMBERT, J. D., E. N. STANLEY & S. B. WOODS. 1950. Proc. Roy. Soc. London. **A200:** 262.
10. DESTY, D. 1957. Nature. **180:** 22.
11. GREGORY, H. & C. T. ARCHER. 1926. Proc. Roy. Soc. London. **A110:** 91.
12. LITTLEWOOD, A. B. Private communication.

## APPENDIX

The derivation of the equations in this paper is primarily from the classic equilibrium equations of thermal conductivity cells.[11] In these, all forms of heat loss are considered. When considering practical katharometers, a number of the ways of losing heat may be ignored, and it can be shown that basically most of the heat lost is by thermal conductivity to the walls of the cell, by thermal conductivity down the supporting leads and, in some cases, by donation to the flowing gas. Therefore, considerable information can be obtained by considering the plot of heat supplied, that is, $i^2R$, and the temperature the wire attains.

The situation is given in EQUATION 4

$$i^2R = Jk''m\theta + Jk\theta(l_1 + l_2) + Jk\theta_k(l_1 + l_2) + Jk'\theta 2\pi\beta l_k$$

Provided the heat lost down the leads is small, a straight-line plot of $i^2R$ against $\theta$ should be obtained. In practice, the determination of $\theta$ depends on an accurate value of the temperature coefficient of resistivity. There is some doubt about this; its determination requires accurate work at several temperatures. It is more convenient to plot the resistance of the filament against $i^2R$, as in EQUATION 7. Obviously, as the resistance of the wire can never fall below $R_0$, a straight line need not necessarily be obtained, as explained previously. From the slope of the straight portion of this plot, it is possible to obtain a value for the rate of loss of heat from the filament. By comparing rates of loss of heat under various conditions, further information may be obtained, as shown under *Tests of Theory*. As pointed out, the departure from linearity also provides information. The factors that affect katharometer sensitivity are fairly straightforward and are discussed fully above.

The statement that noise level is approximately proportional to $\theta$ probably is not true. Subsequently, it has been shown that noise is probably more nearly proportional to the wire current. Obviously, electric noise plays a considerable part in the general noise of the katharometer. This is one of the principal reasons why the object in designing the katharometer is to obtain as big a resistance in as short a filament length as possible. This is shown in TABLE 7, where the wire current is approximately 55 mAmp. in all cases.

Whereas the theory is adequately obeyed when using hydrogen and helium, usually it is not obeyed when using nitrogen. In theory, the katharometer should give a bigger response when using nitrogen than when using helium. While this is true at low wire temperatures and bridge currents, it is not true under all normal working conditions. I have discussed this with A. B. Littlewood,[12] who has been working on a theory similar to the one presented here, but one with a much more fundamental approach to the problem. Littlewood hopes to be able to show that the fall off in response when using nitrogen is as expected and that, ultimately, inverted peaks may be obtained, as have already been shown experimentally. His work also leads to the view that such anomalous behavior should not be expected with hydrogen or helium.

TABLE 8 shows the effect of convection. These results are effective for all reasonable

TABLE 7

| Katharometer resistance (approx.) | Noise | Signal/noise |
|---|---|---|
| 8 ohms | ±1.3 μv. | 5 |
| 30 ohms | ±2. μv. | 50 |
| 100 ohms | ±5 μv. | 500 |

Wire current approx. 55 mAmp. in all cases.

TABLE 8

| | Vertical katharometer | | | Horizontal katharometer | |
|---|---|---|---|---|---|
| Rate of flow, cc./min. | 11 | 23 | 58 | 7 | 34.5 |
| Response, μv. | 20.7 | 43.7 | 46.8 | 6250 | 6080 |

rates of gas flow. However, evidence for its occurrence has been obtained by comparing a vertical katharometer with a horizontal one at very low rates of flow. There is a fall-off in katharometer response with a vertical katharometer, whereas none occurs with a horizontal one. This is illustrated in the table.

Table 6, above, has indicated that the katharometric responses of equal molar quantities of most substances are equal. Some evidence for this was produced at the London Gas Chromatography Symposium, but some workers have found that with hydrocarbons it is equal weights that give equal responses. Obviously, more work is required to determine which is correct; certainly, theory does not explain the subject.

Many other features of katharometer response and wire temperature have been considered, and it would be impossible to discuss all details. The main conclusion to be drawn from this work is the fact that for good katharometer design, the resistance of the filament is of the greatest importance.

# THE 1,2-DIBROMO-1-PROPENES*

Lewis F. Hatch and Jimmie S. Payne, Jr.
*Department of Chemistry, The University of Texas, Austin, Tex.*

During a study of geometrical isomers (*cis*, *trans*) it became desirable to obtain pure *cis*-1,2-dibromo-1-propene and *trans*-1,2-dibromo-1-propene. Van Risseghem[1] has reported the preparation of the two isomers by the dehydrobromination of 1,1,2-tribromopropane:

$$CH_3CHBrCHBr_2 + KOH \rightarrow CH_3CBr{=}CHBr + KBr + H_2O$$

Smith and Line[2] obtained the two isomers by distillation of a commercial mixture prepared by the method of van Risseghem and reported the dipole moments of the isomers.

We obtained a mixture of dibromopropenes from the same commercial source, and two fractions (125° and 135° C.) were separated by distillation through a 3-foot, glass-helices packed column at a pressure of 33 mm. Hg and a reflux ratio of 40:1. The distillation curve (FIGURE 1) is similar to that obtained by Smith and Line, and the physical properties of the fractions correspond closely with those in the previous literature (TABLE 1). However, gas chromatographic analysis indicated that each fraction contained two compounds in a ratio of about 4:1 (FIGURE 2). A 20-foot, ¼-in. copper column containing Curtin X-3 was used for the analysis at 150° C., with helium as the carrier gas. The column had an efficiency of more than 3000 plates, as calculated by the method of James and Martin.[3] The two compounds in the lower boiling fraction were designated $\alpha$ and $\beta$, and the two in the higher boiling fraction, $\gamma$ and $\delta$.

Both fractions gave a molecular refraction for a dibromopropene; thus the 4 compounds were isomeric. The boiling points of the seven isomeric dibromopropenes are given in TABLE 2. The presence of *cis*-1,3-dibromo-1-propene and *trans*-1,3-dibromo-1-propene is not probable because of their relatively high boiling points (153° and 159° C.).[4] Their absence was confirmed by the addition of both isomers to an intermediate fraction of the distillate. Gas chromatographic analysis of the mixture showed no increase in peak height for any of the 4 unknown components.

The presence of 3,3-dibromo-1-propene is not excluded by its boiling point (134° C.), but it is reported to rearrange readily to the 1,3-dibromo-1-propenes:[5]

$$CH_2{=}CHCHBr_2 \rightarrow CHBr{=}CHCH_2Br$$

The other 4 isomers have boiling points close to the boiling range of the 2 fractions separated by distillation and reported to be pure *cis*-1,2-dibromo-1-propene and *trans*-1,2-dibromo-1-propene.

It was not possible to effect a satisfactory separation of either fraction into

---

* The work reported in this paper was supported in part by grants from the Robert A. Welch Foundation, Houston, Texas., and the Phillips Petroleum Company, Bartlesville, Okla.

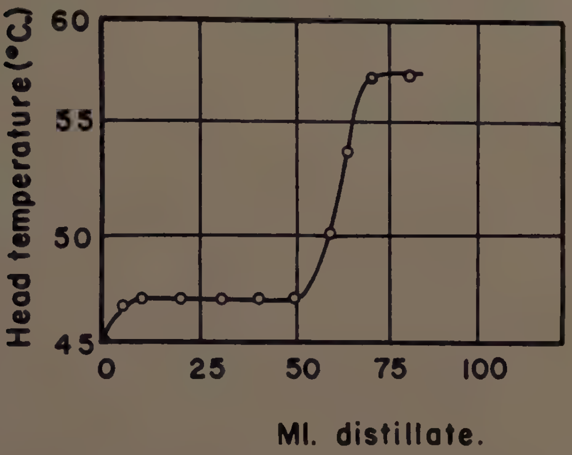

FIGURE 1. Distillation of commercial 1,2-dibromo-1-propenes at 33 mm. Hg pressure.

its components by distillation or by fractional crystallization. Gas chromatography was used to obtain a relatively pure sample of the α compound, but the quantities of the other isomers were not sufficient to permit adequate separation and identification. Because of the difficulty in obtaining pure samples of the unknown compounds, indirect methods were used to characterize them.

A portion of an intermediate fraction of the distillate was treated with alcoholic potassium hydroxide. The conditions for the reaction were: 2 per cent KOH, 70° C., 30 min. The reaction was stopped by the addition of an excess of dilute sulfuric acid. The organic layer was separated, dried, and analyzed by gas chromatography. Both of the higher boiling compounds (γ and δ) apparently reacted with the base more readily than did the lower boiling compounds (α and β). This was indicated by the disappearance of their characteristic peaks (FIGURE 3).

Another portion of the same intermediate fraction was treated with lithium

TABLE 1

PHYSICAL PROPERTIES OF THE TWO FRACTIONS FROM THE DISTILLATION OF THE 1,2-DIBROMO-1-PROPENES

| Fraction | B.p., °C. (mm.) | $n_D^t$ | $d_4^t$ | $MR_D$* |
|---|---|---|---|---|
| Low boiling | 125 (760)† | 1.5369 (17.4)† | 2.0027 (17.4)† | 31.16 |
| | 40.9 (28)‡ | 1.5275 (30)‡ | 1.9743 (30)‡ | 31.15 |
| | 47.0 (33) | 1.5277 (30) | 1.9721 (30) | 31.12 |
| High boiling | 135 (760)† | 1.5337 (17.4)† | 2.0235 (17.4)† | 30.69 |
| | 51.4 (28)‡ | 1.5282 (30)‡ | 1.9900 (30)‡ | 30.72 |
| | 57.0 (33) | 1.5185 (30) | 1.9882 (30) | 30.73 |

* $MR_D$, theory = 31.12.
† Van Risseghem.[1]
‡ Smith and Line.[2]

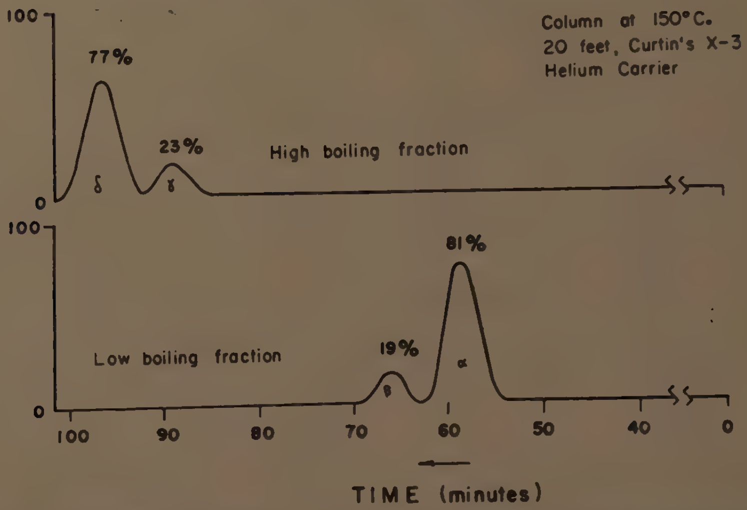

FIGURE 2. Analysis of fractions of 1,2-dibromo-1-propenes by gas chromatography.

aluminum hydride in ether. This reagent will replace allylic halogen atoms by hydrogen, but it will not react with vinyl halogen atoms under the conditions used:[6]

$$4CH_2{=}CBrCH_2Br + LiAlH_4 \rightarrow 4CH_2{=}CBrCH_3 + LiBr + AlBr_3$$

The excess hydride was decomposed by dilute sulfuric acid after the one-hour reaction time at the reflux temperature of ether. The organic layer was separated and dried, and the solvent ether was removed by distillation. The remaining material was analyzed by gas chromatography (FIGURE 4). The

TABLE 2

BOILING POINTS OF THE ISOMERIC DIBROMOPROPENES

| Isomer | Boiling point, °C. (mm.) |
|---|---|
| $CH_3CH{=}CBr_2$ | 127 (750)* |
| $CH_3CBr{=}CHBr$ (*trans*) | 125 (760)† |
| $CH_3CBr{=}CHBr$ (*cis*) | 135 (760)† |
| $CHBr{=}CHCH_2Br$ (*cis*) | 60 (25)‡ |
| $CHBr{=}CHCH_2Br$ (*trans*) | 66 (25)‡ |
| $CHBr{=}CHCH_2Br$ (both isomers) | 154–156 (760)§ |
| $CH_2{=}CBrCH_2Br$ | 40.5 (18)‖ |
| | 141 (760)¶ |
| $CH_2{=}CHCHBr_2$ | 134 (760)¶ |

*Kirrmann.[9]
† van Risseghem.[1]
‡ Hatch and Harwell.[4]
§ Stitz.[10]
‖ Hatch *et al.*[11]
¶ Kirrmann.[5]

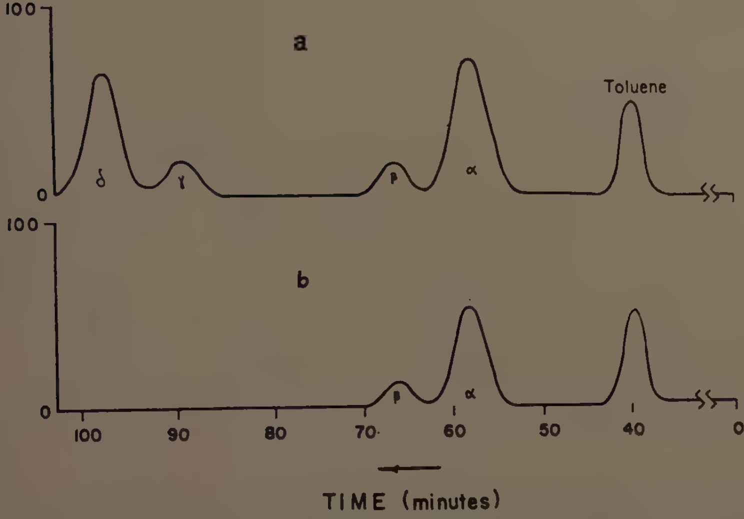

Figure 3. (*a*) Analysis of intermediate fraction of 1,2-dibromo-1-propene and (*b*) of the same fraction after treatment with KOH. Toluene used as a reference standard.

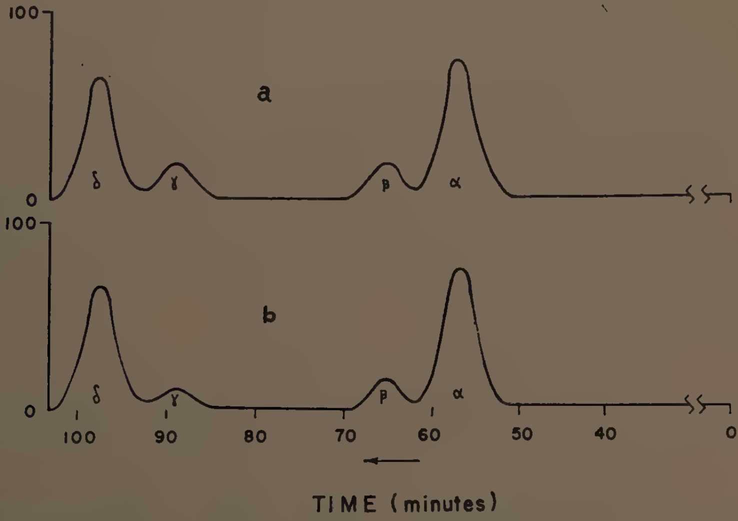

Figure 4. Analysis of intermediate fraction of 1,2-dibromo-1-propene: (*a*) before and (*b*) after treatment with $LiAlH_4$.

results clearly show that the $\gamma$ compound contained allylic bromine. The $\beta$ compound appeared to react to a small extent, but the other two compounds did not react and therefore must contain only vinyl bromine atoms. These data indicate that the $\gamma$ compound is 2,3-dibromo-1-propene ($CH_2{=}CBrCH_2Br$). The characterization is not rigorous because 3,3-dibromo-1-

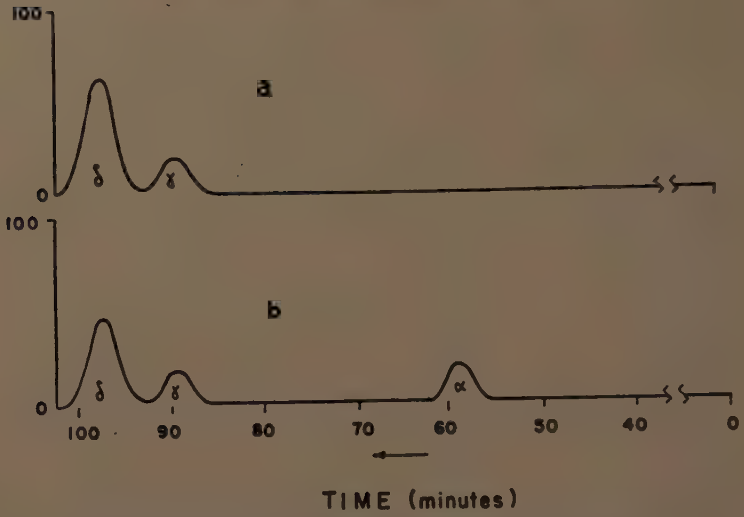

FIGURE 5. Irradiation of high boiling fraction of 1,2-dibromo-1-propene: (*a*) before and (*b*) after irradiation.

propene would show the same qualitative chemical properties. Its presence would not be expected, however, because of its rapid allylic rearrangement to the 1,3-dibromo-1-propenes.[5]

The other high boiling compound must be one of the two isomers of 1,2-dibromo-1-propene. A portion of the higher boiling fraction was irradiated by a strong light in a manner previously reported to isomerize similar geometrical isomers.[7] Gas chromatographic analysis indicated that the δ isomer isomerized to the α isomer (FIGURE 5); therefore, δ and α are the isomeric 1,2-dibromo-1-propenes. Because the δ isomer reacted with alcoholic potassium hydroxide and the α isomer did not, the δ isomer is *cis*-1,2-dibromo-1-propene. The α isomer is *trans*-1,2-dibromo-1-propene:

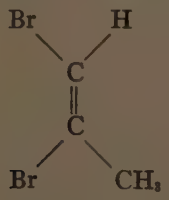

δ

*cis*-1,2-dibromo-1-propene

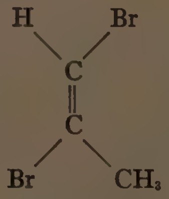

α

*trans*-1,2-dibromo-1-propene

The characterization is based on the greater ease of *trans* elimination in a dehydrohalogenation reaction.[8]

A mixture of an authentic sample of 1,1-dibromo-1-propene and a portion of an intermediate fraction from the distillation were analyzed by gas chromatography (FIGURE 6). The size of the β peak was increased in direct proportion to the amount of 1,1-dibromo-1-propene added. The size of the other

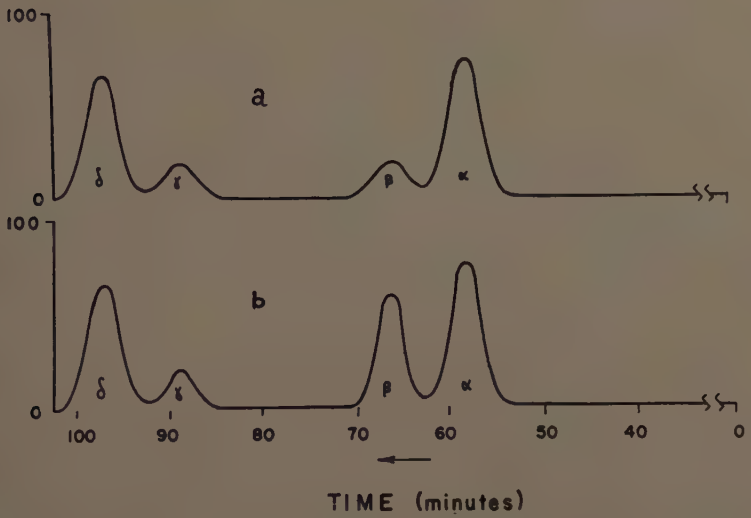

FIGURE 6. Effect of added 1,1-dibromo-1-propene (*b*) to the intermediate fraction of 1,2-dibromo-1-propene (*a*).

peaks remained constant. Therefore the β isomer is 1,1-dibromo-1-propene ($CH_3CH{=}CBr_2$).

TABLE 3 illustrates the probable genesis of the four isomeric dibromopropenes under discussion.

The dipole moment for the lower boiling fraction was reported by Smith and Line[2] to be 1.16D and 1.97D for the higher boiling fraction. From these data they concluded that van Risseghem's assignment of configuration for

TABLE 3

THE DIBROMOPROPENES FROM PROPENE

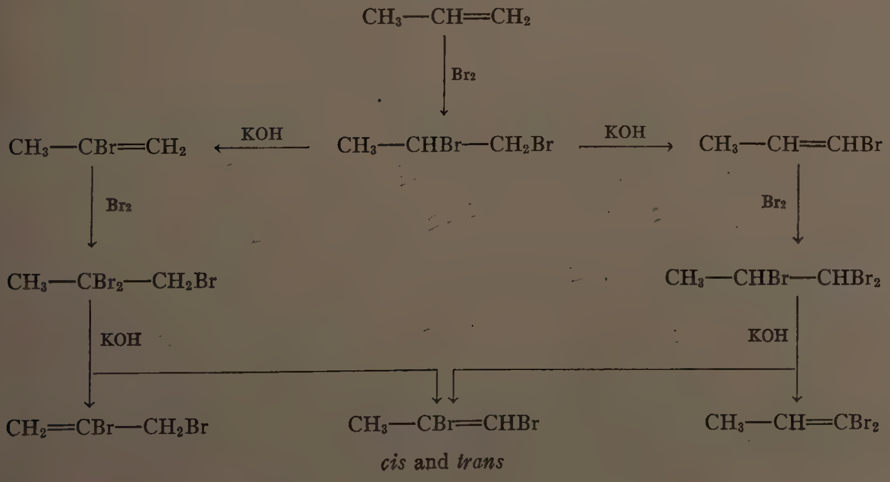

the two 1,2-dibromo-1-propenes was correct. Our work confirms their conclusions in respect to the configuration. Smith and Line rationalized the high dipole moment of the "*trans* isomer" on the basis of a charged resonance structure for the 1,2-dibromo-1-propene. Probably the high value was due, at least in part, to the presence of 1,1-dibromo-1-propene as an impurity.

Our work illustrates the value of gas chromatography in the analysis and identification of small quantities of mixtures of closely boiling compounds. It is especially useful in determining whether one is making exact measurements on impure materials. It is believed that Smith and Line were not working with pure *cis*- and *trans*-1,2-dibromo-1-propene.

## *References*

1. van Risseghem, H. 1919. Bull. soc. chim. Belg. **28:** 376.
2. Smith, H. A. & L. E. Line. 1950. J. Am. Chem. Soc. **72:** 5434.
3. James, A. T. & A. J. P. Martin. 1952. Biochem. J. **50:** 679.
4. Hatch, L. F. & K. E. Harwell. 1953. J. Am. Chem. Soc. **75:** 6002.
5. Kirrmann, A. 1936. Compt. rend. **202:** 1934.
6. Hatch, L. F. & R. H. Perry. 1949. J. Am. Chem. Soc. **71:** 3262.
7. Harwell, K. E. & L. F. Hatch. 1955. J. Am. Chem. Soc. **77:** 1682.
8. Cristol, S. J. 1947. J. Am. Chem. Soc. **69:** 338.
9. Kirrmann, A. 1948. Bull. soc. chim. : 168.
10. Stitz, F. 1947. Österr. Chemiker-Z. **48:** 186.
11. Hatch, L. F., H. E. Alexander & J. D. Randolph. 1950. J. Org. Chem. **15:** 654.

# GAS CHROMATOGRAPHIC ANALYSIS OF MIXTURES CONTAINING OXYGEN, NITROGEN, AND CARBON DIOXIDE

Nathaniel Brenner and Edward Cieplinski
*The Perkin-Elmer Corporation, Norwalk, Conn.*

The versatility and latitude of gas chromatography have increased rapidly in the short years of its history. However, as is often true of rapidly developing analytical techniques, small obstacles to progress are often bypassed rather than overcome. This is illustrated by the application of the technique to the separation of samples containing oxygen, nitrogen, and carbon dioxide. While most conceivable light gas separations had been accomplished by the early workers who then proceeded to separations of much greater challenge, this single, but significant, separation remained unaccomplished.

The use of solid adsorbents such as silica, alumina, and charcoal for the separation of $CO_2$ from the other components of air is well documented.[1–3] The oxygen is separable from the nitrogen only incompletely and at such a greatly reduced temperature (that of liquid nitrogen) that the time required for elution of $CO_2$ is excessive.

The problem of separating oxygen from nitrogen is considerably more difficult. To date only one type of adsorbent has been reported that will perform this separation adequately and conveniently. These are the synthetic zeolites sold commercially under the name "molecular sieves."* These materials succeed in making a complete and rapid separation of $O_2$ and $N_2$ at room, or even elevated, temperatures. Other light gases such as methane, carbon monoxide, and hydrogen also may be separated readily.

Unfortunately, all the molecular sieves developed to date adsorb carbon dioxide irreversibly under those conditions necessary for separation of the other light gases. Therefore, no sample to be analyzed for $O_2$ and $N_2$ content could be analyzed concurrently for $CO_2$ content.

Therefore, all such analyses have been accomplished heretofore by two separate analyses, at a consequent cost in time, equipment, and sample requirements.

The method described in this paper permits the analysis of all three gases, plus other light gases of interest, using a single sample in a single analysis on a standard gas chromatograph.

A "parallel column" system shown in FIGURE 1 was built to permit the passage of a portion of an injected gas sample into each of two flow paths *a* and *b*. A column of 5Å molecular sieve was inserted in one part and a short column of silica gel (Davison type 15, 35 to 60 mesh) was placed in the other part. Therefore, the portions of the sample were being separated in two different modes. In one, the separation was made into oxygen and nitrogen, with $CO_2$ adsorbed irreversibly. This separation alone is shown in FIGURE 2.

---

* Product of Linde Company, Division of Union Carbide & Carbon Corporation, New York, N. Y.

In the other column, a concurrent separation was made of the sample into oxygen and nitrogen as one band and $CO_2$ as another. This separation is shown in FIGURE 3. The combined separation performed by the parallel system is shown in FIGURE 4.

The quantitative analysis of this system must be based upon the use of known standards. The absolute amount of each component analyzed is dependent not only upon its concentration in the sample, but is related also to the relative flow impedances of the two columns *a* and *b*. For example, if the silica has much larger particles than the molecular sieve and has a shorter length or wider diameter, its resistance to flow will be much smaller. If this is the case, a larger proportion of the sample will be swept into this column along with the greater flow of carrier gas. Therefore, it will *appear* that a relatively large quantity of $CO_2$ is present, although usually this is not the case. In practical use, the system very logically might be adjusted in this way to increase the sensitivity to $CO_2$ (usually present in low concentrations) vis à vis $O_2$ and $N_2$ (usually present in high concentrations).

However, provided that a single set of flow, temperature, and column conditions is maintained, the division of the sample between the two columns will remain at a fixed ratio. A convenient analogy may be made between this

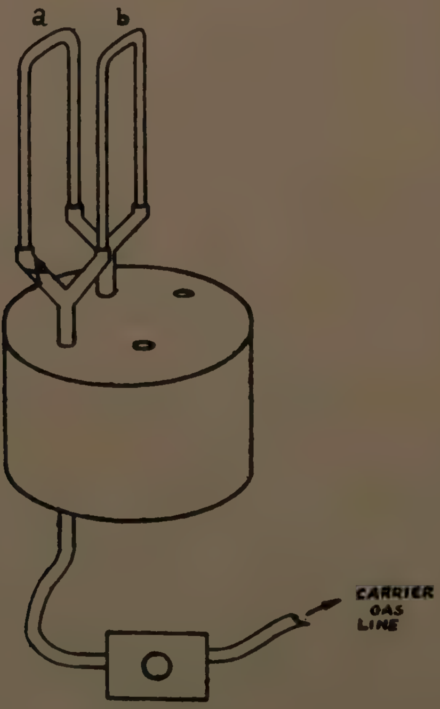

FIGURE 1. Parallel column system.

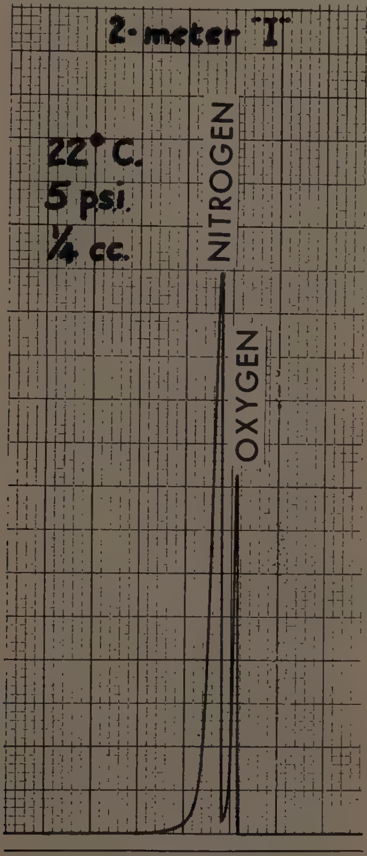

Figure 2. Expired air.

system and a system of parallel resistors in an electrical circuit. In the electric analogue,

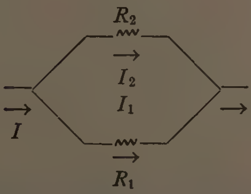

the current $I$, passing through each of the 2 arms will be inversely proportional to the ratio of the resistances $R_1/R_2$ regardless of the absolute value of $I$. This is, of course, Kirchhoff's law.

The same condition of proportionality is attained in our pneumatic system. Therefore, a second sample of gas injected into the instrument as a standard

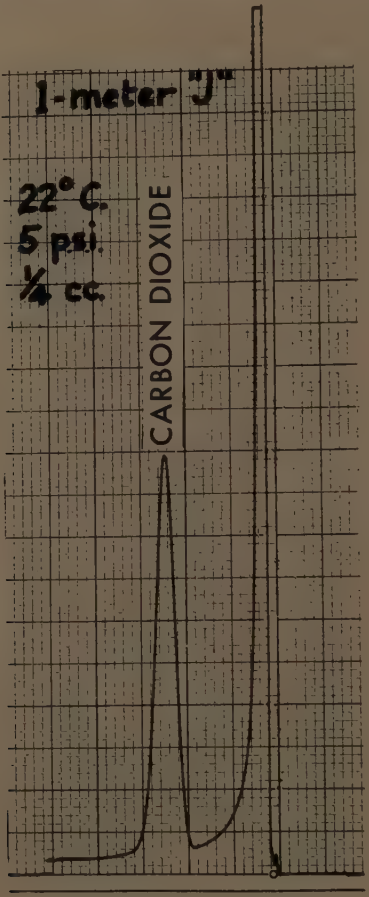

Figure 3. Expired air.

will divide in the same volume ratio as did an unknown gas. Therefore, a series of standards may be used to establish working curves of concentration per unit height of each component band of interest. These curves may then be used directly for immediate calculations of component concentration in unknown mixtures.[4]

Other light gases also may be analyzed together with the $O_2$, $N_2$, and $CO_2$ system. Carbon monoxide, cyclopropane, and ethylene, all of interest in medical and physiological applications, may be analyzed conveniently. Figure 5 illustrates a separation of this type, cyclopropane being the component added. The concentrations of components in this sample are shown in table 1.

Flows were adjusted to each column to give minimum time of elution for cyclopropane and equal sensitivity requirements for $CO_2$, $C_3H_6$, and $O_2$.

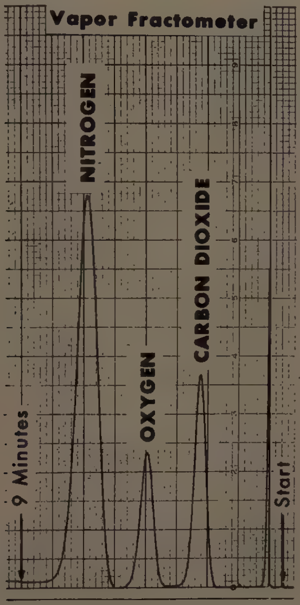

FIGURE 4. Expired air. Perkin-Elmer model 154-C.

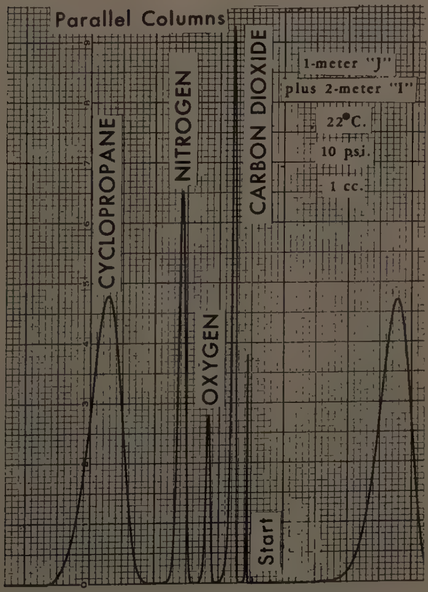

FIGURE 5. Anesthesia mixture.

TABLE 1

| Component | Per cent concentration |
|---|---|
| $O_2$ | 16 |
| $N_2$ | 64 |
| $CO_2$ | 5 |
| $C_3H_6$ | 15 |

The particular run shown here illustrates the reproducibility expected under the least carefully controlled conditions: no thermostat was used to minimize temperature fluctuations during the analyses. The cyclopropane peak may be compared with that of an identical sample run previously (band at right). Had a thermostat been employed, greater precision would be expected.

In many applications, high speed of analysis is essential. Analytical time may be reduced by several procedures: (1) operating the instrument at elevated temperatures; (2) operating at elevated pressures; and (3) using shorter columns of high efficiency. All of these variables may be applied within the limits of resolution of the components of interest.

The result on the analysis time of an increase in pressure is shown in FIGURE 6 where the $O_2$, $N_2$, and $CO_2$ time has been reduced to 2 min. from the 9 min. required originally.

The parallel column system theoretically may be extended in application to

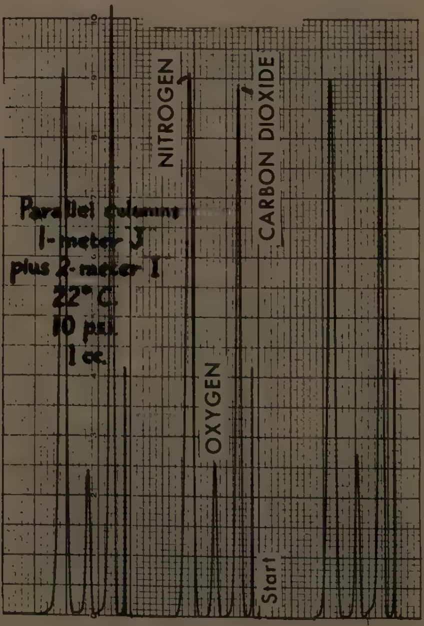

FIGURE 6. Expired air.

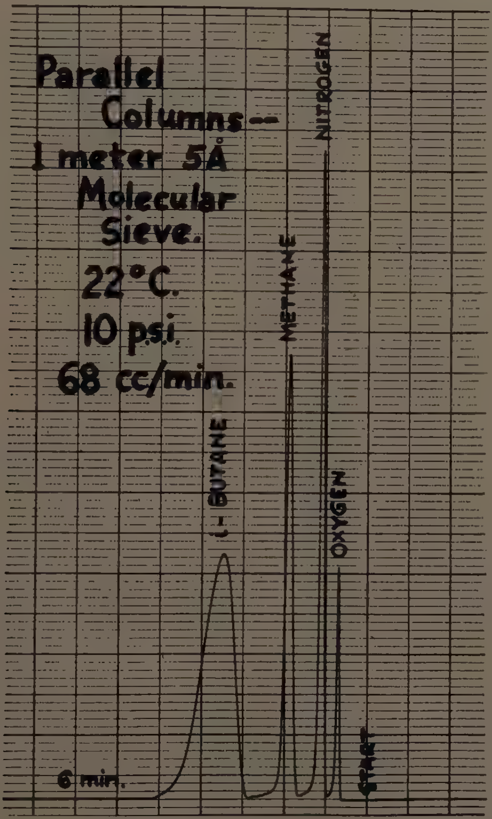

FIGURE 7

any problem in which one column fails to provide complete separation, but practically is limited to cases in which either few components are present or (as in the case of molecular sieves) only a few components are eluted, others being adsorbed.

The $O_2$, $N_2$, and $CO_2$ separation in mixtures containing higher hydrocarbons may be considered. In the mixtures containing no components above $C_3$ and no acetylenic components, the silica gel–molecular sieve system is still useful. However, for higher hydrocarbons, a system of molecular sieve and a partition column capable of separating those hydrocarbons as well as $CO_2$ is recommended.

FIGURE 7 illustrates a "partial" separation of $O_2$, $N_2$, and $C_1$ to $C_4$ paraffins on the molecular sieve column. No peaks are recorded for ethane, propane, or *n*-butane.

FIGURE 8 shows the result of running the same sample on a partition column. $O_2$, $N_2$, and methane are eluted as one band. The complete separation of all components by the parallel column system is shown in FIGURE 9.

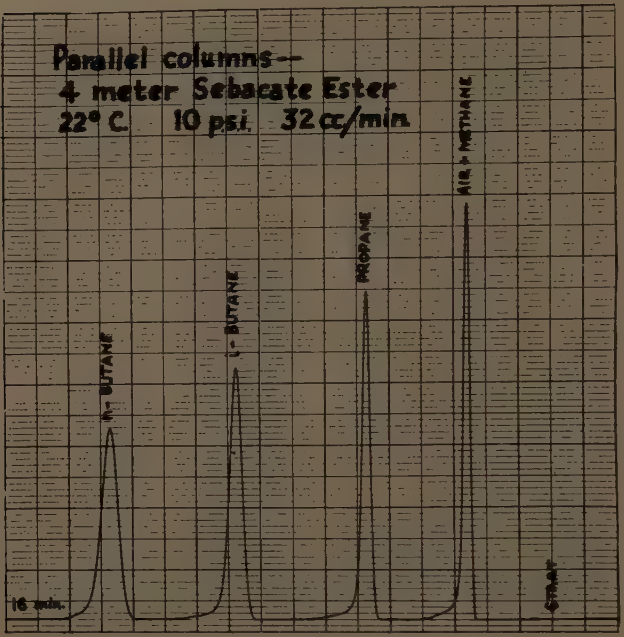

FIGURE 8

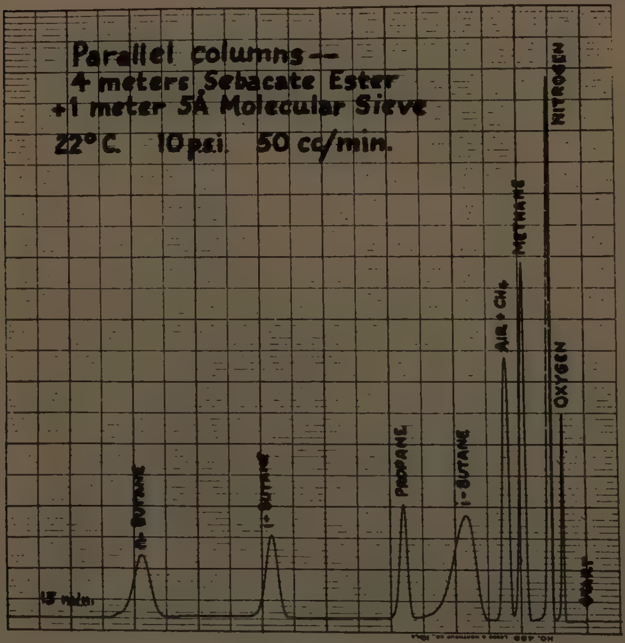

FIGURE 9

## *References*

1. GREENE, S. A., H. L. MOBERG & E. M. WILSON. 1956. Separation of gases by gas adsorption chromatography. Anal. Chem. **28:** 1369–1370.
2. GREENE, S. A. & H. PUST. 1957. Use of silica gel and alumina in gas-adsorption chromatography. Anal. Chem. **29:** 1055.
3. JANÁK, J. 1958. Analysis of natural gas and determination of methane in nine gases. Rept. **No. 13.** Inst. Natl. Industrie Charbonnière. Liège, Belgium.
4. COATES, V. J. & N. BRENNER. 1956. Fuel gas analysis by gas chromatography. Petrol. Refiner. **35**(11): 197–201.

# A RADIO FREQUENCY GLOW DETECTOR FOR GAS CHROMATOGRAPHY

Arthur Karmen and Robert L. Bowman
*Laboratory of Technical Development, National Heart Institute, Bethesda, Md.*

The electric characteristics of an electric discharge in gas have been known to be sensitive to the composition of the gas. Harley and Pretorius[1] reported utilization of this property in the design of a sensing element for vapor phase chromatography that was more sensitive than any previously reported.

In attempting to repeat this work with a discharge tube of similar design, it was noted that the stability of the signal produced was dependent on the stability of the pressure regulation, requiring maintenance of closely controlled reduced pressures, and that the electrode surfaces were sites for the deposition of carbonaceous material that altered the electric properties of the tube.

To reduce the influence of pressure variation, experiments were performed in which a corona discharge was produced between pointed electrodes in helium at atmospheric pressure by a direct current potential of several thousand volts. It was noted that the discharge at the cathode point was more highly concentrated than that at the anode, and that the cathode became more rapidly heated, sputtered and, when organic vapors were passed through the tube, became the site of carbon deposition. All of these factors contributed to a prohibitive amount of electric noise.

Lion[2] reported utilizing measurement of the direct current produced across electrodes in a R.F.-excited gas discharge in the construction of a stable, ultrasensitive mechanoelectric transducer. These observations prompted our investigation of the DC sensitivity of R.F.-excited discharges to small changes in gas composition and of the possibility of utilizing similar measurements in the construction of a sensing device for vapor phase chromatography.

Lion's measurements were accomplished by exciting a discharge by means of an external R.F. electrode in a glass tube filled with gas at reduced pressure, and by measuring the direct current between electrodes placed within the plasma of the discharge. The magnitude of the observed current was reported to be proportional to the geometric and capacitative asymmetry of the probes with respect to the external electrode. For maximum direct current, therefore, a discharge tube was designed consisting of a central wire to which R.F. power was supplied. The wire was mounted along the axis of a shielding metal cylinder that served as the detector cell (FIGURE 1). The cylinder was provided with entry and exit ports for the effluent gases of the chromatographic column and was electrically grounded. The central wire was supplied with power through the secondary winding of a tuned, radio frequency step-up transformer (FIGURE 2). The primary winding of this transformer was connected by a low impedance, coaxial line to the antenna terminal of a conventional, 40-watt, variable frequency oscillator (V.F.O.) stabilized, Viking Navigator radio transmitter.* The secondary winding was grounded through a capacitor. The R.F. circuit through the discharge tube consisted of the grounded metal cylinder of the discharge tube, the gas, the central wire, the secondary winding of the R.F. transformer, and the low impedance pathway to ground through the capacitor. A direct current was measurable between the central wire and the grounded shielding cylinder when electric discharge through the gas was present.

---

* E. F. Johnson Company, Wasica, Minn.

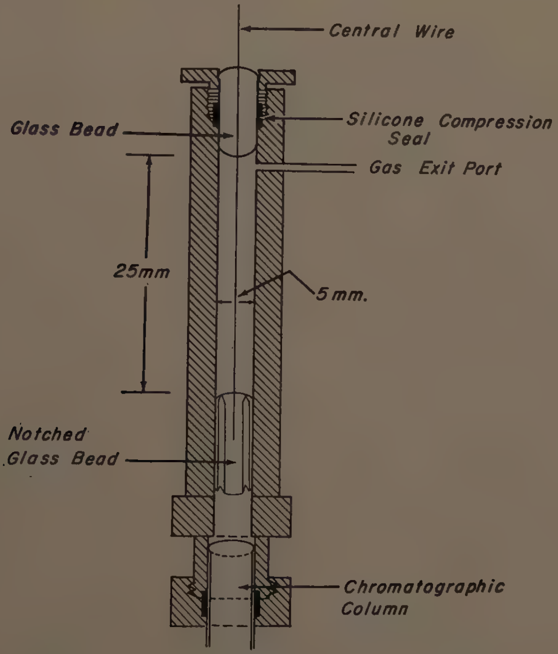

FIGURE 1. Gas discharge tube with metal envelope.

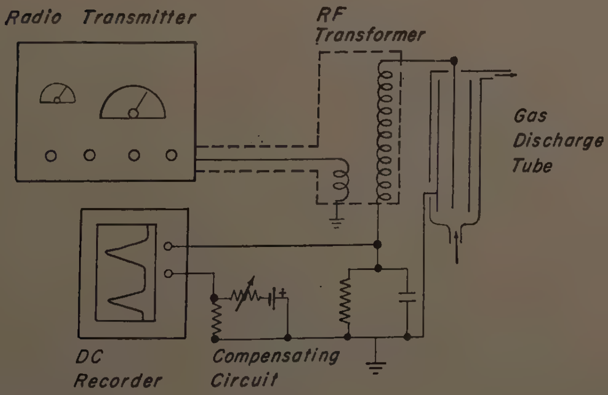

FIGURE 2

This current was measured as the potential drop across a resistor grounding the low side of the secondary transformer winding with respect to direct current. The potential drop across this resistor was applied directly to the input of a standard 5 mv. Speedomax recorder.* The direct current produced by the glow discharge in carrier gas was opposed by the current from a dry cell battery so that a change in current produces a potential only at the input to the recorder.

## *Results*

*Design of discharge tube.* Substituting a cylinder of wire mesh for the solid metal cylinder and enclosing both cylinder and central wire in a glass envelope permitted observation of the discharge. The size and intensity of the glow discharge in pure helium were proportional to the amount of R.F. power supplied. The discharge, utilizing the geometry described, was fairly evenly distributed along, and limited to, the central wire regardless of whether the central wire was connected to the source of R.F. power and the surrounding cylinder grounded, or vice versa. No discharge was visible on the surface of the cylinder. When the power supplied was increased, a localized, powerful arc was seen between the wire and cylinder, which resulted in incandescence of both. The potential of the wire was negative with respect to the cylinder, indicating that the wire was the site of a net collection of electrons, thus resembling the electrode of a DC-activated corona discharge connected to the positive terminal of the power supply. The diffuse character of the discharge showed further resemblance to the positive glow, which seemed fortunate since most of the visible instability of the DC-activated discharge seemed attributable to changes at the cathode surface.

The electric characteristics of the discharge were found to be influenced by the geometry of the discharge tube. Increase in length or diameter of the central wire tended to make the tube more difficult to ignite, possibly because of capacitative losses of the applied R.F. While use of wire of smaller diameter made the discharge easier to ignite, breakdown occurred at lower magnitude of DC signal, probably because of increased heating of the finer wire and resulting secondary emission. Wire diameters between 0.016 and 0.020 in. were generally used in our experiments. The inside diameter of the cylinder, or the spacing between the wire and the cylinder walls, would be expected to influence the internal resistance of the discharge tube, with cylinders of larger diameter causing increase in internal resistance. Because of the desirability of small detector tube size for more rapid indication of changes in gas composition, cylinder diameter has been kept at less than one fourth in. and total wire length below 2 in., with total volume at 1 ml. or less.

Both stainless steel and pure tungsten wires were used; no significant difference between them could be detected, except that tungsten wire was more easily sealed in hard glass for construction of discharge tubes with glass envelopes. The surrounding cylinders have been made of stainless steel, brass, or aluminum.

---

* Leeds & Northrup Company, Philadelphia, Pa.

Under usual operating conditions in pure helium, a DC potential of approximately 50 to 60 volts appears between central wire and cylinder, with internal resistance in the megohm range.

*Effect of small changes in gas composition.* When small quantities of organic vapors are mixed with the helium flowing through the glowing discharge tube, several changes in the character of the discharge occur. The color of the discharge is seen to change from the pale blue observable with pure helium to a brighter, deeper blue color. The radio frequency circuit, of which the discharge tube is a part, is detuned and, if a nonfrequency stabilized power oscillator is used as source of R.F. power, a change in the frequency of the oscillator is observed. The amount of direct current decreases and the extent of the decrease is proportional to the concentration of organic vapor. Among the organic vapors tested that gave this effect were alcohols, ketones, hydrocarbons, and esters of fatty acids. Larger concentrations of these organic vapors extinguish the discharge. When pure helium again passed through the tube, the direct current returned to the starting level.

Small quantities of air mixed with helium caused the color of the discharge to become more purple, and caused an increase in the direct current measurable; larger concentrations of air caused a decrease in DC, progressing to extinction of the discharge. Thus an air peak in the effluent of a column may be qualitatively recognizable.

Since the discharge tube does release heat, its temperature is generally higher than that of its surroundings; in general, cooling the discharge tube was accompanied by a fall in the DC output. When the flow rate of relatively cool helium is appreciably increased, the DC output is decreased, possibly attributable to cooling of the tube elements. Although use of a metal envelope has been found sufficient to buffer temperature transients when the tube is supplied with the effluent of the chromatographic column, the effect of temperature is more marked, with increase in column temperature resulting in a decrease in DC produced. This decrease was accompanied by a change in color of the discharge to the deeper blue characteristic of organic vapors, and the change was attributed to increased volatility of the stationary phase with increase in temperature.

Since small concentrations of organic vapors in helium decrease the DC output of the discharge tube and larger concentrations extinguish the output, it is desirable to increase the DC output in order to extend the range of concentration detection. Therefore the R.F. power supplied usually was increased to the maximum possible, but to less than that required to produce "breakdown" or formation of an arc.

For a given frequency of the exciting field in any given tube, the maximum amount of DC without breakdown was found to be fairly constant. With each of the tubes tested, this amount was found to increase with increase in frequency through the ranges tested (1 to 40 mc.), and the highest frequency obtainable from the transmitter was generally used.

*Sensitivity and stability of the detector.* The amplitude of the signal produced by a given concentration of organic vapor was observed to be proportional to the total direct current produced over the largest part of the range of that current, representing a fraction of that current. Since baseline noise also seemed to be a constant fraction of the total direct current, efforts to increase the sensitivity of the detector could be directed toward increasing the DC output of the tube or toward reducing baseline variations.

The maximum to which the total DC can be raised is limited ultimately only by the power output of the transmitter used, but a more practical limitation is the size and current capacity of the tube. Since current output of the tube was sufficiently large to permit shunting of a large part of the output, most of our efforts have been directed toward reducing baseline noise. Although limiting the current capacity, smaller tube volumes were thought desirable from the analytic standpoint.

Although no data have been obtained thus far concerning the amount of destruction of the organic material passing through the glow discharge, one might expect that this would become more appreciable as the power supplied to the tube increased.

The baseline stability of the system depended on regulation of the R.F. voltage applied to the tube. This was accomplished by the use of regulated power supplies and careful attention to thermal and electric shielding. A large factor contributing to baseline instability is creeping or bleeding of the stationary phase. This is observable as deposition of stationary phase along a portion of the walls of the sensing element, and is more marked at higher operating temperatures with more volatile stationary phases. Since the tube surfaces subjected to the heating influence of the discharge are usually clear, the advisability of separately heating the sensing element and maintaining it at a higher temperature than the column is suggested.

The sensitivity of the detector was estimated with samples of methyl esters of fatty acids, separated on a Celite column using Apiezon L as the stationary phase. Sample operating conditions were: temperature, 190° C.; helium flow at exit, 36 cc./min.; pressure drop 10 psi.

As an example, when methyl laurate, approximately 1.6 $\mu$g., was passed through the column, a peak 2.56 in. high, representing 1.28 mv. and 6 per cent of the total DC signal resulted. The mean mole fraction for this peak of methyl laurate in the helium was calculated to be $5 \times 10^{-7}$. During this experiment the baseline noise level was within 0.1 in., representing 0.3 per cent of total signal. In the units of sensitivity suggested,[3] this may be expressed as $1.6 \times 10^{5}$ mv. ml./mg. for methyl laurate (M.W. 214) with a noise level of 0.05 mv. Separating synthetic mixtures of methyl esters of fatty acids, it was found that the area under each peak appeared proportional

Table 1

| | Methyl laurate percentage | Methyl myristate percentage | Methyl palmitate percentage |
|---|---|---|---|
| Reported | 24 | 15.1 | 60.8 |
| Found | 25.2 | 17 | 57.8 |

to the mole fraction of the ester represented. Close agreement has been obtained between the composition estimated from areas under the peaks obtained with this detector and the percentage composition estimated from separations using a thermal conductivity detector (TABLE 1). Whether there is a change in the response of the detector to large changes in the molecular weight of the substances analyzed has not yet been determined.

## *Summary*

A sensing device for vapor phase chromatography has been constructed based on measurement of the changes in the electrical characteristics of a R.F.-excited glow discharge in helium.

The discharge may be excited at atmospheric pressure, is relatively insensitive to ambient pressure and flow changes, and is only slightly more sensitive to temperature changes.

The signal produced is of such magnitude as to permit measurements with standard DC recorders without additional amplification.

Although ultimate sensitivity has not yet been reached, sensitivity with the present model permits analysis of microgram quantities of organic materials in the effluent of a conventional gas chromatograph operated at high temperature.

## *References*

1. HARLEY, J. & V. PRETORIUS. 1956. A new detector for vapour phase chromatography. Nature. **178:** 1244.
2. LION, K. S. 1956. Mechanic-electric transducer. Rev. Sci. Inst. **27:** 222.
3. DESTY, D. H. 1957. Vapour detectors for gas chromatography. Nature. **180:** 22.

# A NEW TYPE OF IONIZATION DETECTOR FOR GAS CHROMATOGRAPHY

J. E. Lovelock, A. T. James, and E. A. Piper
*National Institute for Medical Research, London, England*

High resolution is attained in gas chromatography only with small loads of volatile substances and this, in turn, demands a highly sensitive device for measuring the low concentrations of vapor emerging from the chromatograph column.

The detection methods so far proposed fall into two principal categories: those measuring the bulk properties of the gas mixture, and those measuring specific properties of the emergent vapors. Detectors in the first category measure differences in the density, thermal conductivity, and ionization cross section of the gas mixture. The principal disadvantage of this type of detector is that the bulk properties of the gas mixture also vary with temperature and pressure and, unless special precautions are taken to neutralize the effects of small changes in these variables, high sensitivities cannot be attained. In these circumstances, it is not surprising that the only detector in this category with a sensitivity sufficient to exploit the full resolution of gas chromatography is the gas density balance (A. J. P. Martin and A. T. James, 1956). In this detector, complex and ingenious methods are used to balance out variations in temperature, pressure, and rate of gas flow. Detectors in the second category include those measuring specific chemical properties, combustibility (R. P. W. Scott, 1956), and specific ionization properties (J. Harley and V. Pretorius, 1957; S. A. Ryce and W. A. Bryce, 1957; and J. E. Lovelock, 1958). Usually, detectors in this category are unaffected by temperature and pressure changes and are sensitive. However, they have the disadvantage of a sensitivity that varies from substance to substance and cannot be calculated from simple physical parameters. The detector described in this paper does not have this disadvantage; it responds similarly to nearly all volatile organic substances. Its sensitivity is such that it will detect $2 \times 10^{-13}$ moles, and it is insensitive to temperature, pressure, and rate of gas flow. In addition to these desirable properties, it is simple and inexpensive to construct.

## *Principles of Operation*

A volume of rare gas exposed to a continuous flux of ionizing radiation contains not only ions, but also a considerable proportion of excited, but non-ionized atoms. These excited atoms are metastable and, after a comparatively long lifetime for metastable atoms ($10^{-4}$ sec.), decay to the ground state following the emission of ultraviolet radiation. If during its lifetime a metastable atom encounters a vapor molecule, energy may be transferred and the vapor molecule ionized. A detector making use of this effect consists simply of an ionization chamber containing a source of radiation. If a rare gas is used as the carrier in gas chromatography, the emergence from the column of vapor molecules causes an increase in the ionization current flowing in the detector. The concentration of metastable atoms in an irradiated rare gas, for example, argon, is less than the concentration of argon ions, so that the increase in current even with a high concentration of vapor will be small. However, it is possible to increase the concentration of excited atoms; if the voltage applied to the chamber is sufficiently raised, the velocity of the free electrons in the gas reaches a value sufficiently high to excite more argon atoms by collision, but insufficient to produce more argon ions. With a typical detector an increase in applied voltage from 400 to 1600 increases the concentration of metastable atoms almost $10^4$ times, without appreciably increasing the concentrations of ions. Of course, the sensitivity of the device is related directly to the concentration of excited atoms, and consequently a wide range of sensitivities can be obtained simply by varying the applied voltage. By a fortunate coincidence, the most suitable rare gas for use with this detector is argon, which is also the cheapest and most readily available. The heavier rare gases, krpyton and xenon, have excitation potentials for their metastable atoms too low to ionize many organic compounds. On the other hand, the excitation potentials of neon and helium are so high that traces of the other rare gases normally present in the commercial product discharge the metastable atoms as fast as they are formed.

### *Construction of the Detector*

The construction of the detector is shown in FIGURE 1. It consists of a cylindrical chamber, 1 in. in diameter and 1 in. deep, of brass or of aluminum. A metal disc, 0.5 in. in diameter and 0.03 in. thick, is supported centrally

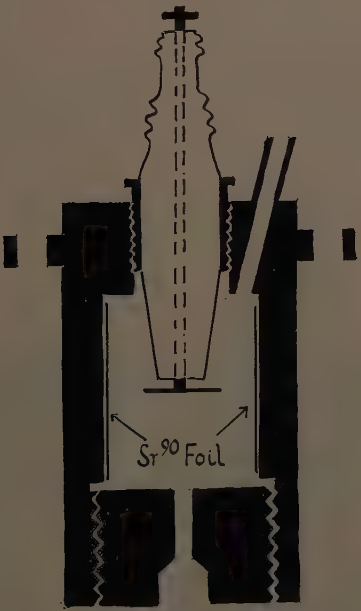

FIGURE 1. The construction of the detector.

within the chamber and serves as the collecting electrode for the negative ions produced in the chamber. The collecting electrode is mounted on the end of a spark plug, and the ceramic insulation of the plug serves to isolate it from the body of the chamber. Gas from the chromatograph column is led into the chamber through a channel drilled in the base and out through a narrow tube close to the plug. None of the chamber dimensions are critical, although wide variations from the dimensions given will produce detectors with different electric characteristics.

The ionizing radiation is provided by a $\beta$-particle source of the type used with industrial thickness gauges. It consists of a thin sheet of silver foil containing 10 mc. of $Sr^{90}$ sandwiched between two inert sheets of silver foil. With pure argon at 25° C., a source of this type gives a saturation current of approximately $10^{-8}$ amp. The radiation from the source is absorbed completely by the walls of the chamber, and the only external radiation from the detector is a small flux of soft X radiation excited by the $\beta$-radiation bombardment of the chamber walls. With the detector described, this flux is less than 10 milliroentgens/hour at the surface of the detector. In normal use the detector is enclosed within a heating chamber and this, in turn, is surrounded by a thick layer of thermal insulation; when this is done the external radiation flux at the surface of the completed apparatus is negligible, and therefore the device does not constitute a radiation hazard. The exposed source emits an intense flux of $\beta$ radiation and, of course, all precautions appropriate to the handling of radioactive substances are essential in the assembly of the detector. No detectable leakage of $Sr^{90}$ from the source is expected, or indeed has been observed with two sources during a year of continuous use at temperatures up to 250° C.

The chromatograph column and the detector are both enclosed within channels in an aluminum rod 4 feet long and 2.5 inches in diameter (FIGURE 2). The aluminum rod is wound with 352 feet of 28 S.W.G., double-glass-insulated, nickel-chrome wire for heating and is thermally insulated by a 2-inch layer of Fiberglas. An electric input of 250 w. is sufficient to maintain a temperature of 250° C. The chromatograph columns were of glass tubing 4 feet long, with a 4 mm. I.D. and a wall thickness of 1 mm. The detector

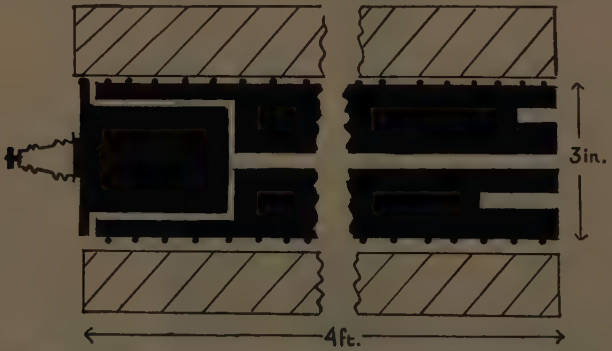

FIGURE 2. The construction of the column support and heater.

end of the column was drawn out to a narrow constriction and a short length of silicone rubber tubing slipped over it. A gas-tight joint between the detector and the column was made by resting the end of the column, with its silicone rubber gasket, in the cone-shaped socket at the top of the detector. With this type of straight column, efficiencies as high as 3000 theoretical plates are obtained consistently, and columns can readily be changed when required. The top of the column is connected directly to the argon cylinder by means of a simple reducing valve. The column is loaded by interrupting the gas flow and introducing the test mixture directly from a micropipette onto the top of the column packing.

The signal from the detector is conveyed to a recorder by means of a simple DC amplifier, for example, that illustrated in FIGURE 3. A suitable value for the input resistance of the amplifier is between 500 and 2000 megohms; with these values the maximum signal from the detector is from 15 to 60 v. In these circumstances no voltage gain is required from the amplifier; indeed, with potentiometric recorders it may be necessary to attenuate the signal several thousandfold. The high level of the signal from the detector enables the recorder and amplifier to be used under conditions where their own inherent drift and noise are imperceptible.

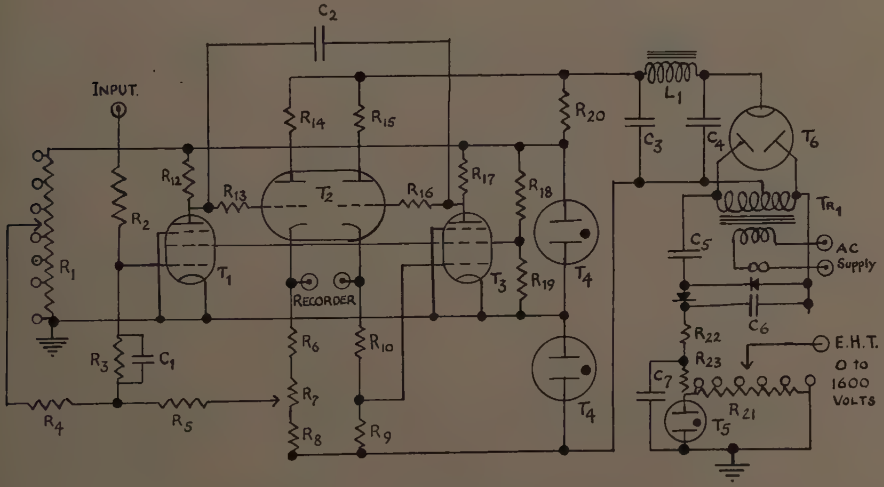

FIGURE 3. Circuit diagram of the amplifier.

*Resistors*

$R_1$ = 6 × 10 k
$R_2$ = 2000 megohms
$R_3$ = 500 megohms
$R_4$ = 4 megohms
$R_5$ = 1 megohms
$R_6$, $R_{10}$ = 4.7 k
$R_7$ = 500 ohms
$R_8$, $R_9$ = 10 k
$R_{12}$, $R_{17}$ = 500 k
$R_{13}$, $R_{16}$ = 1 megohm

$R_{18}$ = 150 k
$R_{19}$ = 250 k
$R_{20}$ = 3.9 k
$R_{21}$ = 5 × 5 megohms
$R_{22}$, $R_{23}$ = 2 megohms

*Capacitors*

$C_1$ = 1000 $\mu\mu$F
$C_2$ = 4 $\mu$F 400 v.
$C_3$ = 32 $\mu$F 400 v.
$C_4$ = 8 $\mu$F 400 v.
$C_5$, $C_6$, $C_7$ = 0.1 $\mu$F 2000 v.

$L_1$ = 10 hy. inductance 50 mAmp.
$Tr_1$ = 300-0-300 v. transformer

### *Performance*

*Sensitivity.* Two factors limit the sensitivity of the detector. First, the current flowing in the ionization chamber suffers random fluctuations as a consequence of the stochastic nature of the emission of $\beta$ radiation from the source. Second, the increase in sensitivity with applied voltage does not progress indefinitely, but reaches a limit in the region of 2000 v. where a further increase in applied potential multiplies not only the concentration of metastable atoms, but also the concentration of ions. At voltages above 2000, although the current for a given concentration of vapor still increases with applied potential as does the noise, the true sensitivity which is a function of the signal-to-noise ratio remains constant.

With an input-time constant of 2 sec. and a 10 mc. source, the random fluctuations of the current flowing in the detector are 0.05 per cent. Under these conditions and with an applied potential of between 1600 and 2000 v., the smallest quantity of vapor that can be detected is $2 \times 10^{-13}$ moles. A chromatographic separation with the detector operating at its maximum sensitivity is illustrated in FIGURE 4. The dilution of the vapor in the retention volume of the column reduces the minimum detectable concentration and, in practice, the least detectable quantity is approximately $10^{-9}$ gm. applied to the column.

If required, it should be possible to increase the sensitivity, perhaps as much as 1000 times. The noise level can be decreased by the use of a more intense source of radiation and a larger input-time constant. Careful attention to chamber design and the use of very pure argon would permit the use of higher applied voltages than described here. In this connection this detector is five times more sensitive than that described previously (J. E. Lovelock, 1958).

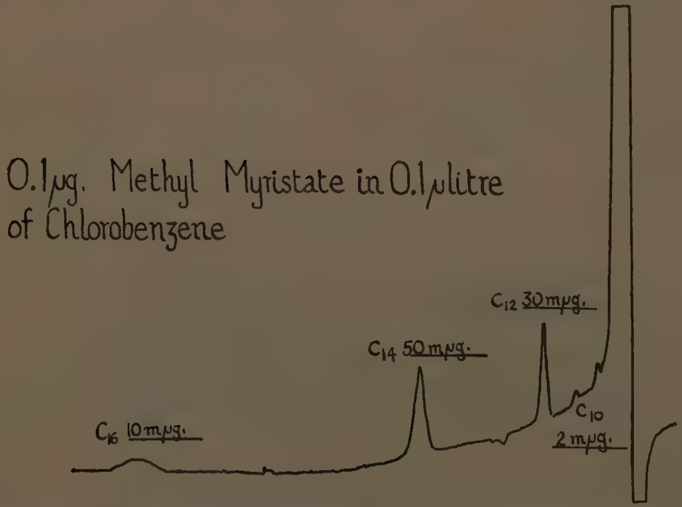

FIGURE 4. A chromatographic separation of 0.1 µg. of commercial methyl myristate, Column temperature 205° C., flow rate 60 ml./min., applied voltage 1600.

### *Effect of Temperature, Pressure and Gas Flow Rate*

The acceleration of free electrons within the ionization chamber is related directly to the applied potential and inversely to the number of argon atoms present. Therefore, at high temperatures where the gas density is lower, the excitation of argon atoms by electron collision occurs at lower applied potentials. The effect of temperature on the performance of the detector is illustrated in FIGURE 5. The diagram shows the variation of sensitivity, which is directly related to the concentration of excited atoms, with applied potential for three different temperatures. It can be seen that the general performance is changed only slightly between 25° and 225° C.; as expected, at the higher temperatures the sensitivity at a given potential is greater. In practice, provided that the minimum operating potential is chosen sufficiently high for the multiplication of excited atoms to occur at the lowest operating temperature, no changes in circuit values are necessary for use at different temperatures.

The current flowing in the cell is inversely related to the absolute temperature, so that between 25° and 225° C. there is a 76 per cent decrease. This drop in current does not affect the sensitivity of the detector, since both the signal and the noise fall equally.

The effects of pressure changes on the performance of the detector are analogous to those of changes of temperature. In practice, the small ambient atmospheric pressure changes have no perceptible effect on the operation of the equipment. The same is true of changes in gas flow rate between 0 and 200 ml./min.

*Linearity.* FIGURE 6 illustrates the variation of ionization current with vapor concentration at different applied voltages. The values shown are calculated from the equation given previously (J. E. Lovelock, 1958) and assume that the cell is connected to a low-impedance source of potential. The experimental relationship determined, using the cell described in this paper and a "low"-value series resistance (10 megohms), is very similar. The

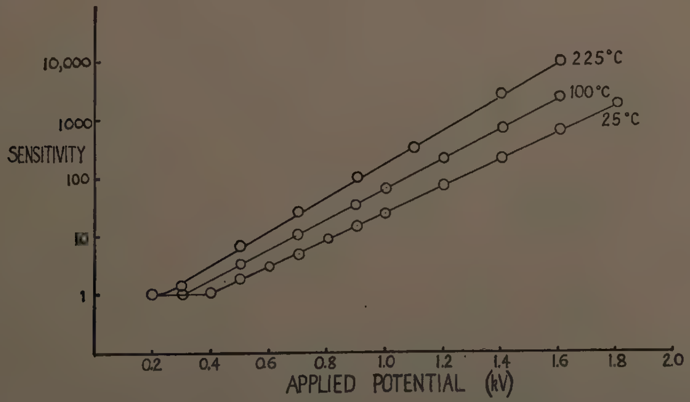

FIGURE 5. The relationship between sensitivity and applied potential at 25, 100 and 225° C.

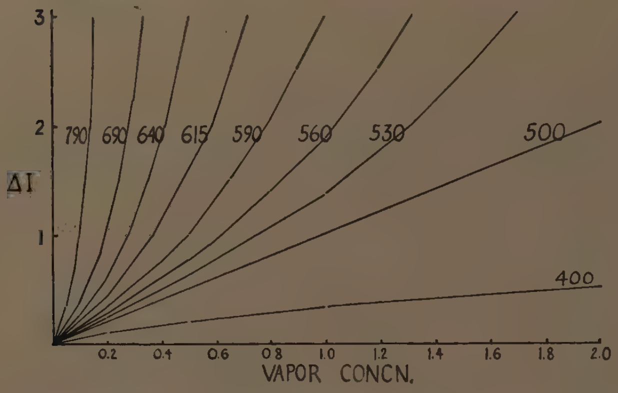

FIGURE 6. The relationship between ionization current and vapor concentration at different applied potentials when the detector is supplied from a low-impedance source of potential.

figure illustrates that there is only one applied potential at which the change of current with concentration is linear; this particular potential is that at which as many metastable atoms are replaced by electron collision as are lost by their collision with the vapor molecules. At higher potentials the production of metastable atoms exceeds their loss by collision, so that the sensitivity rises with increasing vapor concentration.

The restriction of linear response to a single applied potential can be avoided if a resistance of appropriate value is connected in series with the ionization chamber. FIGURE 7 illustrates the change of ionization current with vapor concentration at an applied potential of 800 v. when various resistances are

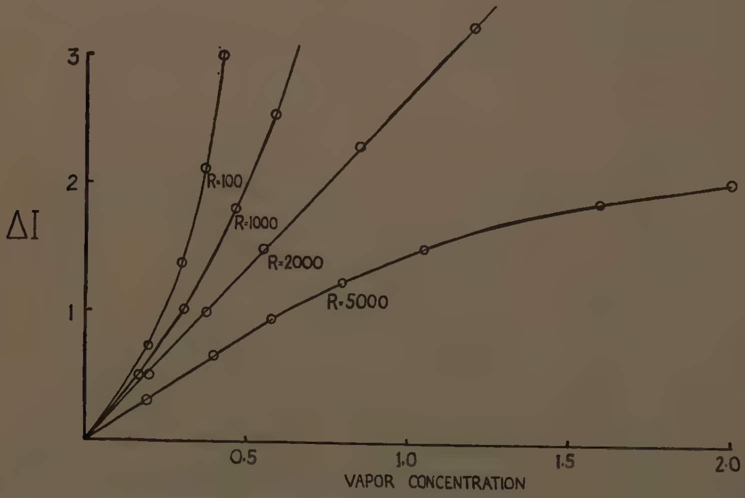

FIGURE 7. The relationship between ionization current and vapor concentration with an applied potential of 800 volts for different values of resistance in series with the detector.

connected in series with the ionization chamber. With a series resistance of 2000 megohms, the response is seen to be linear. The value of the series resistance for linear operation is related directly to the rate of increase of sensitivity with applied potential, and inversely to the current flow in the chamber with pure argon. Both of these factors may be altered with chambers of different design and with different radioactive sources. Provided that the applied potential is at least 100 v. in excess of that required to give a linear response with no series resistance, the resistance required for linear operation is independent of the applied potential. The temperature at which the cell is operated does have some effect on the linearity of response with a given resistance but, provided that a value is chosen appropriate for an intermediate operating temperature, for example, 120° C., the departure from linearity at 20° and 250° C. is small, and normally there is no need to use different resistances for different temperatures.

*Response to different substances and anomalous effects.* Provided that the ionization potential of the colliding molecule is equal to or less than the excitation potential of argon, there is a high probability of ionization by collision. Therefore, the response of the detector to different substances depends on the frequency of collisions between the excited argon atoms and the vapor molecules. FIGURE 8 illustrates the mass and molar sensitivities calculated from the kinetic theory of gases; the calculated sensitivities are shown as solid lines and the observed sensitivities, as points. The diagram illustrates the close agreement between theory and observation for substances with molecular weights below 100; for larger molecules, the observed mass sensitivity falls less rapidly than expected. Indeed, for fatty acid methyl esters and for *n*-primary alcohols with molecular weights greater than 100, the mass sensitivity is constant within the limits of precision of chromatographic analysis. The discrepancy between theory and practice is of great practical convenience,

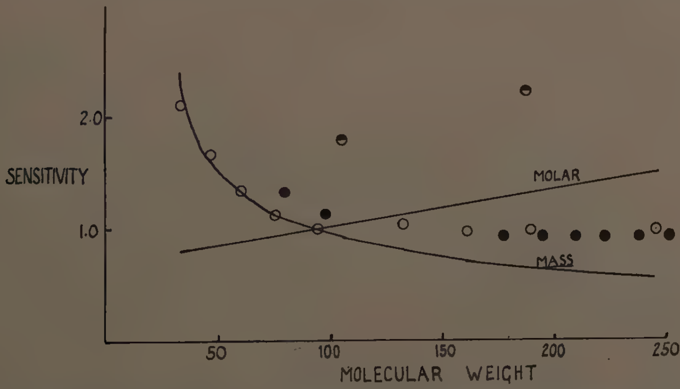

FIGURE 8. The mass and molar sensitivity of the detector for substances of different molecular weight. The solid lines are the calculated mass and molar sensitivities; the points are the observed mass sensitivities for various classes of organic compounds as follows: (○), *n*-primary alcohols; (●), fatty acid methyl esters; and (◒), aromatic hydrocarbons. Both the observed and calculated sensitivities are relative to 1-pentanol; mass sensitivity and molar sensitivity = 1.

since the peak areas of the chromatogram are directly proportional to the mass of substance separated. For substances with molecular weights less than 150, the molar sensitivity changes only slightly with molecular weight so that, for these smaller molecules, the peak areas of the chromatogram are approximately proportional to the molar quantity of substance separated.

The mass sensitivity of the detector for the following aliphatic and aromatic organic substances has been measured: hydrocarbons, alcohols, aldehydes, ketones, ethers, amines, nitriles, nitro compounds, and halogenated compounds. Of these only three classes show considerable divergencies from the expected sensitivities: polycyclic aromatic hydrocarbons, for which the detector has an unexpectedly high sensitivity; and halogenated and nitro compounds, for which it is less sensitive than expected. The high sensitivity of the detector for polycyclic aromatic hydrocarbons is probably attributable to the large cross-sectional area of these molecules, which increases the probability of collision. The low sensitivity of the detector for halogenated and nitro compounds is due to the capture of free electrons by these molecules, which interrupts the chain of multiplication of excited argon atoms. The discrepancy with halogenated compounds is manifest only when the vapor concentration is high and when there is a high proportion of halogen to carbon in the compound, for example, in carbon tetrachloride; substances such as chloro- and bromobenzene show no discrepancy.

The response of the detector fails when the vapor concentration exceeds 1 in $10^3$, by volume. This failure is manifest either by a nonlinear response or by erratic behavior such as double- or triple-peaking with a single component. The introduction of air, or indeed of any other gas, at a concentration exceeding 1 in $10^3$ by volume disturbs the operation of the detector in much the same manner. For this reason care should be taken in assembling the apparatus to avoid leaks. Failure of the detector at high gas or vapor concentrations is a consequence of the reduction of the free-electron velocity that follows nonelastic collisions between electrons and gas or vapor molecules. In practice, 1 part in $10^3$ by volume is close to the upper limit of concentration for the satisfactory operation of the chromatograph columns; consequently, the failure of the detector at these high concentrations is not a limitation to its practical use. For convenience, it is recommended that the amplifier sensitivity be adjusted so that, on the lowest sensitivity range, a full-scale deflection is given by a vapor concentration of 1 part in $2 \times 10^3$, by volume. The erratic response of the detector at high vapor concentration is entirely transitory, and as soon as the concentration falls to the region of normal operation, the correct response is given. No "memory" effects are observed following a gross overload of the detector.

## *Conclusions*

The high sensitivity of the detector permits separations to be made under conditions closely approaching the ideal. This is illustrated by the work of R. P. W. Scott, Watford, England (personal communication), who has used the detector described here with 50-foot columns operating at a pressure of 200 psi, and obtained efficiencies as high as 30,000 theoretical plates; this is sufficient, for example, to separate *m*- and *p*-xylenes. This high efficiency was possible only by using very small loads, approximately 5 μg. for each component. It is unlikely that any other detector available at present would have enabled the high resolution of these columns to be exploited in full.

Perhaps the principal disadvantage of the detector described is that it requires the use of radioactive substance. In view of the increasing stringency of regulations affecting the use of radiation sources, every effort has been made to develop alternative methods of exciting the argon atoms. Detectors have been tested in which the argon was excited by corona, spark, and high frequency electric discharges, but so far their performance has been inferior to those using radioactive sources. The problem of establishing long-term stability with electric discharge devices is formidable, especially at atmospheric pressure and with mixed gases. Therefore, it is probable that the detector using a radioactive source will remain the one most suitable to use for some time to come.

## *References*

HARLEY, J. & V. PRETORIUS. 1957. Nature. **178:** 1244.
LOVELOCK, J. E. 1958. J. Chromatography. **1:** 35.
MARTIN, A. J. P. & A. T. JAMES. 1956. Biochem. J. **63:** 138.
RYCE, S. A. & W. A. BRYCE. 1957. Nature. **179:** 541.
SCOTT, R. P. W. 1957. Vapour Phase Chromatography. D. H. Desty & C. L. A. Harbourn, Eds. Butterworths. London, England.

## *Discussion of the Paper*

STANLEY H. LANGER (*U. S. Department of the Interior, Pittsburgh, Pa.*): What substrate was used for the *m*- and *p*-xylene separation?

LOVELOCK: Apiezon L.

LANGER: Since the xylene separation is of interest, I shall describe some of the work on this separation that we did at the U. S. Bureau of Mines. In addition to the construction of extremely efficient columns, another approach to separating *m*- and *p*-xylene is to use liquid substrates that give favorable separation factors. This may be achieved by taking advantage of differ-

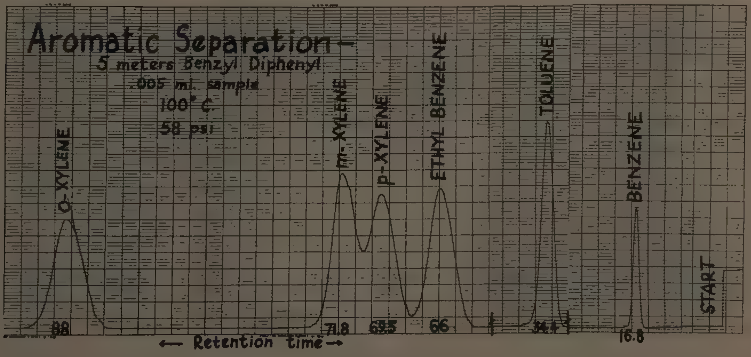

FIGURE 9

ences in the capacity of *m*- and *p*-xylene to act as electron donors in "charge transfer" interactions with a suitable liquid phase. Therefore, we have synthesized several tetrachlorophthalate esters for use as liquid substrates with the thought that these materials may act as electron acceptors. Several of these substrates give separation factors of about 1.04 at 110° C., with *m*-xylene emerging from the column first. With methyl propyl tetrachlorophthalate as a liquid substrate, we have been able to obtain separations adequate for direct quantitative analysis of commercial xylene mixtures with column loads of about 0.5 $\mu$l. for any xylene isomer. For these separations we have used a 27-foot, 5900-plate column operating at inlet pressures of about 35 psi of helium; the 42 to 48 mesh firebrick packing contained 20 per cent liquid phase.

Indications that charge transfer forces are operative are: (1) equal weight mixtures of di-*n*-propyl tetrachlorophthalate and either xylene isomer give increased ultraviolet absorption in charge transfer regions, and (2) di-*n*-propyl tetrachlorophthalate forms solid complexes with durene and hexamethylbenzene.

While work on more efficient columns with greater resolution undoubtedly will increase the power and range of application of gas-liquid chromatography, it should be re-emphasized that development of new and selective liquid substrates also will be of considerable importance in accomplishing this end.

NATHANIEL BRENNER (*Perkin-Elmer Corporation, Norwalk, Conn.*): I have been very interested in the separation of *m*- and *p*-xylene. FIGURE 9 illustrates this separation as performed by a standard column of benzyl diphenyl substrate. The column was made with 20 per cent substrate on 60 to 80 mesh Chromosorb support. This run was the result of work by Lawrence O'Brien and Philip Scholly of The Perkin-Elmer Corporation, Norwalk, Conn., and Albert Zlatkis, University of Houston, Houston, Texas, and will soon be published. It should be noted that the time scale has been compressed somewhat in order to show the entire run, which required 72 min. for the appearance of *m*-xylene.

# PROPERTIES OF THE CALCIUM ZEOLITE AS ADSORBENT FOR GAS CHROMATOGRAPHY

J. Janák, M. Krejčí, and E. E. Dubský
*Laboratory for Gas Analysis, Czechoslovak Academy of Sciences, Brno, Czechoslovakia*

If the problems attendant on the separation of permanent gases are to be solved it will be necessary to utilize the technique of gas-solid chromatography. Activated charcoal,[1, 2] silica gel,[3, 3a] types of activated alumina,[4] and some aluminosilicates[5, 6] already have been used for this purpose. It can be concluded, on the basis of the reported experimental work, that a successful separation may be obtained with adsorbents having a pore structure of the order of molecular size and a surface adsorption of secondary importance only. This necessitates the use of carrier gases that are adsorbed only slightly and consequently do not block up the pores.

From this standpoint, Barrer and Robins' observations are important.[7] These investigators found substantial deviations in the adsorption isotherms of permanent gases, especially of oxygen, nitrogen, and carbon monoxide, on dehydrated crystals of natural, as well as artificial, aluminosilicates. These gases show considerable differences in adsorption energy values, even at normal temperatures. Owing to their regular lattice, these artificial materials have not only very narrow pores resulting from the splitting off of water molecules, but also show a very homogeneous distribution of these pores; therefore they are called molecular sieves.

Practical possibilities of the separation of these gases on commercial calcium aluminosilicate at normal temperatures have been pointed out by van de Craats[8] and by Kyryacos and Board.[9] This new adsorbent, molecular sieve 5Å,* will be used for solving a series of problems. Therefore we shall discuss its properties and behavior.

The molecular sieve 5Å,[10] in pellets,† was crushed before use, selected for 0.2 to 0.4-mm. grain size, and activated for 3 hours at 450° C.; the activated adsorbent was stored in sealed ampules. Its composition was as follows: $SiO_2$, 40.8 per cent; $Al_2O_3$, 36.2 per cent; CaO, 16.0 per cent; heating loss at 950° C., 3.0 per cent; $Na_2O$, 3.75 per cent; $Fe_2O_3$, 0.03 per cent; MgO, 0.04 per cent; $K_2O$, 0.05 per cent; $SO_3$, 0.03 per cent; which corresponds to the molar ratio of $CaO \cdot Al_2O_3 \cdot 2SiO_2$, that is, to the calcium zeolite. In the atmosphere, it adsorbs water vapor (19 per cent maximally) and carbon dioxide (12.6 per cent maximally) intensively, whereby it becomes quite warm. The adsorbed carbon dioxide and the occluded water are released at 105° C., the water of constitution at 300° C. The smaller part of $CO_2$ (up to 3 per cent) remains bound, probably in the form of $Na_2CO_3$.

According to the X-ray diffraction powder analysis of the calcium zeolite (TABLE 1, FIGURES 1 and 2), the lattice of the adsorbent seems to be of a sim-

---

* Product of Linde Company, Division of Union Carbide & Carbon Corporation, New York, N. Y.

† Obtained from the British Drug Houses Ltd., London, England.

TABLE 1

INTERPRETATION OF X-RAY POWDER DIAGRAM DIFFRACTION LINES

| Interlayer distance *d* | Relative visual intensity *I* | Miller's indexes | | | Interlayer distance *d* | Relative visual intensity *I* | Miller's indexes | | |
|---|---|---|---|---|---|---|---|---|---|
| | | *h* | *k* | *l* | | | *h* | *k* | *l* |
| Circle diagrams: | | | | | Strip diagrams: | | | | |
| 12.2 | 8 | 0 | 0 | 1 | 2.023 | 1 | 6 | 0 | 0 |
| 8.64 | 2 | 1 | 0 | 1 | — | — | 4 | 4 | 2 |
| 7.056 | 3 | 1 | 1 | 1 | 1.974 | 1 | 6 | 1 | 1 |
| 5.44 | 2 | 1 | 0 | 2 | 1.906 | 1 | 5 | 4 | 0 |
| 4.42 | 3 | 2 | 0 | 2 | — | — | 4 | 4 | 3 |
| 4.09 | 4 | 0 | 0 | 3 | 1.869 | 1 | 6 | 2 | 1 |
| — | — | 2 | 2 | 1 | 1.724 | 2 | 5 | 5 | 0 |
| 3.687 | 3 | 1 | 1 | 3 | — | — | 5 | 4 | 3 |
| — | — | — | — | — | — | — | 7 | 1 | 0 |
| — | — | — | — | — | 1.673 | 1 | 6 | 4 | 1 |
| Strip diagrams: | — | — | — | — | — | — | 7 | 2 | 0 |
| — | — | — | — | — | 1.617 | 1 | 5 | 4 | 4 |
| 8.65 | 2 | 1 | 0 | 1 | — | — | 7 | 2 | 2 |
| 7.02 | 3 | 1 | 1 | 1 | 1.586 | 1 | 5 | 5 | 3 |
| 5.48 | 2 | 1 | 0 | 2 | — | — | 7 | 3 | 1 |
| 4.979 | 1 | 1 | 1 | 2 | 1.562 | 1 | 6 | 4 | 3 |
| 4.066 | 5 | 0 | 0 | 3 | — | — | 6 | 5 | 0 |
| — | — | 2 | 2 | 1 | 1.465 | 1 | 6 | 5 | 3 |
| 3.677 | 5 | 1 | 1 | 3 | 1.438 | 1 | 6 | 6 | 0 |
| 3.257 | 6 | 2 | 1 | 3 | — | — | 8 | 2 | 2 |
| 2.960 | 4 | 1 | 0 | 4 | 1.409 | 1 | 7 | 5 | 0 |
| — | — | 3 | 2 | 2 | — | — | 7 | 4 | 3 |
| 2.863 | 1 | 1 | 1 | 4 | — | — | 8 | 3 | 1 |
| — | — | 3 | 3 | 0 | 1.389 | 1 | 6 | 5 | 4 |
| 2.785 | 1 | 3 | 1 | 3 | — | — | 8 | 3 | 2 |
| 2.715 | 1 | 2 | 0 | 4 | 1.347 | 2 | 9 | 1 | 0 |
| 2.594 | 3 | 3 | 3 | 2 | — | — | 8 | 3 | 3 |
| 2.496 | 1 | 4 | 2 | 2 | 1.314 | 1 | 4 | 2 | 1 |
| 2.431 | 1 | 0 | 0 | 5 | — | — | 7 | 6 | 1 |
| — | — | 4 | 3 | 0 | — | — | 6 | 5 | 5 |
| 2.337 | 1 | 1 | 1 | 5 | 1.292 | 1 | 9 | 2 | 2 |
| — | — | 3 | 3 | 3 | — | — | 7 | 6 | 2 |
| 2.154 | 1 | 4 | 4 | 0 | — | — | 8 | 4 | 3 |
| 2.089 | 1 | 5 | 3 | 0 | — | — | 8 | 5 | 0 |
| — | — | — | — | — | 1.247 | 1 | 8 | 4 | 4 |
| — | — | — | — | — | 1.215 | 1 | 10 | 0 | 0 |
| — | — | — | — | — | — | — | 8 | 6 | 0 |

ple, cubic structure with the lattice constant $a_0 = 12.182 \pm 0.001$ Å (preliminary indexing of diffraction lines was carried out in accordance with the Hull-Davey diagram; the more detailed indexing, especially in case of higher order diffractions, was performed mathematically).

### *Properties of the Adsorbent*

In order to determine the activation conditions, a differential thermal analysis was carried out. The curve of FIGURE 5*a* shows two endothermic and two exothermic peaks. The first endothermic peak at 100° C. indicates the occluded moisture, the other large peak with its maximum at 300° C. corresponds

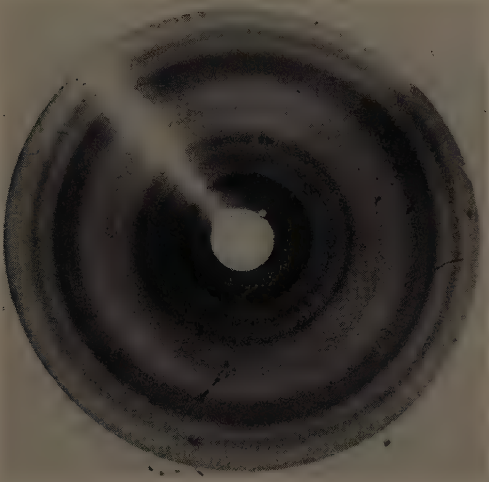

FIGURE 1. X-ray powder diffraction diagram (circle diagram) of the adsorbent. Apparatus Mikrometa; radiation CuK$\alpha$, filtered with Ni-foil at 35 kv. and 28 mAmp.; exposure time 3 hr. Distance between film and layer preparation, 95.4 mm.

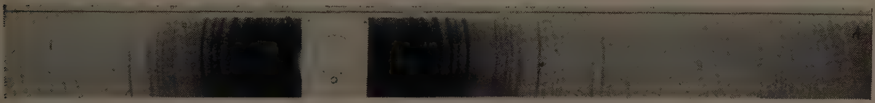

FIGURE 2. X-ray powder diffraction diagram (strip diagram) of the adsorbent. Apparatus Mikrometa; radiation CuK$\alpha$, filtered with Ni-foil at 35 kv. and 28 mAmp.; exposure time 3 hr. Circular camera, 114 mm.; sample in a rotating gelatine capillary.

to the separation of the water of constitution, whereby the true activation of the adsorbent takes place. Sharp exothermic peaks at 810° C. and 950° C. correspond to the lattice destruction by the crystallization of $CaO \cdot Al_2O_3$ and $Al_2O_3 \cdot SiO_2$, accompanied by sintering and melting.

With the progressive release of the water of constitution, a successive change of the adsorbent properties takes place. For the purpose of studying this effect, measurements of chromatographic spectra of some permanent gases were performed on adsorbent with known amounts of water. The $U_g$ values[1] (corresponding to $V_g$ values in gas-liquid chromatography) found are shown in TABLE 2. From these it is evident that with alterations of the water content, substantial changes of $U_g$ values take place and that these changes are of two types.

If the water amount is lowered, the pores of the adsorbent open successively and the sorption-active surface increases. In connection with this effect, the adsorption capacity of the adsorbent increases with regard to all components, as can be seen with all gases examined. In the course of a progressive uncovering of the silicate framework with polar groups of $Al_2O_3$ and $SiO_2$, the effect of polar groups also begins to have an effect. This causes an increased sorption of polar molecules or of those that can be polarized and, thus, a shifting of components in the chromatographic spectrum. A very pertinent exam-

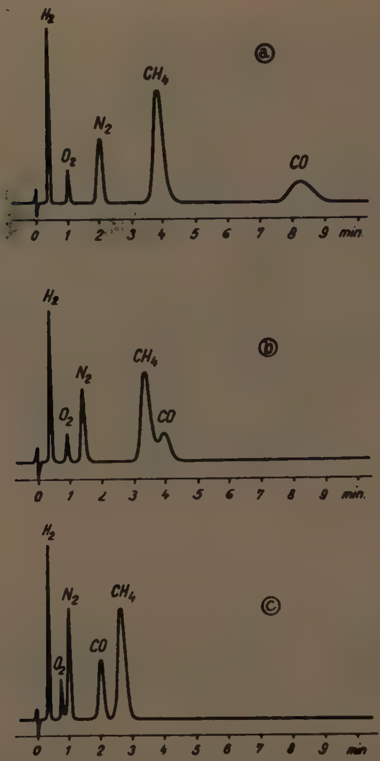

FIGURE 3. Change of the elution order of CO—$CH_4$, caused by change of adsorbent polarity after wetting with water. (*a*) 2.07 per cent $H_2O$; (*b*) 4.18 per cent $H_2O$; (*c*) 9.43 per cent $H_2O$.

TABLE 2

CHANGES OF CHARACTERISTIC ELUTION VOLUME DUE TO PARTIAL WATER DEACTIVATION OF THE ADSORBENT

| Component | $U_g^{22}$ at water amount of weight, percentage | | | | |
|---|---|---|---|---|---|
| | 0.0 | 2.07 | 4.18 | 5.27 | 9.43 |
| Argon as carrier gas: | | | | | |
| Hydrogen | 0.0 | 0.0 | 0.0 | 0.0 | 0.0 |
| Oxygen | 4.44 | 3.19 | 2.78 | 2.22 | 0.78 |
| Nitrogen | 13.3 | 7.32 | 4.72 | 3.54 | 0.78 |
| Methane | 22.1 | 18.4 | 14.2 | 12.3 | 3.94 |
| Carbon monoxide | 84.6 | 33.5 | 14.6 | 8.76 | 1.88 |
| Hydrogen as carrier gas: | | | | | |
| Helium | 0.0 | 0.0 | 0.0 | 0.0 | 0.0 |
| Oxygen | 4.0 | 4.05 | 3.55 | 2.08 | 0.74 |
| Nitrogen | 13.6 | 8.84 | 4.44 | 3.00 | 0.74 |
| Methane | 20.2 | 16.6 | 12.7 | 10.7 | 3.16 |
| Carbon monoxide | 86.5 | 35.6 | 15.2 | 7.73 | 1.34 |

Note: calculation of $U_g$ performed in the same manner as in TABLE 3.

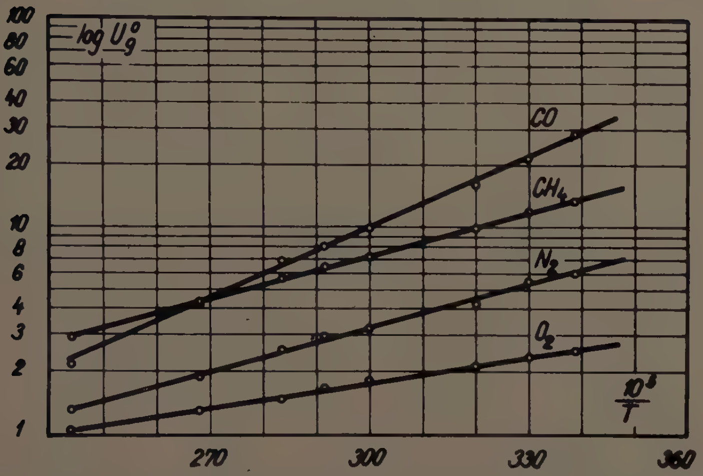

FIGURE 4. Characteristic elution volume as a function of the experimental temperature (the adsorbent contains 3.5 per cent water).

ple is offered by the behavior of carbon monoxide (TABLE 2). In the case of 2 per cent of water, the $U_g$ value for the carbon monoxide is nearly twice the value for methane, although the boiling point of carbon monoxide (−191° C.) is lower by 30° C. than that of methane (−161° C.). The decrease in the carbon monoxide pressure above the adsorbent evidently is due to the selective action of the polar surface on the electrically unbalanced CO molecules. If the adsorbent surface is covered with 4.5 per cent of water, the sorption selectivity decreases so that the tensions of both components, CO and $CH_4$, above the adsorbent are equal, and the components cannot be separated by chromatography. On further covering of the surface with strongly polar water molecules, the external action of surface polarity is so disturbed as to entail an inversion of the elution order of both components. For example, in the case of 9 per cent water, the $U_g$ value for the carbon monoxide is half the value of methane. The inversion of the component order is demonstrated in a practical chromatogram in FIGURE 3.

In addition, the effect of the temperature on the adsorbent capacity and selectivity has been examined. The results are plotted in FIGURE 4. They are proof of the fact[1] that the logarithm of the characteristic elution volume of a substance bears a linear relation to the reciprocal value of the temperature at which the experiment was performed. It may be noted that the decrease of the $U_g$ values is more rapid for carbon monoxide than for methane. At 100° C., an equalization occurs in the pressure of both gases above the adsorbent. At higher temperatures an inversion of the elution order of the two components takes place in a manner similar to that observed with the increase in water content to 9 per cent. It follows that the sorption selectivity of carbon monoxide on the aluminum silicate framework, for the most part, is to be ascribed to the orientated polarization.

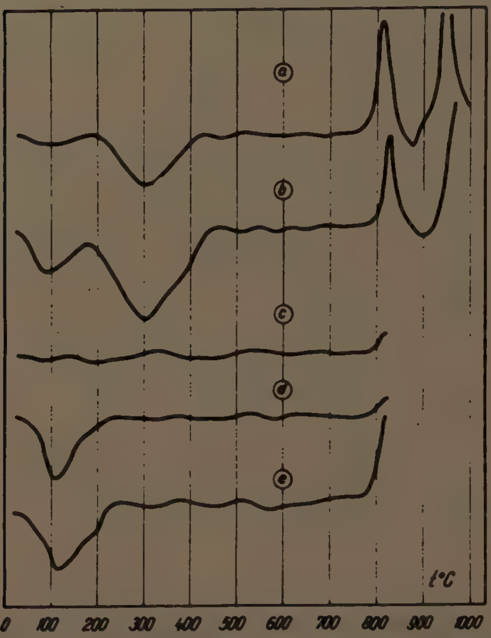

FIGURE 5. Differential thermal analysis of the adsorbent; temperature increase 13.5° C./min. (*a*) Original adsorbent, $Al_2O_3$ as standard; (*b*) original adsorbent saturated with 8 per cent $CO_2$, $Al_2O_3$ as standard; (*c*) adsorbent activated at 450° C., activated adsorbent at 750° C. as standard; (*d*) adsorbent activated at 450° C., saturated with 12.6 per cent $CO_2$, activated adsorbent at 750° C. as standard; and (*e*) adsorbent activated at 450° C., saturated with 12.6 per cent $CO_2$, $Al_2O_3$ as standard.

In further research we have examined the deactivation of the adsorbent by carbon dioxide, using as much as 12.6 weight per cent $CO_2$. The abnormally large exotherm of the process, which is of the magnitude of chemical reactions, led us to the assumption that the change of the silicate involved the formation of calcium carbonate. This suggestion was supported by the fact that, in a stream of carbon dioxide as carrier gas, the adsorbent lost the capacity to separate the gases to be studied. For a detailed verification, X-ray analysis of the lattice and differential thermal analysis were carried out. The comparison of the X-ray powder diagrams of the activated and deactivated adsorbent, performed with the Debye-Scherrer's method (FIGURES 1 and 2), shows that in sorption of the carbon dioxide no change of the lattice form of the silicate occurs, nor can a formation of heterogeneous lattice material be seen. The differential thermal analysis was performed on a sample of an adsorbent containing 9 per cent of water and saturated with carbon dioxide (FIGURE 5*b*). An increase only in the first endothermic deflection with the maximum at 95° C. was observed. To be able definitely to attribute the temperature change to the desorption of carbon dioxide, a thermal analysis was performed on an activated adsorbent that had been saturated with dry carbon dioxide (FIGURES 5*d*, *e*). The deflection appeared clearly with its maximum

TABLE 3

CHARACTERISTIC ELUTION VOLUME (CHROMATOGRAPHIC SPECTRA)

| Component | $t_{\max}$ | $t_{\max}$ to $t_0$ | $U_g^0$ |
|---|---|---|---|
| Argon as carrier gas: | | | |
| Hydrogen | 30 | 0 | 0.0 |
| Oxygen | 101 | 71 | 4.10 |
| Nitrogen | 240 | 210 | 12.3 |
| Methane | 378 | 348 | 20.4 |
| Carbon monoxide | 1360 | 1330 | 78.3 |
| Hydrogen as carrier gas: | | | |
| Helium | 24 | 0 | 0.0 |
| Oxygen | 78 | 54 | 3.70 |
| Nitrogen | 206 | 182 | 12.6 |
| Methane | 296 | 272 | 18.7 |
| Carbon monoxide | 1200 | 1176 | 80.8 |

Temperature, 22° C.; activated adsorbent of grain size, 0.2 to 0.4 mm. Argon as carrier gas: column filling, 18.3 gm.; rate of flow, 1.29 ml./sec.; pressure in front of the column, 391 tor.; pressure behind the column, 476 tor.; correction for pressure drop on the column, 0.896.

Hydrogen as carrier gas: column filling, 19.8 gm.; rate of flow, 1.5 ml./sec.; pressure in front of the column, 741 tor.; pressure behind the column, 681 tor.; correction for pressure drop on the column, 0.966.

at 105° C.; the comparison curve of the activated adsorbent (FIGURE 5*c*) showed only the base line.

For the purpose of chromatography, it is necessary to activate the calcium zeolite at 300° C. The convenient temperatures are 350 to 600° C. The adsorbent, activated in such a manner, shows separation abilities for gases of the category mentioned even at temperatures above 100° C. Because of the unusually high adsorbability for water (it sorbs up to 250° C.), the effect of the moisture in samples to be analyzed is negligible. A longer use of a wet carrier gas causes a loss of adsorption capacity and a slow selectivity change in the chromatographic column packing. The effect of the carbon dioxide is greater, especially at 100° C. and higher temperatures. In a stream of hydrogen or argon, carbon dioxide does not disturb the separation of gases substantially, but is desorbed slowly by the carrier gas and, after a longer time, it appears behind the chromatographic column and alters the basic thermal conductivity of the carrier gas.

## *Characteristic Elution Volume*

Measurements have been carried out on a column containing an exactly known amount of about 20 gm. of activated adsorbent at 22° C., using argon and hydrogen as carrier gases. The results, expressed in milliliters of carrier gas at pressure behind the column and at temperature °C./1 gm. of the adsorbent and corrected for pressure drop of the column,[11] are presented in TABLE 3.

## *References*

1. JANÁK, J. 1953. Chem. listy. **47:** 817; 1954. Collection Czechoslov. Chem. Communs. **19:** 684.
2. GREENE, S. A., M. L. MOBERG & E. M. WILSON. 1956. Anal. Chem. **28:** 1369.

3. Wirth, H. 1953. Monatsh. Chem. **84:** 156; 741.
3a. Szulczewski, D. H. & T. Higuchi. 1957. Anal. Chem. **29:** 1541.
4. Greene, S. A. & H. Pust. 1957. Anal. Chem. **29:** 1055.
5. Barrer, R. M. 1949. Discussions Faraday Soc. **7:** 135.
6. Janák, J. 1957. Erdöl u. Kohle. **10:** 442.
7. Barrer, R. M. & A. B. Robins. 1953. Trans. Faraday Soc. **49:** 807.
8. Craats, F. van de. 1957. Vapour Phase Chromatography. : 245. Butterworths. London, England.
9. Kyryacos, G. & C. E. Board. 1957. Anal. Chem. **29:** 787.
10. Linde Molecular Sieve 5A (Aluminiumcalcium silicate). 1954. Bull. Linde Air Products Co.
11. Littlewood, A. B., S. C. G. Phillips & D. T. Price. 1955. J. Chem. Soc. : 1480.

## Part IV. Process Control and Instrumentation

# PROCESS CONTROL BY GAS CHROMATOGRAPHY IN THE CHEMICAL INDUSTRY

R. F. Wall, W. J. Baker, T. L. Zinn, and J. F. Combs
*Monsanto Chemical Company, Texas City, Texas*

The use of gas chromatography for process control is so new that any discussion must be more prophecy than history and more prediction than reported experience. Reviewing developments briefly, the key paper by Martin and Synge[1] first mentioning gas chromatography appeared in 1941, and the technique was neglected essentially from then until 1951, when an awareness of the potential value of this new analytical technique stimulated rapid development of instrumentation and analyses throughout the world. Although all of the first work was on laboratory analyzers, attention quickly turned to the development of gas chromatographic analyzers for process analysis. This development proceeded more slowly, as the operational requirements are much more stringent. Any process analyzer must operate without attention or adjustment for extended periods of time, and this requires a much higher order of stability than is demanded of a laboratory analyzer.

Maintenance procedures must be simple and standardized. The process analyzer must conform to safety codes and must operate in a plant environment including such factors as vibration, exposure to the elements, and perhaps corrosive fumes. These requirements were well known from experience with other process analyzers, principally the infrared. The necessary development required time, and it was not until 1957 that commercial gas chromatograph process analyzers became available. During that year a number of revisions and refinements of equipment were incorporated to enable the analyzers to meet in-plant installation requirements more fully; 1957 may be considered a year of preparation. There are several commercial units in actual process plant operation; however, little experience with them has been reported other than on prototype units placed by the manufacturer with cooperating users, on instruments that have been developed by process plant instrument engineers and then adopted for manufacture by instrument companies, and on home-built units. Excellent results have been reported for all of these installations. These first applications undoubtedly have received more detailed and expert attention than is normal for the typical process application. The coming year will provide a more nearly final answer: the experience of the average user.

A schematic drawing of a typical process chromatograph is shown in FIGURE 1. The complete instrument is a simple assembly of functional units that individually are uncomplicated and are capable of high precision. The combination of mechanical and functional simplicity, ruggedness, and complete adequacy of control of pressure, flow, and temperature by conventional and proved methods is ideal for an instrument made to be used in the process plant.

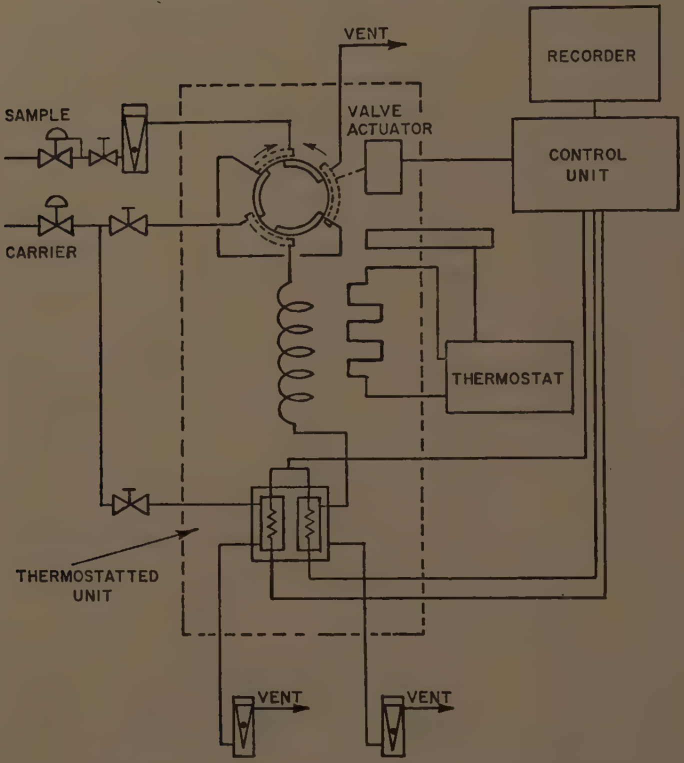

FIGURE 1. Process chromatograph schematic drawing.

The chromatographic column is the key to the success of the analyzer. It appears that a column or combination of columns can be devised that will separate a desired component, or components, from almost any mixture. Although the development of a suitable column system may be a problem for the chemist or engineer, to the instrument man the column is simply a length of stainless steel, copper, or aluminum tubing, usually one fourth of one inch O. D. The column is supplemented by a detector, a precise sample valve, controls for pressure and flow of sample and carrier, a simple thermostating system, and a programming unit to time the introduction of sample and the attenuation and readout of the desired analytical peaks. None of these component parts is very complicated, and all are at least similar to equipment familiar to instrument men. In all probability maintenance can be conducted satisfactorily by normal instrument department personnel with reasonable training.

Process applications require that an instrument be on-stream and operational for a high percentage of the time and that, when maintenance is required, it be rapidly accomplished by normal personnel. On-stream time is particularly important. If maintenance periods are frequent and are of long duration, not only will maintenance costs be high but, more significantly, the unit will be operating more or less blindly during these periods, and incurring all the losses resulting from inadequate control. Experience indicates that actual plant chromatograph maintenance requirements will be relatively low and, in addition, that there will be a relatively low down-time whenever trouble does occur.[2]

The gas chromatograph requires an adequate and careful installation, as does any process analyzer. An adequate shelter must be provided, certainly for the analyzer and, preferably, also for personnel maintaining the instrument. The sample system should be engineered carefully to provide an appropriately prepared sample to the instrument. Perhaps the conditioning requirements are less strict than for the optical analyzer or for the leak system of the mass spectrometer, although this is questionable, for a dirty sample can quickly foul a sample valve and/or the chromatograph column. The sample handling required must be done carefully to ensure that the sample reaching the analyzer is representative of the process stream at the sample point. This may necessitate maintaining a sample as a vapor by steam-tracing the sample line, by condensation or absorption of some materials from the sample stream, or by drying. Each aspect of sample preparation must be considered carefully with regard to the effect on the accuracy of the analysis. A typical sample system is illustrated in FIGURE 2.

If a number of sample streams are analyzed with the same instrument, the sample valving must be arranged to eliminate any possibility of mixing, and the data presentation must be made unambiguous. A careful and complete analyzer installation may appear to be rather elaborate, and is certainly expensive. As a rough rule, installation may cost approximately as much as the analyzer alone.

The chromatographic column almost completely determines the performance characteristics of the process chromatograph; the other operating units of the analyzer are functional only in serving the requirements of the column. The column is the key to the selectivity, sensitivity, and precision of the chromatographic analysis, and is the cause of the limitations in stability and speed, and of the intermittent nature of analysis. The development of a process chromatograph application and instrumentation research directed at improving the chromatograph as a process analyzer are centered on, or subordinate to, the column. The problem of engineering a process chromatograph application involves primarily the design of a satisfactory column system.

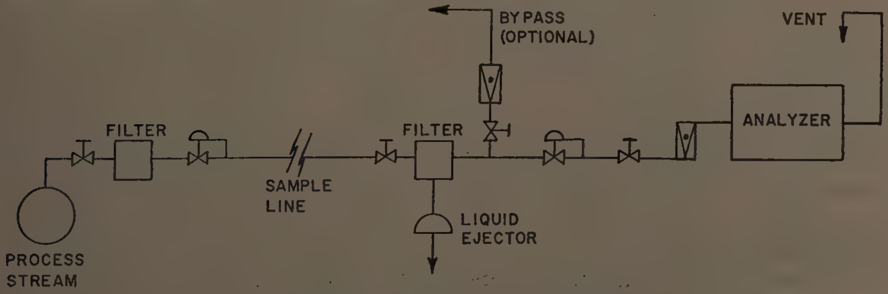

FIGURE 2. Typical sample system.

The usual approach to column development has been a predominantly trial-and-error examination of various columns and operating conditions until a satisfactory combination is found. Fortunately, this is not prohibitatively time-consuming for most problems, and a background of information has been accumulated that usually aids considerably in the search for a column. Much theory has been developed describing the operation of the chromatograph column and explaining the fractionating properties of various liquids.[3-5] Some systematic procedures for column development based on a combination of theory and experience are being evolved.[6] While these methods seldom predict column performance accurately, they serve as very helpful guides and minimize the experimental work required in obtaining a satisfactory column.

The process chromatograph must have a considerably better stability than is acceptable with the laboratory chromatograph, and it is usually much more important in the process chromatograph that the chromatogram scan time be short. As stability and scan time are both determined primarily by the column, column development for process analysis must conform to process standards; many columns that are acceptable for laboratory analyses will be unsatisfactory in process instruments.

Chromatograph stability involves both zero and span stability, and the usual performance standards require drift within 1 per cent for a minimum of 24 hours without adjustment. Minor shifts in such factors as bridge current, temperature, and aging effects appear more as zero drift than as a change of sensitivity and, normally, the zero drift is considerably greater than the drift in span. Daily adjustment of zero almost always will be required if 1 per cent precision is to be maintained. This routine maintenance can be eliminated by adding automatic zero correction, probably with some additional analytical precision; the automatic zero has become almost standard on process chromatographs.

Span stability normally does not require automatic correction. The usual cause of a sensitivity change is a gradual deterioration in the retention characteristics of the column. This can occur with both partition and adsorption columns. A partition liquid that vaporized appreciably during several weeks of operation will result in a column that gradually decreases in retention time and resolution and increases in peak height sensitivity.

The volatility of the liquid used as partition agent should be sufficiently low to prevent its evaporation during several months of steady operation at the column temperature required. This eliminates a number of liquids that have proved valuable for laboratory columns in which long-term stability is of secondary importance.

An adsorbent-type column used on a sample stream containing materials that are irreversibly adsorbed will gradually decrease in activity and therefore in retention time, with an accompanying change in peak height sensitivity. It seems that inevitably the sample will contain some small trace of heavier materials that results in a steadily changing calibration, making the accuracy of the analyses questionable. Our standard practice is to add from 1 to 3 per cent of an oil to the adsorbent and to lengthen the column to obtain the necessary resolution as a means of eliminating this drift in retention time and sensitivity.

Any change in retention time will have an effect on sensitivity and resolution and also may present problems in programming very close peaks. Retention time is affected by temperature and carrier flow rate, which are controlled, and by the column stability, which is obtained by selection of a column packing having the required characteristics. In addition, the sample component distribution will have some effect on the retention time of some components. This may be noticed particularly in samples containing varying quantities of water vapor. At the first part of the column, all components of the sample are together, and the column characteristics will be modified somewhat by the water vapor in the sample. The retention time of certain other peaks may vary slightly in proportion to the concentration of water vapor. The same effect has been observed to a lesser degree with sample components other than water vapor. Johns[7] attributes this type of behavior to residual adsorptivity of the solid support. This effect requires that the column have sufficient resolution to prevent close-spaced peaks having minor changes of retention time from falling outside the programmed interval.

Quite often a column providing a satisfactory analysis will have an undesirably long retention time for process control purposes, either for the components of interest or for other components of the sample that must be cleared before the next sample can be admitted. Techniques using multiple columns and/or complex valving that permit much more rapid analyses and eliminate, or minimize, the time disadvantage are now being developed.

A rapid analysis for light materials in a sample containing heavier components can be made by reverse-flushing the heavier compounds out of the column as soon as the desired analyses have been recorded,[2] as illustrated in FIGURE 3. Perhaps both light and heavy analyses can be obtained rapidly

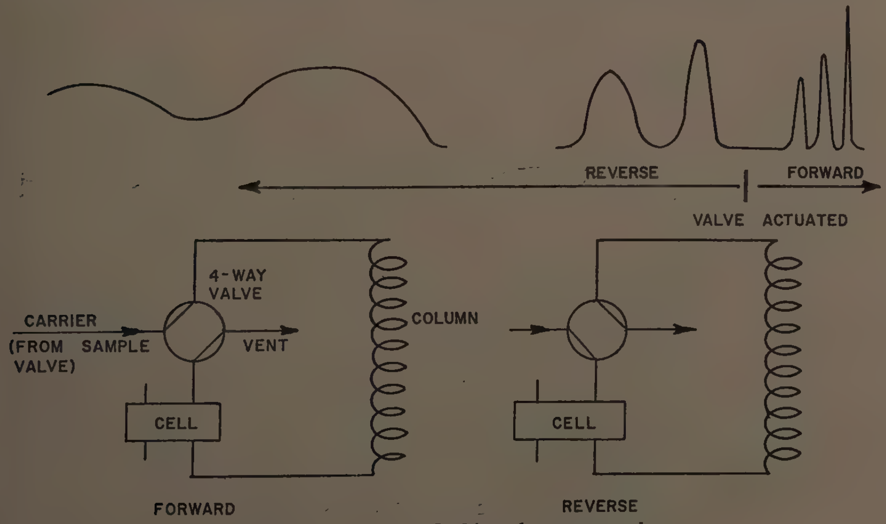

FIGURE 3. Reverse-flushing chromatograph.

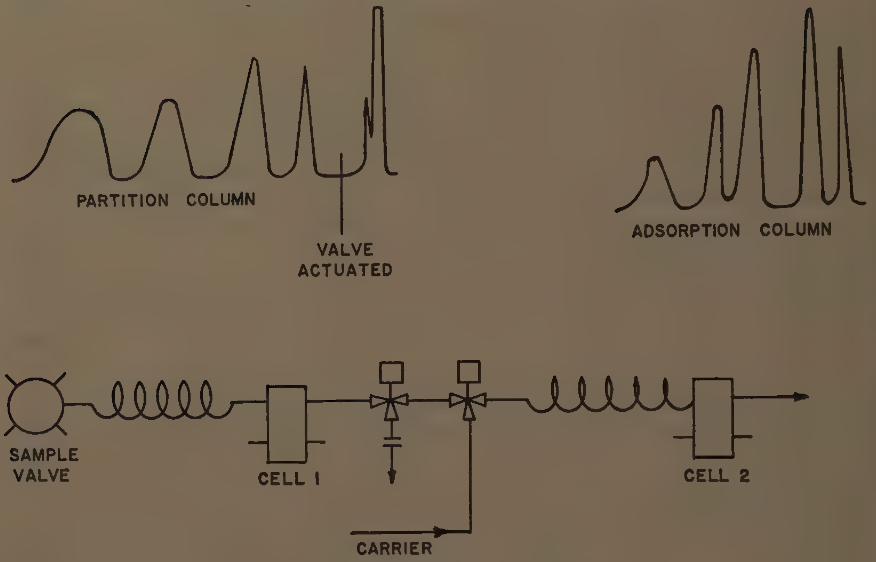

FIGURE 4. Double-column chromatograph.

by increasing the carrier flow immediately after recording the light peaks. Double-column chromatography can be used to obtain a rapid and complete analysis of samples containing light and heavy components,[8] as shown in FIGURE 4. Extension to three or more columns is a distinct possibility. Multiple-column operation is a general and highly versatile technique that may permit many applications of process gas chromatography that otherwise would be impracticable.

Chromatograph analyses are relatively slow, even with the use of multiple-column techniques, and have a time disadvantage that may limit many potential uses of the analyzer. Automatic analytical process control by gas chromatograph is now a particularly difficult problem for fast systems. This may change soon, for Golay[9] has demonstrated very fast chromatographic analyses using capillary columns. When engineered into practical process chromatographs, the capillary column will provide analyses in seconds rather than minutes, and the capillary chromatograph will be one of the fastest of the process analyzers. With an appropriate data conversion unit, this instrument could be used for direct automatic control of fast processes.

The precision of the chromatographic method appears to be remarkably good on favorable peaks. We have observed reproducibilities of 0.5 per cent of scale (95 per cent confidence) maintained for several days on analyzers in operation on process streams, and this experience has been confirmed by others. It appears that the 0.5 per cent deviation is due largely to random variations in barometric pressure, and that the basic precision of the peak-height thermal conductivity readout-type of gas chromatograph that has become standard for process applications is very high. The best precision is obtained for peaks having the highest peak height-to-area ratio consistent with the transient response of the detector and recorder. Very often a desired component can be made a favorable peak, although it may not be possible to obtain a complete analysis at the same time with a single column. Multiple column techniques may be required if a satisfactory multicomponent analysis is to be obtained.

The sensitivity of the process gas chromatograph is excellent, and adequate for normal applications. A minimum range of about 0.5 per cent of full scale is obtained with conventional instruments. A detector more sensitive than the commonly used thermal conductivity cell would make gas chromatography applicable for very low parts-per-million analyses, and would have some other advantages, such as permitting a reduction in sample size to provide a better resolution of components. It is not probable that any detector will displace the thermal conductivity type, except for applications having special requirements. The simplicity, ruggedness, precision, and low cost of the thermal conductivity detector are very difficult to equal, and only a minority of applications will require a more elaborate detector. Considerable work is in progress in the laboratory on the development of highly sensitive detectors for chromatography. The gas density balance of Martin[10] and the hydrogen flame temperature measurement of Scott[11] are examples. A number of detectors depend in some way on the ionization characteristics of the sample. Pitkethly[12] has built a detector using two small glow discharge tubes in a bridge circuit, with the carrier flowing through one and column effluent through the other. The potential drop across the glow discharge is very sensitive to the sample components. Ryce and Bryce[13] have used an ionization gauge operated just below the ionization potential of helium as an extremely sensitive detector. The sample components are ionized and the ion current measured as they leave the column. A number of detectors use radioactive sources for ionization of the sample. Lovelock and James[14] have described a very interesting type in which argon carrier excited by $\beta$ radiation ionizes the sample component in the column effluent, the ion current measurement being proportional to concentration. It will not be long before very sensitive detectors will be available for process chromatography.

One minor problem of gas chromatography is the supply of carrier gas. Helium is ideal, as it is inert, has an unusually high heat conductivity, and is not a normal component of process plant streams. However, the helium supply is restricted and, in some areas, large-scale users of gas chromatographs find it impossible to obtain a sufficient supply. While argon, nitrogen, or similar carrier gases can be used on problems requiring low sensitivity, for most problems hydrogen is the only adequate substitute for helium. The use of hydrogen adds to the problem of safe operation, for hydrogen leakage is particularly difficult to avoid, and the explosive limits with air are very broad. Explosion-resistant analyzer housings are normal for process installation; in addition, an air purge is particularly advisable with hydrogen to ensure that an explosive mixture cannot be formed if hydrogen leakage does occur. A completely safe system requires that a flow-restrictor be used on the hydrogen inlet to effect maximum control of hydrogen leakage and flow switches on the air inlet purge to guard against failure. If nitrogen is available as a purge gas, its use is highly advisable. The use of hydrogen or helium is very advantageous in providing a significantly higher signal-to-noise ratio in the analyzer output. The development of a detector providing adequate sensitivity with nitrogen or argon would have a definite safety advantage for those now forced to use hydrogen as a carrier.

Present process chromatography is limited to the analysis of vapor samples or liquids that will be in the vapor phase in instruments operated at moderately high temperatures. The general class of sample streams containing considerable water can be handled satisfactorily with present instruments. If total vaporization of a sample is not possible, a valve that will measure precisely liquid samples of the order of 0.01 cc. and subsequently vaporize them rapidly and completely in the carrier stream is required. This is a difficult problem of instrument development that has not yet been solved.

Peak height has been used almost exclusively for concentration readout in process gas chromatography. On some problems there is sufficient instability of retention time to make the use of an accurate integrator helpful; however, this technique does not appear to have been applied to process chromatography. The use of peak integration would also facilitate direct process control.

A clearly understood and unambiguous presentation of the multicomponent analysis is required for process plant use. The chromatograph analysis is only a part of the numerous data used in control, and during periods of process upset, when the information is most needed, there is little time for deciphering a confusing analysis display. The identification and value of each component analysis must be clearly and quickly understood irrespective of whether the information has been automatically fed to a process control element; the operator also will need this information.

Initially the chromatograph spectrum was used satisfactorily with proper attenuation of the peaks of interest. Disadvantages are that chart paper is wasted and that only one or two analyses are visible, so that process trends are not readily apparent. This method has been replaced by several means of controlling the chart drive in parallel with the programming and attenuating of the desired analytical peaks. The familiar bar graph predominates; this is obtained by stopping the chart drive while a peak is being recorded and by activating it for a short time between peaks. More elaborate methods of data display are possible; the analyses could be printed on a multipoint recorder of any type or on a digital readout. These have received little attention, probably because of the added expense.

Process analyzers are best used for reset of conventional environmental process controls, either manually or automatically; the control point of a modern large-scale process seldom requires adjustment so rapidly as to make analyzer response-time critical. If automatic reset is used, the response time of the chromatography may present a problem; if manual, probably not, although in adjusting the system to some desired operating point, it may be inconvenient to be forced to wait 15 to 30 min. to find the effect of the last

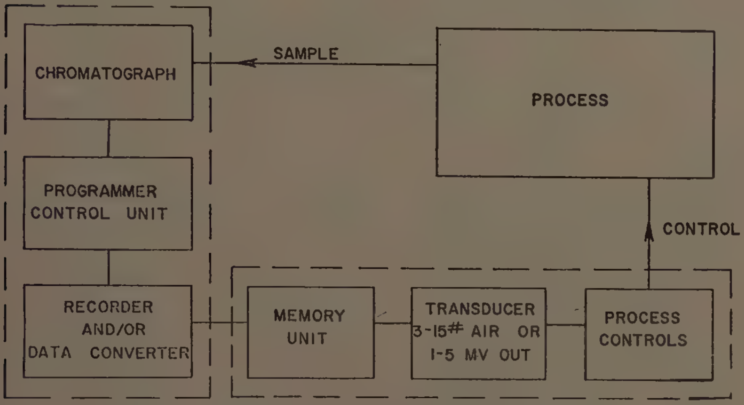

FIGURE 5. Block diagram of automatic control system.

change. Analyzer response is not the only factor involved in analysis lag; a sample lag of from 5 to 10 min. is normal with appropriate filtration and sample preparation, and special attention to the sample system is required if an extremely rapid analysis is to be obtained. The response-time disadvantage of the chromatographic analysis can easily be over-estimated.

The gas chromatograph cannot be used directly for process control because of the intermittent data presentation. A control system of the form shown in FIGURE 5 is required. This includes a memory device to hold the analysis value from one analytical cycle until the next for reset of the process controls. Ayers[15] describes the automatic chromatographic control of a hydrocarbon fractionating unit with this type of system, and mentions the possibility of computation of ratio of component concentrations or of a more complex function of the multicomponent analysis as a more advanced control technique. There is considerable activity in this area, and commercial equipment to adapt the process chromatograph to direct process control should be available soon.

It is interesting to compare process gas chromatography with other process analyzers. This will be done inevitably by the prospective user. There will be little competition with the simpler and less specific analyzers: for example, thermal conductivity. If thermal conductivity will provide a satisfactory analysis obviously it should be used; it is simpler, cheaper, and easier to maintain. Usually the gas chromatograph will be compared with the more specific analyzers, the infrared and the mass spectrometers. All of these instruments are both competitive and complementary; each has certain definite characteristics that may be advantageous or disadvantageous, and the instrument to be selected is the one that best meets the specific requirements for a particular problem. A general comparison of some characteristics of the gas chromatograph, infrared, and mass spectrometer is presented in TABLE 1.

A few examples will illustrate applications typical of process chromatography. Spracklen[16] describes the use of process chromatography to measure the purity of a 90 to 95 per cent chlorine stream. In an excellent discussion of process

TABLE 1
COMPARISON OF GAS CHROMATOGRAPH, INFRARED, AND MASS SPECTROMETER

| | Gas chromatograph | Infrared | Mass spectrometer |
|---|---|---|---|
| Installation in plant | Easy | Easy | Difficult |
| Maintenance | Infrequent; low down-time; simple & easy, average skill, normal training | Moderate; moderate down-time; difficult, high skill, extensive training | Frequent; long down-time; difficult, high skill, extensive training |
| Analysis | Multicomponent, repetitive | Single component, continuous | Multicomponent, repetitive, or single component, continuous |
| Analyzer response | 5 to 15 Min., may be slower or faster | 1 to 2 Min. | 1 Sec., continuous, 5 to 15 min. for multicomponent |
| Selectivity | Very selective | Very selective | Very selective |
| Data interpretation | Direct, easy | Direct, very easy | Usually requires calculation |
| Sensitivity | High | Very high | High |
| Precision | Very high | High | High |
| Versatility | High, requires column change | Low, requires resensitization | Very high |
| Sample | Gas | Gas or liquid | Gas |

chromatography, Ayers[15] describes several applications in considerable detail. The hydrogen-nitrogen ratio in an ammonia-synthesis plant-converter recycle stream is determined in the presence of methane, helium, and argon as inert diluents. A special process analysis for 60 ppm carbon monoxide in ethylene is mentioned. Automatic control of a deisobutanizer column by process chromatograph is described; FIGURE 6 illustrates the principles of Ayers' application. Several process-monitoring analyses of hydrocarbon streams are also mentioned. Dudenbostel and Skarstrom describe a $C_2$ to $C_4$ analyzer using air as a carrier and a heat of adsorption detector.[17]

Obviously, the use of gas chromatography in process control is just beginning and, on the basis of the excellent reports from the present limited applications, the future of the method seems destined to be very good. The process gas chromatograph has some basic characteristics that are unusually well adapted to in-plant use. The analyzer is simple and rugged, and maintenance requirements are reasonable and can be accomplished by personnel with average skill and minimum training. Selective and versatile analyses are possible, and the gas chromatograph has a broad area of potential usefulness. Inherently, the instrument seems to be very precise, and accurate analyses can be obtained. Thus, at the present early stages of development, the gas chromatograph seems assured of a major place in analytical process control. Developments now in progress indicate that in the near future we shall have available chromatographs that can analyze in low ppm ranges with an analyzer response in seconds, and applicable to gas or liquid streams. The potential of gas chromatography as a process analyzer seems unlimited.

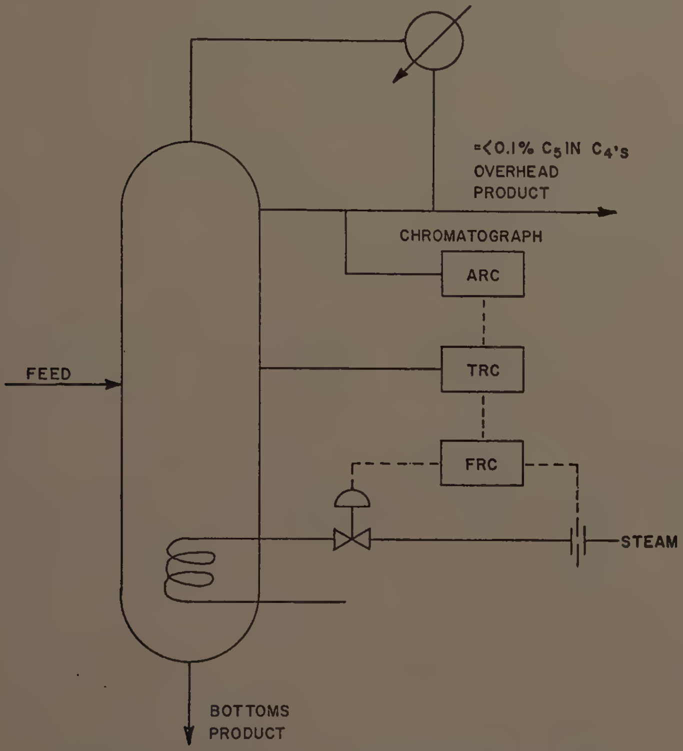

FIGURE 6. Automatic gas chromatograph control system.

## *References*

1. MARTIN, A. J. P. & R. L. M. SYNGE. 1941. A new form of chromatography employing two liquid phases. I. A theory of chromatography. II. Application of the micro-determination of the higher amino acids in proteins. Biochem. J. **35:** 1358.
2. DIETZ, W. A. & B. F. DUDENBOSTEL, JR. 1957. Applications of gas chromatography to chemical processes. Advances in Gas Chromatography. D-171. Preprint of Joint Symposium on Progress in Gas Chromatography. Am. Chem. Soc. Meeting, New York, N. Y.
3. KEULEMANS, A. I. M. 1957. Some theoretical aspects of gas-liquid chromatography. Advances in Gas Chromatography. D-5. Preprint of Joint Symposium on Progress in Gas Chromatography. Am. Chem. Soc. Meeting, New York, N. Y.
4. PIEROTTI, G. J., C. H. DEAL, E. L. DERR & P. E. PORTER. 1956. Solvent effects on gas liquid partition chromatography. J. Am. Chem. Soc. **78:** 2989.
5. PORTER, P. E., C. H. DEAL & F. H. STROSS. 1956. The determination of partition coefficients from gas liquid partition chromatography. J. Am. Chem. Soc. **78:** 2999.
6. BAKER, W. J. & R. F. WALL. 1958. Comparative studies of gas chromatograph column parameters. Presented at the ISA Symposium on Instrumental Methods of Analysis, Houston, Texas.
7. JOHNS, T. 1957. The behavior of the solid support in gas-liquid partition chromatography. ISA Proc. 1957 Intern. Gas Chromatography Symposium, Mich. State Univ., East Lansing, Mich. : 31.
8. DAVIS, R. E. & R. A. SCHREIBER. 1957. Double column gas chromatography: analysis of noncondensable and light hydrocarbon gases by a combined gas-liquid, gas-solid chromatography. Advances in Gas Chromatography. D-91. Preprint of Joint Sym-

posium on Progress in Gas Chromatography. Am. Chem. Soc. Meeting, New York, N. Y.

9. Golay, M. J. E. 1957. Theory and practice of gas-liquid partition chromatography with coated capillaries. ISA Proc. 1957 Intern. Gas Chromatography Symposium, Mich. State Univ., East Lansing, Mich. : 1.
10. Martin, A. J. P. & A. T. James. 1956. Gas-liquid chromatography: the gas density meter, a new apparatus for the detection of vapors in flowing gas streams. Biochem. J. **63:** 138.
11. Scott, R. P. W. 1955. A new detector for vapor phase partition chromatography. Nature. **176:** 793.
12. Pitkethly, R. C. 1957. Symposium on vapor detectors for gas chromatography, Oxford, England. Nature. **180:** 22.
13. Ryce, S. A. & W. A. Bryce. 1957. Ionization gage detector for gas chromatography. Nature. **179:** 541.
14. Lovelock, J. E., A. T. James & E. A. Piper. 1959. A new type of ionization detector for gas chromatography. Ann. N. Y. Acad. Sci. **72** (13): 720.
15. Ayers, B. O. 1957. Chromatographic analyzers in process instrumentation. ISA Proc. 1957 Intern. Gas Chromatography Symposium, Mich. State Univ., East Lansing, Mich. : 11.
16. Spracklen, S. B. 1957. Development of a process gas chromatograph analyzer. Proc. 9th Ann. Symposium on Process Fluid Analyzers. New Jersey Section ISA, Newark, N. J.
17. Dudenbostel, B. F., Jr. & C. W. Skarstrom. 1957. Gas chromatography for plant stream analysis. Advances in Gas Chromatography. D-177. Preprint of Joint Symposium on Progress in Gas Chromatography. Am. Chem. Soc. Meeting, New York, N. Y.

# USE OF ADSORPTION PHENOMENA IN AUTOMATIC PLANT-TYPE GAS ANALYZERS

Charles W. Skarstrom
*Esso Research and Engineering Company, Linden, N. J.*

Automatic plant-type gas analyzers used in oil refineries must meet certain requirements to be successful. First, they must be in an explosion-proof package suitable for their environment. Second, they must provide year-round continuous operation with minimum attention. Third, the instruments must be completely automatic, simple and dependable. Fourth, they should measure the amount of a key component or group of components in a flowing stream, which is useful for the good operation of the plant.

The routine of a gas analyzer in a plant is usually constant. The same analysis is made repetitively. Because the composition of most plant streams changes slowly, higher value is placed on repeatability than on absolute accuracy in the instrument. The early detection of trends in the composition of the stream allows the operator of the plant to minimize costly upsets.

Knowledge of the economics and nature of the chemical process, of the organization of people in the business, and of the physical environment all provide background for the design of useful plant-type gas analyzers.

In an attempt to meet these requirements, several gas analyzers have been built that employ adsorption phenomena of gases on porous solids. Both transient effects and selective adsorption properties have been utilized. An adsorption-type water vapor analyzer and an automatic gas chromatograph will be described. In addition, a continuous adsorption process for drying air without applied heat for regeneration will be discussed.

## *Adsorption Type Detector*

Transient thermal effects in solid adsorbents due to changes in gaseous environment are the basis for these devices. For example, in a continuous gas-flow system through a small solid adsorbent bed, changes of gas composition produce transient temperature changes in the bed. This is true when the components of the stream have different effective heats of adsorption. If the composition of the gas stream is purposely cycled, the resulting temperature cycles in the bed measure the amount of the composition modulation. These temperature cycles are easy to measure, display, and to integrate. This adsorption-type detecting system (U.S. Patent No. 2,826,908, issued Mar. 18, 1958) is used in a water vapor analyzer and in a gas chromatograph.

An adsorption-type detecting system[1] is shown in FIGURE 1. Two gas streams flow steadily through two small beds of solid adsorbent. Flow controls maintain equal and constant flows. The two streams are interchanged every five seconds by timer-operated electric solenoid valves. A bundle of thermocouples or a pair of thermistors measure the temperature differential between the gas flows leaving the two adsorbent beds. It is desirable to have

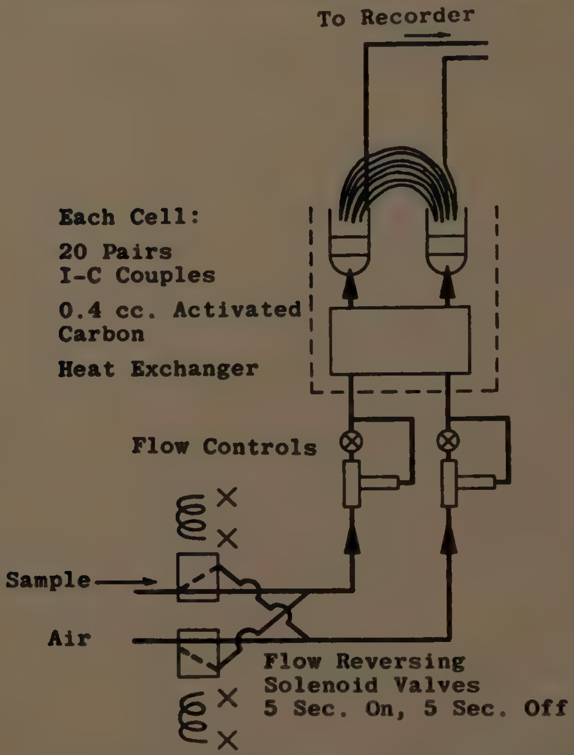

FIGURE 1. An adsorption-type detecting system. Reproduced by permission.[1]

good heat exchange between the two gas streams before they enter the detector cells.

Whenever the two incoming gas streams differ in composition, temperature cycles are produced in the two detector beds. The solid adsorbent must be sensitive to the composition difference. For example, FIGURE 2 shows a burst of oscillations on the recorder chart caused by the signal output from an adsorption detector. The envelope represents the elution of a propylene peak from a gas chromatograph. The carrier and reference gases were dry, $CO_2$-free air, both at 0.2 SCFM. Each detector bed contained 0.4 cc. of activated carbon. The two detector beds are essentially differential flow calorimeters.

This adsorption type detector can be made extremely sensitive to small composition differences. In addition, it can be used in reverse to measure or compare incremental heats of adsorption or coadsorption of gases on various materials.

### *Water Vapor Analyzer*

The adsorption-type detector is employed in a novel water vapor analyzer for use on gas or vapor plant streams.[2] A schematic drawing of the instrument is shown in FIGURE 3. The sample of the plant stream is split; half of it is dried. The dry and moist portions flow alternately through two beds of

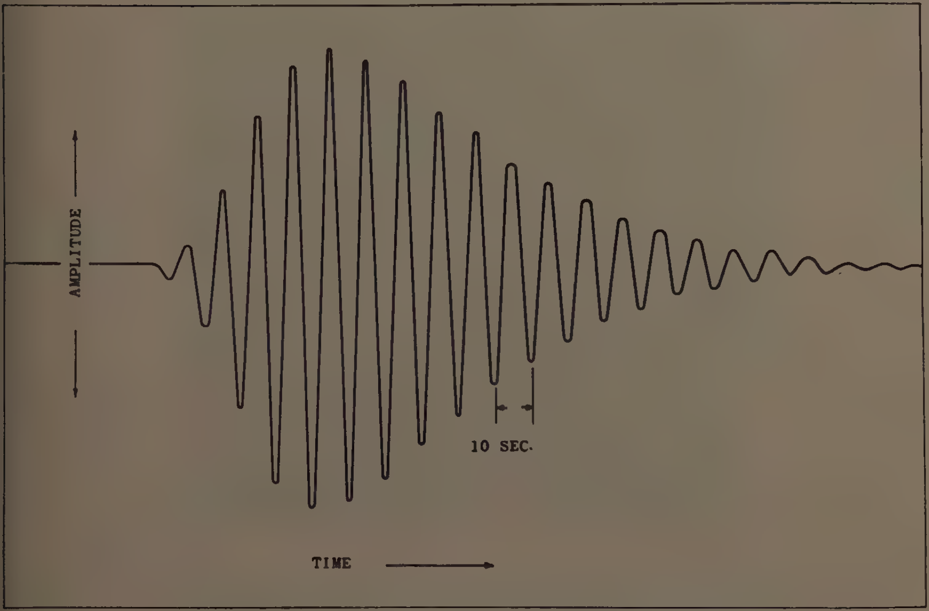

Figure 2. Temperature oscillations in an adsorption detector during elution of propylene from a chromatograph.

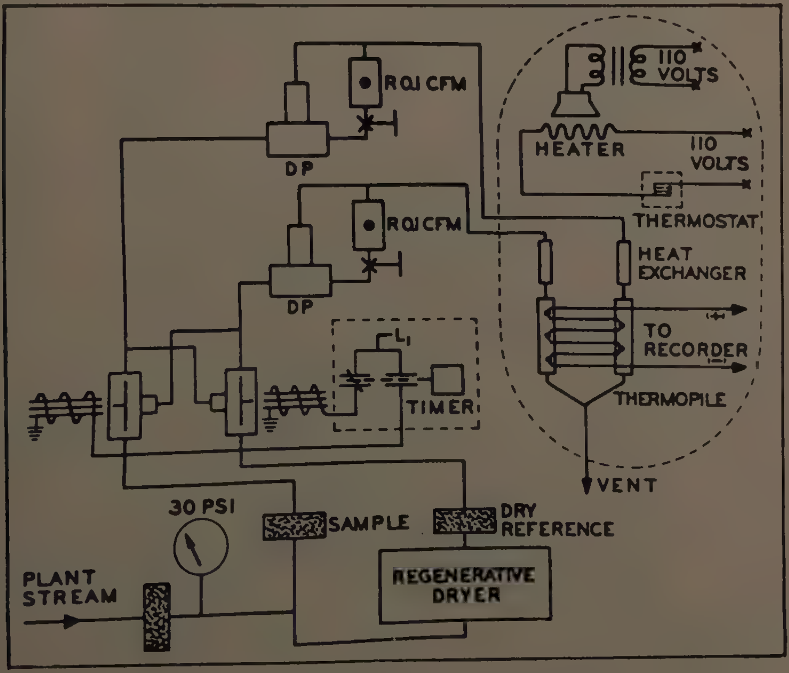

Figure 3. Schematic of water vapor analyzer.

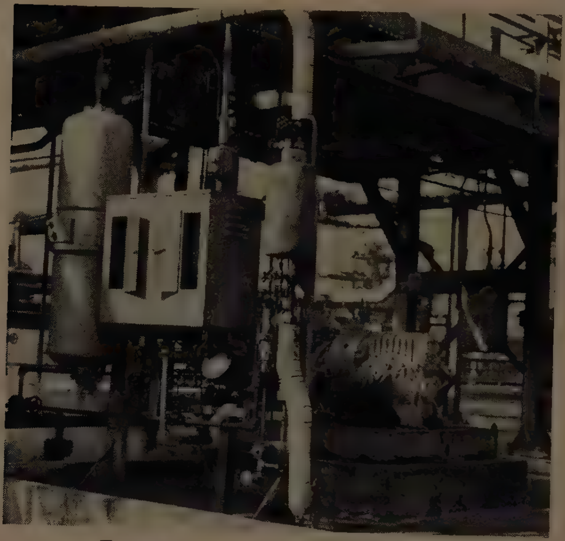

FIGURE 4. Water in LPG analyzer.

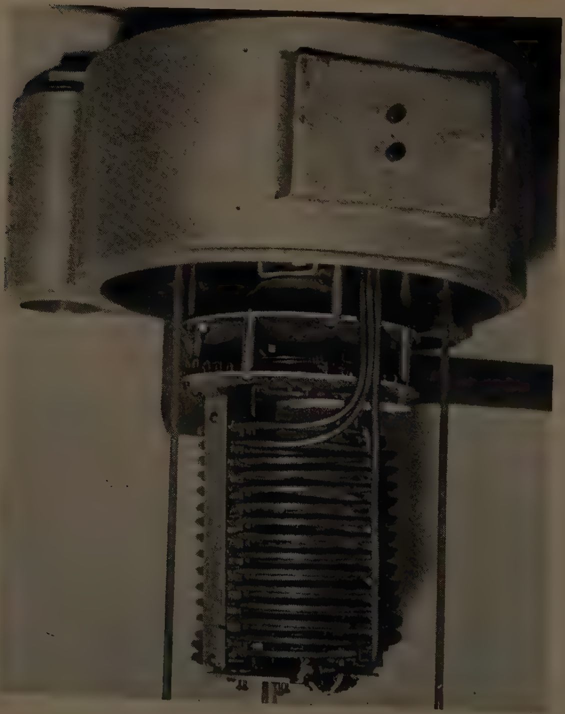

FIGURE 5. Detector assembly.

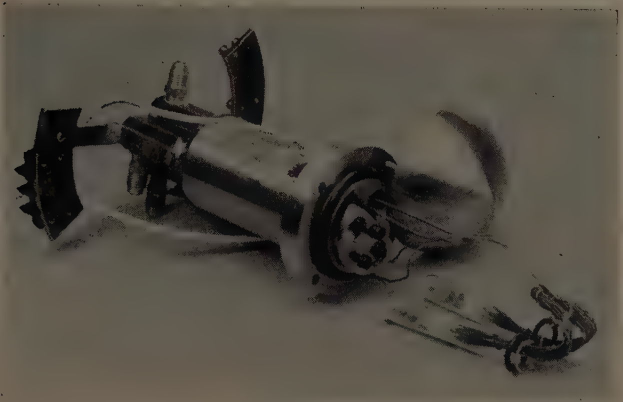

FIGURE 6. Detector cells and bundle of 20 pairs of iron-constantan thermocouples to measure cycling temperature differences.

activated alumina, silica gel, or other solid desiccant. The size of the temperature cycles produced is proportional to the moisture content of the plant stream. In addition, the signals are proportional to the ratio of the total heat of adsorption of water vapor (including the latent heat) to the specific heat of the carrier gas.

FIGURE 4 shows this analyzer installed in an oil refinery. In this application, the analyzer monitors the moisture content of liquified petroleum gas (propane) in the range 0 to 400 mol. ppm. The liquid propane is vaporized by steam before entering the analyzers. The rectangular box in FIGURE 4 holds the regenerative drier. The cylindrical explosion-proof housing contains the thermostated detector cells. FIGURE 5 shows details of the detector assembly, including a loud speaker, blower, heater, thermostat, and heat exchange coils. The detector cells are mounted in the center of the coils. The cells and their container are shown in FIGURE 6. Each cell is filled with 2 cc. of Mobilbeads, a commercial desiccant.* The bundle of 20 pairs of iron-constantan thermocouples produced a signal of 4 $\mu$v./mol. ppm of water vapor. During 5 years of continuous use, the sensitivity of the detector material diminished to one half. This amounts to a little less than 1 per cent per month.

The recorder for this analyzer is located in the control house. The oscillating thermal emf it receives is shown in FIGURE 7 for 50 and 100 ppm of water vapor. The special recorder actually reads out only the peak-to-peak amplitude of this signal, as shown in FIGURE 8. Since the flow switching occurs every 2 min., a new piece of information is recorded every 4 min. Attenuators provide calibration adjustment. FIGURE 8 also shows that the speed of response to water vapor between 0 and 100 ppm is about 16 min. A similar plant-type moisture analyzer is manufactured in the United States.†

* Socony Mobil Oil Co., New York, N. Y.
† Mine Safety Appliance Company, Pittsburgh, Pa.

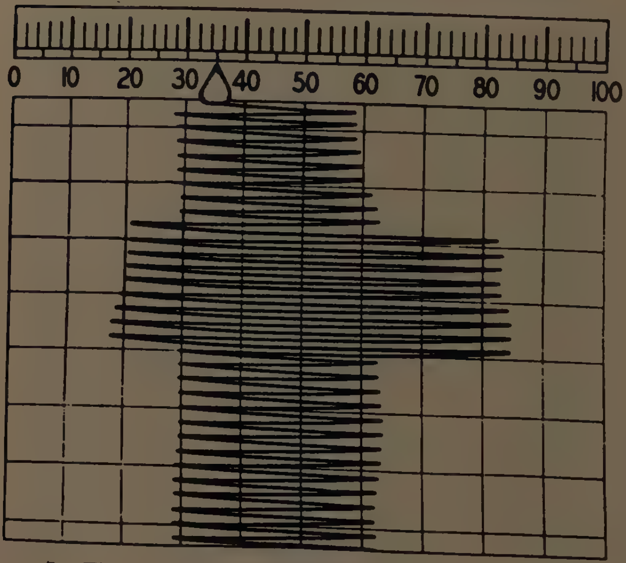

FIGURE 7. The signal from the detector is an oscillating thermal emf.

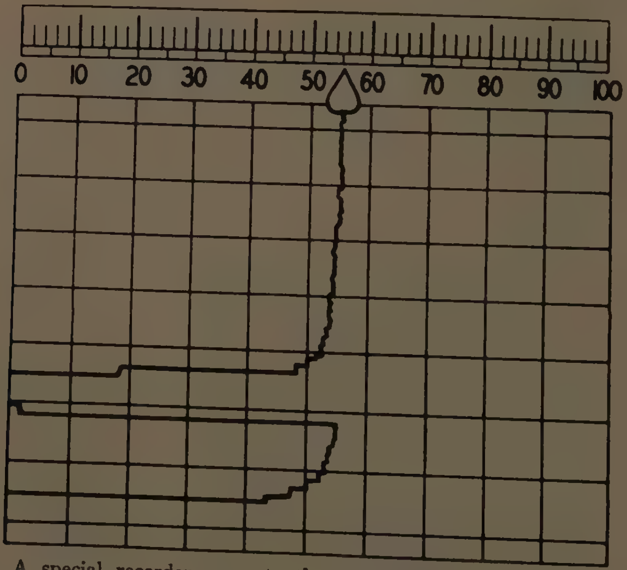

FIGURE 8. A special recorder presents the peak-to-peak amplitude once every four minutes.

## *Gas Chromatograph*

A gas chromatograph is another example of the liberal use of adsorption phenomena in automatic plant-type gas analyzers. Such an instrument is shown in FIGURE 9. It contains a solid adsorbent column and an adsorption-

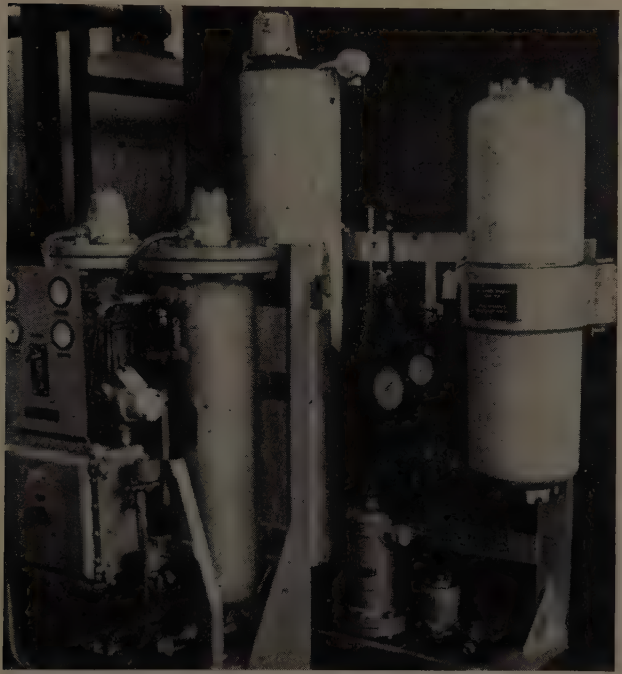

FIGURE 9. Plant-type gas chromatograph using air as a carrier gas through an alumina adsorption column. Air drier is shown at left; column, in center rear; and adsorption-type detector enclosure, at right.

type detector. For carrier gas, it uses dry $CO_2$-free air, prepared by an adsorption drier.

The commercial adsorption drier, shown at the left of FIGURE 9, contains two desiccants in each bed. Mobilbeads are used for high moisture capacity and activated alumina* to hold back oil vapor and $CO_2$. A heating cycle every 6 hours regenerates one 50-lb. bed while the other one is on-stream. Use of this drier at $\frac{1}{250}$ of its normal capacity, provides clean dry air at 15 psig. and 0.4 SCFM for the chromatograph.

A schematic drawing of the chromatograph is shown in FIGURE 10. A vaporized sample of a mixed hydrocarbon gas is periodically injected into the alumina column by a program timer. Different components are carried through the column at different speeds, depending on their heats of adsorption on alumina. The components emerge one at a time. They are then measured by their transient thermal effects in an adsorption-type detector.

In one application, in use for several years in a refinery, an automatic analysis of the LPG product is presented every half hour to the process operator on the recorder shown in FIGURE 11. The signals the recorder receives from the adsorption detector are shown in FIGURE 12. Each component consists of a burst of oscillations, as the close-up in FIGURE 2 shows. For each com-

---

* Aluminum Company of America, New York, N. Y.

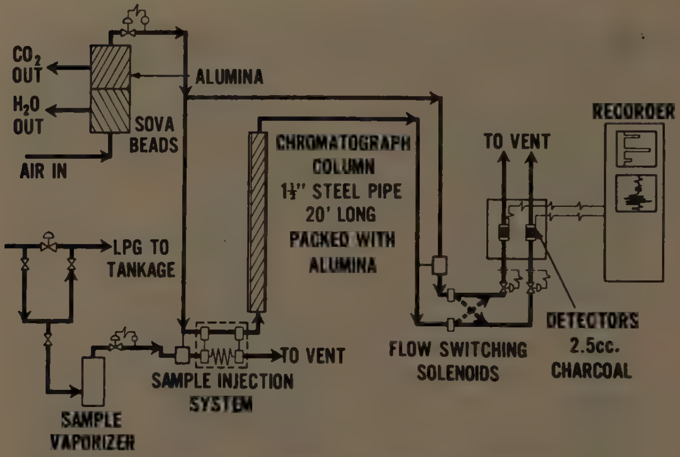

FIGURE 10. Schematic diagram of automatic gas chromatograph.

FIGURE 11. Recorder for the automatic gas chromatograph. Upper recorder is used for bar graph analyses; lower recorder is used to observe signal oscillations. Control box contains attenuators for calibration.

ponent, a mechanism in the recorder adds the peak-to-peak amplitude of each 10-sec. cycle. An integration of the elution peak for each component is thus obtained. The integrals, which are least sensitive to all the instrument variables, are presented to the plant operator as bar graphs. A typical bar graph chart is shown in FIGURE 13.

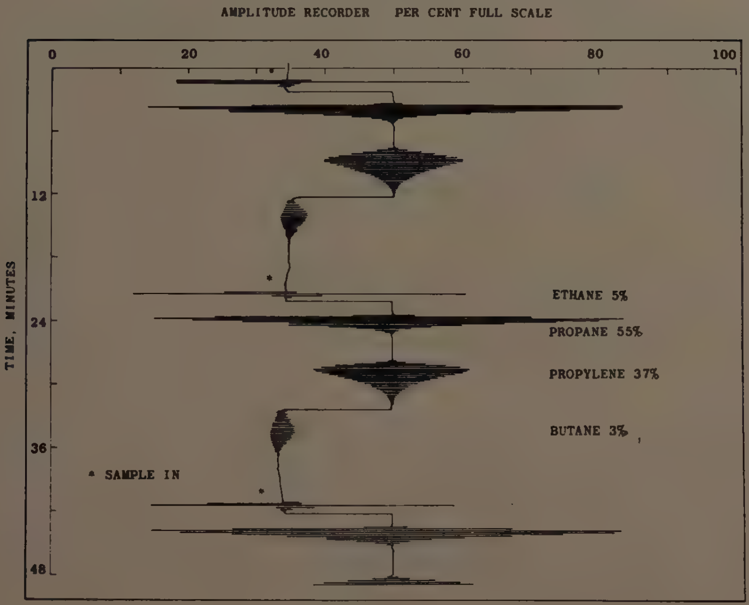

FIGURE 12. Detector output for repetitive LPG analyses, showing bursts of oscillations for the elution of each component.

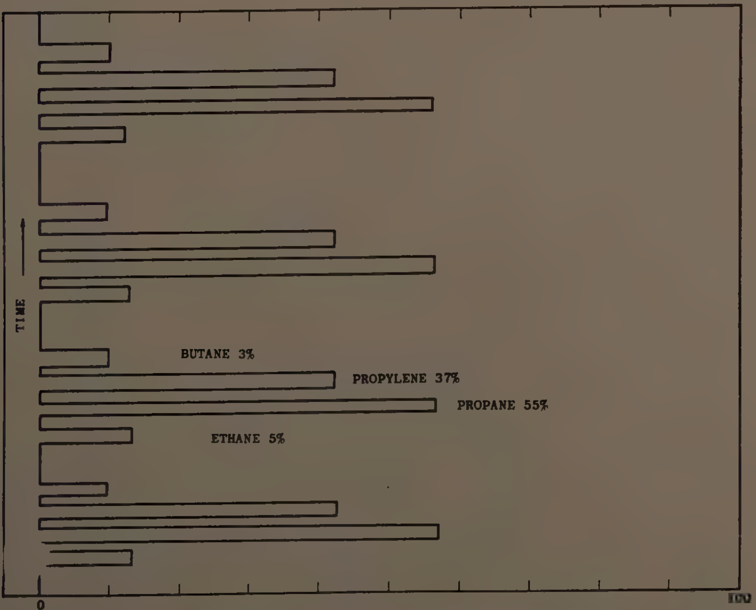

FIGURE 13. Example of bar graph readout of the areas of the elution peaks in LPG analyses.

After calibration for ethane, ethylene, propane, propylene, and total $C_4$'s, the sum of all components added up to 100 per cent. The standard deviation of the analysis was ±0.3 per cent. One year later, without recalibrating, the components added up to 97 per cent. During this time, about 50 years' worth of laboratory analyses were made by this automatic gas chromatograph.

Another application of this chromatograph is the detection of trace impurities. In one refinery, it is used to measure trace acetylene in a relatively pure ethylene product. Large 5-liter samples of ethylene are injected into the column. The detector sensitivity has been increased 400 times by the use of alumina, with thermistors to measure the temperature cycles. The instrument is ranged for 0 to 100 ppm acetylene in ethylene. As little as 3 ppm acetylene can be observed. This is another example of how gas adsorption phenomena on porous solids can be put to good use if the problems are known.

### *Heatless Adsorption Drier*

In the instruments described above, use has been made of gas driers. These driers contain solid adsorbent beds which are periodically heated and backwashed to remove the accumulated moisture. An unusually large and bulky air drier is needed for the gas chromatograph. To simplify the gas drying function in these instruments, a new adsorption drying process has been devised.

The process uses as desiccants such solid adsorbents as alumina and silica gel, which are regenerated without applied heat. In this two-bed system, one bed dries the stream at high pressure; the other bed is backwashed at low pressure with some of the dry product. Roles of the two beds are reversed every several minutes. If the actual volume of backwash flow at low pressure exceeds the actual volume of input flow at high pressure, the system produces

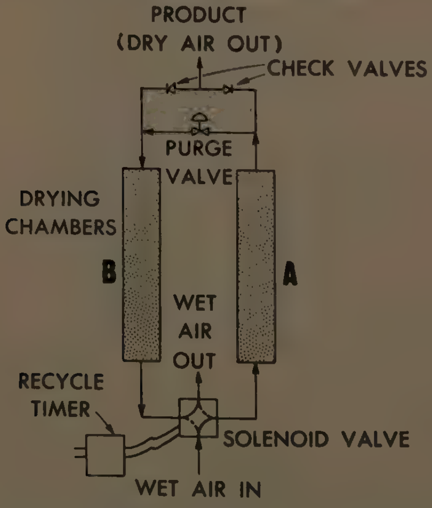

Figure 14. Heatless adsorption drying system.

a very dry air product. Dry air, at line pressure, containing as little as 50 parts per billion of moisture can be attained with commercial solid desiccants.

A schematic drawing of this heatless drying process is shown in FIGURE 14. Bed *A* is connected to the high-pressure moist air line. Moisture is removed in bed *A* while the adsorbent tries to come to equilibrium with the water vapor pressure existing in the high pressure line. Meanwhile, bed *B* is backwashed at atmospheric pressure with some of the dry product from *A*. Bed *B* tries to maintain the same partial pressure of water vapor in the purge as exists in the high-pressure line.

The beds are interchanged every several minutes by a time-operated solenoid valve. If the purge flow is adjusted to exceed the actual incoming flow, more water vapor is rejected from the system than enters. This continues to an equilibrium condition, where the first 4 to 6 in. of each bed does all the drying.

Because of the rapid switching between drying and purging, the heat liberated when moisture is adsorbed is retained in the bed. It is available to supply the heat for desorption during the purge cycle. The temperatures of the beds normally cycle several degrees above and below the ambient. When a heatless drier is first turned on, the desiccant usually contains water. During initial operation, the beds become cool. In this conditioning period, the drier itself is drying out.

The conditioning of a heatless drier is shown in FIGURE 15. The observed moisture content of the dry output is plotted as a function of time. At the start, the product air contained 4000 mol. ppm of moisture. This was the moisture content of the 40 psig air line. After several hours of operation,

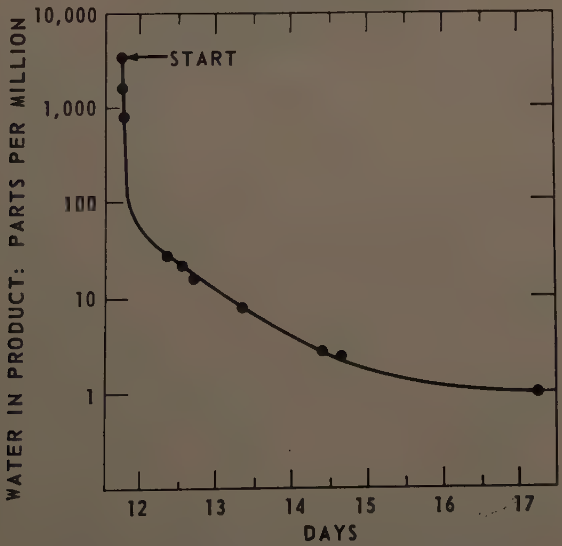

FIGURE 15. Conditioning of a small heatless drier.

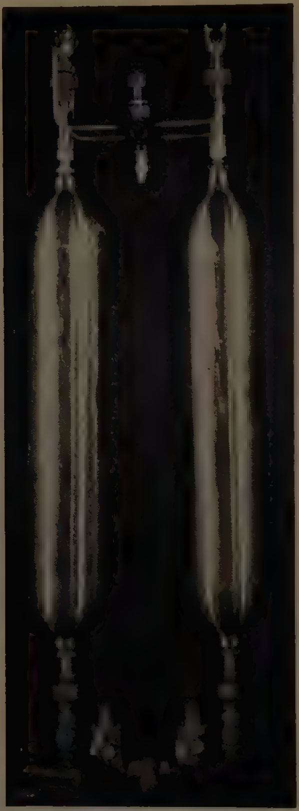

FIGURE 16. Heatless air drier for gas chromatograph contains alumina desiccant This continuous adsorption system rejects water vapor, oil vapor, and carbon dioxide without applied heat for regeneration.

the dry air product contained less than 100 ppm of water vapor. Three days later, the moisture in dry product was down to 2 ppm. Eventually, the product dryness leveled off below 1 ppm. The drier consisted of two 1-lb. beds of Mobilbeads which were switched every 3 min. Product and purge flow were kept at 0.5 SCFM each.

FIGURE 16 shows another heatless drier designed for use with the gas chromatograph. The two 1-gallon size beds each hold about 6 lb. of activated alumina. This air drier supplies dry, $CO_2$- and oil vapor-free air for the chromatograph. The air product moisture content is down to 0.05 mppm. Mechanically and functionally, it is superior to the large heat regenerated drier shown in FIGURE 9.

This drying process is another example of the effective use of transient phenomena when gases flow over solid adsorbents. Heatless adsorption driers* have operated successfully at pressures from 15 to 3500 psig, with ambient temperatures from −20 to +170° F., and with desiccant bed sizes from 25 gm. to 300 pounds. Currently, they are being manufactured in the United States* and are finding increasing use in the electronic, power generation, telephone, rocket, oil, and other process industries.

---

* U. S. Patent applied for.

## *Summary*

The ability of porous solids to adsorb various gases has been employed in the design of two automatic plant-type gas analyzers.

(1) A water vapor analyzer uses temperature cycles in a small adsorbent bed to measure the moisture content of a gas stream. The temperature cycles are produced by alternately flowing a moist and a dried stream through the bed.

(2) A gas chromatograph, suitable for certain oil refinery stream analysis problems, uses a solid adsorbent in the column, and dry, $CO_2$- and oil vapor-free air as carrier gas. Line air is processed by an adsorption drier for use as carrier gas. Detection of the elution peaks is done by an adsorption-type detector, similar to that used in the water vapor analyzer. The chromatograph is completely automated and reads out bar graph analyses of integrated elution peaks of the different components.

The strong memory of solid adsorption desiccants for water vapor pressure is used in a new adsorption process to dry air without applied heat for regeneration. At line pressure, this heatless adsorption drier can produce dry, $CO_2$- and oil vapor-free air containing as little as 50 parts per billion of moisture. Wide application of the process is another example of effective use of transient phenomena when gases flow over solid adsorbents.

## *References*

1. Dudenbostel, B. F., Jr. & W. Priestley, Jr. 1956. Ind. & Eng. Chem. **48:** (Sept.) 56A.
2. Editorial. 1956. Solution to line moisture problems. Gas Age. **117:** 20–23.

---

* Trinity Corporation, Roselle Park, N. J.

# THERMAL CONDUCTIVITY DETECTORS FOR PROCESS CONTROL

F. C. Snowden and R. D. Eanes
*Leeds & Northrup Company, Philadelphia, Pa.*

## *Introduction*

Leeds & Northrup Company has had a long and continuing interest in instrumentation designed for the analysis of process streams containing volatile substances and vapors. Because of the great importance of this type of analysis to the process industries, our company has traditionally oriented its interest in these measurements toward instruments for process analysis and control. The requirements for instrumentation for in-stream measurements on processes in operating plants differ in some basic points from instruments directed primarily toward laboratory measurements. These differences reside in the requirement of the process industries for reliability and stability of the measurement above all other criteria. It has been traditional that such desirable characteristics as high sensitivity, extreme flexibility of instrumentation, low cost, and high precision be subordinated to factors that would produce a rugged and relatively maintenance-free piece of equipment having response-time characteristics suitable for automatic control. In developing detectors for thermal conductivity gas analyzers, for thermomagnetic oxygen analyzers, and for process-type vapor phase chromatographic equipment, we have given precedence to the needs and requirements for applications in process analyzers.

The detecting elements described in this paper are especially applicable and adaptable to the new field of vapor analysis that is presently undergoing great expansion. Vapor phase chromatography has two highly desirable advantages for the designer and manufacturer of process analysis instrumentation. The high specificity and high resolution that can be achieved with relatively simple equipment make this method most attractive. Furthermore, methods of analysis that may be worked out on laboratory equipment may, in many instances, be translated directly into process application. The advantage of this latter point can be realized fully only by those who have attempted to calibrate other types of analyzers on process streams.

The detectors that are the subject of this paper may be used with simple modifications in analyzers for thermal conductivity gas analysis, for thermomagnetic oxygen analysis, and for vapor phase chromatography measurements. The design incorporates the following features: small size; low electric power input requirements; high sensitivity and fast response to changes in sample composition; a high degree of corrosion resistance; the elimination of heat losses by convection; the absence of any effects from cell position; the minimizing of sensitivity to sample flow rate; and the absence of any sensitivity to vibration and shock. These features impart to the new cells dimensional and performance characteristics that are notably superior to those of existing designs for process instrumentation use.

### *Operating Principles*

The fundamental operating principles of the newly designed cells do not differ from those of other hot-wire thermal conductivity cells. All such cells consist basically of a cylindrical envelope in which a hot-wire element is mounted coaxially. This element is made of a material that has a relatively high thermal coefficient of resistivity. A known thermal gradient, or temperature rise, is imposed between the hot-wire element and the cell wall under standard conditions: for example, with cell envelope held at a constant temperature (usually 50° C.), and with dry air flowing to the atmosphere through the cell block at a known rate. Thus, when a sample gas mixture flows through the cell block under the same conditions, heat is conducted away from the hot-wire element at a rate that depends upon the thermal conductivity of the gas mixture present in the cell at a given moment. This causes the temperature of the hot-wire element and, consequently, its electric resistance, to vary with the thermal conductivity of the sample gas mixture. This hot-wire element is placed in one arm of a bridge circuit; a second element, located in another cell operating under certain reference conditions, is placed in an arm of the bridge adjacent to the first. The output of the bridge varies as a function of the resistance of the element exposed to the sample gas mixture, and it can be calibrated directly in terms of a percentage of some particular component present in the sample being measured.

### *Heat Loss Considerations*

*Determination of heat loss characteristics.* When a thermal conductivity cell of the hot-wire type is connected to a source of power, and the electrically heated cell element is exposed to a gas sample of constant composition—for example, air—an equilibrium is established between the electric power input and the energy lost by heat transfer from the cell element. The heat losses within the cell fall into several well-defined categories: (1) by conduction through the gas surrounding the heated element (thermal conductivity); (2) by convection; (3) by radiation; and (4) by conduction through the supporting structure of the cell element and through the external electric connecting leads. Collectively, the latter losses are called end losses.

Ideally, a thermal conductivity cell should have only gaseous thermal conduction losses. Such an ideal cell would have maximum sensitivity. However, while it is impossible to eliminate all the heat losses occurring by the other mechanisms mentioned, it is definitely possible to eliminate losses due to convection and to minimize the end losses. Fortunately, the radiation losses, about which not much can be done, represent only a small portion of the total heat losses when the hot-wire element is operated at a temperature difference between element and cell wall not exceeding 300° C.

A cell that has a diameter large enough for convection currents to be present is sensitive to changes in its mounting position. This is caused by a changing pattern of convection currents as the cell is tilted away from its normally vertical position. The two extreme cases, of course, are the purely vertical and the purely horizontal mounting positions. Thus, if all other conditions are held constant, the difference in the electric power input required to maintain a constant element operating temperature when the cell is mounted in the two extreme positions is attributable to the difference in convection losses in the two cases. If no difference is observed in the electric input power required, it can be inferred that no convection losses are present within the cell.

Losses from convection have been eliminated, for all practical purposes, from the thermal conductivity cell described in this paper. A series of earlier studies indicated that convection losses are not present in cylindrical hot-wire cells if the I. D. of the cell envelope is less than approximately 5 mm. The restrictions imposed on the free motion of gas within a cell of such narrow confines preclude the formation of convection currents.*

The I. D. of the envelope of the new cell being considered here was restricted to about 5 mm. when used as a diffusion-filled thermal conductivity cell. For thermomagnetic oxygen measurements the principle of operation of the analyzer depends upon the induction by the magnetic field of a thermal convection current. In this application the diameter of the cell envelope is opened up to 9 to 10 mm. In using the subject detectors for vapor-phase chromatography equipment, advantage is taken of the fact that the flow through the chromatography column must be rigidly controlled for proper functioning of the column. In this case the thermal conductivity cells do not operate as diffusion-filled cells, but are in series with the flow of the gas stream. For this application, high stability and fast speed of response are the essential characteristics for the detectors.

The other types of heat losses found in thermal conductivity cells are all present in the new cell design. Ideally, a thermal conductivity cell should have only gaseous thermal conductivity losses. Practically, however, some radiation and end losses will always be present. The amount of radiation losses is dependent on the operating temperature of the cell element, since heat loss by radiation is a function of the fourth power of the absolute temperature of the radiating body. End losses cannot be eliminated, but they can be minimized.

The first step to be taken in an analysis of the heat losses that occur in a thermal conductivity cell is to obtain, under normal operating conditions, a plot of the equilibrium values of the cell element operating temperature corresponding to a series of given power inputs to the cell element. To obtain these values the cell under study is mounted in an appropriate cell block in a constant-temperature oil bath. Air is caused to flow through the cell block at a rate of 200 ± 20 ml./min. under conditions of normal atmospheric pressure.

The current through the cell is adjusted by varying the power decade resistor until the voltage drop across a standard resistance indicates that the desired value has been reached. The voltage drop across the cell element is measured at known values of the current.

The resistance of the cell element at 50° C. is determined by measuring the voltage drop across the element with a current of only 5 mAmp. This small current is low enough to eliminate substantially any self-heating of the element, and the 50° resistance of the element calculated from the data thus obtained will be referred to henceforth as the cold resistance. Next, the current flow through the cell element is varied from 10 mAmp. to 80 or 90 mAmp. in 10-mAmp. steps. In each instance, the corresponding voltage drop across the element is measured after an equilibrium has been established. From these voltage-current data a series of power input values and the corresponding values of the operating resistance of the cell element may be calculated. Each of these operating resistance values is then divided by the known cold resistance of the element. From these ratios one can determine the operating temperature of the cell element for each value of power input. In FIGURE 1, curve *A* represents the power input to the cell element, in milliwatts, plotted against the operating temperature of the cell element, in °C. From this plot one can find the total heat, expressed in terms of milliwatts input, dissipated by the cell element at any operating temperature from 50° C. to 350° C.

---

* Unpublished work of R. H. Cherry, Development Division, Leeds & Northrup Company.

When a gas is under normal pressure in a cell, the coefficient of thermal conductivity, $K$, is a function of the product of $\eta$, the coefficient of viscosity, and $C_v$, the specific heat of the gas at constant volume. This may be expressed mathematically as:

$$K = \epsilon \eta C_v \tag{1}$$

where $\epsilon$ is a constant that empirically is found to be independent of temperature and pressure over a wide range. It appears to depend chiefly on the number of atoms in the gaseous molecule. Eucken found the value for $\epsilon$ to be approximately 2.5 for monatomic molecules such as He, Ne, and A, and approximately 1.9 for diatomic molecules such as $H_2$, $N_2$, and $O_2$. These values were confirmed by later investigators. Since the coefficient of viscosity $\eta$ is independent of pressure and $C_v$ is a constant, it follows that the coefficient of thermal conductivity, $K$, is also independent of pressure. However, the above statement is valid only so long as the mean free path of the gas molecules remains small.

At reduced pressures the number of gas molecules, and thus the number of collisions per unit time between them, becomes small. As a consequence, the mean free path of the gas molecules becomes proportionately large. When the pressure in a thermal conductivity cell is reduced to the point where the mean free path of the gas molecules is large with respect to the dimensions of the cell envelope, the actual free path of many of the molecules will be restricted only by the cell envelope. In the new cells being discussed here, the mean free path is considered large with respect to cell dimensions if it equals the distance from the element to the cell wall, or approximately 2.5 mm. The mean free path, $\lambda$, of the molecules in a gas can be expressed:

$$\lambda = \frac{1}{\sqrt{2}\pi n \sigma^2} \tag{2}$$

where $n$ is the number of molecules per unit volume and $\sigma$ the collision diameter of an individual molecule. At 50° C. and at atmospheric pressure, the value for $n$ is $2.3 \times 10^{19}$ molecules per cc. The diameter $\sigma$ of most gas molecules is on the order of $2 \times 10^{-8}$ cm. Substituting in EQUATION 2, we find that the mean free path of molecules in a gas at atmospheric pressure at a temperature of 50° C. is about $2.3 \times 10^{-4}$ mm. Since $\lambda$ is inversely proportional to $n$ and $n$ is directly proportional to pressure $p$, it follows that $\lambda$ is also inversely proportional to $p$. Thus, the product of the mean free path and the gas pressure is constant:

$$\lambda_1 p_1 = \lambda_n p_n \tag{3}$$

Applying this to the new cells, where the cell radius equals 2.5 mm., substitution in EQUATION 3 shows that a pressure of about $10^{-1}$ mm. Hg is required to give a mean free path equal to the cell radius of 2.5 mm. Under these conditions of reduced pressure the influence of the viscosity effect is altered, and many of the gas molecules will pass directly from the hot-wire element to the envelope wall without becoming involved in a single intermolecular collision. In such cases heat from the element is carried directly to the wall by individual gas molecules. The thermal conductivity of the gas in the cell has become a function of pressure, inasmuch as the number of gaseous molecules available for the direct transport of heat from the element to the envelope is directly proportional to the pressure.

The above relationship between thermal conductivity and pressure exists, for most thermal conductivity cells, in the approximate pressure range $10^{-1}$ mm. to $10^{-4}$ or $10^{-5}$ mm. Hg. Below pressures of $10^{-4}$ or $10^{-5}$ mm. Hg, the number of gas molecules is relatively small, so the thermal conductivity of all gases, for most practical purposes, becomes zero. Thus, if a thermal conductivity cell is evacuated to a pressure of about $10^{-4}$ mm. Hg, the heat losses from thermal conduction by the gas in the cell virtually have been eliminated, and the losses that are measured at this reduced pressure are due solely to radiation and end losses. Thus, evacuation of cells to very low pressures is a valuable tool for studying cell heat-loss characteristics.

Curve *B* of FIGURE 1 shows the total cell heat losses plotted against element temperature after the cell has been evacuated to a pressure of $10^{-4}$ mm. Hg. It can be assumed that all the heat losses represented by this curve are from radiation and end losses only.

The mass of the cell element supporting structure and the cross-sectional area of the escape path for end losses are both constants. Thus, the end losses of these thermal conductivity cells should be a linear function of the operating temperature of the hot-wire element. Furthermore, if there is no electric power input to the cell element, its operating temperature will be the same as the temperature of the cell envelope, which is 50° C. for all the tests made on these cells. Under such conditions the heat radiated by the element will be balanced by the radiated heat it receives from the envelope. Thus, the net radiation loss from the element is zero at an operating temperature of 50° C. when the temperature of the envelope is also 50° C. Therefore, in FIGURE 1 the tangent *C* to curve *B* at the element operating temperature of 50° C. represents the end losses that occur in the cell, while the difference between the tangent *C* and curve *B* represents the radiation losses.

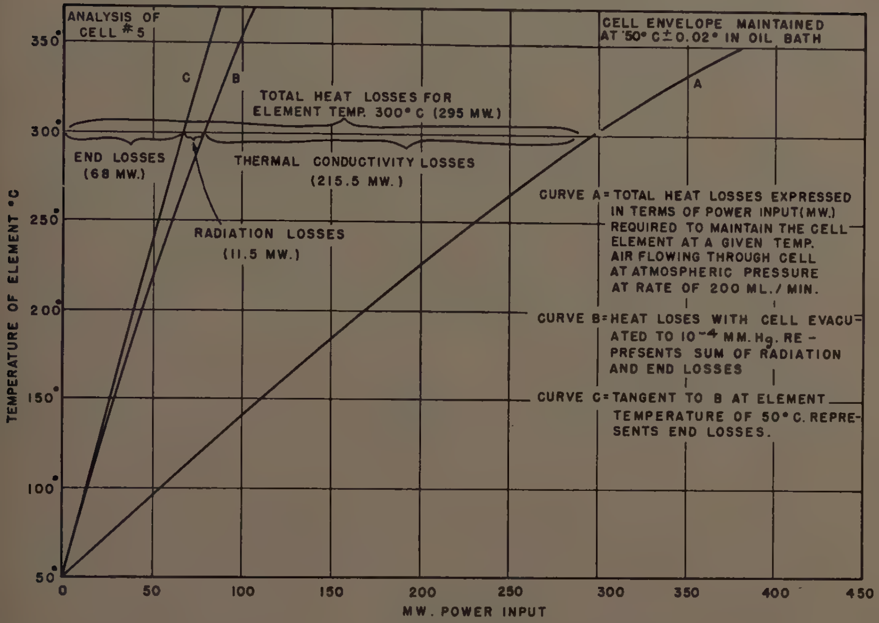

FIGURE 1. Analysis of the heat loss characteristics of a typical cell of the new design.

The validity of the separation of radiation and end losses by the method outlined above is confirmed by plotting the differences between points on tangent *C* and curve *B* obtained for several particular values of the element operating temperature against the fourth powers of the corresponding absolute temperatures. A straight line plot in agreement with theory* results, as shown in FIGURE 2. Additional proof of the method is found when the line of the plot is extrapolated to zero radiation loss, at which point it crosses the fourth power absolute temperature axis at the value corresponding to 50° C.

Thus, with curves *A*, *B*, and *C* of FIGURE 1, one can find, for any cell element operating temperature from 50° C. to 350° C., the total heat losses of this element expressed in terms of milliwatts power input and what proportion of these losses are caused by: (1) thermal conductivity through the gas in the cell; (2) radiation from the hot element; and (3) end losses. An analysis of the situation at 300° C., the normal element operating temperature, is shown on the plot.

*Minimizing end losses.* In the development of the new thermal conductivity cells the minimizing of end losses was of paramount interest. FIGURES 3*A* *B*, *C*, *D*, and *E* show five possible supporting structures for helically wound hot-wire cell elements. FIGURE 3*A* illustrates the type of supporting structure

---

* Theory states that radiation is a linear function of $T_2^4 - T_1^4$, where $T_2$ = temperature of the radiating body, $T_1$ = the temperature of the absorbing body. If $T_1$ is constant, as the cell wall in this case, radiation is then a linear function of the fourth power of the absolute temperature of the radiating body, the cell element in this case.

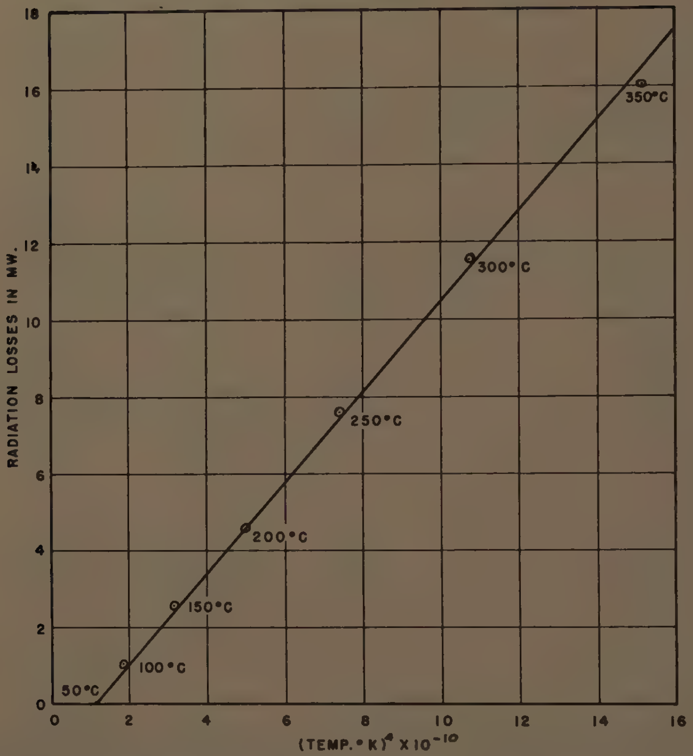

FIGURE 2. Radiation losses versus the fourth power of the absolute temperature of a typical cell element.

used as a control design in these studies. This structure consists of a solid glass stem having a relatively large mass and cross section, and a mandrel approximately 6.5 mm. long. The mandrel is located coaxially in the envelope of the completed cell; it positions and supports the hot-wire helix. The mandrel consists of a length of platinum wire, approximately 12.5 mils in diameter, overlaid with a thin, 2.5-mil coating of insulating glass. The platinum wire serves a dual purpose: it provides the mandrel with sufficient mechanical strength, and it serves as the external electric connecting lead for one end of the hot-wire helix.

The flow of heat from the mandrel surface occurs through the platinum lead, through the glass stem, and thence to the environs of the cell. The structural details suggest that the high end losses (50 to 55 per cent) are primarily the result of two factors: (1) the large cross-sectional area of the glass stem that supports the mandrel, thereby providing a low resistance path for heat flow from the mandrel to the cell envelope; and (2) the presence of the good conducting platinum wire of relatively large diameter at the core of the mandrel. The thin insulating glass coating around the wire is inadequate in cutting down

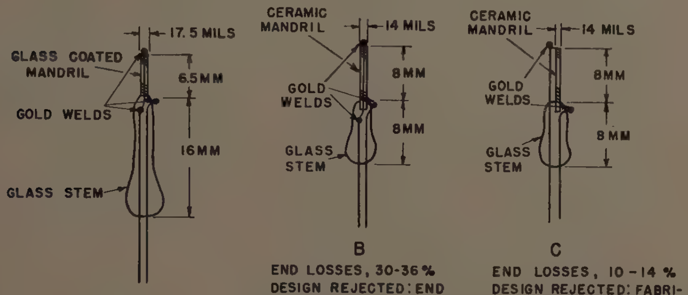

B

END LOSSES, 30-36%
DESIGN REJECTED: END LOSSES TOO HIGH.

C

END LOSSES, 10-14%
DESIGN REJECTED: FABRICATION COMPLICATIONS.

A

END LOSSES, 50-55%
DESIGN REJECTED: END LOSSES TOO HIGH.

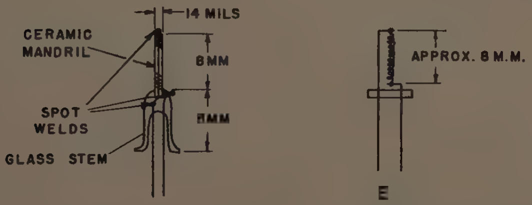

D

END LOSSES, 22-25%
DESIGN ADOPTED: ACCEPTABLE COMPROMISE.

E

END LOSSES, PROBABLY < 10%
DESIGN REJECTED: SHOCK SENSITIVE; NOT RIGID AND THUS UNSTABLE; POSITION SENSITIVE.

FIGURE 3. Some representative cell element designs.

losses. Furthermore, the intimate contact between the insulating glass coating and the platinum wire, along the mandrel length, encourages the transfer of heat from the surface of the mandrel to the highly conductive core.

The above analysis suggests several means by which end losses may be reduced: (1) decrease the cross-sectional area of the glass stem by decreasing its diameter; (2) increase the proportionate thickness of the insulating layer with respect to the total diameter of the mandrel; (3) find another way to impart mechanical strength to the mandrel, so (4) the diameter of the platinum lead through the core of the mandrel may be decreased; and (5) eliminate the intimate contact between the insulating layer and the mandrel core, thus providing for a less efficient transfer of heat to the mandrel core.

Mechanical strength of the mandrel was maintained by using a length of extruded ceramic tubing to support the helical winding. The wall thickness of this tubing is approximately 4.5 to 5.0 mils, and it provides an effective insulating layer between the hot-wire element and any lead wire that might extend through the center.

In most of the cells that were built and tested (one exception is described below), a small platinum wire passes through the ceramic tube. This wire does not contribute to the mechanical strength of the mandrel, but serves simply as the electric connection for one end of the cell element. Intimate contact does not exist between this wire and the insulating ceramic walls of the tube.

A series of thermal conductivity cells with various modifications of the element-supporting structure were designed, built, and characterized with regard to their heat loss distributions. Some of the more successful designs are shown in FIGURES 3*B*, *C*, and *D*. The average end loss obtained for each of these designs is noted under each drawing and is expressed as a percentage of the total heat dissipated by the cell element.

The design represented by FIGURE 3*C* was the best evolved from this work, if one considers it only from the standpoint of minimizing end losses. As shown in the drawing, there is no platinum lead up through the center of the ceramic mandrel. Instead, a self-supporting length of platinum wire is located parallel to the mandrel at a distance of about 1 mm., extending slightly beyond the end of the mandrel to provide the return connection for the far end of the hot-wire helix. The elimination of the wire from the center of the mandrel removes the path of lowest resistance to the flow of heat and reduces significantly the quantity of heat that escapes to the external environs of the cell. A large reduction in end losses is observed for cells having elements of this design.

However, the external location of the platinum lead wire in this design is responsible for some fabrication problems that would be difficult to overcome in any attempt to produce cell elements of this design in quantity. Difficulties arise in winding the helix on the mandrel. In addition, serious problems are encountered in attempting to mount the element coaxially in the cell envelope. The time required to accomplish these steps, the high rate of breakage, and the large percentage of rejections were all out of proportion to any advantage that might accrue from the low end losses observed. For these reasons, the design represented by drawing 3*C* was not accepted.

The element-supporting structure finally accepted is shown in FIGURE 3*D*. The principal differences between this design and that of drawing 3*B* are: (1) further reduction in the mass of the supporting glass stem; and (2) a large decrease in the effective cross-sectional area of the stem. Both of these improvements are the result of the adoption of a flared, bell-shaped stem. The thin, annular cross section of this stem offers a considerably higher resistance to the flow of heat away from the mandrel than does the heavy, solid-bead construction previously used (FIGURES 3*A*, *B*, and *C*). Cells made with these elements have end losses in the range of 22 to 25 per cent of the total heat loss, less than half that of the original cell element design.

The cell configuration shown in FIGURE 3*E* has extremely low end losses, well below 10 per cent of the total heat loss, and it is relatively easy and inexpensive to produce in quantity. However, this design was found to yield cells of inferior performance. The hot-wire helix is not rigid because it is unsupported. In turn, this causes the cells to be shock- and position-sensitive. Unsupported elements tend to sag or droop when they expand with heating; this causes a displacement from the normal coaxial mounting and introduces an eccentricity to the element. The calibration curves of analyzers built with such cells become nonlinear. A further disadvantage is the difficulty of mounting such elements coaxially in the cell envelopes. This would have the undesirable result of compounding the eccentricity effect.

Summarizing this part of the study, the element design finally adopted was not the one that exhibited the lowest end losses. It was the best of all the designs tested from an over-all consideration of the ease and cost of manufacture, complete cell performance, and low percentage of end losses.

### *Cell Performance Characteristics*

The cell performance characteristics that were considered in this study are: (1) total response, expressed in mv. output; (2) relative sensitivity expressed in mv. output/v. cell input; (3) response times in seconds required for the cell output to indicate initial response and to reach nine tenths of the total response; (4) sensitivity of the cell to deviation from the vertical position of operation; (5) sensitivity to the flow of gas through the sample line; and (6) sensitivity of the cell to vibration and shock.

The experimental conditions were similar for all the measurements made. The temperature of the cell envelopes was always maintained within the range 50 ± 0.2° C. All gas flow rates were regulated to 200 ± 20 ml./min., except when the cells were being tested for sensitivity to changes in the flow rate.

The total response of all the cells tested was measured relative to air for each of the five gases: $O_2$, $N_2$, $H_2$, A, and $CO_2$. These gases were selected because they differ widely in their thermal characteristics and present a good cross section of the properties most likely to be encountered in the laboratory and in industrial gases ordinarily analyzed by thermal conductivity equipment. The actual gas samples used were obtained from commercially available pressure tanks. No attempt was made to remove or reduce the amount of any impurities that might have been present. However, in every measurement both the sample gas and reference air were dried to eliminate the effects of an otherwise variable water vapor concentration. Water-pumped $N_2$, rather than Seaford $N_2$, was used as the $N_2$ sample in these tests because of the interferences caused by the residual $H_2$ present in Seaford $N_2$. The small amount of $O_2$ remaining in water-pumped $N_2$ caused no difficulty.

To measure total response of the test cell to any gas $X$, the bridge output is adjusted initially to a value of approximately zero with air flowing in the cell block positions of both the reference cell and the test cell. The change in bridge output, measured when the gas flow of the test cell is changed from air to 100 per cent gas $X$, is called the total response of the test cell to gas $X$. The change in bridge output is called positive if gas $X$ exercises a cooling effect on the cell element, that is, if the thermal conductivity of gas $X$ is greater than that of air. Conversely, the change in bridge output is called negative if the thermal conductivity of gas $X$ is less than that of air.

TABLE 1 presents the total response data measured for 14 of the new thermal conductivity cells. The data are given in terms of millivolts change in bridge output when the gas flow through the test cell is changed from air to 100 per cent of the gas indicated at the top of the column.

TABLE 1

TOTAL RESPONSE OF FOURTEEN THERMAL CONDUCTIVITY CELLS OF NEW DESIGN TO $O_2$, $N_2$, $H_2$, A, AND $CO_2$

| Cell No. | Total response in millivolts to | | | | |
|---|---|---|---|---|---|
| | $O_2$ | $H_2$ | $N_2$ | A | $CO_2$ |
| 2 | +28.9 | +759 | −7.7 | −217 | −127 |
| 4 | +29.8 | +717 | −8.2 | −231 | −127 |
| 5 | +27.2 | +707 | −7.5 | −210 | −121 |
| 9 | +30.3 | +799 | −7.5 | −226 | −130 |
| 13 | +27.4 | +683 | −7.5 | −207 | −115 |
| 14 | +29.2 | +766 | −7.4 | −218 | −125 |
| 19 | +33.6 | +792 | −7.7 | −251 | −136 |
| 20 | +30.1 | +730 | −8.2 | −232 | −128 |
| 23 | +31.0 | +775 | −8.7 | −242 | −133 |
| 24 | +33.0 | +760 | −8.5 | −253 | −137 |
| 26 | +31.9 | +758 | −8.7 | −246 | −129 |
| 28 | +27.2 | +651 | −7.5 | −210 | −115 |
| 29 | +27.9 | +654 | −7.9 | −216 | −117 |
| 30 | +28.1 | +665 | −8.1 | −222 | −123 |
| Median............... | +29.5 | +744 | −7.8 | −224 | −127 |

TABLE 2

RELATIVE SENSITIVITY OF FOURTEEN CELLS TO FIVE GASES

| Cell No. | Relative sensitivity in millivolts per volt | | | | |
|---|---|---|---|---|---|
| | $O_2$ | $H_2$ | $N_2$ | A | $CO_2$ |
| 2 | +7.76 | +204 | −2.06 | −58.3 | −34.0 |
| 4 | +8.50 | +204 | −2.34 | −65.8 | −36.1 |
| 5 | +7.56 | +197 | −2.08 | −58.4 | −33.5 |
| 9 | +7.29 | +192 | −1.81 | −54.4 | −31.1 |
| 13 | +7.83 | +195 | −2.14 | −59.2 | −32.7 |
| 14 | +7.61 | +200 | −1.93 | −56.8 | −32.5 |
| 19 | +8.73 | +206 | −2.00 | −65.3 | −35.2 |
| 20 | +7.79 | +189 | −2.12 | −60.0 | −33.2 |
| 23 | +8.16 | +204 | −2.29 | −63.7 | −34.9 |
| 24 | +9.17 | +211 | −2.36 | −70.3 | −38.0 |
| 26 | +8.91 | +212 | −2.43 | −68.9 | −36.0 |
| 28 | +7.93 | +190 | −2.18 | −61.2 | −33.5 |
| 29 | +8.10 | +189 | −2.29 | −62.6 | −33.8 |
| 30 | +8.27 | +196 | −2.38 | −65.6 | −36.2 |
| Median............ | +8.02 | +198 | −2.16 | −61.9 | −33.9 |

The relative sensitivity of a thermal conductivity cell to any gas *X* is derived by dividing the total response of the cell to gas *X* by the voltage input to the cell required to maintain an element operating temperature of 300° C. when air is flowing through the cell block. The relative sensitivity is expressed in terms of millivolt output per volt of cell input. TABLE 1 shows the cells considered; TABLE 2 presents the corresponding sensitivities.

FIGURE 4 indicates the relative sensitivity of a typical cell for the five test

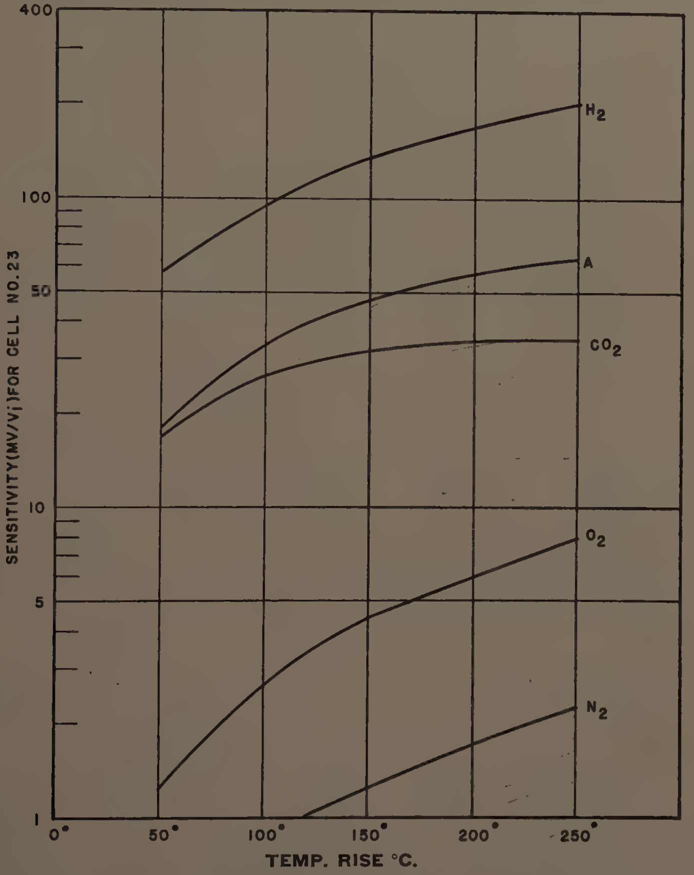

FIGURE 4. Log of the cell sensitivity versus temperature rise for five gases.

gases measured. The data are presented in terms of millivolts cell output per volt cell input as a function of cell temperature rise. In order to present data for gases having thermal conductivities widely different from that of air, the ordinate is a log plot. On this curve helium, which is of such current interest and importance in gas chromatography studies, would fall between argon and hydrogen.

The speed of response of a primary element is an important characteristic in adapting analysis instrumentation to measurement and control of processes. In many cases the acceptance or failure of an application to a process depends upon whether the control loop can be made to have a tolerable time constant. This inevitably involves the speed of response of the measuring system and of the sampling system. FIGURE 5 illustrates the effect of mandrel diameter of the new thermal conductivity cells upon the speed of response of the bridge. The curves shown represent the time for the cells to respond to a change in gas composition from a gas containing 18 per cent $CO_2$ in nitrogen to a gas

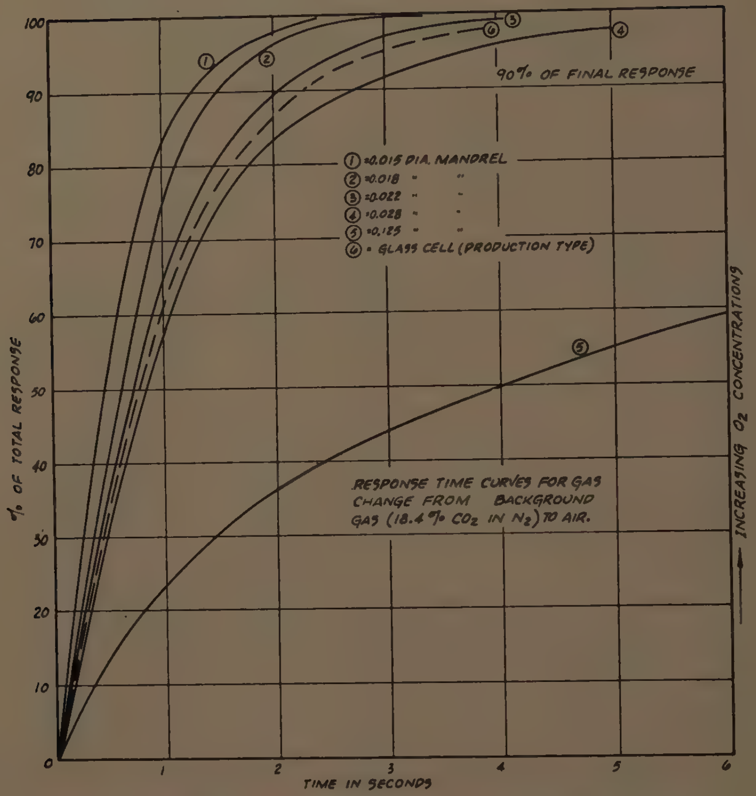

FIGURE 5. Response time curves plotted as a function of mandrel diameter.

containing 20 per cent oxygen in nitrogen or, in other words, air. The data shown were obtained for a diffusion-type cell used for thermal conductivity measurements, and will also hold true for the same cells when used for thermomagnetic oxygen measurements. When used in gas chromatography equipment, where the measuring cell is series-fed rather than diffusion-fed, both the initial response time and the 90 per cent response time are substantially improved. While exact measurements are difficult to obtain on changes occurring as rapidly as those in gas chromatography detectors, we have reason to believe that essentially these elements respond completely in substantially less than 1 second.

A study of the plot indicates that there is a definite relationship between speed of response and mandrel diameter, and this relationship holds approximately for the effect of mandrel diameter upon sensitivity. It will be noted that in increasing the mandrel's diameter from 0.015 in. to 0.028 in., the 90 per cent response time is doubled. However, a compromise must always be made in a high quantity production item between desirable characteristics and practical manufacturing considerations. For the cells that are the subject

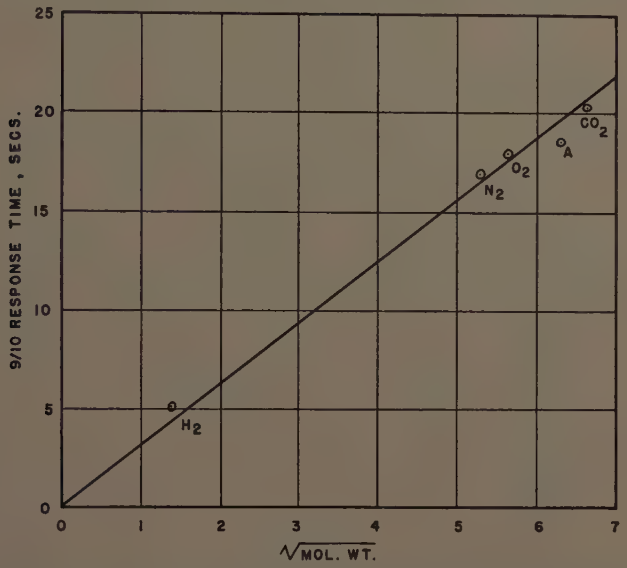

FIGURE 6. Plot of nine tenths response times versus the square root of the molecular weights for five gases.

of this paper, a mandrel diameter of 0.018 in. with a center hole of 0.007 in. to 0.008 in. was used.

Graham's law of diffusion states that the rate of diffusion of a gas is inversely proportional to the square root of its density. It follows that the rate of diffusion also should be inversely proportional to the square root of the molecular weight. The response times of the new thermal conductivity cells should be proportional to the rates of diffusion of the respective gases tested if the cells operate on the diffusion exchange principle. That the cells do operate on this

TABLE 3

EFFECTS OF CHANGES IN GAS FLOW RATE IN A TYPICAL CELL OF NEW DESIGN

| Flow rate ml./min. | Galvanometer reading in volts for flow of | | | | Total response in volts, corrected for zero shift | | | Percentage change from response at 200 ml./min. flow for | | |
|---|---|---|---|---|---|---|---|---|---|---|
| | $N_2$ | $H_2$ | $CO_2$ | Air | $N_2$ | $H_2$ | $CO_2$ | $N_2$ | $H_2$ | $CO_2$ |
| 370 | −0.0649 | +0.6656 | −0.1859 | −0.0570 | −0.0079 | +0.7226 | −0.1289 | 0.00 | +0.01 | −0.08 |
| 300 | −0.0649 | +0.6656 | −0.1860 | −0.0570 | −0.0079 | +0.7226 | −0.1290 | 0.00 | +0.01 | 0.00 |
| 250 | −0.0649 | +0.6656 | −0.1860 | −0.0570 | −0.0079 | +0.7226 | −0.1290 | 0.00 | +0.01 | 0.00 |
| 200 | −0.0649 | +0.6655 | −0.1860 | −0.0570 | −0.0079 | +0.7225 | −0.1290 | 0.00 | 0.00 | 0.00 |
| 150 | −0.0648 | +0.6654 | −0.1860 | −0.0569 | −0.0079 | +0.7223 | −0.1291 | 0.00 | −0.03 | +0.08 |
| 100 | −0.0648 | +0.6653 | −0.1860 | −0.0569 | −0.0079 | +0.7222 | −0.1291 | 0.00 | −0.04 | +0.08 |
| 50 | −0.0648 | +0.6652 | −0.1859 | −0.0569 | −0.0079 | +0.7221 | −0.1290 | 0.00 | −0.06 | 0.00 |
| 25 | −0.0647 | +0.6649 | −0.1858 | −0.0568 | −0.0079 | +0.7217 | −0.1290 | 0.00 | −0.11 | 0.00 |
| 0 | −0.0646 | +0.6643 | −0.1853 | −0.0567 | −0.0079 | +0.7210 | −0.1286 | 0.00 | −0.21 | −0.31 |

principle is indicated in the plot of FIGURE 6, which shows the response times of a typical cell to be a linear function of the square root of the molecular weights of the five gases tested.

The effects of cell-mounting position on cell response were determined by two measurements of the total response to $H_2$ and $CO_2$ as compared to air. In the first measurement, the total change in output of the thermal conductivity bridge to $H_2$ and $CO_2$ was observed with both the measuring and reference cells in a vertical position. The same measurements were then made with the cell under question mounted in a horizontal position; the reference cell remained in a vertical position. The behavior of cells in the two extreme mounting positions was thus studied. In no case was a significant difference in cell output detected between the two positions. The absence of position sensitivity in these cells permits us to conclude that natural convection currents have been eliminated in this cell design.

The effects of changes in sample flow rate through the cell block were measured. The air flow of the reference cell was held to 200 ± 20 ml./min., while the flow rate of gas of the measuring cell was varied from 0 to 370 ml./min. The gases used in these tests were $N_2$, $H_2$, $CO_2$, and air. Varying the flow of air of the measuring cell enabled us to determine the amount of zero shift caused by flow changes. This zero shift was then applied to the correction of the range changes observed for the other gases. The flow data measured appear in TABLE 3. It is seen that no zero shift occurs in the flow range 200 to 370 ml./min., and a shift of only 0.1 mv. for flows down to 50 ml./min. The data observed for a flow of 200 ml./min. are used as the reference in calculating the percentage change in bridge output or total response.

TABLE 3 indicates only very small changes in total cell response as a result of variations in sample flow between 0 and 370 ml./min. For flows in the range 50 to 370 ml./min., the zero shift observed is of insignificant proportions.

# ADAPTING GAS CHROMATOGRAPHY TO AUTOMATIC PROCESS STREAM ANALYSIS

H. N. Claudy, C. C. Helms, P. R. Scholly, and D. R. Bresky
*The Perkin-Elmer Corporation, Norwalk, Conn.*

## *Introduction*

Gas chromatography possesses many features that make it attractive as an analytical method, but its simplicity and the possibility it offers for the determination of several components in a sample are undoubtedly the features that make it particularly suitable for adaptation to process instrumentation. Previous process analyzers have been rather complex in their construction and operation, and generally have been limited to measuring one component only. The importance of the advantages of gas chromatography has been well illustrated by the fact that commercial process chromatographic analyzers appeared on the market only a few years after the introduction of such equipment for laboratory use.

## *Description of Instrument*

A typical process chromatographic instrument is shown in FIGURE 1. It consists of the analysis unit, the programmer, and the recorder. The analysis unit (FIGURE 2) is enclosed in an explosion-proof dome. Because of its similarity to equipment previously described, I shall mention only a few features that are characteristic of this particular design. Thermostating is accomplished by mounting all temperature-sensitive parts in close thermal contact with a temperature-controlled aluminum mandrel. This includes detector, sampling valve, column, and preheat coils for carrier and sample. The detector is of a parallel-flow design; a separate stream of carrier flows through the reference cell and to a vent common to it and the measuring cell, resulting in improved stability. This vent leads to an opening under the cover of the rotary sampling valve. After passing around the valve, this essentially inert gas flows to the main vent line. This continuous purge prevents the build-up of explosive vapors inside the analyzer if valve leakage ever occurs. The valve itself is polished to an optical flat on both of its moving surfaces and can be operated without lubrication, eliminating the problem of absorption of sample components in lubricant.

Normal operating temperature of the analyzer can be selected at any point between 50 and 100° C. The lower temperature is dictated by the necessity of maintaining the analyzer warmer than the highest expected ambient temperature in order to maintain control by its thermostat.

The programmer unit (FIGURE 3) provides timing functions for the analyzer and separate signal attenuation factors for each of four peaks, which are normally recorded as bars on the recorder chart. Timing for the peaks is set by positioning the tabs on the timer disc to correspond with the elution times of the components of interest. This permits elimination of the ordinary multiple-cam timing switch entirely. All switching, both for signals and for

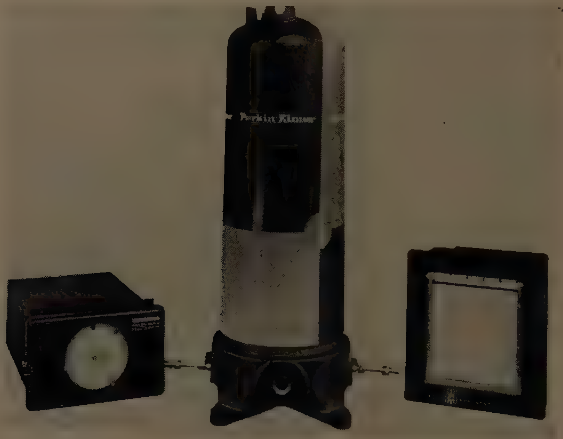

Figure 1. The process vapor fractometer programmer.

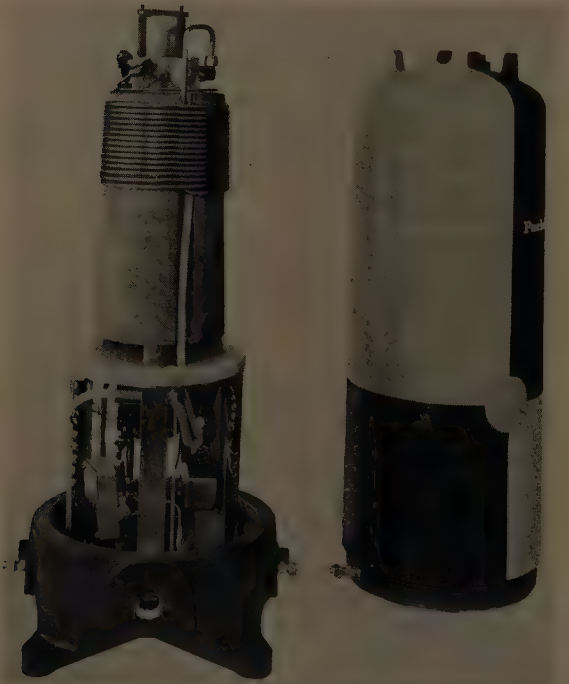

Figure 2. The analysis unit with explosion-proof dome and insulation removed.

power circuits, is done with hermetically sealed switches (figure 4) so that air-purging of the case is not required. If necessary, the bridge zero is adjusted by an automatic servomechanism once in each analytical cycle. Independent signal outputs are provided for each of the four components of interest, in

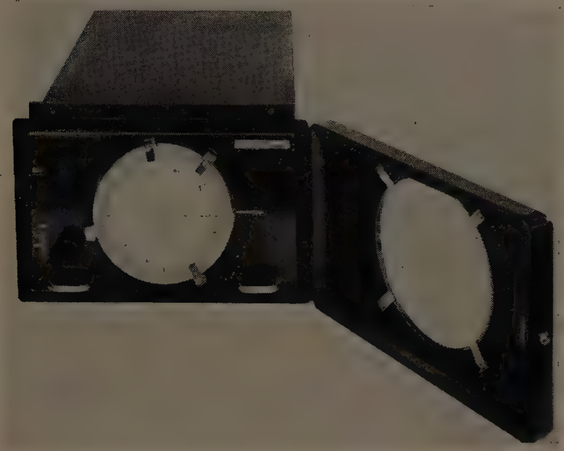

FIGURE 3. The programmer with door open.

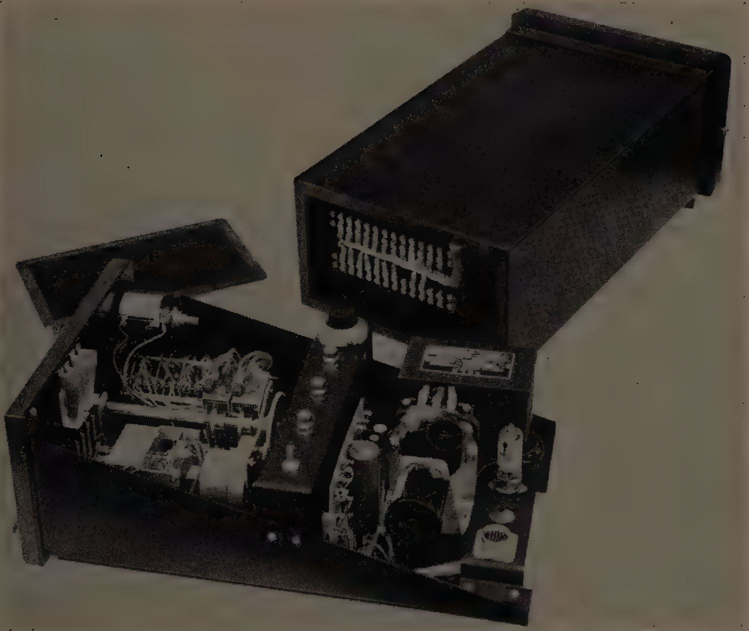

FIGURE 4. The programmer removed from its case.

addition to the common output to the main recorder. This permits use of auxilliary equipment.

Provision of a variable test signal permits setting the attenuators to record component concentrations directly in percentage full-scale ranges such as 0 to 1, 0 to 10, 0 to 50, or 0 to 100 without laborious cut-and-try methods or computation.

In addition to the normal bar graph data presentation, the unit may be operated as a conventional chromatographic analyzer, so that complete analyses of the process stream may be made whenever desired.

The analysis unit and the programmer have been designed to be as simple and flexible as possible in order to retain the chief advantages of gas chromatography while adapting the equipment to the ruggedness and reliability required of process instrumentation.

### *Application*

The analyzer requires sample in the vapor phase at the operating temperature selected, which may be anywhere between 50 and 100° C. Columns up to 50 feet long may be used, the length depending upon a compromise between resolution of components and cycle time, which should be between 5 and 60 min., the shorter times being preferable. Within these limitations, the analyzer is capable of performing any analysis that can be done with conventional laboratory equipment.

The bulk of present applications is represented by the analysis of hydrocarbons from methane through the $C_5$'s. Techniques for the separation of paraffins, olefins, and diolefins in this boiling point range have been well worked out and such mixtures are among many important refinery and petrochemical process streams. These analyses include applications to fractionating column operations, alkylation processes, and butane dehydrogenation.

One of the most general problems in the application of process gas chromatographic analyzers, as in analytical instrumentation as a whole, is that of obtaining a representative sample from the process stream. The location of the sampling point, if badly chosen, can limit the utility of the entire system dependent upon it. The sample should be obtained from a point in the process where the stream does not contain solid material, partly condensed liquids, droplets of water, or bubbles of gas. The sample point should be chosen to reduce the transport lag between critical process equipment and the analyzer, which should be installed as close to the sample point as possible. The internal volumes of sample-handling equipment such as piping, vaporizers, and strainers must be kept low. When handling liquid streams that must be vaporized before introduction to the analyzer, it is often advisable to provide a bypass loop back to the process through which a fairly large flow rate of liquid can be maintained, with a side stream for the vaporizer taken off close to the analyzer location. The same technique is used occasionally for vapor-phase sample streams.

When the process equipment itself has an appreciable time constant, better results sometimes can be obtained by location of the sample point where changes in stream composition occur most rapidly. For example, the sample point for a fractionating column is often placed on a tray some distance from the top of the column, making the analyzer more responsive to changes in column operation before they affect the final product. This also effectively increases the measured concentration of minor components.

Difficulties are sometimes encountered in reproducibly vaporizing liquid-phase sample streams. The problem here is to avoid fractionation of the sample, which is especially likely to occur if it contains materials having a wide boiling point range. Needle valves usually do not perform well for this purpose, but commercial vaporizers of various designs are available. Essentially, they are based on confining the vaporization to a very small area. Properly applied, they have proved quite satisfactory, but equivalent or even better performance may be obtained by vaporizing the sample as it passes through a heated capillary tube; this system has the advantages of simplicity and low cost.

Usually vapor-phase sample streams containing relatively high-boiling components must be steam-traced to prevent recondensation of the sample.

When there are components in the sample stream which either interfere with the separation desired or contaminate the chromatographic column, there are two approaches that may be taken. Pretreatment of the sample before introduction to the analyzer may solve the problem. For example, in the analysis of nitrogen, hydrogen, methane, and inerts in ammonia synthesis feed gas, water and ammonia are both irreversibly adsorbed on the molecular sieve columns used. However, both of these components may be removed easily by scrubbing the sample with concentrated sulfuric acid, and this technique has been used with success for the analysis of such process streams. Water is often a problem. Another pretreatment that has been adopted to deal with it consists in passing the sample through calcium carbide, which reacts with the water to form acetylene. The acetylene can then be considered as any other component in the stream and can be measured to determine the original water content. Such pretreatment techniques are most effective when the concentration of the interferent in the sample is low.

An alternative approach to such problems has been suggested in the use of analyzers employing provision for backflushing either the entire chromatographic column or the first of two columns in series. This approach is the more generally useful in that it is capable of dealing with a wider variety of contaminants. It is necessary only to select for the first column a substrate that will retain the unwanted components long enough for the others to pass through it into the second column and that will then give up the unwanted components when backflushed. Of course, the remaining components pass on through the second column and are measured by the detector. Such an approach is a virtual necessity when attempting to analyze with an adsorbent column a sample containing an appreciable concentration of high-boiling materials. When only a very low concentration of such materials is present, it is sometimes sufficient to precoat the adsorbent with a small amount of liquid substrate. This greatly reduces the effect of the addition of heavy materials from the sample and enhances the stability of the adsorbent column.

In fact, column instability can arise from two sources. One is the gradual build-up of high-boiling materials that are eluted very slowly if at all, or the actual reaction of the substrate with a sample component. The other is the loss of substrate resulting from its gradual elution by the carrier gas. Among the substrates presently used in process chromatographic analyzers, dimethylsulfolane undoubtedly has the highest vapor pressure. Its use is limited to

50° C, and even at this temperature one would expect a dimethylsulfolane column to have a rather limited life. However, such columns have been in continuous operation for periods of over a year with little sign of change. Perhaps this unexpected stability is due to adsorption of the dimethylsulfolane on the column support. In any case, the life of these columns exceeds that which would be predicted on the basis of vapor pressure alone.

## *Process Control*

The demand for process-stream analyzers has arisen from an increased awareness on the part of processing personnel that environmental measuring and controlling instruments based on such factors as pressure, temperature, level, and flow rate are, at best, only inferential in determining the most important process variables: the actual composition of the product being made, the raw materials fed to the processing unit, and the loss of valuable components in waste or low-value streams. These are the factors whose control is ultimately desired, and upon which operation of a process must be based in order to achieve maximum economic return.

Making this information available on a continuous basis to operating personnel has already resulted in a striking improvement in the control of many processes. However, the process chromatographic analyzer in its present state of development still requires a human operator. He must interpret the analytical results and make whatever adjustments he considers necessary in the process.

The next step in the application of gas chromatography to process control obviously involves including the analyzer in the control loop, so that corrective action is made when necessary without the intervention of a human operator. Such action will require from the analyzer a continuous output signal that is proportional to the concentration of the component of interest; in other words, the sampled data of the chromatographic analyzer must be converted into a step-changed, continuous output signal. Equipment for this purpose is now under development and test and may be expected to be available in the near future.

In addition to permitting control of a process based on the concentration of one component in a process stream, this equipment will permit, with modifications, such sophisticated techniques as control based on the ratio of two components in a stream, on the ratio of concentration of a component in an inlet stream to that in an outlet stream, or on the difference or sum of concentrations of the same component in different streams or of components in the same stream. Simple analogue computations of these types can be accomplished with minor changes of conventional process control equipment and promise to open up new areas in the field of process control. More refined computations involving many measured variables can be made with the data-logging computers now beginning to appear in control rooms, and it should be noted that the increased use of these machines virtually will demand the employment of more process analytical instrumentation to provide the information needed to produce meaningful results and to make operation truly effective.

Inclusion of the process chromatographic analyzer in the control loop will intensify the problem resulting from the inherent time lag in chromatographic analysis. Analyses made by the process instrument currently require between 5 and 60 min. for a complete cycle; 15 min. is probably an average figure. Although this time lag is perhaps not a serious one for many slow-reacting processes, it is certainly excessive for others. Thus, a future development of considerable importance will be the shortening of the analytical cycle, either by improving the efficiency of present equipment or by a radical departure from present practice.

### *Conclusion*

Manufacturers and users alike recognize that thus far process analytical instruments have had much less success than was originally predicted for them. Unquestionably, part of the blame for this situation lies in the fact that many such instruments, because of the analytical principles they employed, have been so complex and difficult to maintain that the advantages of the information they made available have been largely offset by the problems they introduced. However, because the process chromatographic analyzer is both simple and versatile, it offers a hope for a breakthrough in the process analytical area.

The great financial rewards in terms of plant-operating economies resulting from the proper use of process analytical instruments can be expected to spur their application, and indicate that gas chromatography, in its importance in this field, ultimately may equal or surpass the position it has already achieved in the laboratory.

*Printed in the United States of America*

# MONOGRAPHIC PUBLICATIONS

# OF

# THE NEW YORK ACADEMY OF SCIENCES

(LYCEUM OF NATURAL HISTORY, 1817–1876)

(1) The ANNALS (octavo series), established in 1823, contain the scientific contributions and reports of researches, together with the records of meetings of the Academy. The articles that comprise each volume are printed separately, each in its own cover, and are distributed immediately upon publication. The prices of the separate articles depend upon their length and the number of illustrations, and may be ascertained upon application to the Executive Director of the Academy.

Current numbers of the ANNALS are sent free to all Members of the Academy desiring them.

(2) The SPECIAL PUBLICATIONS, established in 1939, are issued at irregular intervals as clothbound volumes. The price of each volume will be advertised at time of issue.

(3) The MEMOIRS (quarto series), established in 1895, are issued at irregular intervals. It is intended that each volume shall be devoted to monographs relating to some particular department of science. Volume I, Part 1 is devoted to Astronomical Memoirs, Volume II to Zoological Memoirs. No more parts of the Memoirs have been published to date. The price is one dollar per part.

(4) The SCIENTIFIC SURVEY OF PORTO RICO AND THE VIRGIN ISLANDS (octavo series), established in 1919, gives the detailed reports of the anthropological, botanical, geological, paleontological, zoological, and meteorological surveys of these islands.

Subscriptions and inquiries concerning current and back numbers of any of the publications of the Academy should be addressed to

EXECUTIVE DIRECTOR
*The New York Academy of Sciences*
*2 East Sixty-third Street*
*New York 21, N. Y.*